TO MY FAMILY

PROPAGATING ACTION POTENTIALS AND THE REGENERATION OF *ACETABULARIA MEDITERRANEA* - A PILOT STUDY

A thesis

submitted in fulfilment

of the requirements for the Degree

of

Doctor of Philosophy in Physics

by

SOMSAK LERTSITHICHAI

University of Waikato,

Hamilton, New Zealand.

1980

ABSTRACT

A study of the relationship between the cell membrane electrical activity and the observed polar regeneration in anucleate isolated stalk segments of *Acetabularia* may help answer the question of how a single cell can 'break symmetry' and establish a definite polarity. Such studies have been carried out extensively by Novak and Bentrup and their colleagues since 1972, but their results contain unresolved inconsistencies and although their experimental technique overcomes the problems arising from conventional microelectrode techniques, it gives a restricted and electrically perturbative environment for the cell.

In an attempt to overcome these limitations the work in this thesis describes the development of a new technique for measuring the electrical activity of the cell membrane with minimum perturbation from the measuring system. In addition it gives more precise and detailed information about the region of action potential initiation and subsequent propagation.

The results of measurements using this technique on a variety of intact cells and various cell segments, including anucleate stalk segments are presented and discussed. The results provide strong evidence for the hypothesis that the region of action potential initiation is strongly correlated with the region of current growth. They do not however appear to provide any support for the suggestion of Novak and Bentrup that propagating action potentials are an essential component of the mechanism for 'symmetry breaking'in initially unpolarised anucleate stalk segments.

ACKNOWLEDGEMENTS

This work would not have been completed without the invaluable advice,encouragement and enthusiasm of Dr R.A. Sherlock. I am particularly indebted to him and offer him my most sincere thanks.

I am also grateful to

Professor D.F. Walls for his encouragement throughout this work,

Mrs J. Miller for the corrections of my thesis writing,

Drs H.W. Morgan and C.G. Harfoot for their advice about the culture techniques,

Dr P.C. Molan for his comments on the membrane concepts,

Mrs J.R. Tait and Mrs C. Coates for their skillful and careful typing,

The Ministry of Foreign Affairs of New Zealand for the scholarship, and finally,

my family for their understanding my absence during the weekends and holidays.

Somsak Lertsithichai

June, 1980

CONTENTS

LIST OF TABLES

LIST OF PLATES

CHAPTER 1

INTRODUCTION

1.1 Perspective

One of the most interesting problems in biology is that of understanding the principles and mechanisms that govern the development of an organism from the single cell zygote to the very much more complex and differentiated structure of the mature form. In most cases of course the mature form is a multi-cellular organism. By mechanisms at present unknown the organism must generate a 'map' of morphogenetic potential so that a given cell knows 'where it is' in relation to the other cells, and so only expresses the appropriate features of its full genetic potential. (Every cell of course carries the same complete set of genetic information, or genome, and so in principle has the potential to develop into any of the morphologically distinct cell types of the organism).

This problem is so complex that to date little progress has been made, and the nature of the 'morphogenetic map' and the way it is established in an initially homogeneous system is little more than a matter of speculation. Obviously there are great difficulties involved in even the simplest forms of experimental investigation due to the small size and susceptibility to damage of any developing embryo.

A possible step towards a solution to this impasse is the selection of an organism which is sufficiently simple and robust to permit some detailed measurement of parameters of possible relevance, and at the same time complex enough to exhibit a definite differentiated development or morphogenesis. A likely candidate is the marine alga *Acetabularia* (in particular the species *A. mediterranea*) already well known from the elegant experiments of Hammerling and co-workers (e.g. see Bonotto, et.al. 1976), demonstrating that the species dependant characteristic

morphogenesis is ultimately controlled by the nucleus. Although a single-cell organism, *Acetabularia* is unique for its large size (a mature cell may be 60 mm long with a stem diameter of 0.4 mm and a cap diameter of 8 mm) and its well differentiated structure (Plate 2.1.1). The mature cell consists of at least three morphologically distinct regions - the rhizoid by which the cell attaches itself to the ocean floor and in which the single well defined nucleus resides, the stem, and the cap in which the reproductive cysts are formed. The cells can be maintained in a laboratory culture and are relatively robust in that fragments cut from a complete cell are able to exhibit further growth and differentiated development in appropriate circumstances. Experimental monitoring of various cellular parameters associated with these developmental or redevelopmental processes and the identification of the morphogenetic control mechanisms in this organism is thus a real possibility. The work described in this thesis is concerned in particular with possible relationships, suggested by the work of Novak and Bentrup (1972a) between the observed electrical activity of the cell (plasmalemma) membrane and the morphogenetic control system in *Acetabularia mediterranea*.

It is of course the long term hope that any mechanisms identified in this specific organism may have a more general applicability. Given the extensive subset of structures and processes known to be common to all living cells this would seem to be not too unreasonable on expectation.

1.2 Morphogenesis in *Acetabularia mediterranea*

It is generally accepted that the morphogenesis in a normally growing *Acetabularia* cell is governed by a morphogenetic map. Demonstrable features of this map are an apico-basal gradient of 'cap-forming' morphogens and a baso-apical gradient of 'rhizoid-forming' morphogens (Werz, 1974) although these are clearly simplified observations. The morphogenetic substances (MS's) have been shown to be of nuclear origin and are believed to be stable m-RNA's (Brachet and Bonotto, 1970). They are species specific.

The MS's are produced in the vicinity of the nucleus and transferred into the cytoplasm where they become distributed heterogeneously. The evidence that the establishment and maintenance of the morphogenetic map is dependent on normal illumination (see e.g. Hammerling, 1963) suggests that photosynthesised ATP is an important source of the energy necessary to maintain such a non-equilibrium situation. There is some evidence that they may be loosely bound to specific receptors (capable of interacting with the MS's) in the cytoplasmic membrane at the developing region (see Bonotto, et.al., 1976 for references).

The MS's are produced well in advance of the time when they are needed for a particular stage of development (morphogensis), i.e. they can be stored in the cytoplasm stably for long periods. The expression of their appropriate morphogenetic development at the right time is believed to be triggered by some special proteins which are non species-specific (Werz, 1974).

In addition to the morphogenetic gradients, there is ample evidence to demonstrate the existence of other gradients in the cytoplasm, e.g. the spatial difference in metabolic activity (more activity at the apical end), the non-uniform spatial distribution of cytoplasmic substances

e.g. enzymes (Werz, 1974) and chloroplasts (Hoursiangou-Neubrun, et.al., 1977). The gradient of chloroplasts consists of the lightest chloroplasts containing the highest DNA content (most likely the highest transcriptional activity) at the apical end and the heavier ones, which exhibit more complex supramolecular organisation, in the other regions (Mazza, et.al., 1977).

Information about the establishment of the morphogenetic map can be obtained by placing stem sections cut from complete cells in the dark for several days, during which time their original polarity is lost, and then monitoring their redevelopment when illumination is restored. The results of such experiments, pioneered and pursued for many years by Hammerling are now summarised from Hammerling (1963).

When a normal growing complete cell (CC) is cut into two halves, resulting in a basal stalk segment (BSS) containing the nucleus (nucleate segment) and an apical stalk segment (ASS) without a nucleus (anucleate segment) the following behaviour is seen:

A. If the BSS is kept in the dark,

(i) there is no further growth,

(ii) there is a degradation of nuclear material,

(iii) the size of the nucleus is reduced, but it continues to synthesize MS's and some of them are transported and stored at the cut apical end, and

(iv) the gradients of the MS's are still maintained.

When the BSS is re-exposed to light normal physiological activities resume and normal redevelopment to a complete (fertile) cell is obtained.

B. An anucleate ASS is capable not only of surviving for weeks or even months but also of

regenerating, provided it has exposure $\lesssim$ 7 days after cutting to light, into

(i) a rhizoid-like structure at the cut end,

or (ii) sterile whorls (or even a cap) at the apical end,

or (iii) both (i) and (ii).

C. If the rhizoid and nucleus of a BSS are removed an anucleate isolated stalk segment (ISS) results. This can survive > 100 days (Schweiger, et.al., 1975) under normal culture conditions (Section 2.2). If it is kept in the dark (for $\gtrsim$ 1 day), the existing morphogenetic polarity soon disappears. When illumination is restored, the polarity is usually unambiguously re-established, though not necessarily in the same direction, and subsequent apical-like and rhizoid-like redevelopment at the cut ends is seen.

Since the reformation of the morphogenetic gradients in an ISS is totally governed by the remaining cytoplasm (i.e. is not dependent on the presence of the nucleus), it has been suggested that the re-establishment of concentration gradients of the MS's would be facilitated by two main physical factors, hydrodynamic and electrical forces (Novak, 1975a; Zubarev and Rogatykh, 1975; and Bonotto, et.al., 1976)

It should also be remembered that in the normal development of a complete cell phototropism and geotropism are important factors (Gibor 1966, 1977; Bonotto and Sironval, 1977) but as will be seen these effects are not essential to the gradient establishment process.

1.3 Theoretical Models

In this section some general ideas which have been suggested as providing a possible mathematical description or basis for the process of morphogenesis are very briefly reviewed. A more detailed discussion is then given of a model proposed by Goodwin (1976) which is particularly concerned with single-cell systems such as *Acetabularia*.

1.3a General models of morphogenesis.

A number of theories attempting to explain morphogenesis or pattern formation in a developing organism have been suggested since 1895 (e.g. see references in Babloyantz and Hiernaux, 1974). The morphogenetic process is usually divided into two stages: the formation of morphogenetic gradients or map and the subsequent differentiation of cellular processes which leads to a visible structural differentiation (Wolpert, 1969; 1975).

In the first stage, the distribution of MS's in the embryo (or the single developing cell) is assumed to be homogeneous, symmetrical and unstable. Subsequently a coordinate system, which is an ordered spatial inhomogeneity in the morphogenetic field, is established by some gradient-generating mechanism. Such processes have been demonstrated in several relatively simple model reaction schemes (e.g. see Turing, 1952; Wolpert, 1969; 1975; Babloyantz and Hiernaux, 1974; 1975; Goodwin, 1975; 1980; Nicolis and Prigogine, 1977; and Haken, 1978). However, none of these is an explicit biological model and an example of gradient formation via some known biochemical reaction scheme has yet to be disconcerted.

In the second stage the information of the morphogenetic map is translated into molecular differentiation of visible structural forms. This process is also discussed in the above references but again there is a severe lack of real biological information.

1.3b Goodwin's Model of Morphogenesis in One Dimensional Systems.

Goodwin (1976) has reviewed a range of evidence which suggests that membranes are the sites of organisation and maintenance of morphogenetic gradients. He then presents a simple model of a 'metabolically excitable' membrane in which a gradient of a membrane bound metabolite could be established and maintained by repetitive waves of metabolic activity initiated in a pacemaker region.

In the cytoplasm, there is considerable metabolic activity associated with membranes, in addition to their more familiar properties of electrical excitability and selective ionic permeability. Although the most familiar form of excitability is the well-known electrical action potential phenomenon, biochemical 'activity waves' similar to propagating AP's but not necessarily accompanied by membrane depolarisation and the flow of ions across the membrane are also possible. Briefly the mechanism of the activity wave generation can be described (p. 142-148, Goodwin, 1976; and Fig. 1.3.1 a and b) as follows.

A membrane bound enzyme E_1 is activated by an activator S to catalyse the transformation of some metabolite M_1 to another, M_2. This reaction also produces more S's that can spread by diffusion, i.e. there is a positive feed-back loop and an 'activity wave' of excited E_1's spreads along the membrane. This chain-reaction process is stabilised by the third metabolite M_3, resulting from the catalysis of M_2 by a second enzyme E_2, which acts as an inhibitor of E_1. If there are membrane binding sites for M_2 (identified as the morphogen) then the passage of such an activity wave can result in a gradient of M_2 concentration which has its maximum at the wave origin and elsewhere decreases monotonically, i.e. a morphogenetic gradient. Further details of this calculation are given in Goodwin (1976, p. 241-3) and the results are reproduced here in Fig. 1.3.1b. The gradient is temporarily formed

Fig. 1.3.1 (after Goodwin, 1976)

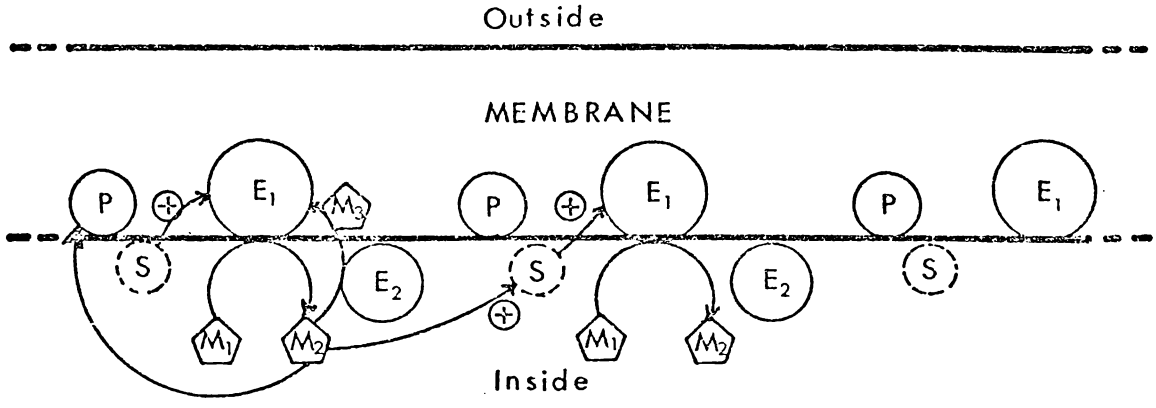

a) Goodwin's Model of the metabolic system of a membrane forming a spatial morphogenetic gradient.

Suggested equivalent substances in *Acetabularia mediterranea* and the model

E_1 = adenyl cylase

E_2 = phosphodiesterase

M_1 = ATP

M_2 = cyclic AMP

M_3 = AMP

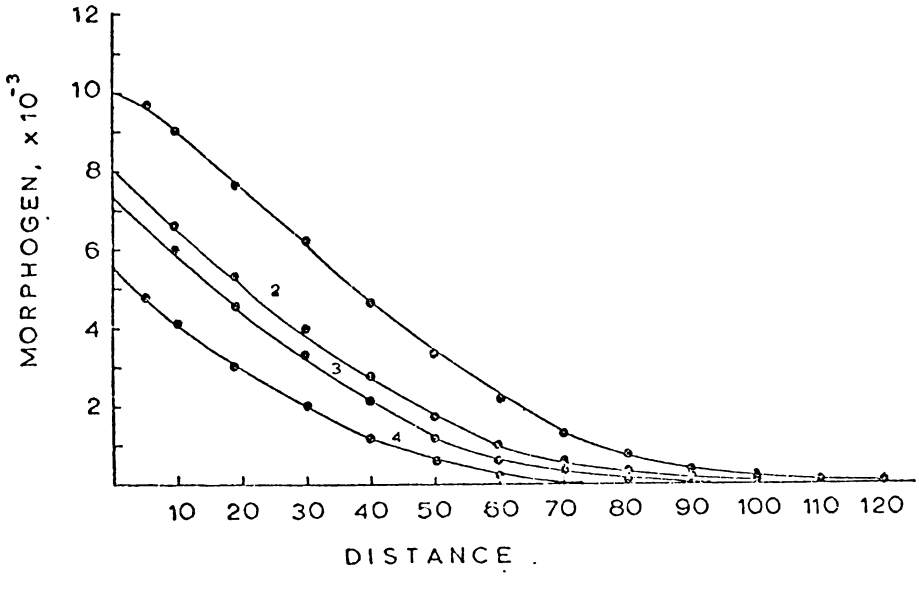

b) Curves showing the spatial distribution of morphogen (M_2 binding to the membrane at site P) as computed from a particular form of the wave propagation model at different values of time delay.

by a single activity wave. Its stabilisation requires the regular recurrence of waves initiating periodically from the origin.

Goodwin points out the possible correspondence between this model and the experimental observations of the spontaneous AP's initiating at the rhizoid in *Pelvetia* eggs(Nuccitelli and Jaffe, 1974) and at the apical end in the *Acetabularia* cell (Novak and Bentrup, 1972a). However these experiments have not so far shown that the electrical waves are in any way correlated to the establishment of the morphogenetic gradient in these developing cells.

1.4 Questions Arising from the Current State of Electrophysiological Investigations.

Novak and Bentrup (1972a and b) made an extensive study of the electrical activity of the dark-treated anucleate posterior stalk segments (in this work referred to as ISS's - isolated stalk segments) during the early stages of their light-triggered redevelopment. These experiments (as well as others subsequently performed by them and their various co-workers) were made using a special cuvette (Fig. 1.4.1) which divided the ISS and the external medium into two or more electrically isolated compartments. Their measurements implied that a small membrane potential gradient (typically 5-10 mV) established itself at an early stage (~ 29 hours after exposure to light), and that this gradient always correlated with the polarity of the subsequent regeneration. The new apex was at the end of the segment where the (internal) membrane potential was most negative.

In addition to the establishment of the steady gradient in the membrane potential, action potential depolarisations were also observed, occurring at both ends of the ISS during the initial stages and then exclusively at the regenerating (more negative membrane potential) end when the potential gradient was established. However it should be noted that the highly perturbative experimental set-up prevented the propagation of these AP's along the cell, and indeed at the time of this work no demonstration of propagating AP's in *Acetabularia* had ever been given. Nevertheless, in their conclusions Novak and Bentrup (1972a) suggest that propagating AP's are an essential mechanism in stabilising fluctuations in the membrane potential and establishing a steady gradient. This type of interpretation was also made by Goodwin (1976) in support of his model described above.

Unfortunately however, in addition to these experimental limita-

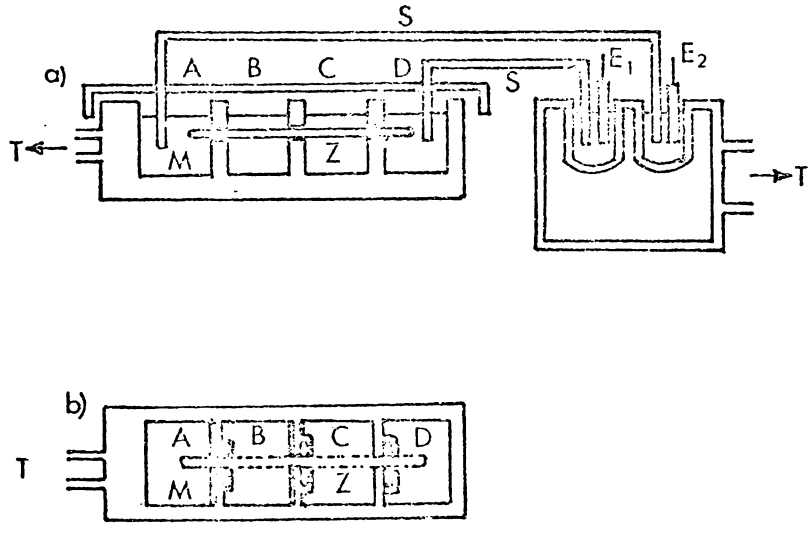

Fig. 1.4.1 Special Cuvette for the measurement of the potential differences along the ISS by means of external electrodes (Calomel electrodes via salt bridge) used by Novak and Bentrup.

a) Side view

b) Front view

A, B, C, and D = Electrically isolated compartments

S = Salt bridge

E_1 and E_2 = Calomel electrodes

M = Medium

Z = Cell segment (ISS)

T = Thermostat

(After Novak and Bentrup, 1972a).

tions there are a number of internal inconsistencies between the original and subsequent work by Novak and Bentrup. For example the transcellular current resulted by the membrane potential gradient was firstly reported flowing internally away from the regenerating end (Novak and Bentrup, 1972a), contrary to the reports in all later papers (Novak and Bentrup, 1972b; Novak and Sironval, 1975; 1976; Novak, 1975a and b; Christ-Adler and Bentrup, 1976; and Bentrup, 1977).

Considerable ambiguity also exists concerning the relative importance of the membrane potential gradient and the resulting current (if any) in relation to the regeneration. The first paper (1972a) mentioned that the regeneration was induced by the membrane potential gradient independent of cytoplasmic current flow whereas other papers (e.g. Novak and Sironval, 1975) reported that an actual current flow was essential to the redevelopment.

Novak (1975a)has concluded eventually that both trans-cellular current and AP propagation induce the MS's towards the growing tip, and therefore, control the beginning of the regeneration processes.

An opposing view was taken by Christ-Adler and Bentrup (1976), and Bentrup (1977) who performed experiments on the ionic concentration gradients between two cut ends of the ISS's and found that the regeneration could be induced by lower concentrations of either K^+ or Cl^- ions. Bentrup (1977) concluded that neither the transcellular current nor AP initiation was necessarily related to the initiation process of the regeneration. Both electrical and morphogenetic events were derived from a common functional pattern developed by the membrane at its immediate vicinity. This conclusion agrees with the hypothesis of an intracellular localization mechanism, proposed for the morphogenetic events in other kinds of seaweed eggs (Jaffe et.al., 1974).

These ambiguities arise in large part from the difficulty in

performing the electrophysiological experiments. In particular the electrical isolation of the medium and the ISS into compartments inhibits the flow of the local action currents during an AP occurance from one compartment of the medium to another, i.e. the propagation of the AP is suppressed within the initiating compartment (Section 3.4). Because of this major limitation the role of propagating action potentials in the morphogenetic processes involved in the redevelopment of *Acetabularia* ISS's was considered undefined at the start of the present work.

1.5 Objectives of Present Work.

As a pilot study of the role of action potentials in developmental processes of *Acetabularia mediterranea* the work described in this thesis falls into three categories.

(1) Development of culture techniques for *Acetabularia mediterranea* to meet the local material supplies and the requirement of the experiments (Chapter 2).

(2) Development of a new experimental technique for investigating the relevant electrical activities of *Acetabularia* cells in the medium that can overcome most of the problems arisen in using conventional microelectrode techniques and the techniques employed by Novak and Bentrup (Section 1.3). In other words the spontaneously initiating AP's are monitored in as near natural an environment as possible so as to minimize the perturbation to current flow patterns or any other parameters (Section 4.1). This technique was developed to enable the transmembrane current to be simultaneously recorded in several positions (typically 8) along the cell and stored for analysis of the initiating position (Chapter 4).

(3) Utilization of the above experimental technique for obtaining details of AP initiation and propagation characteristics in complete cells (CC's) and various cell fragments in relation to their developmental and redevelopmental behaviour (Chapter 5).

CHAPTER 2

CULTURE TECHNIQUES AND SPECIMEN PREPARATION.

2.1 Introduction.

The green marine algae, including *Acetabularia*, are *Chlorophycea*. *Acetabularia* belongs to the family *Dasycladaceae* which is characterized by the development of specialized branches that at their apices become the reproductive organs of the plant. Of about twenty species in this family, only a few are used as laboratory materials. The most frequently employed are *A. mediterranea* and *A. crenulata*.

In nature, *A. mediterranea* is found growing as seaweed several centimetres in height with an umbrella shaped cap with diameter of up to 10 mm. The basal end, where the only nucleus is, develops a branched tendril-like root called the rhizoid which attaches the cell to the sea bed (see Plate 2.1.1).

Acetabularia grows very slowly, taking about six months to complete the life cycle from the initial germination to the fertile plant forming the reproductive cap (see Fig. 2.1.1, and also Bonotto, et.al., 1976). There is only one nucleus during the entire period of growth. When this period ends the cap matures to become the reproductive organ of the cell. The nucleus begins to divide into thousands of nuclei which migrate into the cap. The contents in the radial chambers (rays), which are the accumulation of almost all of the protoplasm of the alga, break up into rounded masses approximately 50 μm in diameter. They become surrounded by a thickened membrane and are then called cysts. By the destruction of the cap, the cysts are freed and are dispersed by sea currents. After a few months of being disseminated, the protoplasm of the cysts divides to produce highly active, biflagellate elements of

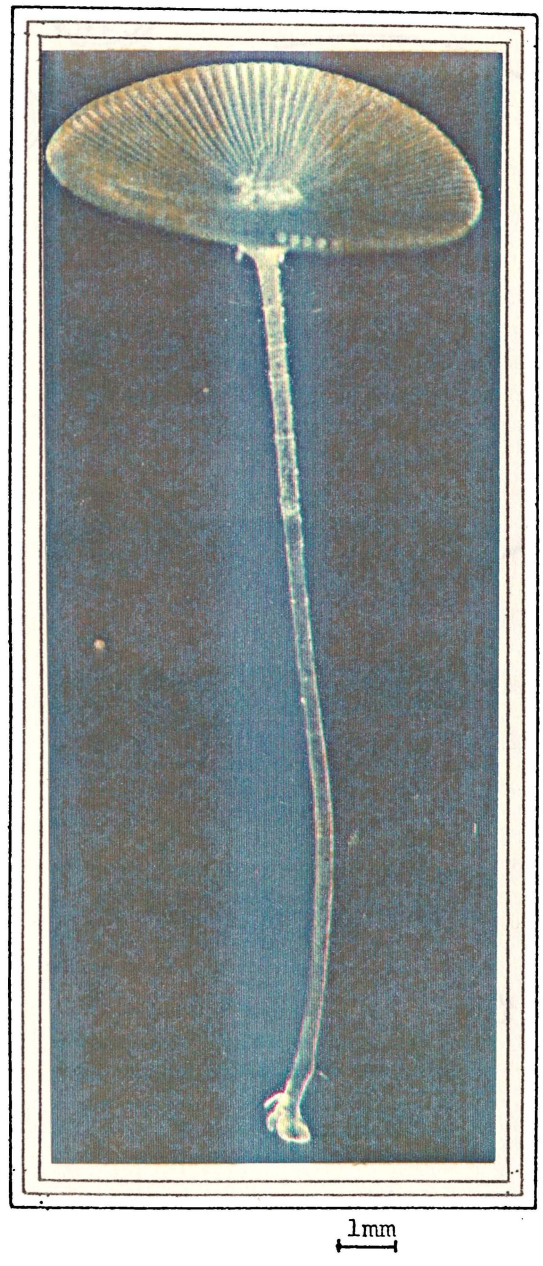

Plate 2.1.1 Mature cell of *Acetabularia mediterranea*

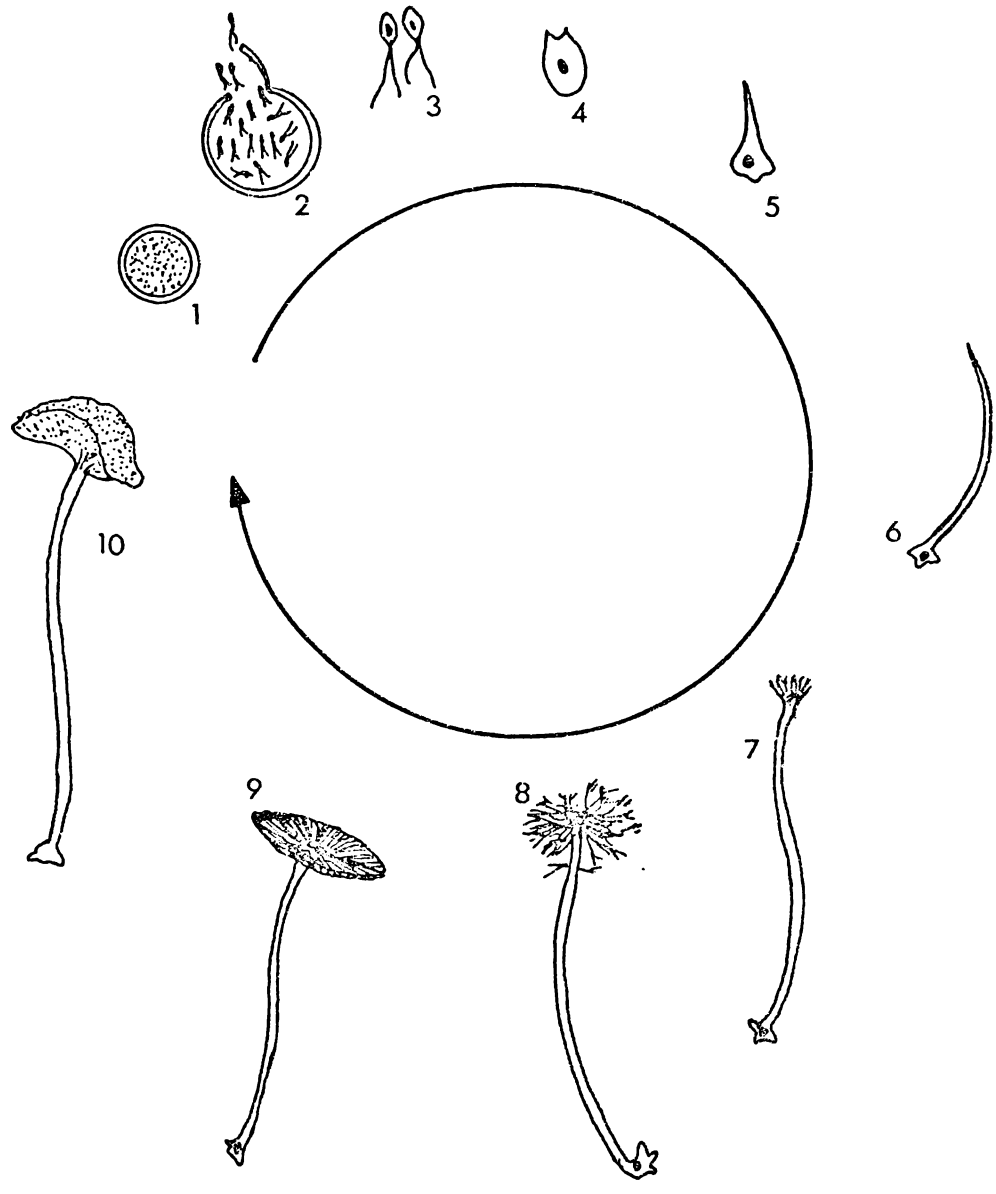

Fig. 2.1.1. The most frequently occuring reproductive cycle of *A. Mediterranea*.

1. Mature cyst, 2. Opening of lid, releasing gametes, 3. Fertilisation of two gametes, 4. Zygote; fusion of two gametes, 5. Early growth phase cell, 6. Young cell, 7. Young cell with whorl, 8. Cap developing cell, 9. Mature cell, 10. Cyst formation.

pyriform shaped zoids. They measure 2 to 3 µm in width and 5 to 8 µm in length and bear a more or less well-defined 'eye-spot'. These zoids emerge from the cysts, which burst open by means of readily observable lids (Puiseux-Dao, 1970). They are positively phototactic at first, then negatively: they then lose their flagellae and round off, to become attached to the ocean bed and transformed into young seedlings. This type of reproduction which is called cyst germination occurs most frequently in *A. mediterranea*. In addition, at the cyst level, there are several types of reproduction found possible in the laboratories (Fig. 2.1.2). They can be sexual and asexual reproductions, e.g. the sexual fertilization by isogamous gametes formed in cysts, each cyst supplying zoids of only one sex, was found by Hammerling (1931). The alga also multiplies asexually by aid of zoospores liberated from the cysts as well (Puiseux-Dao, 1970). Little plants which derive from direct germination of the cysts are also known to occur.

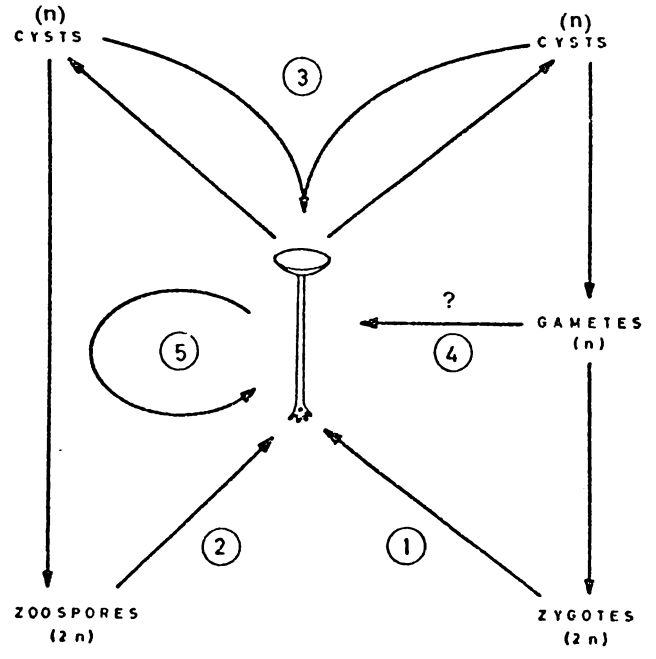

Fig. 2.1.2. Scheme showing the different possible types of reproduction of *Acetabularia mediterranea* 1. by gamete fusion ; 2. by zoospore formation; 3. by cyst germination; 4. by gamete parthenogenesis; 5. by germination of basal cytoplasm. (After Bonotto, et.al., 1976).

2.2 Culture Medium and Physical Conditions.

The first successful laboratory culture of *Acetabularia* was established by J. Hammerling and his colleagues in 1926 (Hammerling, 1931). The growth medium was artificial sea water supplemented with the undefined Erd-Schreiber solution (Hammerling, 1931, 1963). A few attempts have been made to grow *Acetabularia* in purely synthetic media (e.g. Keck, 1964 ; Shephard, 1970), but these have not been very successful (Puiseux-Dao, 1970). Recently, Schweiger and his colleagues have presented a completely defined synthetic medium that fulfils the requirements of *Acetabularia* cells to at least the same extent as the undefined Erd-Schreiber medium. Furthermore, cells grow excellently in a flow-through system containing unsupplemented sea water. (Schweiger, et.al., 1977).

The medium that was found suitable for the present work is the modification of Hammerling's original medium (Lateur and Bonotto, 1973). It is called AE 50 by C.C.A.P. (Culture Centre of Algae and Protozoa, Cambridge, England), who supplied the recipe and the original stock culture of *A. mediterranea*. AE 50 consists of two equal main parts, ASP 2 and Erd-Schrieber solutions. The preparation of this medium is described in detail in Appendix I.

Shephard's purely synthetic medium (Shephard, 1970), was tried without success, the cells remaining alive but exhibiting very little growth.

Important factors of culture conditions, in addition to an adequate growth medium, are temperature and light. Usually, *Acetabularia* is cultured at a temperature ranging from 18 to 25°C, preferably at 21 ± 1°C. with an alternating light/dark rhythm of 12/12 hours, the light source supplying 1,000 to 3,000 lux (~ 10 - 30 watts/m^2.).

A temperature higher than 30°C is noxious, and the plastids of

Acetabularia become yellow and the membrane strongly calcified. On the other hand, below 10°C growth is stopped and the protoplasm of the algae contracts within the siphon, where it remains in a dormant state until conditions become favourable again. However, optimum culture temperatures can also favour the growth of contaminations.

Small amounts of light, less than 10 watts/m^2., could cause the cells to grow very slowly. The more light (the more energy) they receive, the more quickly *Acetabularia* grow, the more rapidly they form fertile caps, and the shorter are the stalks which carry them. For very high intensities, more than 100 watts/m^2., however, the rate of development is again reduced.

The spectrum of the light can affect the development considerably. Continuous red light tends to reduce the rate of development to nearly nil, but normal development is resumed when the blue light is applied (Puiseux-Dao, 1970).

In practice, the cells are cultured in one litre Roux flasks, each containing about 400 ml of AE 50. The number of cells in the flask depends on the sizes of the cells (see Section 2.3). Up to sixteen culturing Roux flasks are kept in a wooden cabinet and partly immersed in a circulating water bath where the temperature is kept constant at 21 ± 1°C. The temperature is controlled by a regulated water bath heater in conjunction with a continuously operating cooling unit made from a domestic refrigerator.

The cabinet (Fig. 2.2.1) is reasonably light-tight but well ventilated. It has two sections of the dimensions 45 × 75 × 50 cm^3, one of which is normally kept dark and at a lower temperature for long term storage. The illumination is given by two 65 watts, no. 55 daylight, Thorn fluorescent lamps. The lamps are about 250 mm above the mouths of the Roux flasks and about 450 mm above the water level in the

Fig. 2.2.1. Diagram of Culture Cabinet.

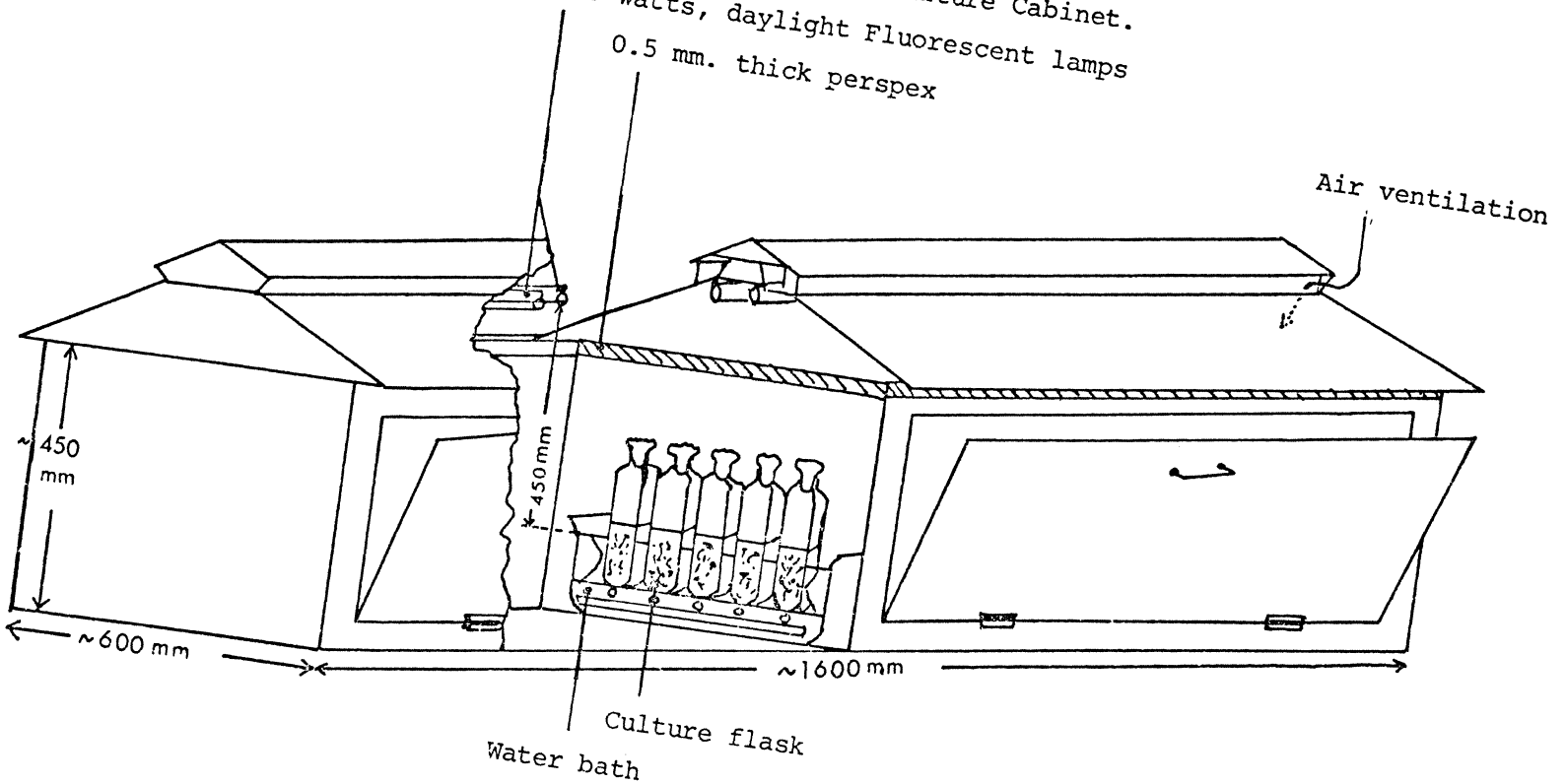

bath. The water bath level is always brought up to the level of the medium in the flask to ensure an even temperature. The light passes through a 0.5 mm thick white perspex sheet and gives a measured intensity of about 2,000 lux (20 watts/m^2) at the water level in the bath.

An interesting observation was made concerning the effect of agitation of the growth medium on the development of the cells. If under good culture conditions the culture flask was shaken for 2 min. once a day for several weeks, the size of the cells and the caps in that flask were larger (by up to 30%) than those in a similar but unshaken flask. This observation may have been confirmed now by Schweiger, et.al. (1977).

During the growth period, a number of culture conditions can be modified to accelerate or to slow down the development. Richer medium, more light intensity, pumping medium through cells, and optimum temperature can help cells grow faster. Under proper culture conditions, the life-cycle can be shortened to as little as a third of the normal time, which is about six months (Schweiger, et.al. 1977). Normally it takes 4 - 7 months, under the general standard laboratory culture conditions, for a very young cell to develop to a mature one.

2.3 Culture Maintenance.

When a cell reaches its maturity, the nucleus begins to divide to produce thousands of nuclei which migrate from the rhizoid into the cap. This is indicated by the loss of colour in the stalk as cytoplasm migrates into the cap as well. When this cap maturation process, which takes about 6 weeks, is complete, the mature cap is full of round cysts. The dormant period then starts and mature caps are generally harvested. This is the best stage at which to transport them. Indeed, the cysts (*A. mediterranea* and *A. crenulata*) normally survive several months or even a year or more. However, the healthier the culture, the shorter is this dormant period, which may even be lost. For normal duration of the dormant period, the reproductive caps should be kept in the dark at a low temperature (about 6 to 16°C); they should be exposed to light for twelve hours a month to avoid the degeneration which may set in if they are kept too long in the dark (Shephard, 1970).

Cysts are more resistant to mechanical, osmotic and chemical treatments than cells and this stage offers the best possibility for ridding the culture of contaminant organisms (Keck, 1964; Shephard, 1970). Before the treatments, the selected mature caps [1] are kept in the dark for 12 - 15 weeks to ensure maturation of cysts (Koop, 1975). Then the cysts are released from the rays of the caps by some physical means, e.g. cutting the cap, blotted between two layers of sterile filter papers, into small pieces (Lateur and Bonotto, 1973). The cysts now are ready for decontamination treatments (see also Gibor and Izawa, 1963;

---

(1) Since the reproductive potential of one *Acetabularia* cell is about 10,000 new young cells, only a small percentage of the cells is needed to be carried on to maturity. However, selection for healthy and normal cells at the late growth phase should be done to ensure a large safety margin.

Schweiger,et.al., 1977), or stored in the dark at low temperatures for future use.

There are various techniques suggested to initiate cyst germination. In order to facilitate the liberation of zoids from the cysts, they can be treated with osmotic shock, by putting them for a few minutes in distilled water, or thermal shock by slightly heating the medium (Puiseux-Dao, 1970). Germination may be simply obtained within two days from mature cysts which are kept in dark or within four days from cysts exposed to light (Koop, 1975). Generally this process is done by keeping the mature cysts alternatively in dark and light 2 and 5 days respectively (Lateur & Bonotto, 1973; and Appendix 2). When the lid of the cyst bursts and the zoids are liberated, a clound of flagellate elements showing positive phtotactism is obtained. It is preferable to have the culture wrapped up in black paper for 24 hours in order to encourage uniform distribution of germination. At this stage, the culture should have the medium renewed and should be kept 10 days in an alternating 12/12 hours, light/dark rhythm, at 21 ± 1°C, at which temperature the cells are cultured during the entire growth phase. As the cells are young, renewal of the medium is required approximately once in every five days three times, then monthly until the cells are fully grown. Before the mature caps are harvested, the culture should have the medium changed once in every three days three times (see Appendix 2 for details and procedures).

To ensure a continuous experimental cell supply, when the cells of the first generation of *A. mediterranea* of this work were about 2 - 3 mm long, they were separated into three batches; A, B and C. Batch B was cultured according to the procedures detailed in Appendix 2. Batch C was kept in sterile pure sea water, in dark at room temperature (20 ± 5°C), exposing to light 12 hours/month, and with the sea water changed monthly.

The growth rate of batch C was retarded considerably. Batch A was cultured in AE 50 supplemented with double strength of soil extract, the medium to cell ratio was also doubled and it was changed every two weeks. The flask was shaken once a day during that period. The growth rate of this batch was accelerated considerably. The experiments were started with cells in batch A, then B. As soon as batch A was used up, batch C was cultured as was done for batch B, the standard culture maintenance procedures - Appendix 2.

It is difficult to obtain and culture axenic cells (Koop, 1975). Although the decontamination processes using chemical treatments (listed in Shephard, 1970) were tried, a simpler treatment was found sufficient in this work. The mature cysts were kept in sterile pure sea water, in the dark, at 10 ± 1°C for a month. They were then exposed to light for 12 hours, the sea water was renewed, and returned to the same condition for another month with the sea water being changed weekly. The contaminations in the culture treated by the above process were found to be negligible. However, it is essential at any stage of the culture that the medium should be renewed at least once a month.

2.4 Specimen Preparation.

The cells used in these studies were those which had entered the late growth phase stage, i.e. while they were forming whorls and young caps (see stages 7 and 8 in Fig. 2.1.1). They were aged 4 - 7 months after germination. The stalks were approximately cylindrical, 20 to 30 mm long, and 0.20 to 0.40 mm in diameter.

An isolated stalk segment (ISS) was prepared by modifying the cutting procedures used by Novak and Bentrup (1972a). The reasons for this are given in Section 1.2. It was done by hooking a number of cells into a sterile plastic dish containing > 2 ml of AE 50 per cell. About 2 - 3 hours later, the apices were cut off first by using a pair of aseptic sharp scissors or a slightly flamed razor (which was more satisfactory). The resulting basal stalk segments (BSS's) were then kept floating horizontally in the same petri-dish at room temperature (20 ± 5°C) and in the dark for 6 days. Then the rhizoid containing the nucleus was cut off to give an approximate cylindrical ISS with the length that suited the cell holder (14.25 ± 1.5 or 24 ± 0.75 mm, see Section 4.2). These ISS's were kept in the dark at room temperature for another 24 hours. The best specimen was chosen to be transferred into the cell holder after being kept in the petri-dish for about 12 hours. The experiments were started in the dark (cabinet) for 8 - 12 hours before the light was turned on to elicit the redevelopmental processes.

A single cut specimen (BSS or ASS) was prepared by cutting the apices or rhizoids respectively off a number of cells which had been kept in fresh medium, in a petri-dish, in normal room conditions, for 24 hours. The remaining segments were kept in the same conditions for another 2 - 24 hours, until the best specimen had recovered. Then this specimen was transferred into a cell holder and the experiment was

commenced.

During the specimen preparation, only sharp cutting tools were used (to avoid damaging the cut ends) with a minimum movement. The movement of either the medium or the cut cells was found to cause the loss of turgor pressure in the cells. Consequently they became floppy and clear patches were formed at the ends. The slight movement might result in the formation of the transverse bands of chloroplasts as described by Sironval, et.al. (1977).

For an experiment where the internal membrane potentials were investigated, i.e. micropipettes were to be inserted into a normal cell, it was hooked into the open cell holder type A, (see Fig. 4.2.3a). It was held firmly, without squeezing, by a piece of rectangular perspex near the point of electrode insertion. This clamp was released after the micro-pipettes were introduced. The insertion was facilitated by the use of a micro-manipulator.

CHAPTER 3

IONIC RELATIONS AND ACTION POTENTIAL IN *Acetabularia mediterranea*.

3.1 Membrane Concept.

A biological membrane can be defined in simple terms as tenuous partition or interface between two phases of the substance of the cell, or between the cell and its environment.

Membranes are essential in the organisation of cell structure and function. Prokaryotic organisms (bacteria and blue-green algae) do not have a defined nucleus. They have an external plasma-membrane, but further differentiation of membrane systems within the cells is limited. In eukaryotic cells (cells of animals, plants, fungi, and protista) there is usually a variety of cytoplasmic organelles with structures which involve membranes (Fig. 3.1.1). A plasma-membrane (also known as cytoplasmic or cell surface membrane) may exist alone or be a part of a more complex cell surface structure. Within cells the membranes delineating compartments are different in their quantity and complexity depending on the type of cells. It is believed that there is a considerable degree of functional continuity between different intra-cellular membranes and between these and the plasma-membrane.

The thickness of the cell membrane as seen in the electron microscope varies between 8 to 9 nm. It has an identifiable characteristic trilamellar feature as pairs of closely spaced, and generally continuous, parallel dense lines separated by a less dense region (see Fig. 3.1.1).

Most membranes are composed principally of 50% to 60% proteins and 50% to 40% lipids. The lipids include phospholipids, neutral lipids, cholesterol and glucolipids. Membrane proteins can be classified in two categories: the extrinsic (peripheral) proteins which are loosely

Fig. 3.1.1. Cell Structures of Prokaryotic and Eukaryotic organisms. (After Finean et.al., 1974).

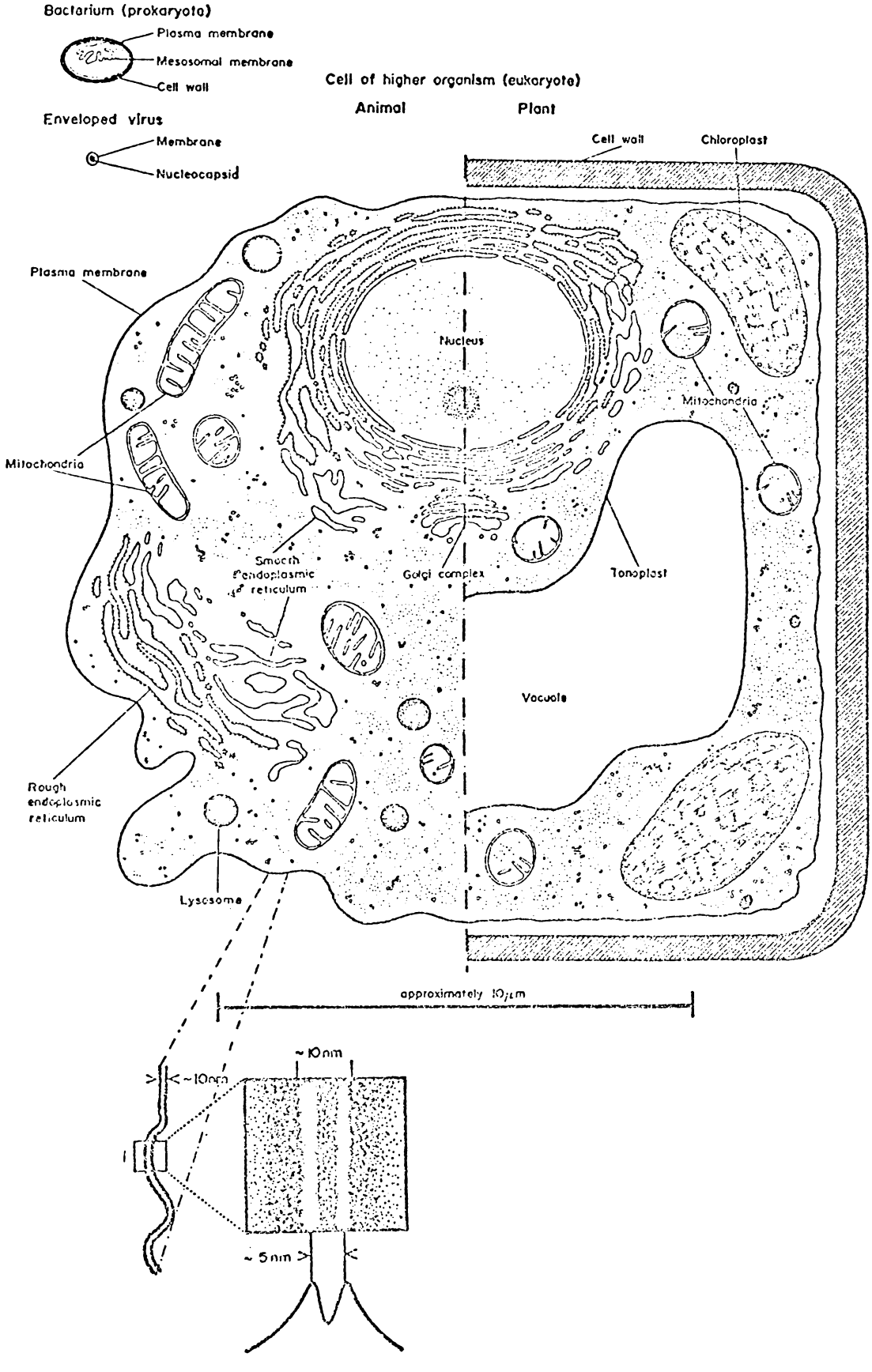

attached to the membrane surface, and the intrinsic (integral) proteins which make up 70% or more of the total membrane protein and are very tightly bound to the lipid portion (Lehninger, 1975).

There is evidence that these components may be arranged in a highly ordered fashion. The most satisfactory model of the membrane structure to date appears to be the lipid-globular protein mosaic model (the fluid mosaic model; Fig. 3.1.2; see also Lehninger, 1975; White, et.al., 1978). The phospholipids of membranes are arranged in a bilayer to form a fluid, liquid-crystalline matrix or core. In this bilayer individual lipid molecules can move laterally, endowing the bilayer with fluidity, flexibility, and a characteristically high electrical resistance and relative impermeability to highly polar molecules. The membrane proteins are globular and asymmetric in structures. Each of them has one polar end and one non-polar end which is embedded in the fluid lipid matrix. Some are partially embedded, others are completely buried in it.

The surface membrane of the cell, particularly important in its structural role in maintaining the integrity of the cytoplasm, is also able to control or influence the passage of a wide range of materials into and out of the cell. Among the enzymes associated with the cell surface is adenosine triphosphatase (ATP-ase) which releases energy required to drive the electrogenic pump(s), an ionic transport system which is located in the cell membrane and is thought to be essential for the maintenance of the normal membrane potential of the cell. In otherwords, the normal membrane potential, so-called the resting potential, is maintained electrically negative with respect to the environment by both the selective diffusion of the ions between the cytoplasm and the medium through the cell membrane and the active pumping process at the membrane to import or export ions between those two fluids. This is discussed further in Section 3.2.

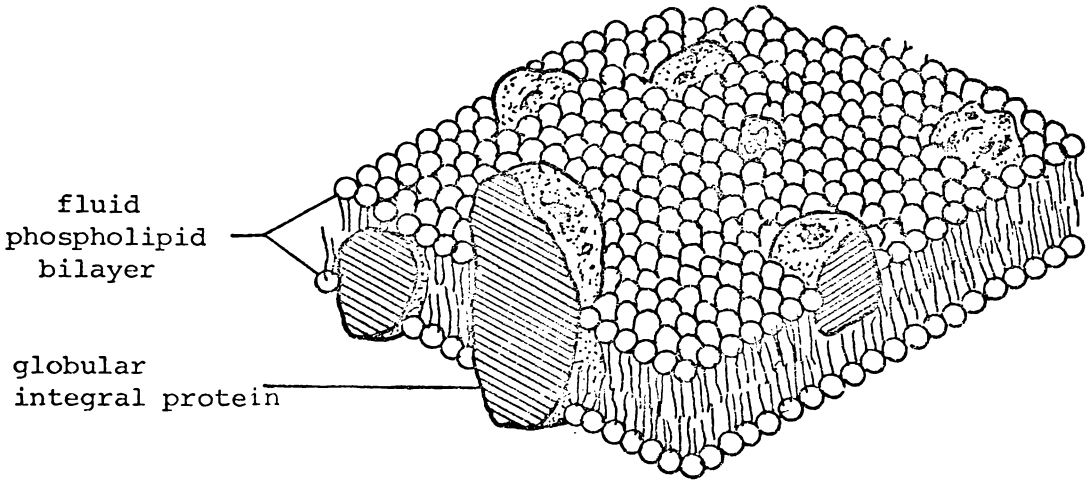

Fig. 3.1.2 Schematic three-dimensional and cross-sectional view of the fluid mosaic model of the membrane structure. (After White, et.al., 1978).

One of the most important properties of the membrane is that, in response to some kinds of stimulation, it can adjust its pores (or channels or gates) to close or open for certain specific ions. The resulting ionic currents may change the membrane potential, making it electrically less negative or even reversing its polarity. In such states the cell is said to be depolarised or reverse-polarised respectively. In many cases a stimulus exceeding a certain threshold will give rise to a large depolarisation followed by a repolarisation. The resulting 'spike' in the membrane potential is known as an Action Poteneial (AP) and is discussed in Section 3.3.

In a cylindrical cable-like cell, such as nerve and muscle fibers and certain giant algal cells, e.g. *Nitella* and *Acetabularia*, during the generation of an AP the cytoplasmic current in the active region flows into and excites the adjacent inactive membrane to depolarise and so spread the depolarisation along the cell. This non-decremental propagating signal is known as a propagating AP and is discussed in Section 3.4.

Two special problems about the concept of the plasma membrane potential in plant cells need to be mentioned here. The first concerns the complication of non-uniform ionic concentration in the cytoplasm due to the presence of cytoplasmic organelles. This arises because of the capability of the active transport of the organells; the differences in various organelles may arise because of concentrations of diffusible and indiffusible ions; and the cytoplasm itself is not homogeneous. This is a considerable difficulty, for example, in the concept of ion concentration in the cytoplasm because of the presence of complex plane and tubular membrane systems (Hope and Walker, 1975). The p.d. (potential difference) between the cytoplasm and the medium may not reflect the p.d. across the plasma-membrane itself because we do not

know exact ionic composition of cell walls under various conditions, and thermodynamic equilibrium is not obviously satisfied.

The second problem arises because the measured membrane potential is the sum of two components: the wall p.d. and the plasma-membrane p.d.. Several attempts to measure a wall p.d. under various conditions in *Charophyte* cells (e.g. *Chara* and *Nitella*) have been reported (listed in Table 5.1, p. 59, Hope and Walker, 1975). However, the wall p.d. in *Acetabularia* has not been studied so far. In this work p.d. across both cell wall and the plasma-membrane, i.e. the p.d. between the cytoplasm and the external growth medium, is regarded as the membrane potential. Also the complication of the non-uniform ionic distributions in the cytoplasm is not specifically considered in the simple treatments described in this chapter.

3.2 Resting Membrane Potential and Ionic Relations.

3.2a The Nernst Equation.

This well known equation is extremely useful in describing the p.d.'s appearing at the boundaries between two electrolyte solutions in simple physical terms. Its original derivation is based on the principles of simple reversible thermodynamics (Katz, 1966) that the condition of electrochemical equilibrium of the two solutions separated by a membrane is governed by the electrical work (required to move a small quantity of ions across the boundary) and the osmotic work (required to move the same quantity of the opposite direction).

Suppose, for example the electrolyte solutions on either side of an ion selective membrane (permeable only to potassium ions) are potassium salts with concentrations k_1 and k_2, and let $k_2 = 10k_1$. The electrical work (W_e) required to transfer 1 mole of potassium against the potential difference, E, is EF, where F = charge per mole of univalent ion, i.e. Faraday constant. Hence

$$W_e = EF \tag{3.2.1}$$

The osmotic work (W_o) required to move 1 mole of potassium from the lower concentration (k_1) to the higher (k_2) is considered as the analogous mechanical work (W_m) done in compressing 1 g. equivalent of an ideal gas reversibly to $\frac{1}{10}$ of its original volume. If this is done extemely slowly and isothermally in a cylinder with a movable piston which is exerted by a pressure (p) and the volume of gas (v) changes gradually from v_1 to v_2, this work done is given by

$$W_m = \int_{v_2}^{v_1} p \, dv \tag{3.2.2}$$

By the gas law,

$$pv = RT. \tag{3.2.3}$$

(R = universal gas constant, T = absolute temperature).

Substituting $p = \frac{RT}{v}$ in eqn. (3.2.2) we obtain

$$W_m = RT \int_{v_2}^{v_1} \frac{dv}{v} = RT \ln \frac{v_1}{v_2} \tag{3.2.4}$$

This result is exactly applicable to the osmotic work done in moving solute molecules from a lower to a higher concentration. If this is done reversibly, W_o is given by

$$W_o = RT \ln \frac{k_2}{k_1} \tag{3.2.5}$$

When this procedure establishes an equilibrium potential that just balances the 'diffusion pressure', we obtain,

$$W_e = W_o \quad , \quad \text{or}$$

$$EF = RT \ln \frac{k_2}{k_1} \quad ,$$

$$\text{i.e.} \quad E = \frac{RT}{F} \ln \frac{k_2}{k_1} \quad . \tag{3.2.6}$$

Equation (3.2.6) is known as the Nernst equation.

For an ion of charge z, the general Nernst equation is given by

$$E_{21} = \frac{RT}{zF} \ln \frac{C_2}{C_1} \tag{3.2.7}$$

where C_2 and C_1 are concentrations (strictly activities) of the ion on either side of a permeable boundary.

In the more complex general case when there are several ionic species involved we can compare the Nernst potential given by Eqn. (3.2.7) for each ion with the measured membrane potential. If the values

are not equal (the usual case) then that ion is not in equilibrium and will be subject to a net driving force across the membrane i.e. the system will slowly 'run down' in the absence of any active maintenance of the ionic concentrations.

With a membrane boundary having different permeabilities (conductivities) for several different ionic species the membrane potential will lie between the extreme values of the various Nernst potentials, and can be calculated using the simple electrical equivalent circuit given in Fig. 3.2.1.

Examples of the calculation of membrane potentials for various model situations are given in Katz (1966) p.51-53.

3.2.b Resting Membrane Potential in Squid Axon.

Since it is probably the most studied and best understood biological system the squid axon will be taken as an example to illustrate the application of the above ideas. In Table 3.2.1 the experimentally measured concentrations of the three main diffusible ions, Na^+, K^+ and Cl^-, in the cytoplasm and in the external environment are given. In Fig. 3.2.2 the Nernst potentials for each of three ions (calculated using Eqn. 3.2.7) is shown on a potential energy diagram. Also shown is the resulting driving potential $V_m - E_i$ for each ion, where V_m is the experimentally observed resting membrane potential.

During the steady state, the nerve cell membrane is more selectively permeable to K^+ ion than others (Table 3, p.59, Katz, 1966) which implies that the conductance of K^+ channels is much greater than the Na^+ and Cl^- channels. This is borne out by experiments in which the external K^+ concentration is changed and the resulting change in V_m is in good agreement with the Nernst equation (Hodgkin and Keynes, 1955; and Adrian, 1956).

Even though the channel conductances of Na^+ and Cl^- ions

Fig. 3.2.1

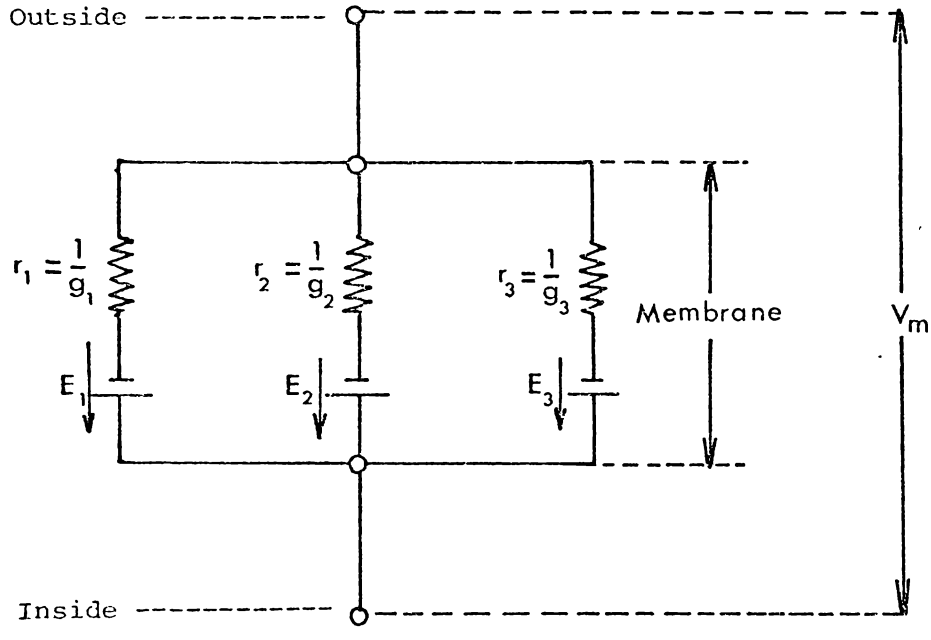

E_i = Nernst potential of ionic species i

$$= \frac{RT}{z_i F} \ln \left(\frac{C_i^{in}}{C_i^{out}} \right)$$

z_i = charge of ionic species i

C_i = concentration (activity) of ionic species i.

$r_i (g_i)$ = resistivity (conductivity) of channels for ionic species i.

TABLE 3.2.1.

CONCENTRATIONS ($^{mM}/_{\ell}$) OF MAJOR IONS IN THE CYTOPLASM AND THE EXTERNAL MEDIUM, THEIR NERNST POTENTIALS (E_i), AND THE OBSERVED RESTING MEMBRANE POTENTIALS (V_m) IN SQUID AXON AND *Acetabularia*. (Modified from Katz, 1966 and Saddler, 1970a).

Ion	Squid Axon			*Acetabularia*		
	Medium	Cytoplasm	E_i/mV	Medium	Cytoplasm	E_i/mV
Na^+	460	50	+55	470	60	+51
K^+	10	400	-92	10	400	-92
Cl^-	540	70	-51	550	490	-3
V_m	-60 mV			-170 mV		

Fig. 3.2.2. Potential Energy Diagrams Showing Nernst Potentials (———) Potential Driving Passive Leakage (----), and Passive Pathways of Major Ions of Squid Axon and *Acetabularia*. (Modified from Katz, 1966 and Saddler, 1970a)

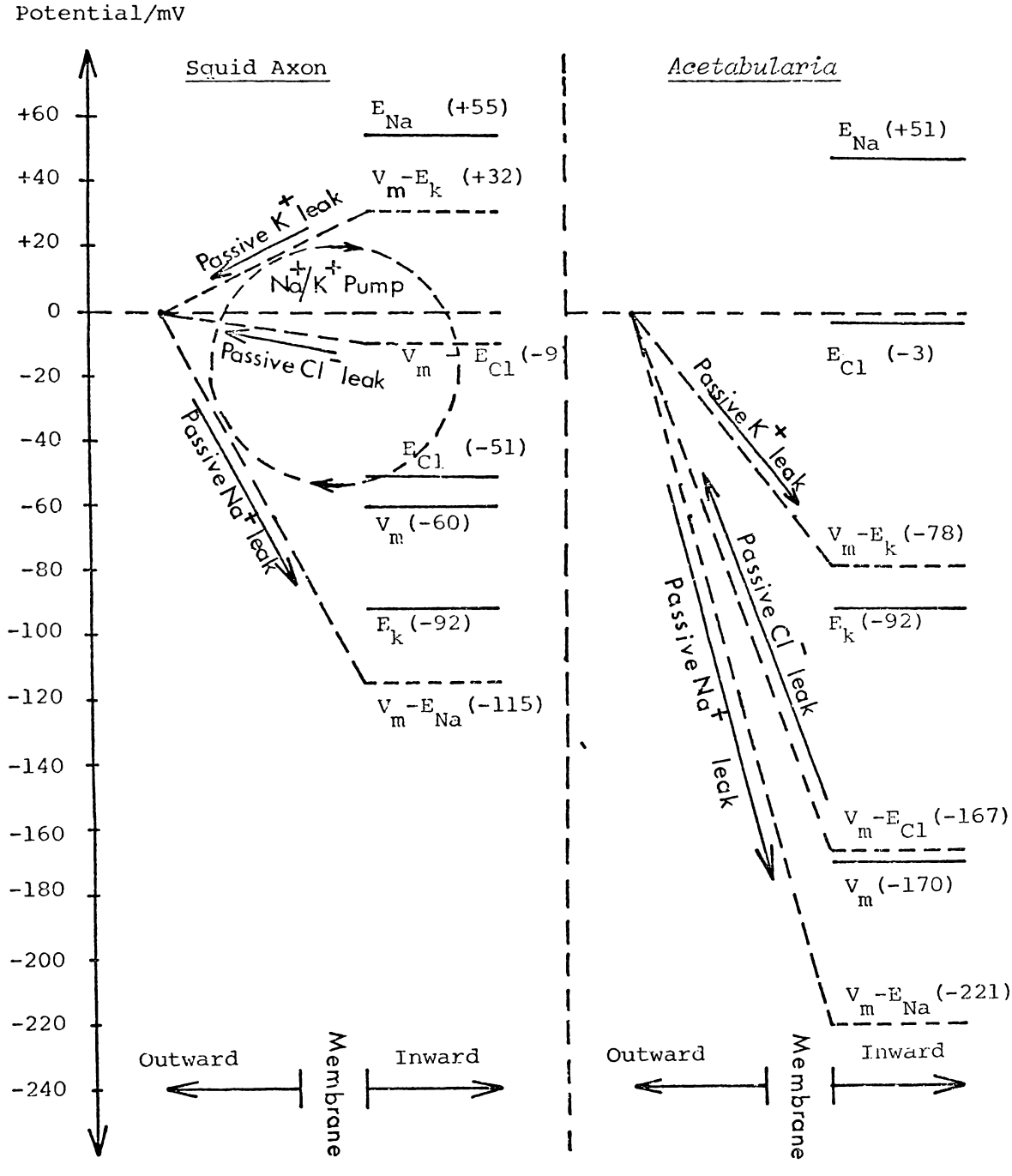

are small there will be an inevitable passive diffusion of Na^+ into the cytoplasm and Cl^- out of it. This is also a passive outward diffusion of K^+. For the cell to maintain its ionic concentrations these fluxes must be counterbalanced by some metabolically driven active transport mechanism. The details of this are not known but there is some evidence to suggest that there is a 'coupled pump' which exports one Na^+ ion for every K^+ ion it imports (p.65, Katz, 1966).

V_m is usually measured directly (Section 3.2d) but it can be estimated by the diffusion equation, concerning the movements of the ionic species through the membrane, proposed by Goldman (1943) and Hodgkin and Katz (1949). Recently a new theoretical analysis taking account of the surface potentials due to the membrane possessing fixed charges has been proposed by Ohki (1979). It is clear that this fact needs to be taken into account since experimentally measured membrane potentials are usually only in approximate agreement with the calculated value using the Goldman-Hodgkin-Katz model. However, this model still gives valuable insights into the relation between changes of channel conductivity and membrane potential.

3.2c Resting Membrane Potential in *Acetabularia*.

Like most of the algal cells, the membrane of *Acetabularia* is permeable by three major ions; K^+, Na^+ and Cl^-. The differences of the ionic concentrations of these ions between the cytoplasm and the environment (Table 3.2.1) give rise to the consequent Nernst potentials and ionic driving forces shown in Fig. 3.2.2.

The two largest ionic driving forces for Na^+ and Cl^- ions in *Acetabularia* suggest two active pumps; an outward transport of Na^+ and an inward transport of Cl^-. This is in common with the great majority of plant cells. The function of these pumps is to import Cl^- ions and export Na^+ to maintain the resting membrane potential during

the steady state.

Owing to the high measured resting membrane potential ($V_m \simeq -170$ mV) of *Acetabularia*, higher than any Nernst potentials (for the major ions), it has been suggested that H^+ ions may be actively expelled (Saddler, 1970a). However variation of the external applied pH from 4 to 9 was found to have no effect on the resting membrane potential (Gradmann and Klemke, 1974). This means the H^+ permeability is so low that it can be ignored from the electrical point of view.

So far, no ion other than K^+ and Cl^- in the external medium has been reported to affect the resting membrane potential of *Acetabularia*, i.e. it is mainly controlled by the electrogenic (active) pump of Cl^- and the passive diffusion of K^+ ions. However, it is clear that our understanding of the *Acetabularia* membrane is far from complete and the simple models developed to date must be used with caution. Almost certainly the discrepancy arises from the presence of large fixed changes in the membrane as discussed above (Ohki, 1979).

3.2d Experimental Measurement of the Membrane Potential.

The internal resting membrane potential, V_m, of a cell can be measured directly by inserting a micro-electrode through the membrane into the cytoplasm. A second electrode is left in the external salt medium. In general V_m is maintained at a steady level, negative with respect to the external medium, so long as the microelectrode tip remains inside the cytoplasm without blocking and provided that no stimulus is applied to the cell.

There are two kinds of microelectrodes, metal and glass-micropipette. The latter, most frequently used in measurements of the absolute membrane potential, consists of a small glass tube with one end pulled down to a diameter, at the tip, of less than 1 μm. The tube is filled with an electrolyte, generally saturated or 3M KCl and electrical contact

is made via an Ag/AgCl or a similar type of reversible electrode (see e.g. Adrian, 1956; Frank and Becker, 1964; Lavallée,et.al., 1969; and Ferris, 1974).

A pair of glass microelectrodes immersed in a common medium may produce a non-zero p.d. owing to some assymmetry in the system. However with careful fabrication of the electrodes this can usually be sufficiently small and free from drift to be ignored.

Electrodes of this kind can also be used for stimulating the cell by connecting them to a suitable current source. This technique enables measurement of electrical properties of the membrane to be made (see e.g. Gradmann, 1975, 1976).

Owing to the fact that the cell wall of *Acetabularia* that holds the liquid cytoplasm is thick and made up of solidified compounds (see e.g. Puiseux-Dao, 1970; Saddler, 1970a) the insertion of a glass micropipette can easily damage the cell and the tip of the pipette is invariably found to be broken by the time it has been inserted into the cytoplasm. In addition the turgor pressure is lost at the time of penetration (Hope and Walker, 1975). Due to the broken tip there is a relatively large diffusion of electrolyte from the pipette into the cytoplasm. 'Clear patches' become apparent in the cytoplasm within a few hours and the cells rarely survive for > 15 hours. Thus the use of micropipette electrodes is very restricted with this organism and they are completely unsuitable for long-term investigations. However, since they provide the only method of measuring the absolute membrane potential then use is unavoidable, but must be restricted to short-term measurements.

Fabrication and related practical details are given in Appendix 3.

3.3 The Action Potential in *Acetabularia*.

In the normal resting state, the membrane potential, V_m, of a cell is directed so that the inside is negative with respect to the outside. When the magnitude of the membrane potential, $|V_m|$, is reduced in some region, by electric current stimulation for example, so that V_m becomes less negative the membrane in that region is said to be depolarised. Changes in the membrane potential in adjacent regions produced by such depolarisations can be classified into three levels according to the strength of the stimulus. These are (i) a passive electrotonic potential, (ii) an active local response, and (iii) an AP. (see Fig. 3.3.1).

Mainly, the amplitude of an electrotonic potential is a linear function of the stimulating current strength. It rises and falls exponentially (determined by the membrane time constant). In contrast the generation of either a local response or an AP causes the membrane impedance to fall considerably. The relationship between the applied current and the response potential is non-linear. (For further details of the similarities and differences of these three potential changes, see Khodorov, 1974).

The global properties of an AP in both animal and plant cells are similar in many aspects (Hope and Walker, 1975) and so it is worth considering briefly the mechanism of AP generation in squid axon, a much studied animal system. Considering only the three main ions, the membrane equivalent electric circuit model can be given as in Fig. 3.3.2. The mechanism of the changes of the membrane potential during an AP can be well explained in terms of this model by the theory of Hodgkin and Huxley (1939). It can be analysed in terms of three processes (Katz, 1966):

(i) The increase of Na^+ permeability.

Fig. 3.3.1.

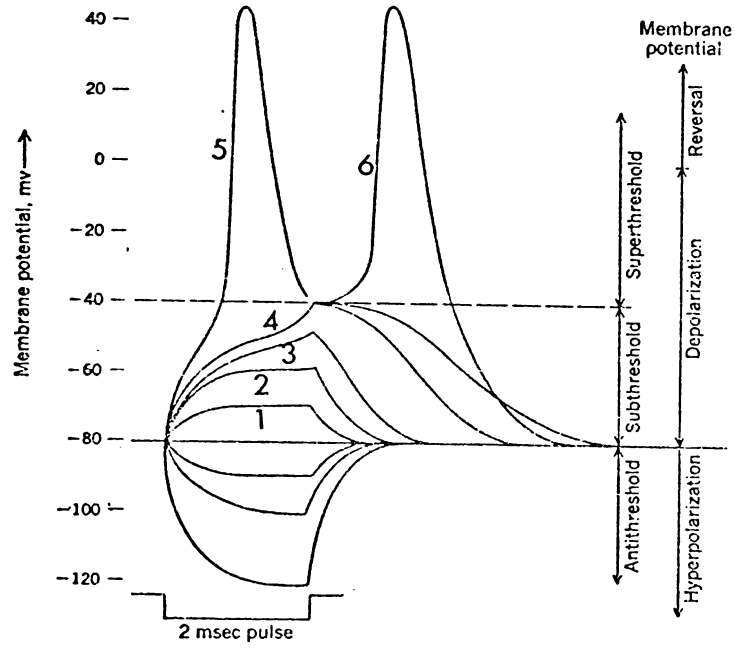

Variations of reponses in membrane potential produced by current pulses of fixed duration (indicated below) but variable size and polarity:

Curves 1 & 2: are passive electrotonic potentials produced by weak current pulses;

Curves 3 & 4: are active local responses produced by current pulses approaching the threshold level.

Curve 5: is an AP produced by a current of threshold strength.

Curve 6: is an AP produced by local responses.

(After Katz, 1966).

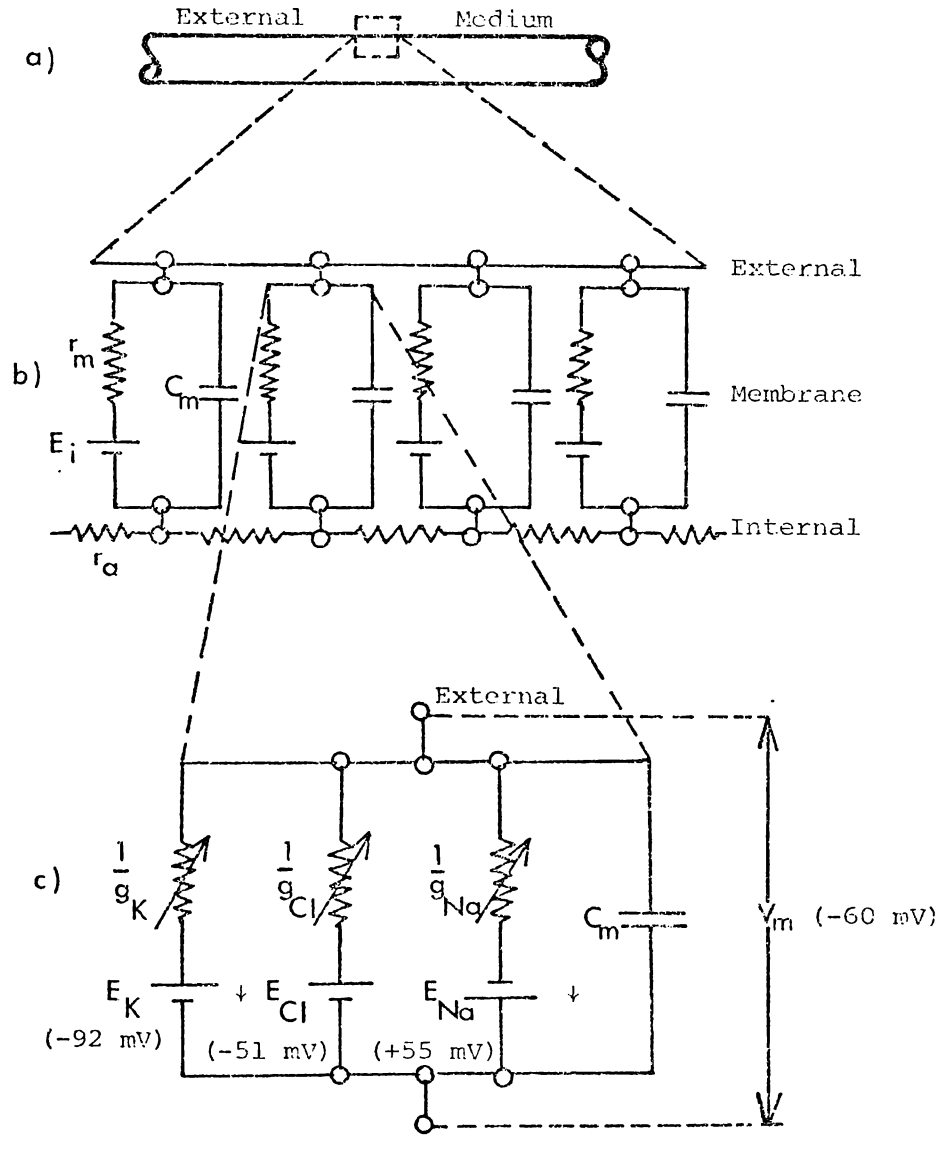

Fig. 3.3.2. The Cable Model of a Nerve Fiber.

(a) Representation of squid axon fiber,
(b) Its electrical analog, and
(c) Equivalent circuit of unit membrane.

r_m = Membrane resistance

C_m = Membrane capacitance

r_a = Cytoplasmic resistance

E_i = Ionic Nernst potential

g_i = Ionic membrane conductance.

At normal resting potential, Na^+ conductance, g_{Na} is very small, but it increases when $|V_m|$ is lowered. As a result, Na^+ ions will enter the cell at an increased rate and, by carrying their positive charge across the membrane, will reinforce the initial lowering of the resting membrane potential. This in turn causes the Na^+ permeability to increase further. Thus the process becomes self reinforcing once the threshold level is reached. The potential change (and the coupled increased g_{Na}) will increase rapidly and displace the membrane potential to $\simeq$ + 40 mV, toward Nernst potential for Na^+ (Fig. 3.3.3).

(ii) The decline of Na^+ permeability.

When the cytoplasm acquires sufficient positive charge to balance the chemical potential gradient of Na^+ ions, the Na^+ permeability begins to decline, i.e. the Na^+ gates close and g_{Na} becomes small again.

(iii) The increase of K^+ permeability.

At the same time as (ii), the K^+ conductance, g_K, begins to increase, reaching a peak when the Na^+ gates have closed. This accelerates the return of the system (repolarisation) to the resting condition, i.e. the initial level of potential, ionic concentrations and excitability.

The mechanism of generation of an AP in *Acetabularia* is relatively much more complicated and is by no means as well understood as in nerve cells. In Fig. 3.3.4 a membrane equivalent circuit proposed by Gradmann (1975) is shown and the evidence is clear that the large effluxes of Cl^- and K^+ ions are coincident with the occurrence of an AP (Gradmann, et.al., 1973; Mummert and Gradmann, 1976; see also Fig. 3.3.5). These two fluxes cause the depolarisation and the repolarisation respectively. This is the same situation as observed in other algal cells, for example *Nitella* (Mullins, 1962). However in *Acetabularia* the

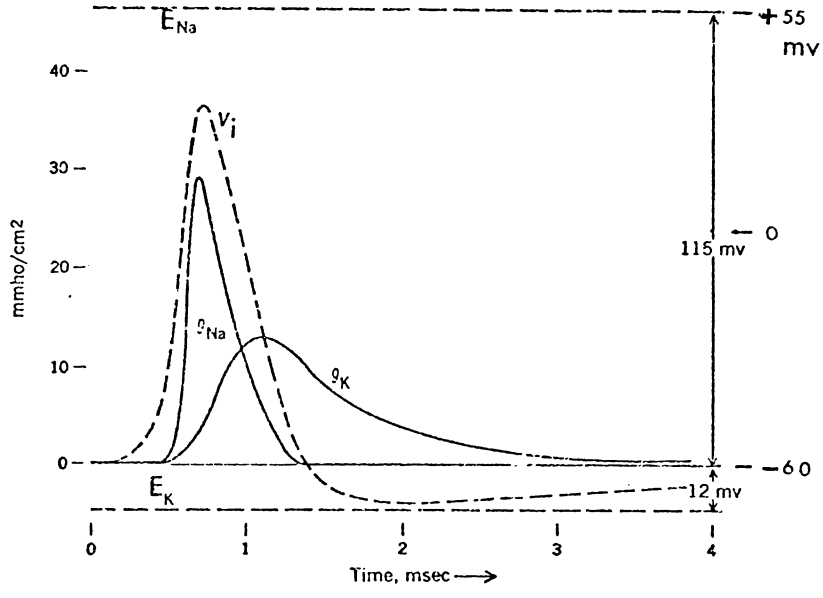

Fig. 3.3.3. Theoretical reconstruction of a propagated action potential (curve V_i) and sodium and potassium conductances, using experimental constants appropriate to 18.5°C. Total calculated entry of sodium = 4.33×10^{-12} mole/cm^2; total loss of potassium = 4.26×10^{-12} mole/cm^2. Calculated velocity of propagation = 18.8 m/sec (observed velocity = 21.2 m/sec). (From Hodgkin and Huxley, 1952).

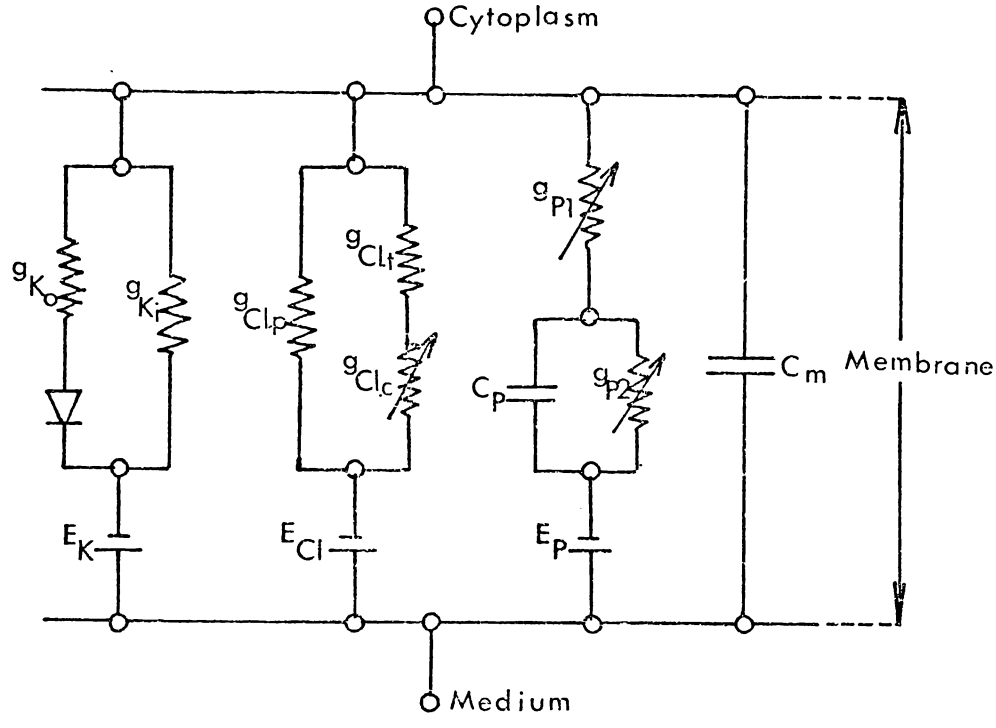

Fig. 3.3.4. Detailed analog circuit of *Acetabularia* membrane. (After Gradmann, 1975).

g_{Ki}	(inward K^+ conductance)	15 μmho cm^{-2}
g_{Ko}	(outward K^+ conductance)	600 μmho cm^{-2}
$g_{Cl.p}$	(Cl^- conductance of plasmalemma)	12 μmho cm^{-2}
$g_{Cl.t}$	(Cl^- conductance of tonoplast)	1 μmho cm^{-2}
$g_{Cl.c}$	(Cl^- conductance of cytoplasm)	500 μmho cm^{-2}
E_K	(K^+ Nernst potential)	-90 mV
E_{Cl}	(Cl^- Nernst potential)	0 mV
E_p	(e.m.f. of the active pump)	-190 mV
C_m	(membrane capacitance)	5 μf cm^{-2}
C_p	(a quasi-capacitor)	3000 μf cm^{-2}

Fig. 3.3.5. Coincidence between the AP Generation and the Effluxes of K^+, and Cl^- ions.

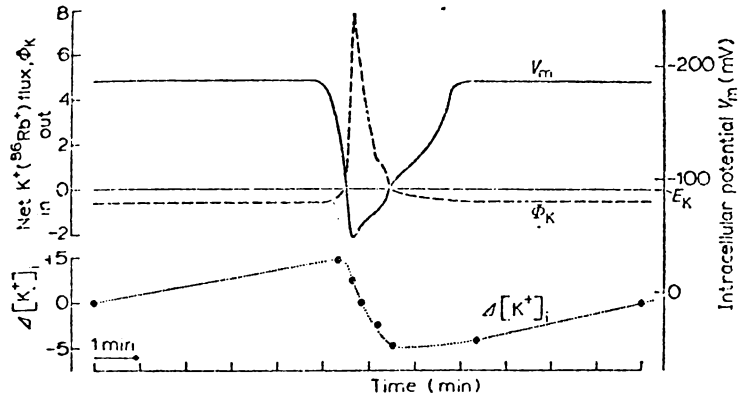

a. Example of the time course of net K^+($^{86}Rb^+$) flux, Φ_K (pmol $K^+ \cdot cm^{-2} \cdot s^{-1}$), (– – –); and change of internal K^+ concentration, $\Delta[K^+]_i$ (μM), (. . .); during a spontaneous action potential (—); horizontal line indicates E_K.

(After Mummert and Gradmann, 1976)

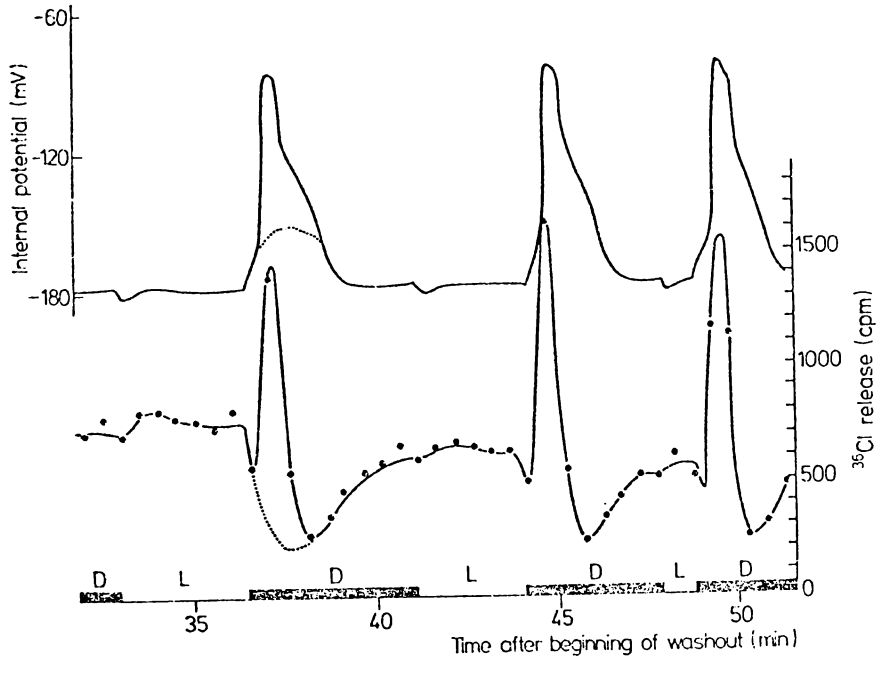

b. Internal potential, V_i (———) and $^{36}Cl^-$ release (o——o). Example from an *A. mediterranea* cell in a light/dark regime. Coincidence of action potentials and enhanced Cl^- efflux.

(After Gradmann, 1976)

mechanism of the AP appears to be dependent on the turning off and on again of the electrogenic pump which in the steady state operates to import Cl^- ions (see e.g. Saddler 1970a; b; c; and 1971; Gradmann, 1975). Its suppression during the AP results, therefore, in a formal Cl^- export. During the initial stages of a depolarisation, there is an enhanced K^+ conductance and an inhibition of the Cl^- import pump. The membrane potential falls to $\simeq$ - 80 mV, between the Cl^- and K^+ Nernst potentials (Fig. 3.2.2). If the cell is in a low metabolic state (e.g. due to low temperatures or metabolic inhibitors), this plateau can be prolonged i.e. the pump does not operate to import Cl^- ions again. The repolarisation takes place relatively quickly at first, slowing down later. The involvement of a metabolically driven active pump causes the time course of an AP in *Acetabularia* to be slower than that in other plant and animal cells by two and four orders of magnitude respectively. It may last 15 to 200 sec. depending on the stimulation; Gradmann (1976; 1978) has used the term 'metabolic action potential' to describe this unusual situation.

3.4 Propagating Action Potentials.

An AP usually propagates unless the length of the cylindrical cell is effectively short (Jack, et.al., 1975). The mechanism of the propagation depends on the current flow from the local circuit of the active region (Fig. 3.4.1a) to excite the inactive neighbouring region to depolarise. This excited region similarly re-excites the next adjacent inactive region and so on throughout the whole length of the fiber (see also Katz, 1966; Brazier, 1968; Jack, et.al., 1975).

During the generation of an AP, the 'action currents' flow in a local circuit from the active region along the inside of the cell, outward through the adjacent resting parts of the membrane, back through the external medium, and inward through the active membrane, so completing the circuit. It is clear from Fig. 3.4.1a that the net longitudinal current which flows through any one cross section is zero because at any point the currents along the cell core are of equal strength and opposite direction to those flowing along the external fluid. But the density of the longitudinal current and the longitudinal p.d. between two points are not necessarily the same inside and out. The axial current inside, i_a, is concentrated within the narrow tube of the cylindrical cell, and the current along the outside, i_o, is distributed among the external fluid. The membrane current is i_m.

From Fig. 3.4.1b, representing a one dimensional core conductor model of a cylindrical cell in a large uniform medium, we may derive some equations during the steady state linear regime by using Ohm's law,

$$i_o = \frac{-1}{r_o} \frac{dV_o}{dx} \qquad (3.4.1)$$

where V_o = potential on the surface,

$\frac{dV_o}{dx}$ = external potential gradient,

Fig. 3.4.1. Diagram of a Propagating Action Potential.

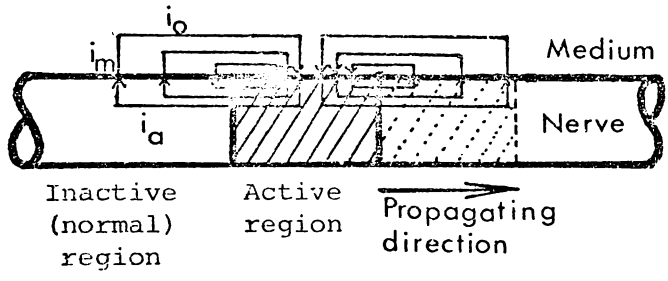

(a) Circuit showing the flow of the Action Current.

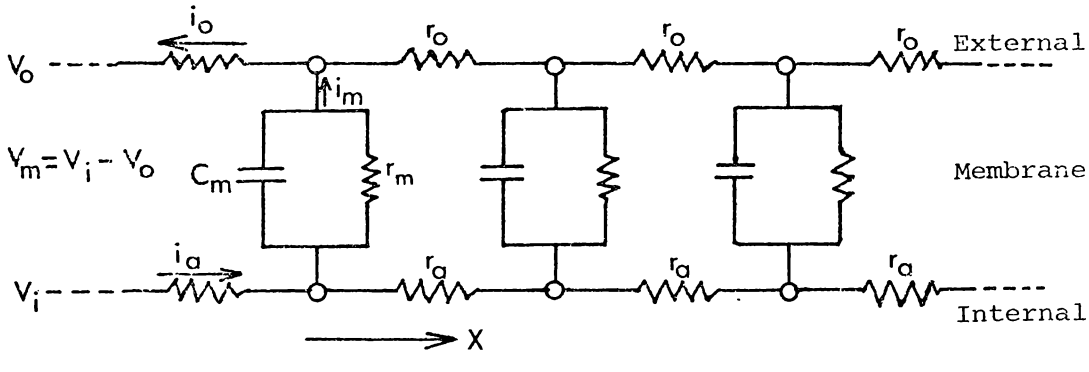

(b) One-dimensional core conductor (cable) Model of an Axon in a Large Uniform Medium.

r_o = resistivity of the outside medium.

(The negative sign is in accordance with the convention that the direction of electric current is positive along a falling (negative) gradient of potential).

Similarly

$$i_a = \frac{-1}{r_a} \frac{dV_i}{dx} \tag{3.4.2}$$

$$i_o = - i_a \tag{3.4.3}$$

and

$$i_m = - \frac{di_a}{dx} = \frac{1}{r_a} \frac{d^2V_i}{dx^2} \tag{3.4.4}$$

where V_i = internal membrane potential,

$\frac{dV_i}{dx}$ = internal potential gradient,

r_a = resistivity of the core cytoplasm.

If we ignore r_o and regard V_o as constant, then when a signal of amplitude V_s (p.d. across the membrane) has been applied at one internal point of the fiber, $x = 0$, Eqn. 3.4.4 becomes

$$V_i = \frac{r_m}{r_a} \frac{d^2V_i}{dx^2} \qquad (r_m = \text{membrane resistivity})$$

and the solution of this differential equation is

$$V_i = A \exp\left(\frac{-x}{\sqrt{r_m/r_a}}\right) + B \exp\left(\frac{+x}{\sqrt{r_m/r_a}}\right) .$$

Since at $x = \infty$ $V_i = 0$, and at $x = 0$ $V_i = V_s$, the particular solution is

$$V_i = V_s \exp\left(\frac{-x}{\sqrt{r_m/r_a}}\right) . \tag{3.4.5}$$

Therefore the signal decays exponentially with a characteristic distance

$$\lambda = \sqrt{r_m / r_a} \qquad (3.4.6)$$

i.e. λ is the length or cable constant of the fiber.

Since $r_m = \frac{R_m}{\pi d}$, and

$$r_a = \frac{4R_a}{\pi d^2}$$

where R_m = specific resistance of one cm^2 of membrane

R_a = specific resistance of one cm^3 of cytoplasm

d = fiber diameter,

then

$$\lambda = \sqrt{\frac{dR_m}{4R_a}} \quad . \qquad (3.4.7)$$

When r_o is taken into account equation (3.4.6) becomes

$$\lambda = \sqrt{r_m / (r_a + r_o)} \quad . \qquad (3.4.8)$$

The above derivation for the cable constant clearly shows that the propagation of an AP is dependent on the fiber size or the core (cytoplasmic) resistance. The greater the diameter (the smaller r_a) is, the longer distance the 'signal' from a local perturbation of membrane potential propagates. (It also depends on the rate at which the membrane capacity ahead of the impulse is discharged beyond the threshold level - see Jack, et.al., 1975 for a detailed treatment).

During this process, the cell membrane behaves linearly at first, i.e. during the steady state, before the potential change affects the ionic conductivities, then non-linearly (Hodgkin and Huxley, 1952; Katz, 1966; Clark and Plonsey, 1966; 1968; and Jack, et.al., 1975).

It is not known whether the propagation of an AP in *Acetabularia* is an information carrying process (as it is a nerve cell), or just an ionic movement in response to the immediate situation. Certainly if

information is internally transmitted by the *Acetabularia* AP (see p.241, Novak and Bentrup, 1972a) it is a completely different level being an intracellular 'message' rather than a message in a multicellular system. Zubarev and Rogtykh (1975) have suggested that the apex-amputated *Acetabularia* may send 'signals' to the nucleus for transporting morphogentic substances for the regeneration process but at present this is an unconformed hypothesis.

3.5 Intra- and Extracellular Measurement of the Action Potential.

The occurrence of an AP in *Acetabularia* or nerve cells can be measured either directly using an inserted microelectrode (Section 3.2d) or indirectly from the outside by an external electrode.

From Section 3.4, if we integrate Eqns. 3.4.1 and 3.4.2, from which we may obtain the ratio of the change of the external potential, ΔV_o and the change of the membrane potential $\Delta V_m = V_i - V_o$ as

$$\frac{\Delta V_o}{\Delta V_m} = \frac{-r_o}{r_o+r_a} \qquad (3.5.1)$$

From Eqn. 3.5.1, the relationship between the changes of the external and membrane potentials is just the same as with an ordinary potential divider, i.e. a fraction, that depends on the ratio between shunt resistance r_o and the sum of the total - inside plus outside - resistances (r_o+r_a), is being monitored.

Incidentally, the electric sign of the external potential change during an AP is negative going, i.e. the opposite of the positive going membrane potential change (ΔV_m).

The membrane potential (V_m) and the intracellular potential (V_i) are known to be monophasic in nature (Clark and Plonsey, 1966), the external potential $(V_o = V_i - V_m)$ recorded in a large uniform medium is triphasic. (See Clark and Plonsey, 1966; 1968; for an analytic calculation and Barker, et.al., 1979 for a numerical analysis applicable to cylindrical cells in cylindrical volumes of conducting medium.) The comparison of the intra - and extracellular potential waveforms is shown in Fig. 3.5.1b.

There are two important aspects needed to be pointed out in relation to the measurements of the external electric field to be described in Chapter 4:

(i) Radially, the magnitude of the external potential falls

Fig.3.5.1. (After Clark & Plonsey,1966)

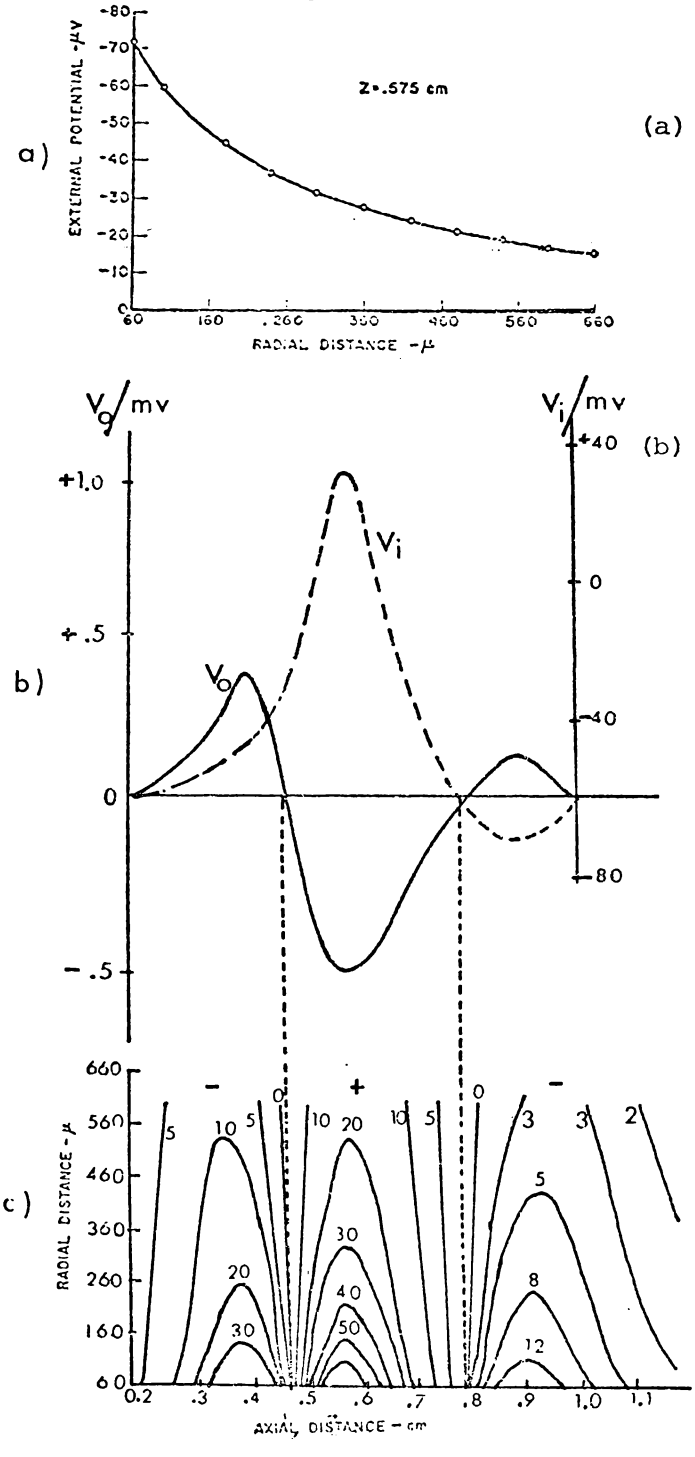

(a) Plot of radial fall-off in external potential at z = 0.575 cm. (Outer membrane surface of axon is located at r = 60μ).

(b) Plots of extracellular (Solid line, V_o) and Intracellular (Broken line, V_i) potential distribution in the medium vs. axial distance.

(c) Calculated external potential field of 120μ crayfish lateral giant axon immersed in an extensive volume of sea water for various values of radial distance (r) and axial distance (z). The values of the isopotential lines in this figure are in microvolts. Since the radius of the axon is 60μ, the radial distance r = 60μ corresponds to the outer membrane surface of the axon.

off as the distance increases from the cell wall (Fig. 3.5.1a). At a radial distance of about 15 times of the cell's diameter, the situation corresponds to an essentially infinite medium environment for the cell (Clark and Plonsey, 1966).

(ii) The longitudinal field (Fig. 3.5.1c) is composed of three distinct zones that are delineated by two zero iso-potential lines located at some distance apart. Since the current density field is orthogonal to the potential field it, too, consists of three zones.

CHAPTER 4

MULTIPLE EXTRACELLULAR ELECTRODE RECORDING METHOD.

4.1 Introduction.

A new technique of recording the occurrence of AP's in *Acetabularia* has been developed which involves measurement of the potential gradients in the external growth medium due to the circulating 'return currents' from any locally depolarised cell membrane. This enables the regenerating stalk segment (SS) to be maintained in a close to natural environment with minimal pertubation by the measuring system. This is in direct contrast to the highly artificial and restrictive system of Novak and Bentrup (1972a) and avoids the well known problems of long term implanted glass microelectrodes (see e.g. Novak and Bentrup, 1972a). In this Chapter the method is described in detail and a number of experimental results involving both internal and external potential measurements are presented to demonstrate the validity of the analysis of the initiation and subsequent propagation of AP's.

Fig. 4.1.1 shows the block diagram of this system. A cell SS lies freely in a cylindrical glass cell holder of diameter at least three times that of the SS (Fig. 4.2.1b). Growth medium is gravity fed through the cell holder continuously throughout the experiment (Section 4.2). There are 8 recording electrodes and one common electrode spaced along the length of the cell holder. They are durable Ag/AgCl electrodes (for fabrication, see Appendix 3). The cell holder and the high input impedance pre-amplifiers are situated in a metal shielded cabinet to reduce electrical interference. Illumination of the cell is given by a 12 V tungsten halogen lamp, with a blue filter to give an approximate daylight spectrum, from the top of the cabinet. Both light intensity and temperature are measured by transducers in or close to the cell

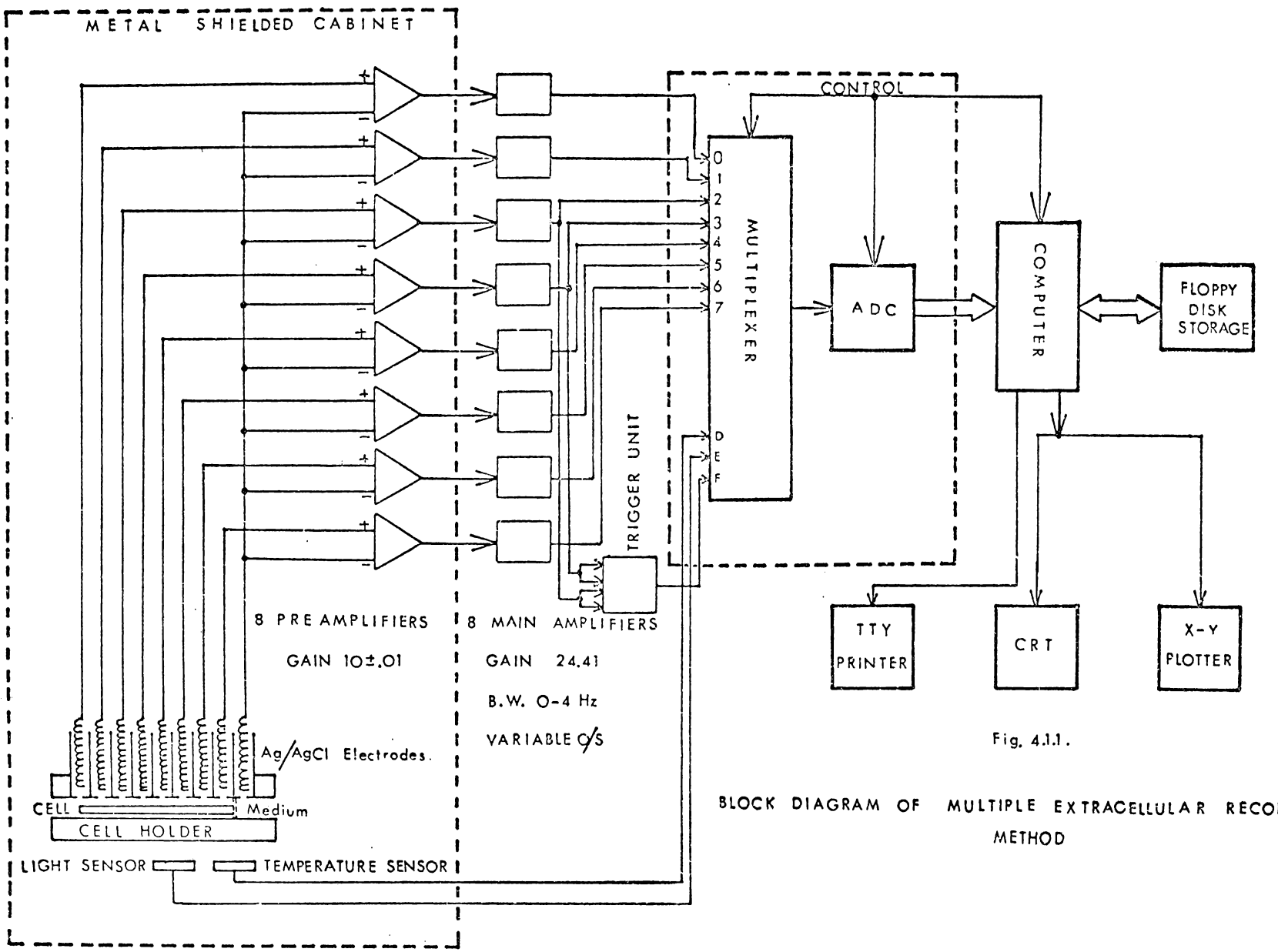

Fig. 4.1.1.

BLOCK DIAGRAM OF MULTIPLE EXTRACELLULAR RECORDING METHOD

holder and monitored by the computer.

The output of each preamplifier is connected to a main amplifier which incorporates a variable D.C. offset (for backing off steady electrode potentials) and a low-pass anti-aliassing filter. The main amplifier outputs are connected to a computer controlled multiplexed analog-to-digital converter (ADC) and up to four of them can also be connected to a hardware trigger detection unit with adjustable thresholds so that the occurrence of any transient AP's is detected. The computer controls continuous sampling of all data channels as well as the trigger detector output and acts as a transient recorder with retention of pre-trigger as well as post-trigger information. Captured transient AP's are displayed on a storage CRT and logged on a Teletype during the experiment, and each complete data record is stored on a Floppy Disk for subsequent processing and graph plotter display. Details of the hardware are given in Section 4.3 and the computer software is outlined in Appendix 4.

In Section 4.4 the analysis of the recorded waveforms to give the initiation and propagation characteristics of the AP is developed and Section 4.5 presents some typical experimental results to illustrate various features of the analysis and types of behaviour.

4.2 Cell Holders.

4.2a Mechanical Details.

There are several important factors in the design of the cell holder, e.g. the optical transparency, dimensions that restrict the external electric field in the medium for a sufficient voltage to be measured by the electrodes, and the medium feed systems. By trial experiments on a number of cell holders, two types were found to satisfy well most of the requirements. They are shown in Fig. 4.2.1.

Type A is used for the experiments on normal complete cells (CC's) for investigating the internal membrane potentials by the inserted microelectrode technique, and relating this to the simultaneously recorded external potentials at any positions by the external electrodes. It is made up of a clear perspex slab with nine (or more) cylindrical 'L' shaped holes (smaller at the lower ends). Each hole contains an Ag/AgCl electrode embedded in solidified (5 - 20%) Agar + AE 50, or in pure AE 50. One, at the end of the row, is used as common electrode. The cell is laid in the groove with cross section $\gtrsim$ 2.5 times that of the cell stem. It is held lightly in position by perspex clamps (1-3), and a micropipette can be introduced into the cytoplasm of the cell with the aid of a micromanipulator.

Cell holder type B was specially designed for investigation of AP's by the multiple external electrode technique in experiments on the regeneration of ISS's. It is made up of a thick walled glass tube (I.D. = 1 mm, O.D. = 7.25 mm.), in which the cell SS lies, with a longitudinal slot that communicates with either 9 or 17 closely spaced capillary tubes (Fig. 4.2.1b). Each of the capillary tubes contains AE 50 and an Ag/AgCl electrode. At one end, it is flamed to a small opening (~ 100 μm), the other is sealed round the electrode with epoxy resin (e.g. Araldite) or silicone glue. Two sizes of capillary tubes

Fig. 4.2.1a. Diagram of Type A Cell Holder.

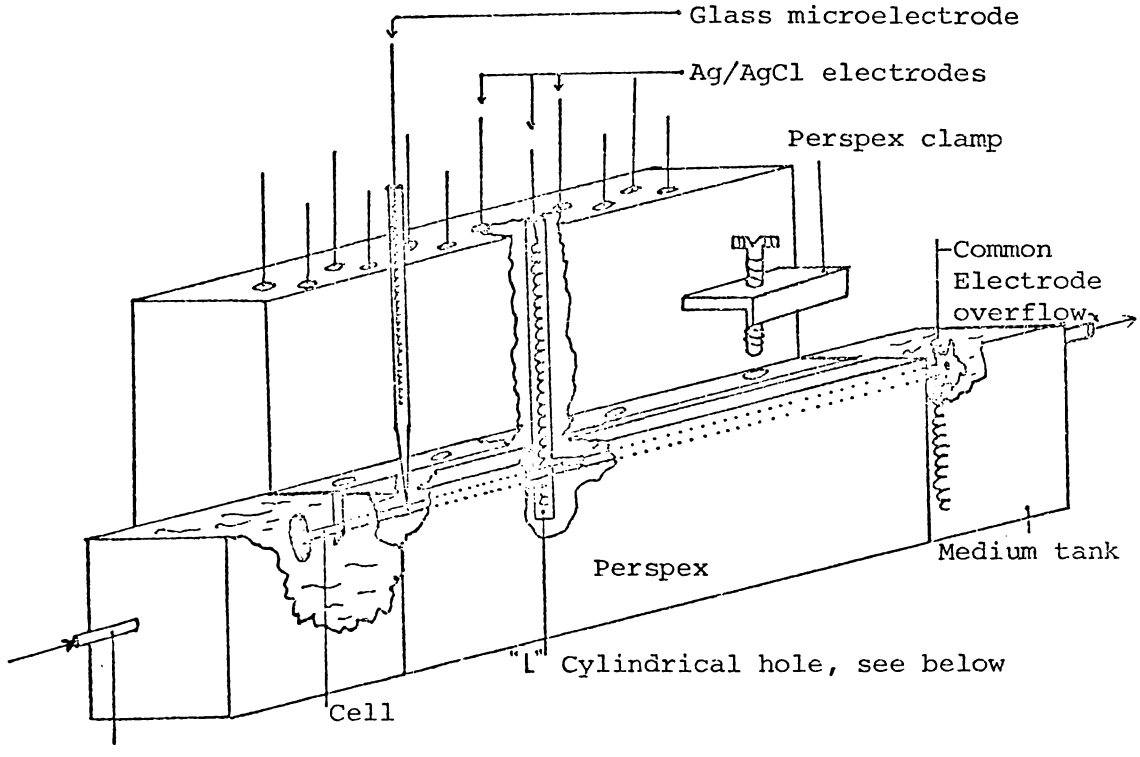

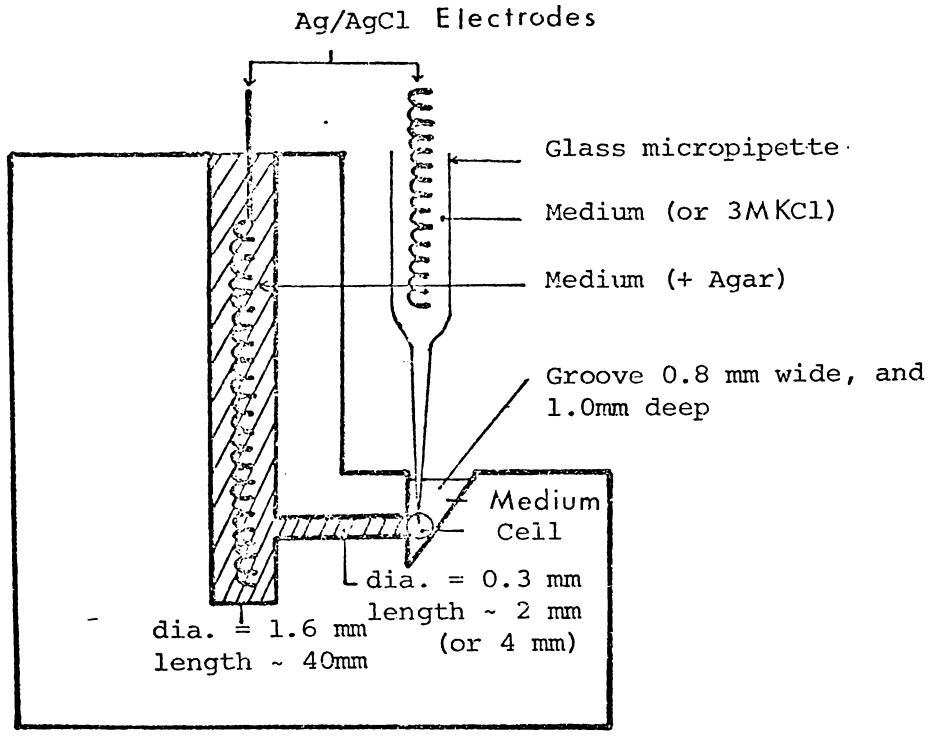

Extended X-Section of Type A Cell holder showing "L" cylindrical hole, and location of the cell.

Fig. 4.2.1b Diagram of Type B Cell Holder.

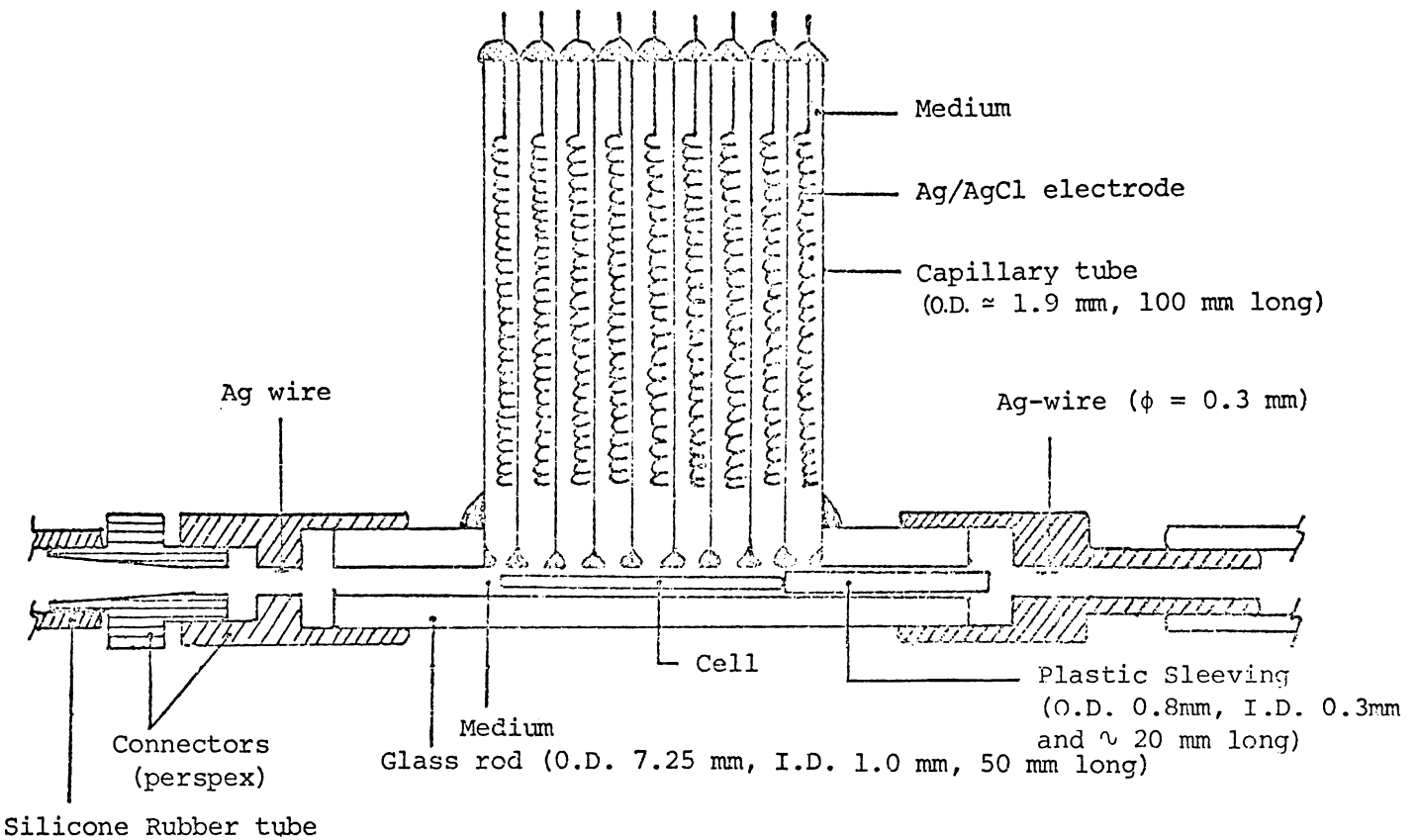

were used, O.D. = 1.6 ± 0.1 mm and 1.9 ± 0.2 mm, to suit the slot (on the glass rod) cut by the two sizes of the available diamond saws. Thus the electrode spacings were 1.6 mm or 1.9 mm., and in the holder with seventeen 1.6 mm tubes, use of alternate electrodes gave an effective inter-electrode spacing of 3.2 mm. Using eight electrodes (plus one common reference) for the extracellular voltage records therefore meant that equally spaced electrode arrays spanning 12.8 mm, 15.2 mm, or 25.6 mm were available. The ISS's were cut to be just less than one of these lengths so they could lie wholly within the electrode span. For all of the "main series" experiments (Chapter 5) the 1.9 mm electrode-spacing holder was used.

A short length of a glass tube with O.D. ≈ 0.8 mm and I.D. ≈ 0.3 mm, or a piece of plastic tube of equivalent dimensions, is fixed at the distal end of the cell holder to retain the cell in the required positions. The remaining slot space on the glass-rod (after the capillary tubes are mounted) is filled with clear epoxy resin. For the purpose of determining the electrical resistivity of the growth medium by injecting a small current from a current source into the cell holder, a pair of Ag-wires are also fixed at the ends of the cell holder, either along the cut slot or at the perspex joints with the medium feed system.

This design does not allow the transducers for measuring the light intensity and temperature to be fitted inside the holder, i.e. the measurement cannot be made directly, but they can be mounted in close proximity.

4.2b The Ag/AgCl Electrodes.

This kind of electrode consists of a pure metallic Ag substrate coated with AgCl and is in contact with an electolyte solution which contains a soluble chloride, such as NaCl or KCl. It is widely used because it has several practical advantages, e.g. it is

reasonably reversible (non-polarizable), the chloride has low solubility, and the electrode exhibits low noise after stabilization (Ferris, 1974).

There are various techniques for producing these electrodes (Geddes, 1972). In this work a simple electrolysis was used as shown in Fig. 4.2.2. The electrolyte and cathode material shown in that diagram are among many alternatives (see e.g. Ferris, 1974). The critical parameters are the purity of the Ag substrate (e.g. wires), the cleanliness of the cathode and the container (beaker), the use of reagent grade electrolyte, and doubly distilled water. The chloriding process is best carried out in the dark. The detailed procedure is described in Appendix 3b.

To ensure the durability and stability of the electrodes, the coated area should be as large as possible ($\gtrsim 1\ cm^2$). Experimentally this can be achieved with a wire of 0.3 - 0.5 mm in diameter in two ways; coiling the wire into a tight helix, or electrically depositing pure Ag grains on the wire. The deposition of extra Ag on a Ag wire offers greater area and purity, i.e. a better electrode. However, the deposition is sometimes too spiky so the wire cannot be put into the capillary tube. The deposition process can be done in a similar set-up to that shown in Fig. 4.2.2. The electrode wires are now the cathode and a cylinder of Ag foil is used for the anode. The electrolyte is 0.1 N $AgNO_3$. At the current density of 1 - 5 mA/cm^2, this deposition takes 4 - 24 hours. The chloriding is the same as is done for the wire helix except that the time is doubled.

All freshly produced Ag/AgCl electrodes need $>$ 2 days ageing in 0.1% NaCl or 0.01 N HCl solution to stabilize the electrode potential. The typical noise produced by any pair of these aged electrodes is less than 10 μV r.m.s.

To store the electrodes, it is recommended to keep them in pure

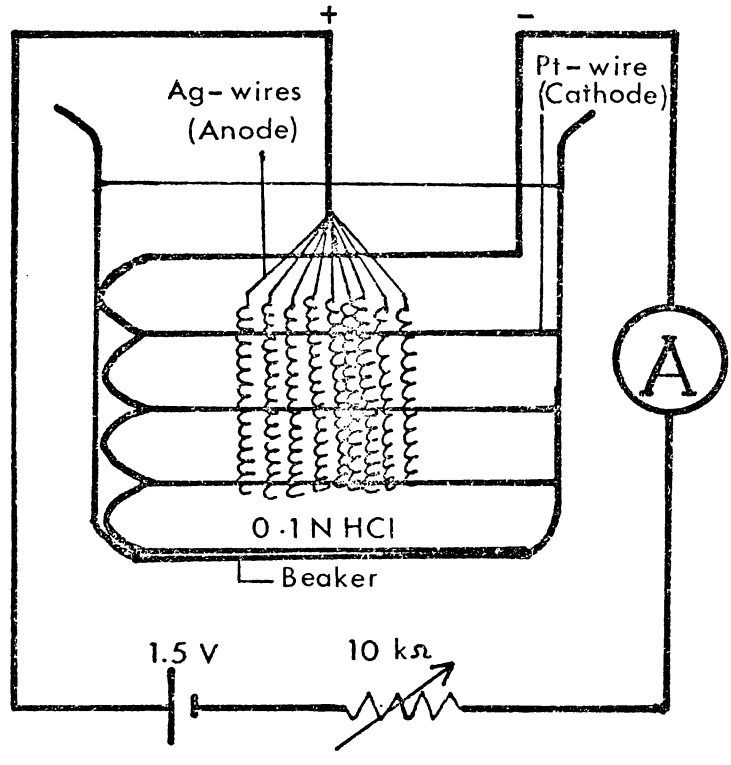

Fig. 4.2.2. Diagram of Electrical Chloriding Apparatus.

distilled water at ~ 5 - 10°C and in the dark.

4.2c The Medium Feed System.

It was found that an ISS needed a minimum fresh medium feed of ≈ 2 - 3 $^{ml}/_{hr}$. Below this rate the cell was found colourless within 12 hours and eventually dead. This is most likely due to lack of nutrition. The clear patch is believed to be the result of the contraction of the chloroplasts (Sironval, et.al., 1977). Slow feeding rates also facilitated the growth of the contaminants in the cell holder. As a result, the cell may not regenerate although it remained alive throughout the whole experimental period. The optimum feed rate was found to be ≈ 10 - 20 $^{ml}/_{hr}$. Usually this rate enabled an ISS to regenerate within 24 hours of exposure to light.

Pumping the medium through the cell holder by an electric peristalic pump was found unsuitable as the rhythms of the pump were picked up by the sensitive preamplifiers. A simple gravity feed was quite satisfactory. This system consisted of a bottle containing sterile medium, a controllable roller valve, a filter with 0.22 μm filter paper, and a drainage (Fig. 4.2.3a). The flow rate was adjustable from the difference between the medium levels in the bottle and in the draining hose, and by the roller valve.

For other details of the set up, see Fig. 4.2.3b.

Fig. 4.2.3. Diagram of the Medium Feed System.

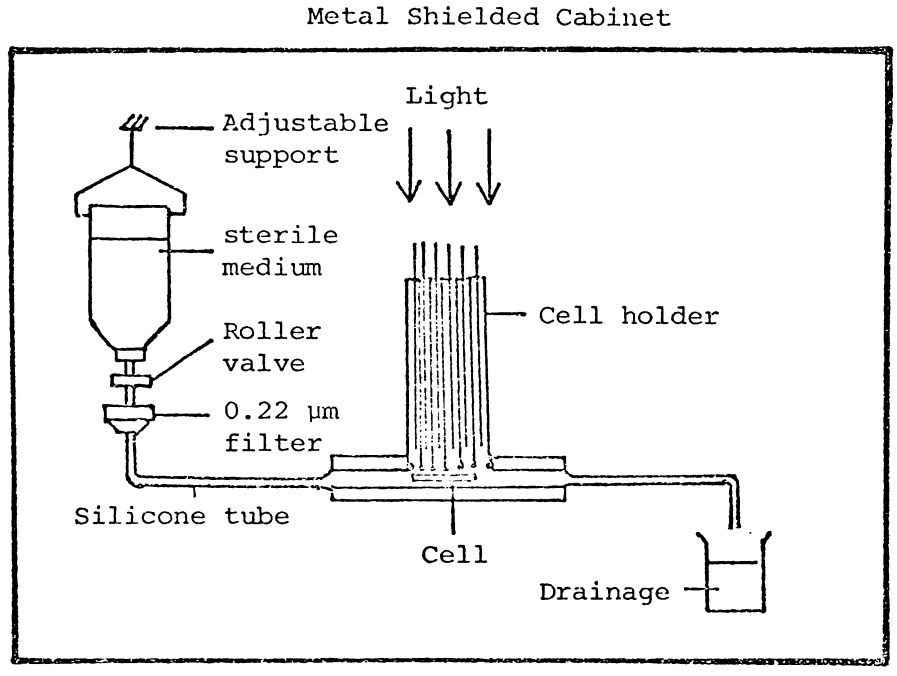

(a) Set-up (Front View)

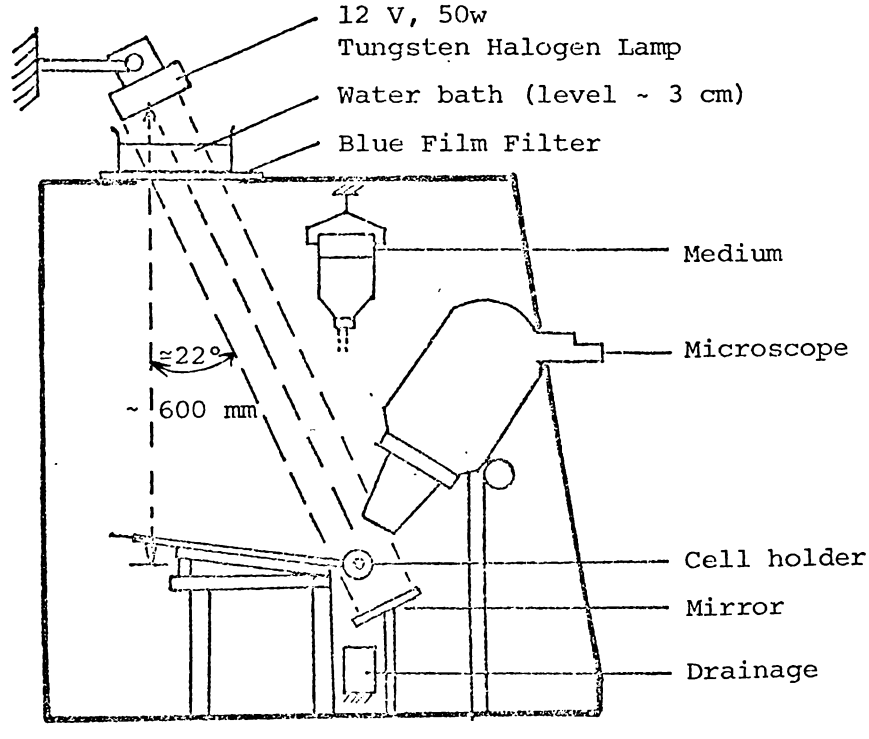

(b) Accessories
(Side View)

4.3 Signal Processing and Computer Data Acquisition.

The overall block diagram is given in Fig. 4.1.1. The signals picked up by the electrodes are immediately connected to the pre-amplifiers based on National Semiconductor type LF 352 instrumentation amplifiers (Fig. 4.3.1). These provide a high input impedance ($2 \times 10^{12}\Omega$) buffer stage with a low bias current (3 pA). Their voltage gains are trimmed to be 10.0 ± 0.01. The pre-amplifier outputs are connected to the main amplifiers, while also provide their power supply, via multi-core screened cable.

Each main amplifier (Fig. 4.3.2) consists of a voltage follower (RCA CA3140 op-amp), a voltage amplifier (National Semiconductor LM 301 op-amp), and a two-pole Butterworth low-pass filter (National Semiconductor AF 100). It offers the device of a.c. or d.c. input coupling but since the d.c. drift of the electrode potentials could be reduced to $\lesssim \pm 2\mu$V/hr d.c. coupling was used satisfactorily.

The gain of the main amplifier was trimmed to be either 2.441 or 24.41 depending on whether it was to be used with a microelectrode inserted in the cytoplasm or an external electrode in the growth medium. With the pre-amplifier this gives a system gain of 24.41 or 244.1 so that the ± 5 V range of the 12 bit ADC gives the convenient scaling of 1 bit ≡ 100 or 10 μV respectively, i.e. in the low gain case the digital output of the ADC is + 204.7 to - 204.8 mV in 0.1 mV steps and in the high gain case it is + 20.47 to - 20.48 mV in 0.01 mV steps. This choice of system gain facilitates programming (which was all done at assembler level) as it avoids the need for any floating point operations to scale the data into convenient physical units.

The low pass filter has a cut off at ~ 4 Hz for protection against aliassing errors (the usual sampling frequency was 10 Hz).

The hardware trigger unit (Fig. 4.3.3) consists of four comparators

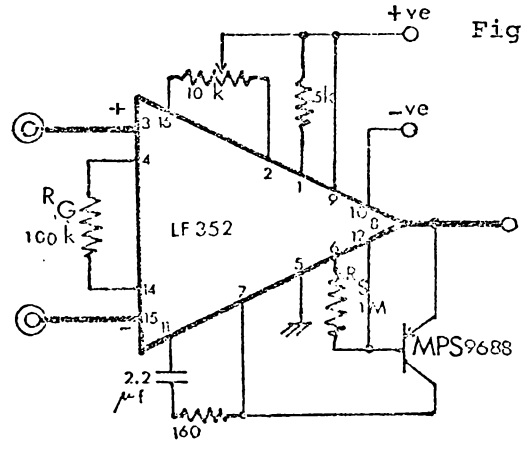

Fig. 4.3.1. Circuit Diagram of Preamplifier

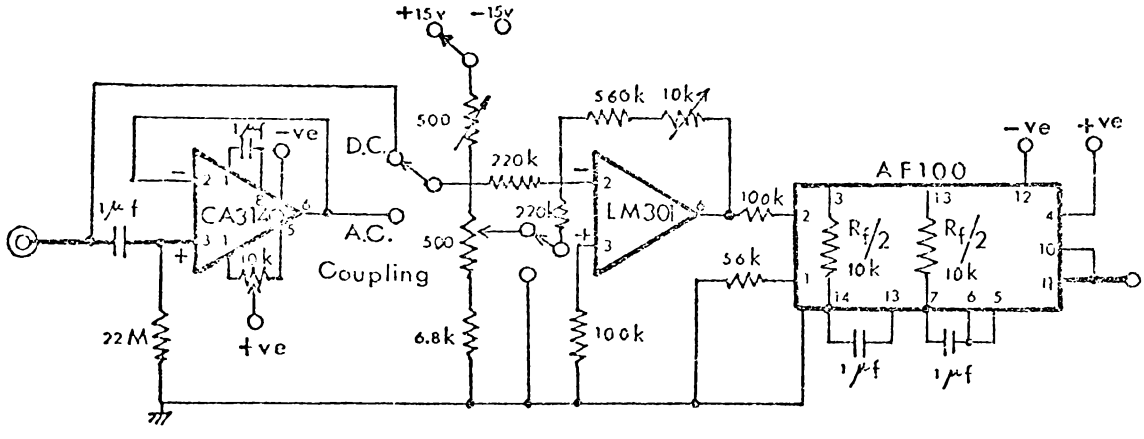

Fig. 4.3.2. Circuit Diagram of Main Amplifier.

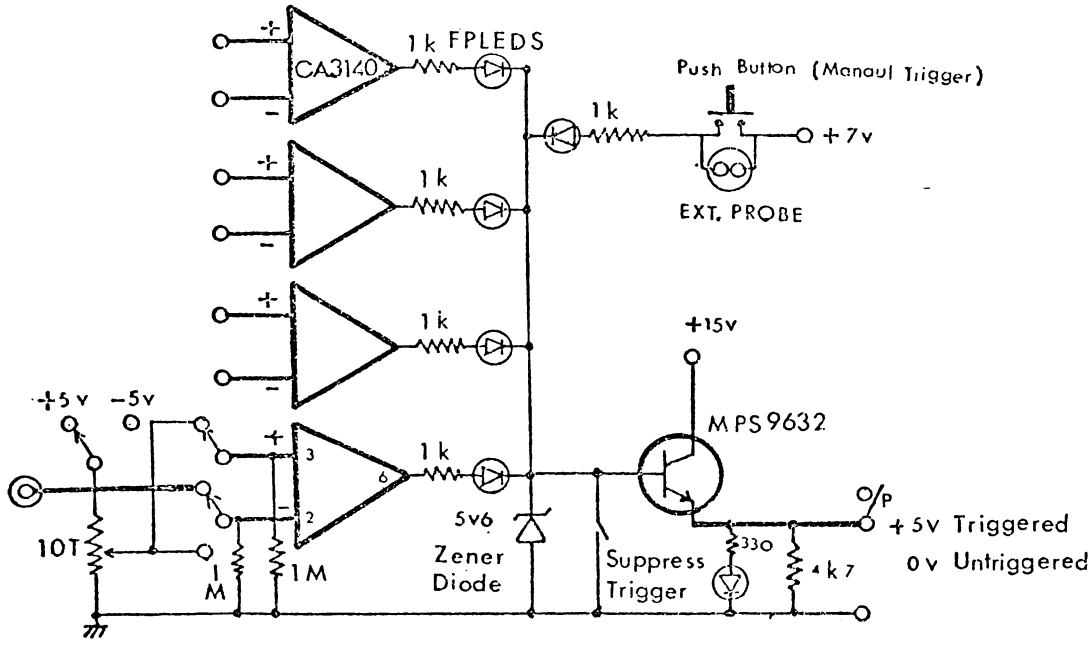

Fig. 4.3.3. Circuit Diagram of Trigger Unit.

whose outputs are logically OR-ed together with a manual push button. Each comparator threshold is adjustable for both sign and magnitude and can be set to respond to either a positive or negative going transition through the threshold. By connecting an appropriate set of the main amplifier outputs to the four trigger inputs the generation of a trigger level at the output could be guaranteed for every transient depolarisation of the cell. (This unit was very much more versatile than the earlier method of a software trigger detection routine as it enables thresholds to be adjusted to compensate for drifts in the steady electrode potentials over long experiments). The unit was also designed to allow the suppression of triggering, manual triggering, inhibition of the trigger while adjusting the triggering levels, and LED indication of the triggering input(s).

Together with the outputs from the main amplifiers (channels 0 to 7) and the trigger unit (channel F); the outputs from the light and temperature transducers (Texas Instruments TIL67 and National Semiconductor XL 5600 respectively) are connected to the multiplexer channels D and E. The voltages from the transducers are amplified to give the converted reading ranges of 10 - 40 watts/m^2 and 10° - 30°C.

The multiplexer and the ADC are an ADAC corporation type ADAM-12 data acquisition module. It contains a 16 channel multiplexer, differential amplifier, high speed sample and hold, 12 bit analog to digital converter, tri-state byte oriented output buffer and all the logic neccessary to have the unit work as a complete system. It is interfaced to the minicomputer, a Computer Automation Alpha LSI 2/20 with 32k 16 bit words of memory, via a "General Purpose Intelligent Cable" on the Distributed I/O System. The data word transfer rate is $\simeq 16 \times 10^3\ s^{-1}$, i.e. the time between samples of successive channels in the scan is $\simeq$ 60 μs. This is completely negligible in comparison with

the time between scans (~ 0.1s); so in each scan all channels are measured effectively simultaneously.

The transient recorder data acquisition program and off-line data processing and display program are described in detailed flow-chart form in Appendix 4.

4.4 Analysis of the Multiple Extracellular Voltage Waveforms.

In Fig. 4.5.4a is shown a typical set of voltage waveforms arising from an AP transient and measured using the techniques described above. Fig. 4.5.4b shows the differential voltages $d_n = v_n - v_{n+1}$ computed from the same data. Ideally we should like to be able to analyse these data to give the time dependence of the current distribution through the cell wall and hence have a complete definition of the initiation and subsequent propagation of the depolarised region. Although this cannot yet be done with the present system it will be shown that the boundaries of the depolarised region can be located with reasonable accuracy and so useful information can be obtained.

4.4a Lumped Element Circuit Analysis.

Fig. 4.4.1a represents the situation of an ISS in the type B cell holder (cf. Fig. 4.2.1b). The electrodes are assumed to be equally spaced and the ISS is taken as a uniform cylinder situated in a cylindrical volume of electrically conducting growth medium.

Fig. 4.4.1b is the simplest one-dimensional lumped-element electrical equivalent circuit where the ISS is represented by a "black box" with eight terminals. It is obviously a very complex black box containing generators and highly non-linear elements. R_o is the resistance of the cylindrical sheath of growth medium between each pair of electrodes.

By Kirchhoff's law $\sum_{n=0}^{7} i_n = 0$ and the relationship between the currents i_n and voltages v_n as defined in Fig. 4.4.1b is readily derived as:

Fig. 4.4.1. Diagrams for Lumped Element Circuit Analysis

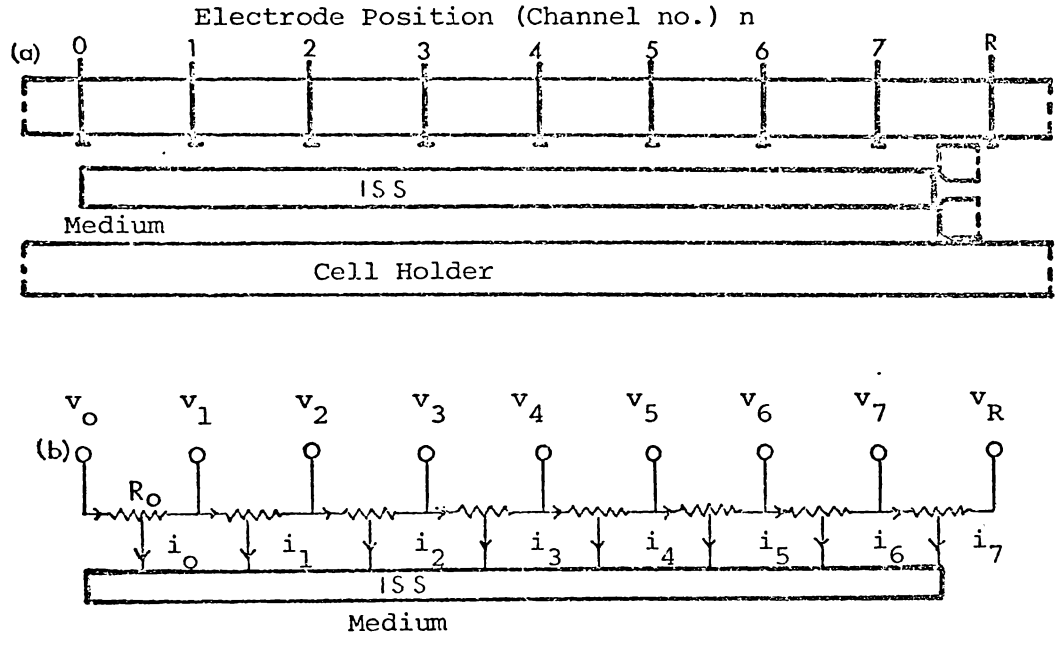

(a) Representation of an ISS in Type B Cell Holder.

(b) One Dimensional Lumped Element Electrical Equivalent Circuit.

$$\begin{bmatrix} v_0 \\ v_1 \\ v_2 \\ v_3 \\ v_4 \\ v_5 \\ v_6 \\ v_7 \end{bmatrix} = \frac{R_o}{2} \begin{bmatrix} 1 & 3 & 5 & 7 & 9 & 11 & 13 & 15 \\ 0 & 1 & 3 & 5 & 7 & 9 & 11 & 13 \\ 0 & 0 & 1 & 3 & 5 & 7 & 9 & 11 \\ 0 & 0 & 0 & 1 & 3 & 5 & 7 & 9 \\ 0 & 0 & 0 & 0 & 1 & 3 & 5 & 7 \\ 0 & 0 & 0 & 0 & 0 & 1 & 3 & 5 \\ 0 & 0 & 0 & 0 & 0 & 0 & 1 & 3 \\ 0 & 0 & 0 & 0 & 0 & 0 & 0 & 1 \end{bmatrix} \begin{bmatrix} i_0 \\ i_1 \\ i_2 \\ i_3 \\ i_4 \\ i_5 \\ i_6 \\ i_7 \end{bmatrix}$$

or $\underline{v} = \frac{R_o}{2} [A] \underline{i}$. (4.4.1)

Alternatively, in terms of the differential extracellular voltages

$d_n = v_n - v_{n+1}$

$$\underline{d} = \frac{R_o}{2} [B] \underline{i} \qquad (4.4.2)$$

where $[B] = \begin{bmatrix} 1 & 2 & 2 & 2 & 2 & 2 & 2 & 2 \\ 0 & 1 & 2 & 2 & 2 & 2 & 2 & 2 \\ 0 & 0 & 1 & 2 & 2 & 2 & 2 & 2 \\ 0 & 0 & 0 & 1 & 2 & 2 & 2 & 2 \\ 0 & 0 & 0 & 0 & 1 & 2 & 2 & 2 \\ 0 & 0 & 0 & 0 & 0 & 1 & 2 & 2 \\ 0 & 0 & 0 & 0 & 0 & 0 & 1 & 2 \\ 0 & 0 & 0 & 0 & 0 & 0 & 0 & 1 \end{bmatrix}$

In principle both Eqns. 4.4.1 and 4.4.2 can be inverted to give explicitly the required $\underline{i}$ in terms of the measured $\underline{v}$ or $\underline{d}$. However this is not readily applicable in practice since the inverse matrices $[A^{-1}]$ and $[B^{-1}]$ are ill-conditioned and small errors in the measured $\underline{v}$ or $\underline{d}$ can give rise to unacceptably large errors in the calculated $\underline{i}$.

For this reason we adopt the opposite approach of calculating the expected $\underline{d}$ from a postulated $\underline{i}$ and showing that the boundaries of the

depolarised region can be identified to within an electrode spacing from these plots.

4.4b Identification of the Depolarised Region.

In Fig. 4.4.2 are shown the sketches of some membrane current distributions corresponding to various possible positions of a single depolarised region, and the resulting differential voltages calculated using Eqn. 4.4.2. These of course represent the situation at some definite instant in time, both $\underline{d}$ and $\underline{i}$ being time dependent. The current distributions have been drawn so as to be consistent with the cable constant $\lambda \sim 6$ mm for the normal resting *Acetabularia* membrane (Sections 3.3 and 3.4) and a much shorter cable constant ($\lambda < 1$ mm) for the regions of depolarised membrane (due to the much greater membrane conductance). These diagrams demonstrate the obvious and useful result that when d_n is positive the depolarised region is to the right of electrode n and when d_n is negative the depolarised region is to the left of electrode n. Also, since the membrane current $\underline{i}$ has its maximum magnitude in the depolarised region immediately adjacent to the boundary with the normal region, d_n will have maximum magnitude when one of the pair of electrodes n, $n+1$ is situated at the boundary of the depolarised region with the other adjacent to normal region (Fig. 4.4.3). Hence the following rules of interpretation apply:

(i) If at some instant of time d_n is positive and $d_n > d_{m\neq n}$ then the depolarised region has its boundary in the vicinity of electrode $n+1$ and extends to the right of this boundary.

(ii) If, on the other hand, at some instant of time d_n is negative and $d_n < d_{m\neq n}$ then the depolarised region has its boundary in the vicinity of electrode n and extends to the left of this boundary.

It is readily seen that when these rules are applied to the voltage distributions of Fig. 4.4.2 the depolarised regions are correctly

Fig. 4.4.2. Representation of the Membrane Current and the External Differential Voltage Distribution at Various Positions for a Single Depolarisation.

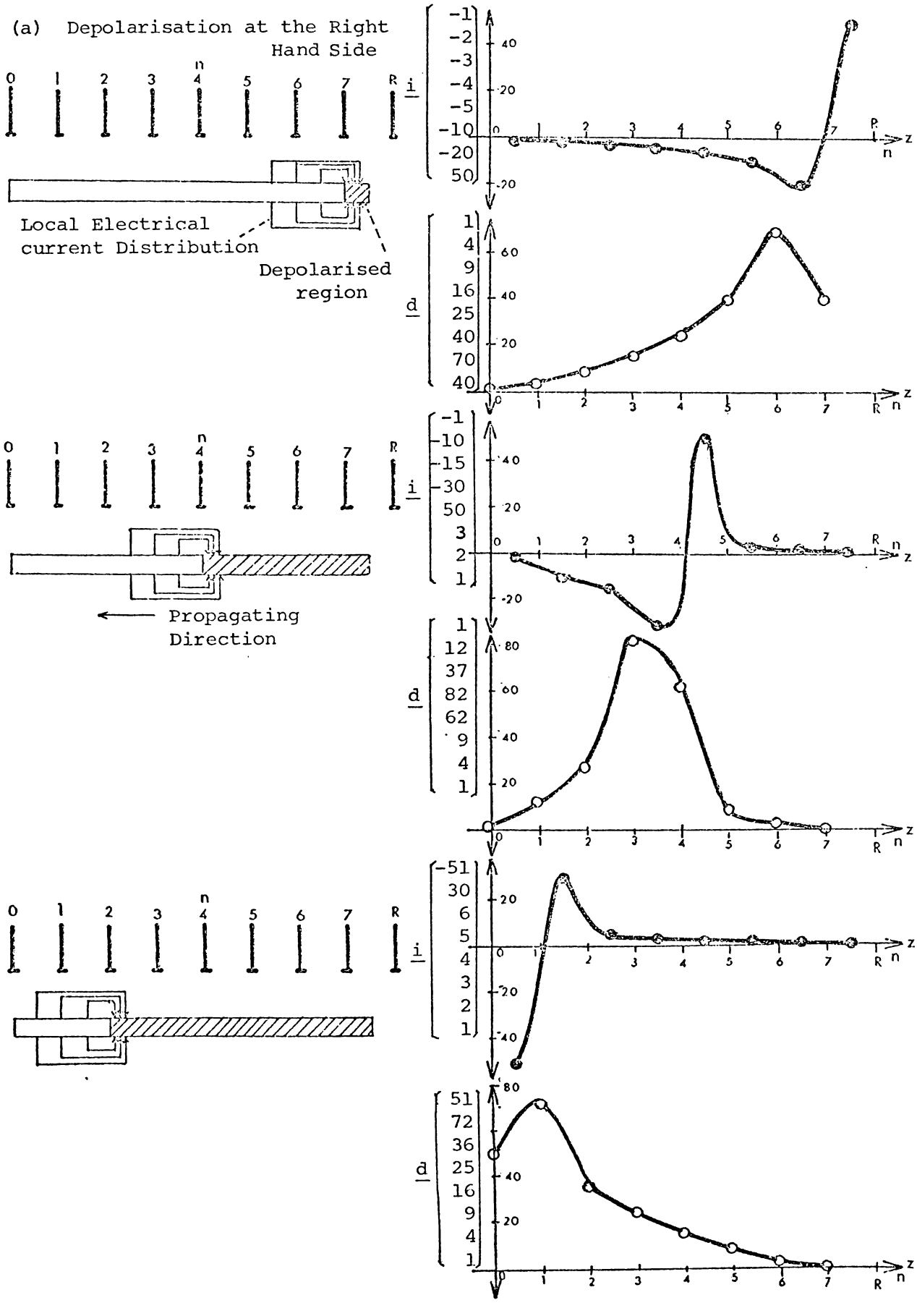

(b) Depolarisation at the Left Hand Side

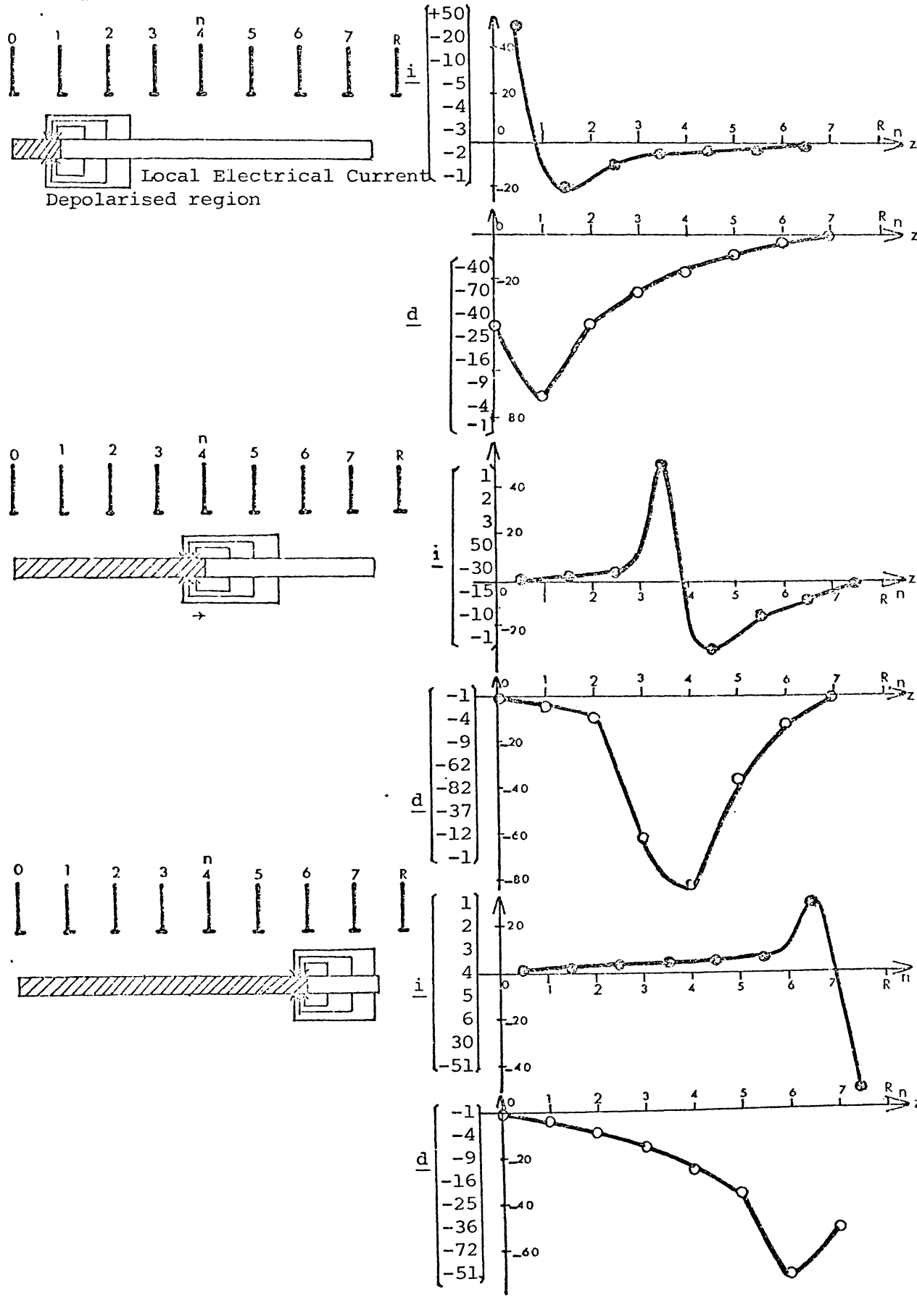

(c) Depolarisation at the Middle

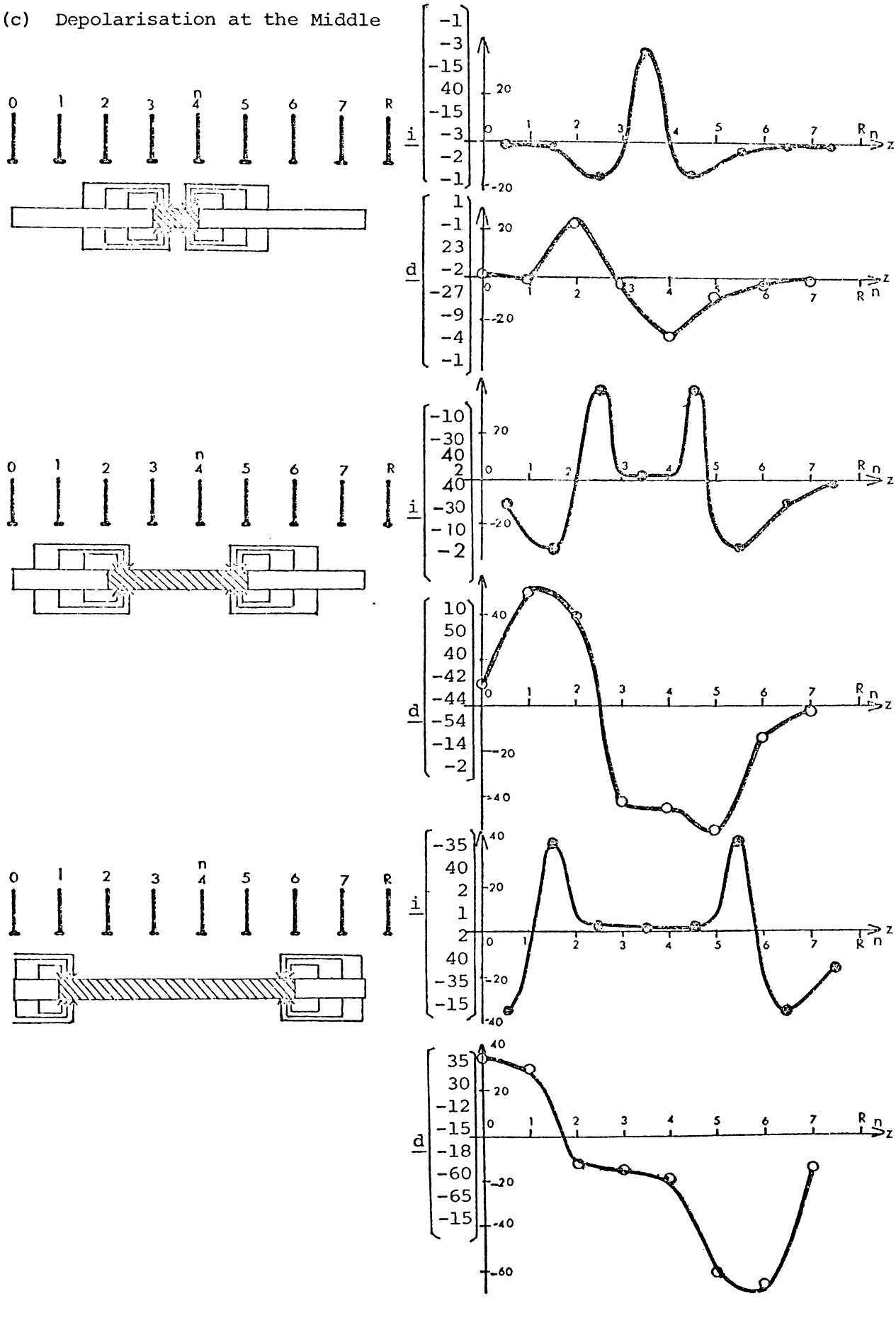

Fig. 4.4.3. The Position of the boundary of the depolarised region of the cell stalk for maximum magnitude - differential voltage d_n between electrodes n and n+1.

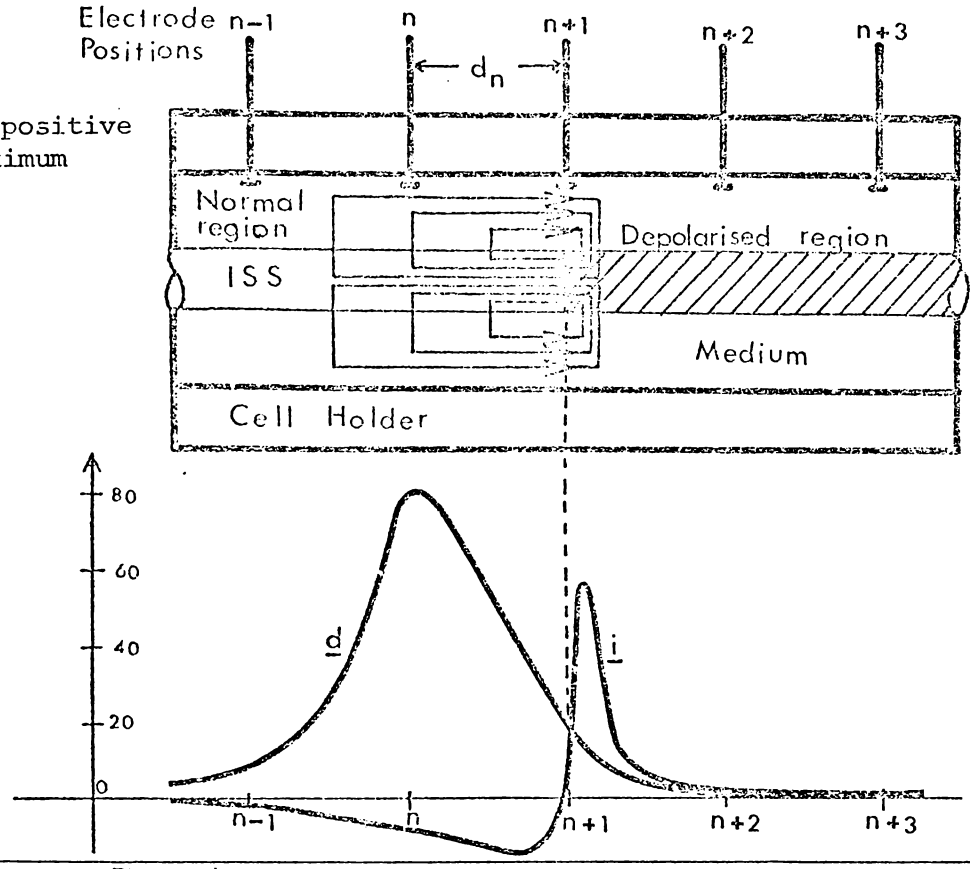

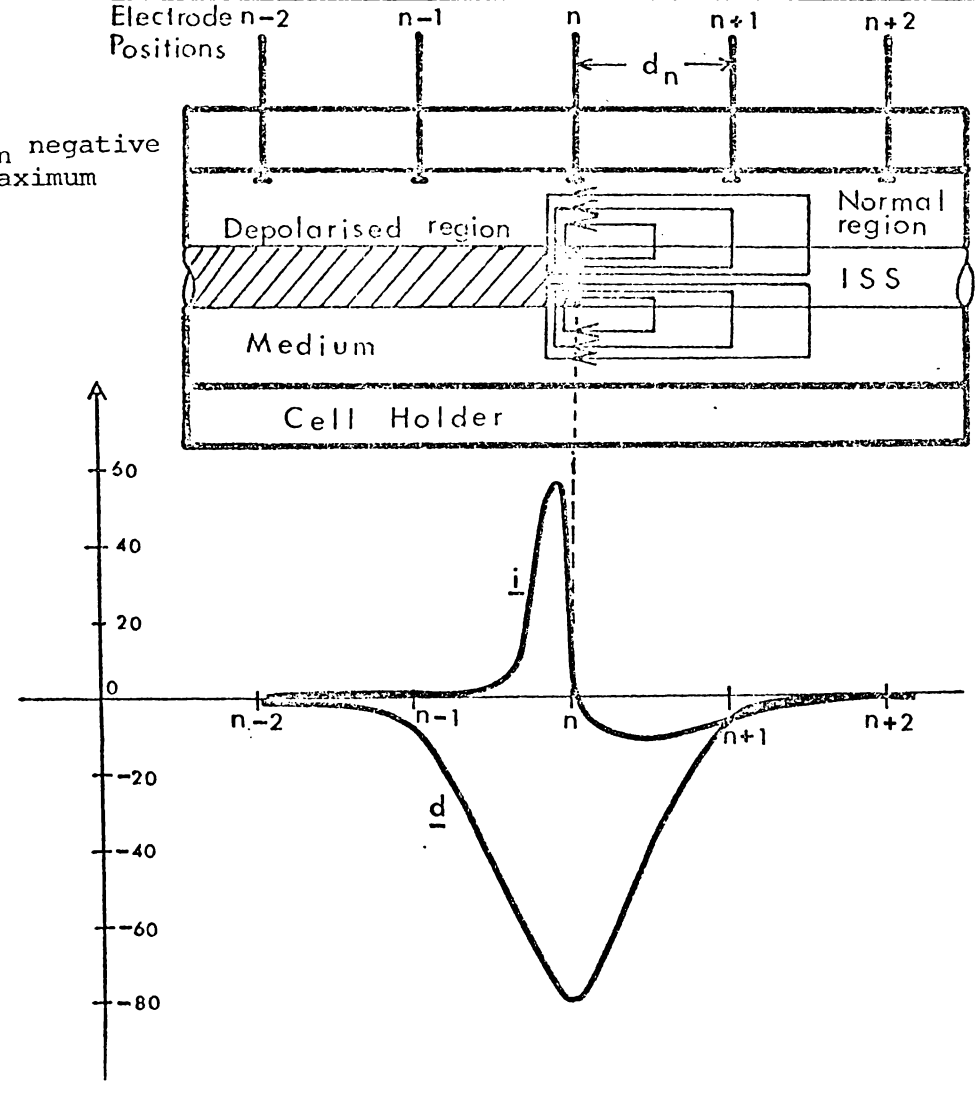

identified.

4.4c Interpretation of the $\underline{d}(t)$ Waveforms.

The usual form of data display (Fig. 4.5.4b) gives the time dependence of the eight differential voltages d_n in $\underline{d}$ over the duration of an AP transient. In principle plots of $\underline{d}$ vs. n such as given in Fig. 4.4.2 can be constructed at successive times. From these the spreading of the depolarised region throughout the duration of the AP can be mapped in some detail, and a number of characteristically different types of behaviour observed (see Appendix 5).

However, this is a time consuming procedure and in the present work rather less detailed information is needed, namely the identification of the region in which the depolarisation initiates and whether it subsequently propagates (i.e. whether it is a true propagating AP or a non-propagating local depolarisation).

Clearly with a non-propagating local depolarisation the differential voltage waveforms $\underline{d}(t)$ will all be the same to within a scale factor. This situation is usually obvious but is easily checked by normalising all the traces to the same height using the appropriate data reduction and display routines (Appendix 4). An example of such a transient is shown in Fig. 4.4.4.

In the case of a propagating or spreading AP then $\underline{d}(t)$ will depend both on the inherent time dependence of the AP depolarisation and also on the change in position and extent of the depolarised region. However, the interpretation of Fig. 4.4.3 can still be used to identify the position of the boundary of the depolarised region and this is conveniently applied by noting the times at which the d_n's take their extremal values and plotting the resulting boundary positions as a function of these times. Examples of the application of this procedure to a range of experimentally obtained $\underline{d}(t)$ plots (cf. Figs. 4.5.6 and 4.5.7)

Fig. 4.4.4. Differential Voltage Waveforms, $\underline{d}(t)$ a non-propagating, local depolarisation.

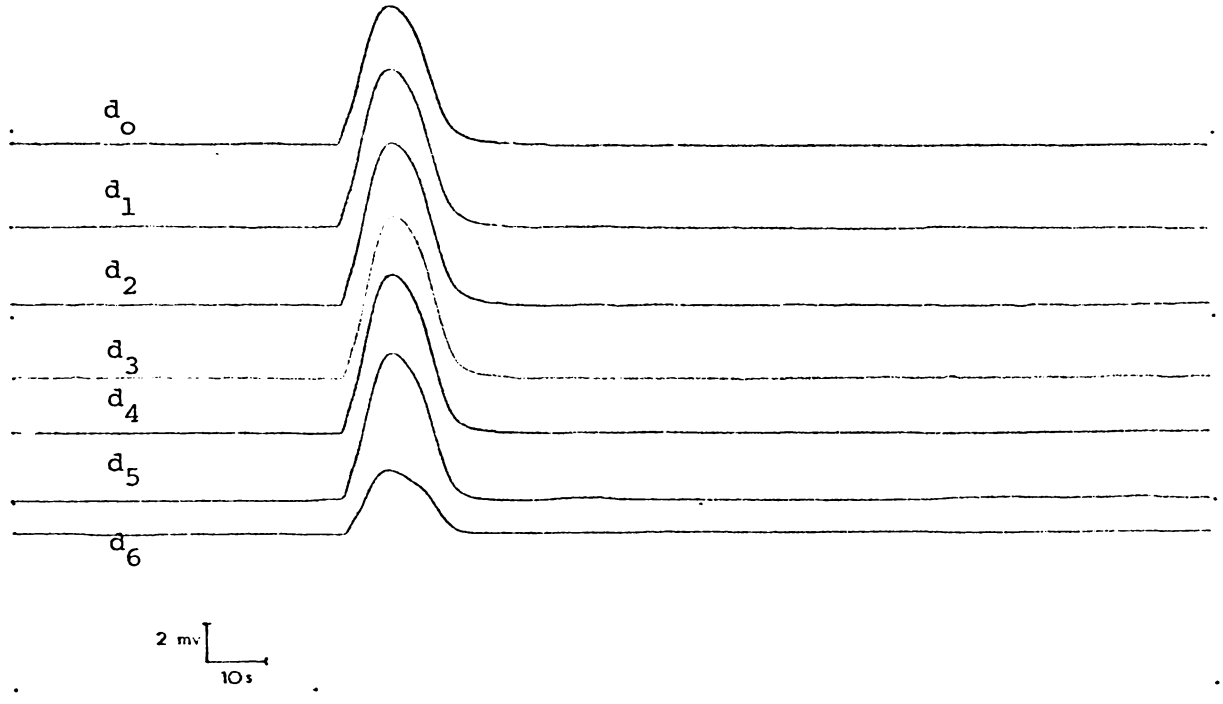

(a) Raw data

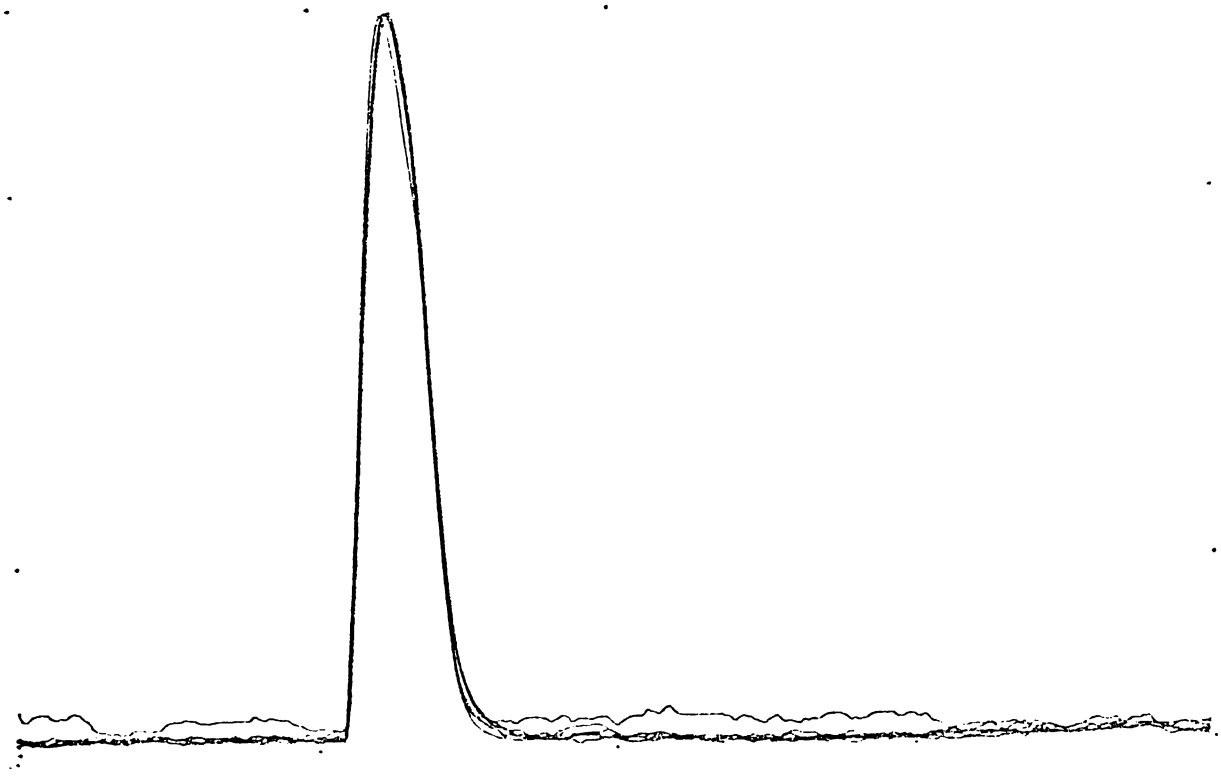

(b) Data normalised to same peak height.

are given in the next section.

4.5 Typical Experimental Results.

In this section some typical experimental measurements of AP's in *Acetabularia* are presented, using both traditional inserted micro-electrodes and the multiple external electrode system described above.

4.5a Simultaneous Internal and External Measurements of the AP.

The intra- and extracellular measurements of AP transients could be recorded singly on an X-T chart recorder, but usually they were simultaneously captured and displayed by utilizing the computer data acquisition programs (Section 4.3 and Appendix 4).

For example, in the experiment represented by Fig. 4.5.1, the X-T chart records of typical internally recorded AP's are shown in Fig. 4.5.2. By the computer acquisition method, the typical internal and external voltage waveforms of an AP were simultaneously recorded and are shown in Fig. 4.5.3.

The internally measured AP waveforms are in good agreement with those reported by other workers (e.g. Gradmann, 1975; 1976) and Fig. 4.5.3 clearly shows the correspondence between the externally measured signals and the occurrence of the AP.

4.5b Multiple External Electrode Measurements and the Identification of the AP Initiation and Propagation.

A typical set of v_n and corresponding computed d_n waveforms from a propagating AP on an ISS in the type B cell holder is shown in Fig. 4.5.4. Also shown are the logging printouts and the analysis of the peak positions provided by the data analysis program. In Fig. 4.5.5 these waveforms are shown normalised to the same peak-peak size and the delay between the negative peaks at successive channels owing to the propagation is clearly displayed (cf. Fig. 4.4.4). In Fig. 4.5.6 the times of the negative peak values are plotted against

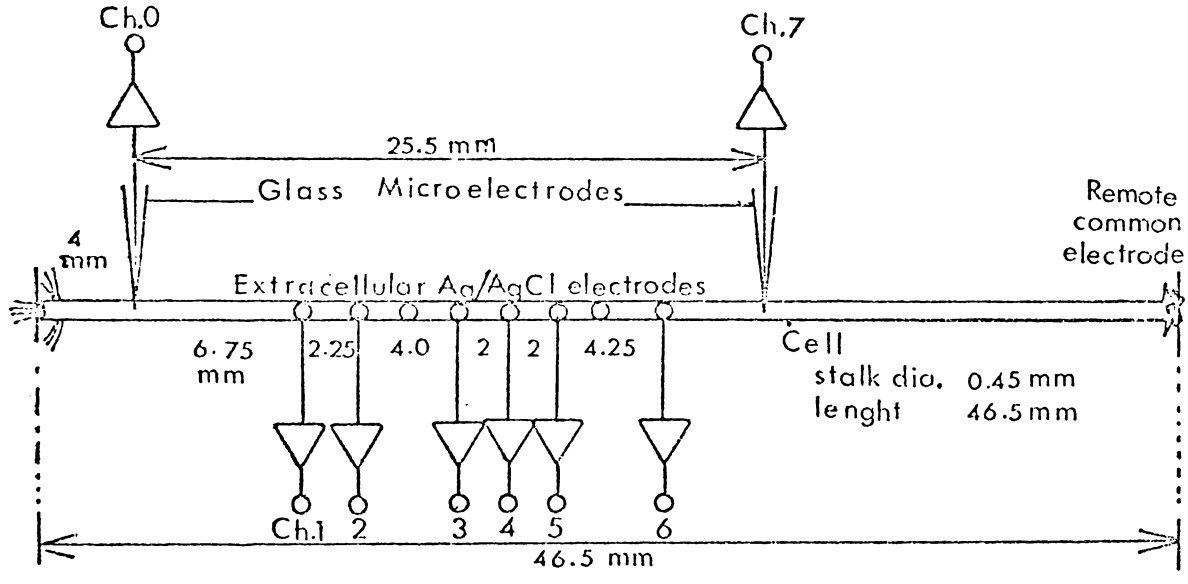

Fig. 4.5.1. Diagram of the Experiment for Simultaneous Recordings of the Intra- and Extracellular Waveforms of the AP Transients.

Fig. 4.5.2. Typical Internal Membrane Potentials Recorded on an X-T chart Recorder.
(Light-triggered Action Potentials)

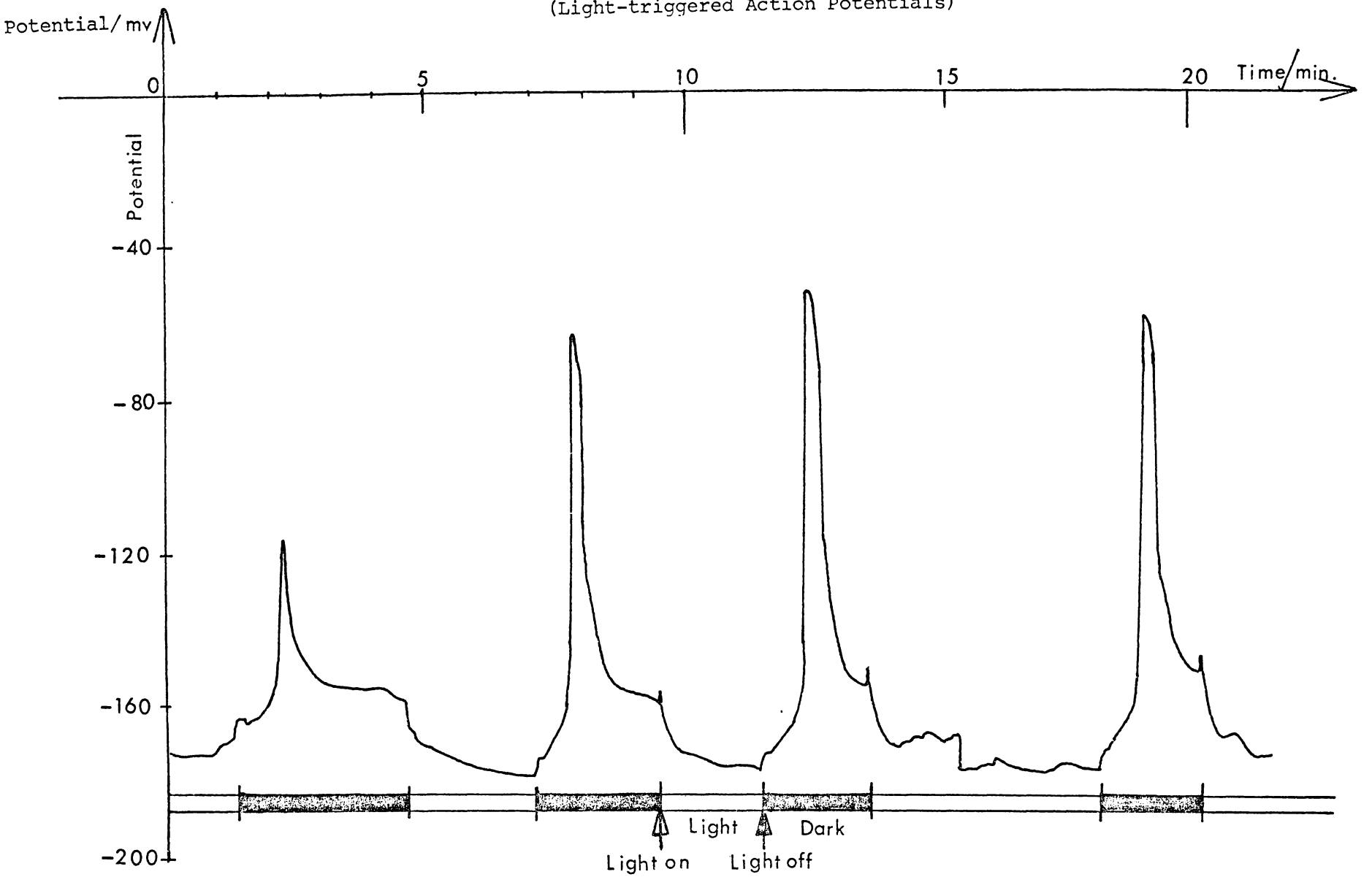

Fig. 4.5.3. Typical Simultaneous Measurement of Intracellular (Ch.0 & Ch.7) and Extracellular (Ch.1 to Ch.6) Waveforms of an AP Transient.

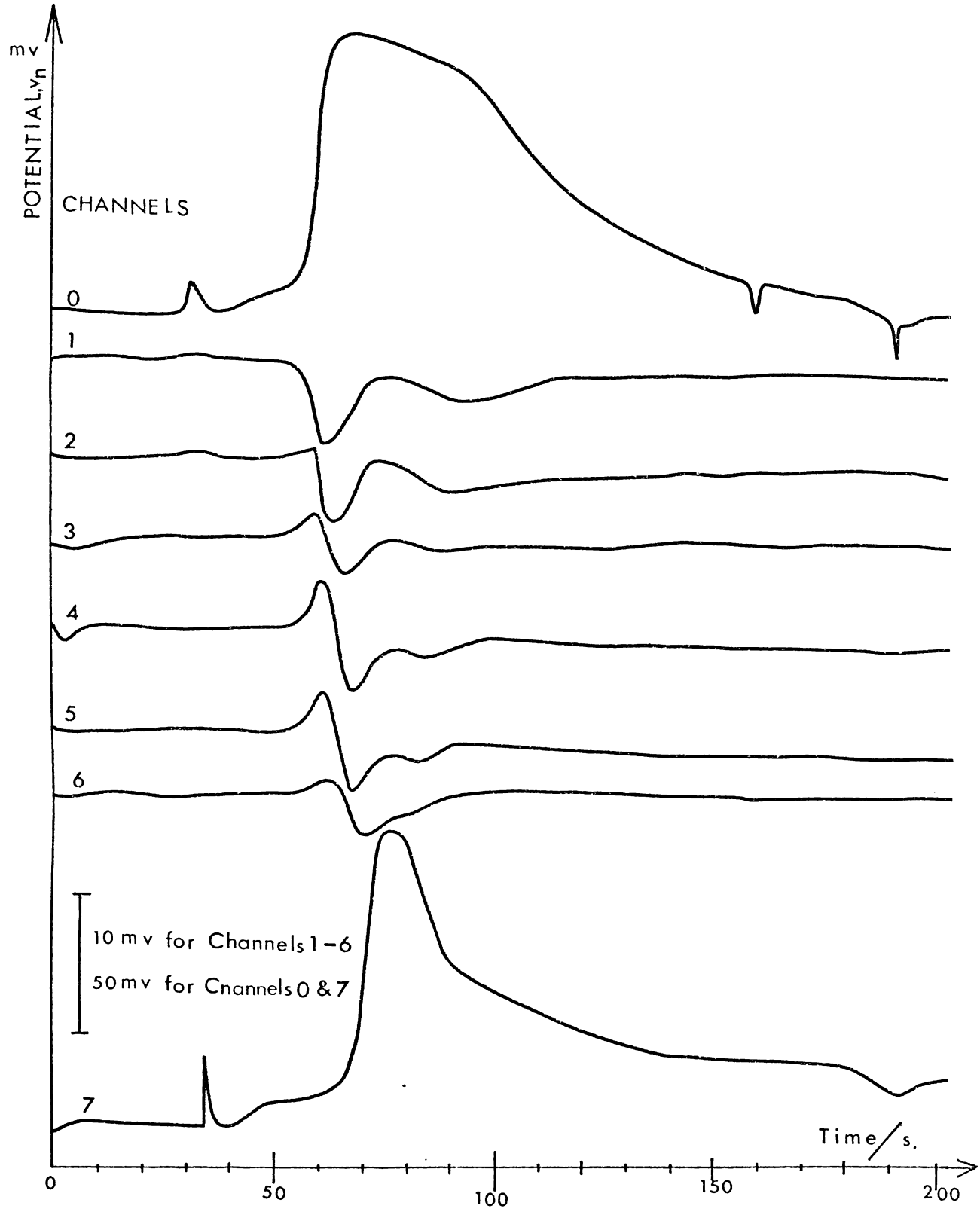

Fig. 4.5.4. Time Dependent Waveforms and Printouts of a Typical AP Transient (Raw Data)

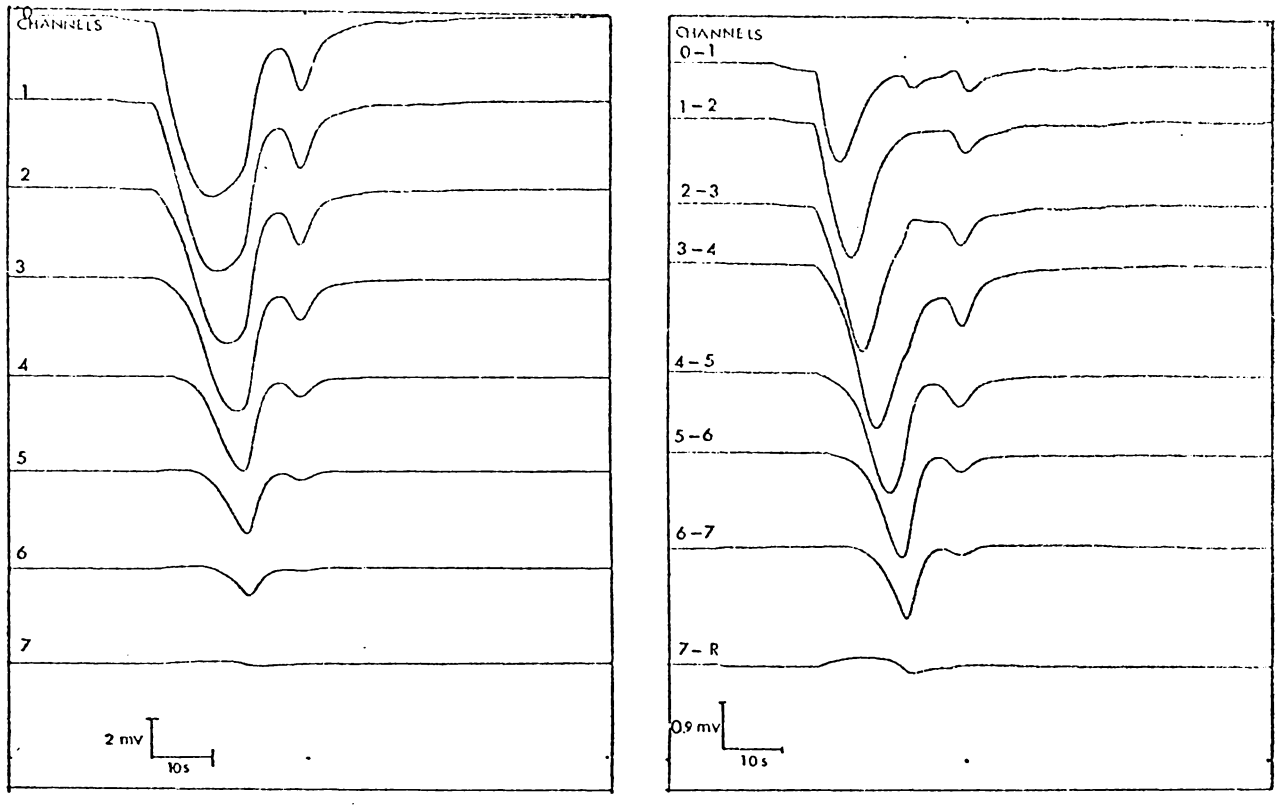

(a) Voltage Waveforms, V(t)

(b) Differential Voltage Waveforms d(t)

```
****  DATA FILE TX2016 LOADED  ****

?Y.
 CHAN   MINVAL MINPOS MAXVAL MAXPOS   SPAN   AV-F100 AV-L100

  :0   -0945     85   -0032   255   +0913   -0306   -0045
  :1   -0897     86   -0036   255   +0861   -0273   -0046
  :2   -0790     91   -0013   255   +0777   -0199   -0020
  :3   -0710     96   -0043   231   +0667   -0169   -0046
  :4   -0460     99   +0031    66   +0491   -0037   +0024
  :5   -0372    101   -0016    66   +0356   -0057   -0029
  :6   -0204    103   -0016    75   +0188   -0037   -0031
  :7   -0039    103   +0002    79   +0041   -0012   -0017

?ZX.
 CHAN   MINVAL MINPOS MAXVAL MAXPOS   SPAN

 0-1   -0185     70   +0013    65   +0198
 1-2   -0264     78   -0020   205   +0264
 2-3   -0255     82   +0070   104   +0325
 3-4   -0379     88   -0065   254   +0314
 4-5   -0169     93   +0082   104   +0251
 5-6   -0197     99   +0007    30   +0204
 6-7   -0167    102   -0006   139   +0159
 7-R   -0039    103   +0002    79   +0041

?
```

(c) Printouts of the Maximal and Minimal Values of the Peaks and their Time Corresponding Positions of Voltage (X) and differential Voltage (ZX) waveforms.

Fig. 4.5.5. Normalised Waveforms

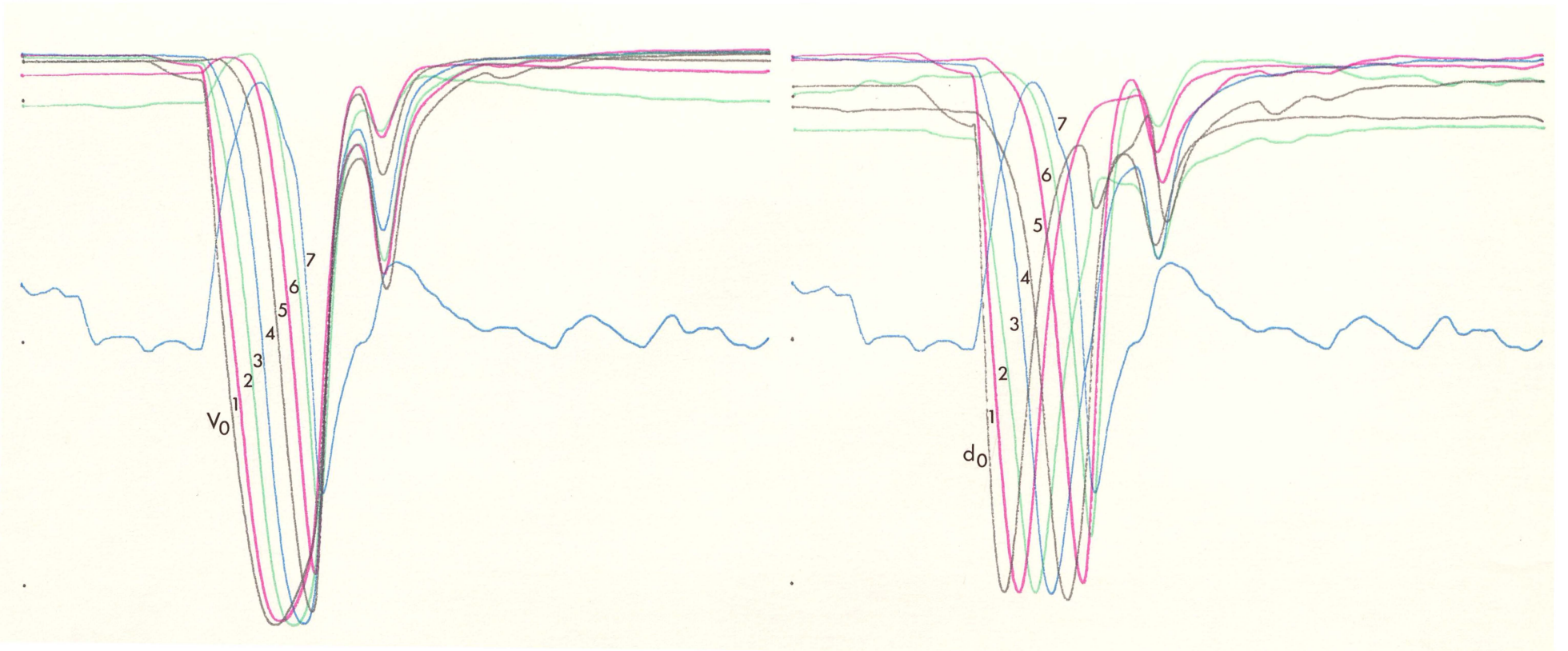

(a) Voltage Waveforms, $\underline{v}(t)$

(b) Differential Voltage Waveforms, $\underline{d}(t)$

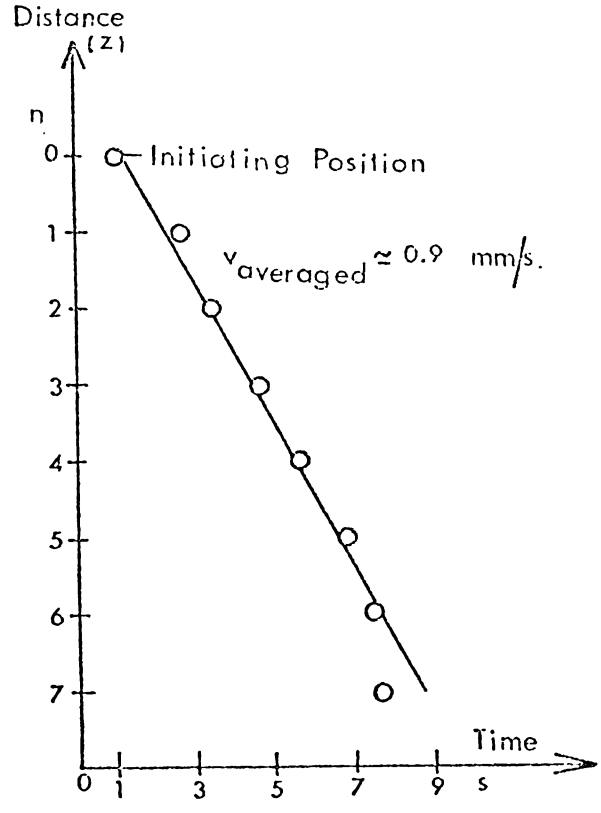

Fig. 4.5.6. Initiation/Propagation Plot.
A plot of the times of the negative peak (extremal) values of d_n vs. distance, z (or electrode position, n).

distance as described in Section 4.4c and it is seen that following initiation in the vicinity of channel 0 the boundary of the depolarised region spreads along the SS with a uniform speed of ~ 0.9 $mm.s^{-1}$.

In Fig. 4.5.7 the $\underline{d}(t)$ waveforms and their initiation/propagation plots are given for a variety of AP's to indicate the range of behaviour observed.

4.5c System Check and Medium Resistivity Measurements.

To check the operation of the transient capture system, the integrity of the electrodes and make a measurement of the growth medium resistivity a constant current was passed along the cell holder, as shown in Fig. 4.5.8.

Fig. 4.5.7. The $\underline{d}(t)$ Waveforms and Their Initiation/Propagation Plots at Various Initiating Positions.

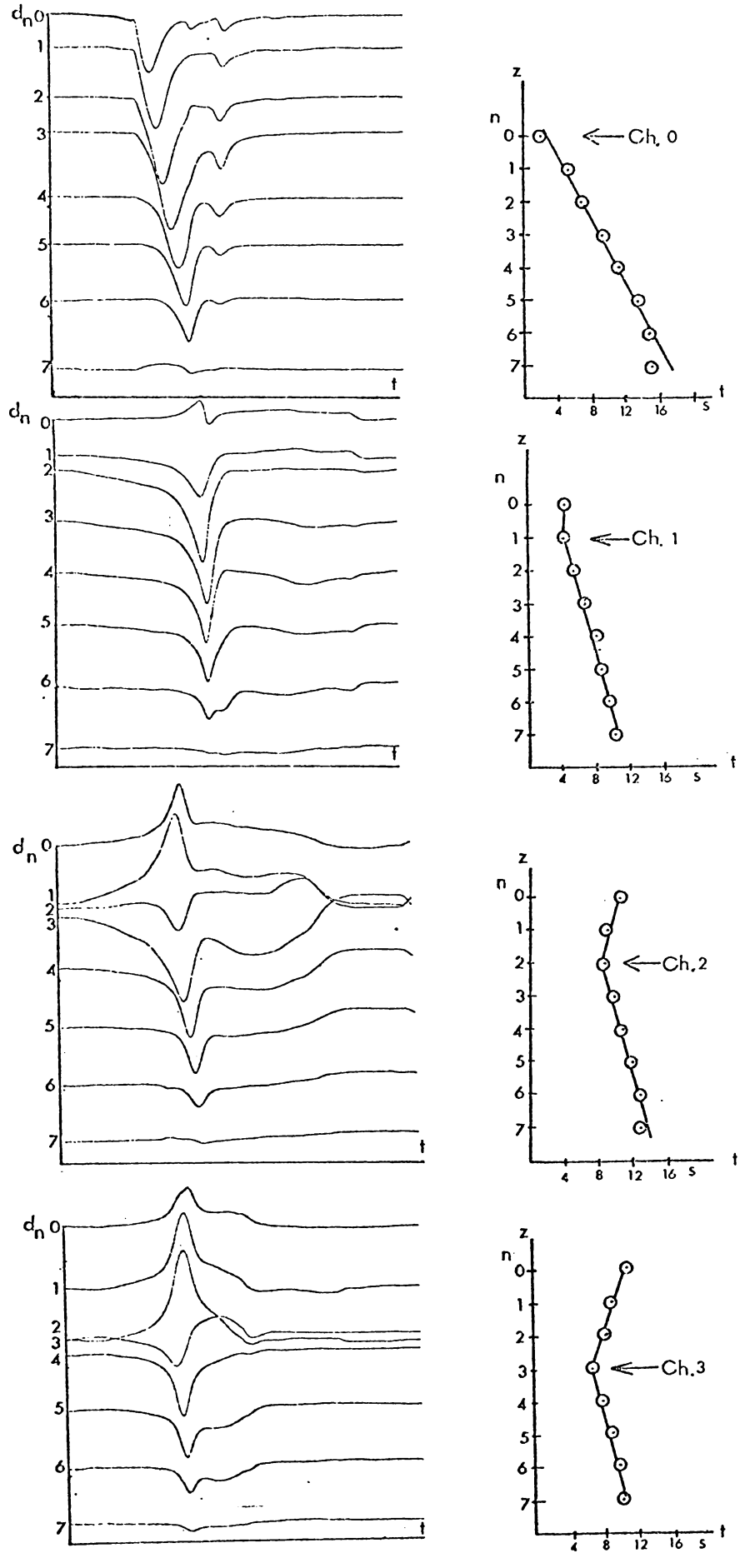

Fig. 4.5.7. (Cont.)

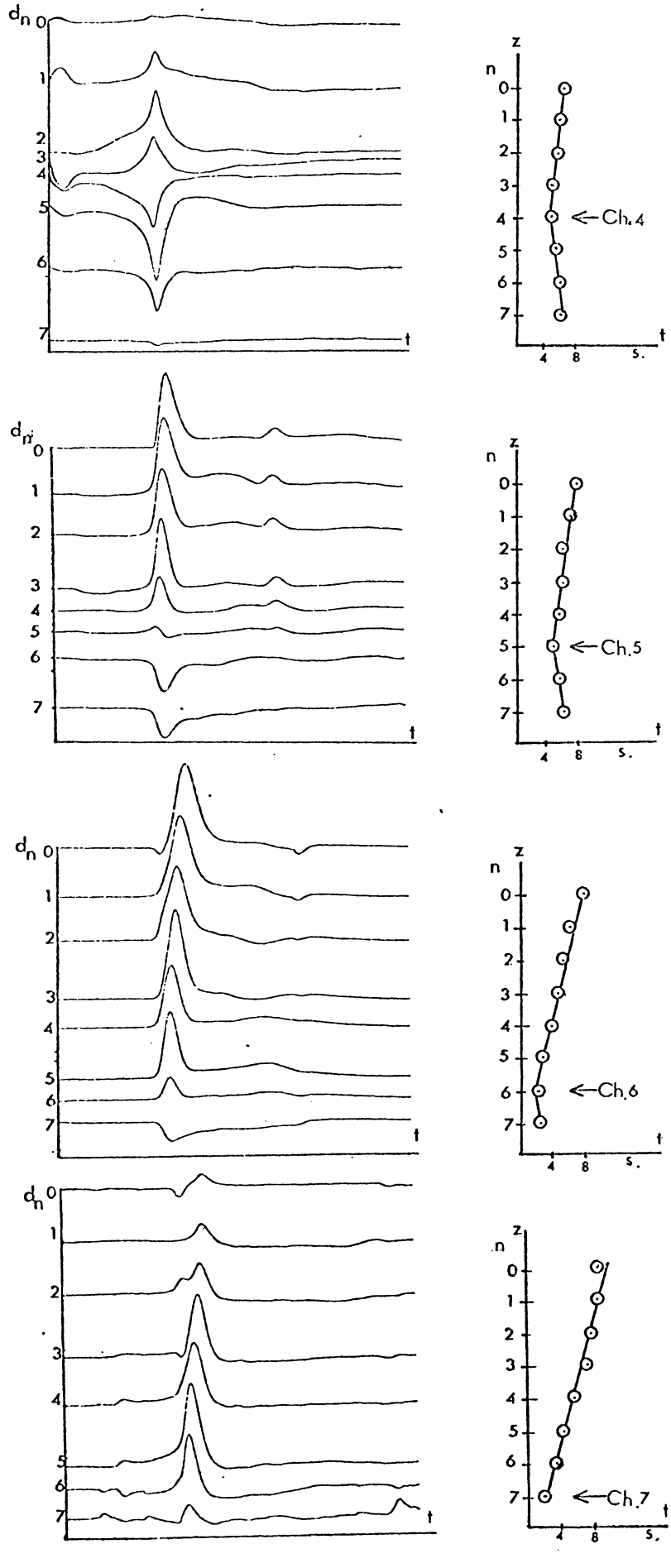
d_n 0
1
2
3
4
5
6
7
t
z
n
0
1
2
3
4
5
6
7
t
4
8
s.
←Ch.4
←Ch.5
←Ch.6
←Ch.7
Scale for all d_n waveforms
1 mv
10s

Fig. 4.5.8. Measurement of the Medium Resistivity.

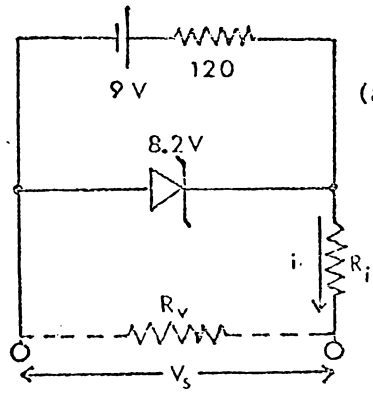

(a) Circuit Diagram of the Constant Current (Voltage) Source.

R_i	i	R_v	v_s
820k	10μA	1k	10mV
8.2M	1μA	1k	1mV

(b) V_n and d_n waveforms produced by the injection of ± 1μA currents.

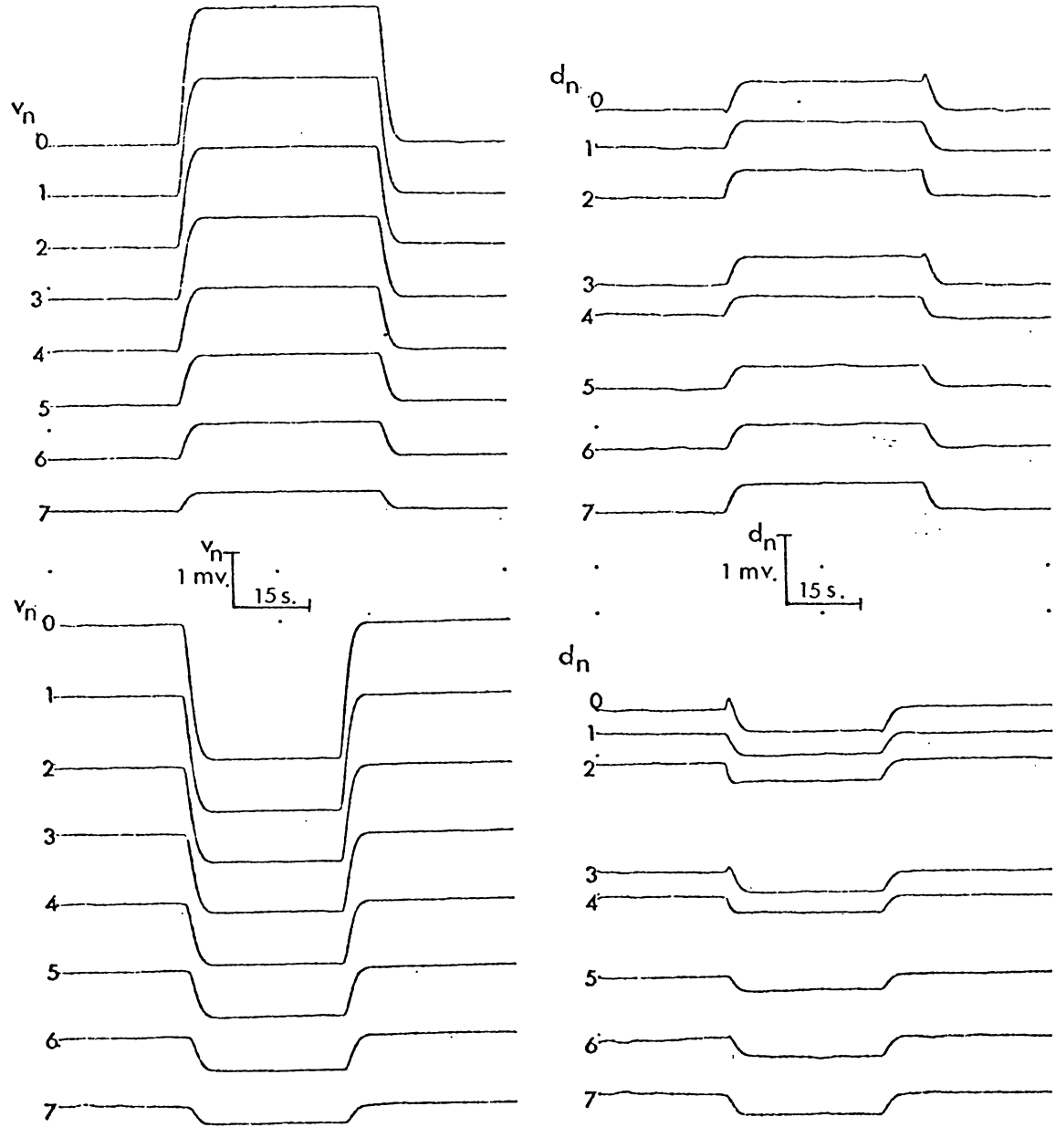

CHAPTER 5

SUMMARY OF EXPERIMENTAL RESULTS.

5.1 Introduction.

The experiments in this work may be divided into four categories, as follows;

(a) General Observations on the Redevelopment of Cut Cells.

Cells which had undergone various cutting procedures were allowed to redevelop while floating horizontally in shallow petri-dishes of growth medium. The statistical frequency of the various types of redevelopment was thereby obtained for conditions comparable to those in the experiments in which the electrical activity was monitored. These results are given in Section 5.2.

(b) The Preliminary Experiment Series (Section 5.3).

These experiments were done on complete cells (CC's) to obtain typical extra-cellular recordings of AP waveforms and some comparisons of extra-cellular and intra-cellular recordings. Both spontaneous AP's and AP's stimulated by illumination changes and insertion of metal needles and glass micropipettes were observed.

(c) The Intermediate Experiment Series (Section 5.4).

In these experiments the electrical activity during redevelopment of single cut cells (both BSS's and ASS's) was monitored and the effect of various external conditions observed. An attempt was made to distinguish between the normal behaviour of the redeveloping cell and the responses to unfavourable conditions.

(d) The Main Experiment Series (Section 5.5).

Detailed measurements of the patterns of electrical activity of developing ISS's are given and the initiation of AP's is correlated with the region of regeneration.

The results presented in this chapter are discussed in detail in Chapter 6.

5.2 Basic Features of the Redevelopment of Cut Cells.

Two groups of cells were studied: (i) young cells aged 17 to 28 weeks (grown normally in the standard culture conditions, Appendix 2, after germinating) having hairy whorls or young caps; and (ii) old cells aged 54 to 63 weeks having young to fully grown caps (c.f. Fig. 2.1.1). The growth of these old cells was retarded by the techniques mentioned in Section 2.3.

The old cells were found to be more easily damaged especially at the cut ends which were sealed off very slowly. They often formed permanent clear patches at the bruised regions, more frequent AP's were obtained (see Section 5.4) and they generally redeveloped at a slower rate.

In contrast the young cells were capable of redeveloping and recovering at a higher rate generally gave less frequent AP's (cf.Tables 5.4.1 & 5.4.2) The ISS's prepared from them showed all the five types of initial redevelopment (Table 5.2.1 and Fig. 5.2.2) but only rarely formed a complete new cap. The ISS's of the old cells rarely showed type V behaviour and were generally able to regrow a complete cap. Typically the regeneration times (time when regeneration is first seen under microscope after exposure to light) of the ISS's from young and old cells were 14 - 50 hours and 48 - 150 hours respectively.

The usual redevelopment of a single cut cell was to replace the lost part. A BSS always regenerated to give a new apex, and an ASS produced a rhizoid-like end (Fig. 5.2.1), provided it was exposed to light within $\leq$ 7 days of cutting. These redevelopments were found to initiate from as soon as $\simeq$ 10 hours to up to $\simeq$ 72 hours after the cells had been exposed to the light. A BSS was obviously capable of regenerating a new complete mature cap, but an ASS (> 13 mm. long) can only regenerate the rhizoid-like end with the existing apex exhibiting

Fig. 5.2.1 Schematic Diagrams of the Developments and/or Re-developments of Single Cut Cells.

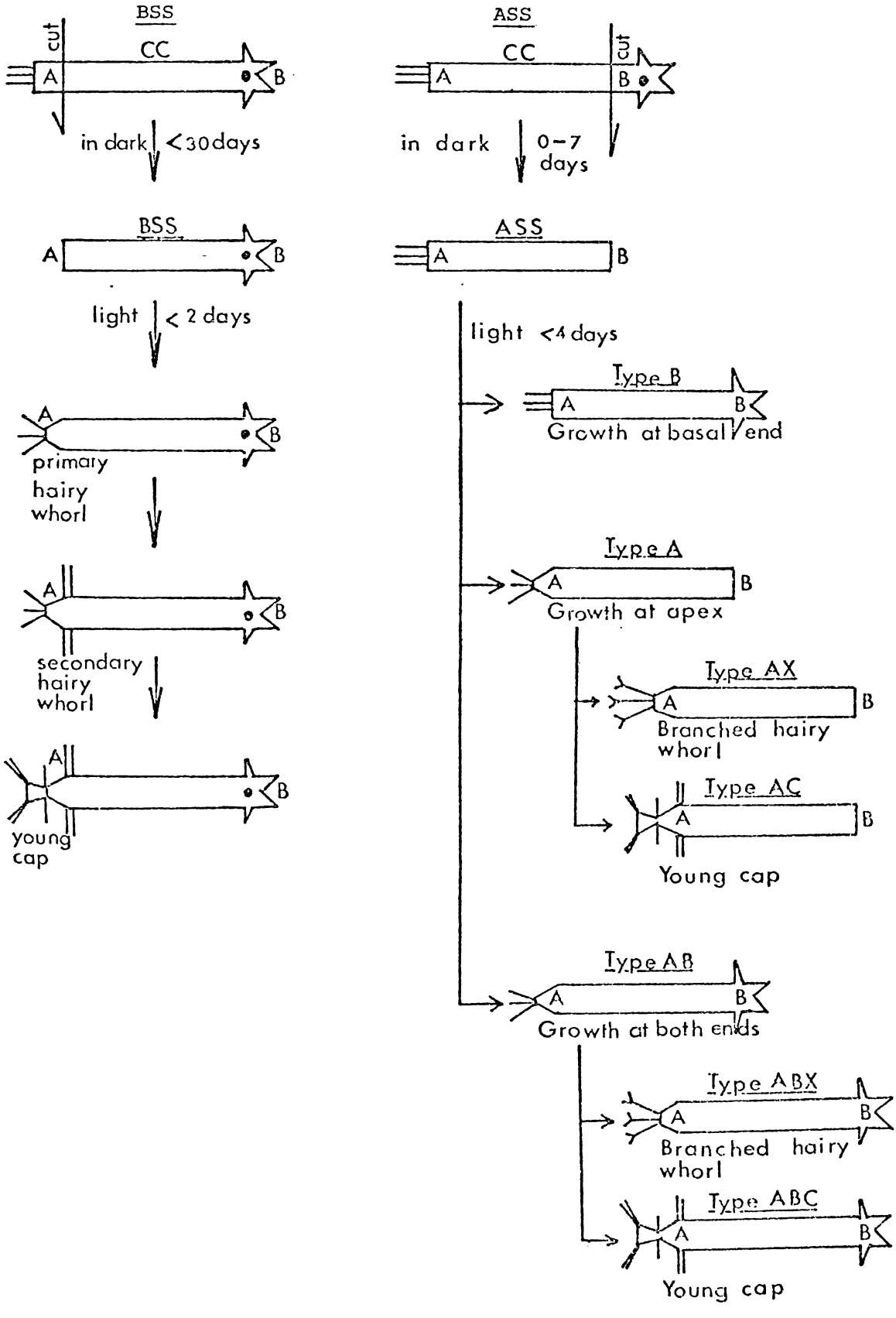

limited further development, e.g. from a hairy whorl to a young cap. Development of a full cap was rarely seen, presumably due to the lack or shortage of 'cap-producing morphogens' in this anucleate system. (Similar limitations were also seen in redeveloping ISS's.) A shorter ASS (≤ 8 mm. long) was likely to regenerate a hairy-whorl-like end (Plate 5.2.1). The more advanced the apex (larger cap) and the shorter the ASS, the more complicated was the regenerating end. This may be indicative of the higher amount of 'cap-producing morphogens' accumulated in the apical end, as has been suggested by Hammerling's experiments (1963).

Experiments on ISS's showed several different degrees of redevelopments which may be classified into five types (Fig. 5.2.2, and Plate 5.2.2):

Type I Absolute Single Regeneration.

The new apex, either a hairy whorl or a young cap, is regenerated at one end (former apex A or former base B), while the other end shows no significant changes, i.e. it is just sealed off and the nearly uniform cylindrical stalk is still maintained at that end.

Type II Single Regeneration with Changing End.

The new apex is regenerated while the other end changes to be either a match head-like (dome-shaped) or a flat protuding end. This type was the most common case in this experiment.

Type III Double Regeneration with one Real Apex.

Both ends regenerate, usually B first in > 3 days, then followed by A, to be two pointy ends. Then one of them develops further into a more advanced stage of cap formation, i.e. a secondary hairy whorl or a young cap is formed while the other remains pointy and its further redevelopment is terminated.

Type IV Double Regeneration with two Apices.

Both regenerating ends can go on redeveloping very slowly (> 7 days)

Plate 5.2.1. Hairy whorl-like Regeneration at cut basal ends of ASS's < 8mm long with various cap forming stages.

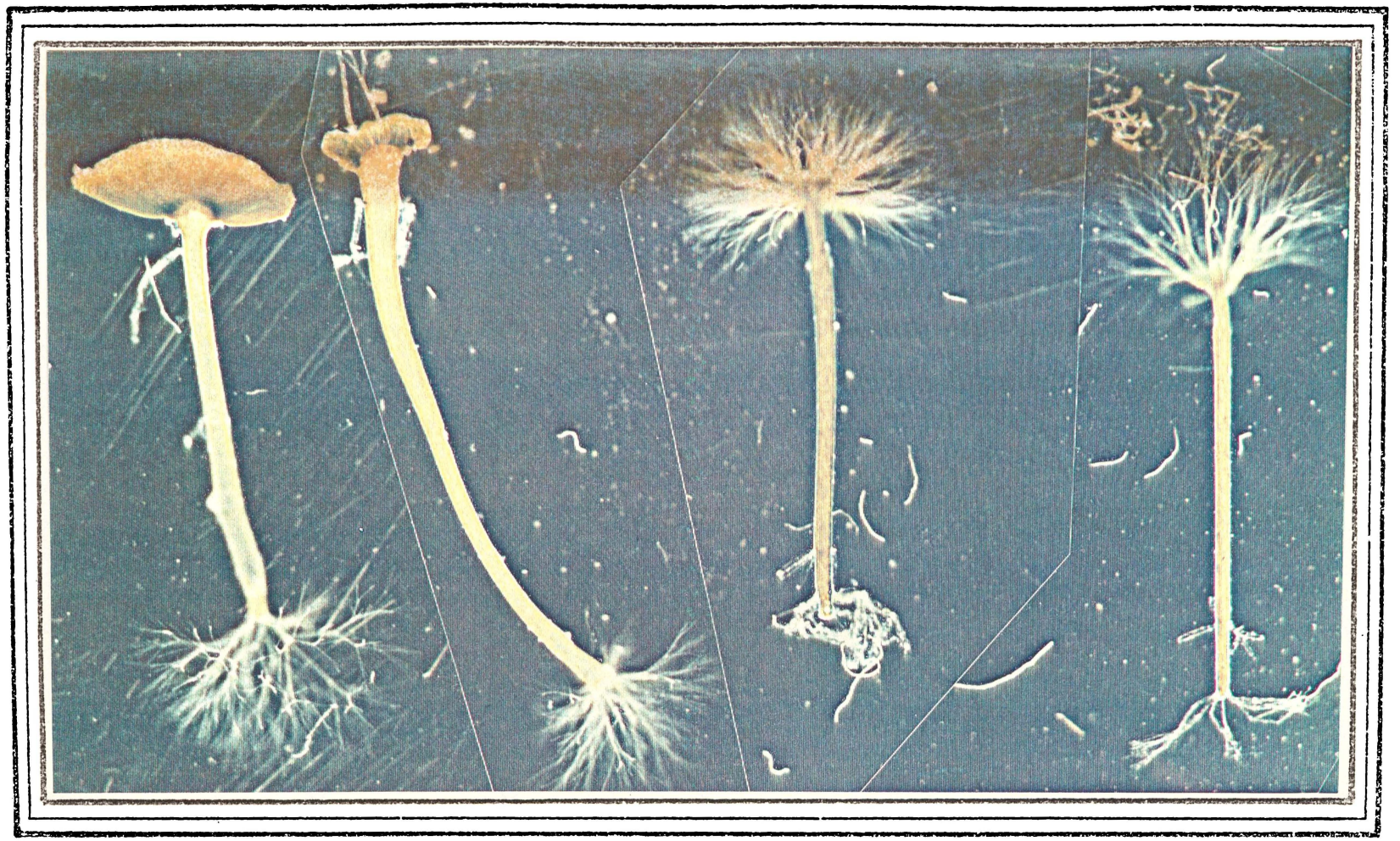

Scale: 1mm 1mm 1mm 1mm

Fig. 5.2.2. Schematic Diagram of the Types of Re-developments in an ISS.

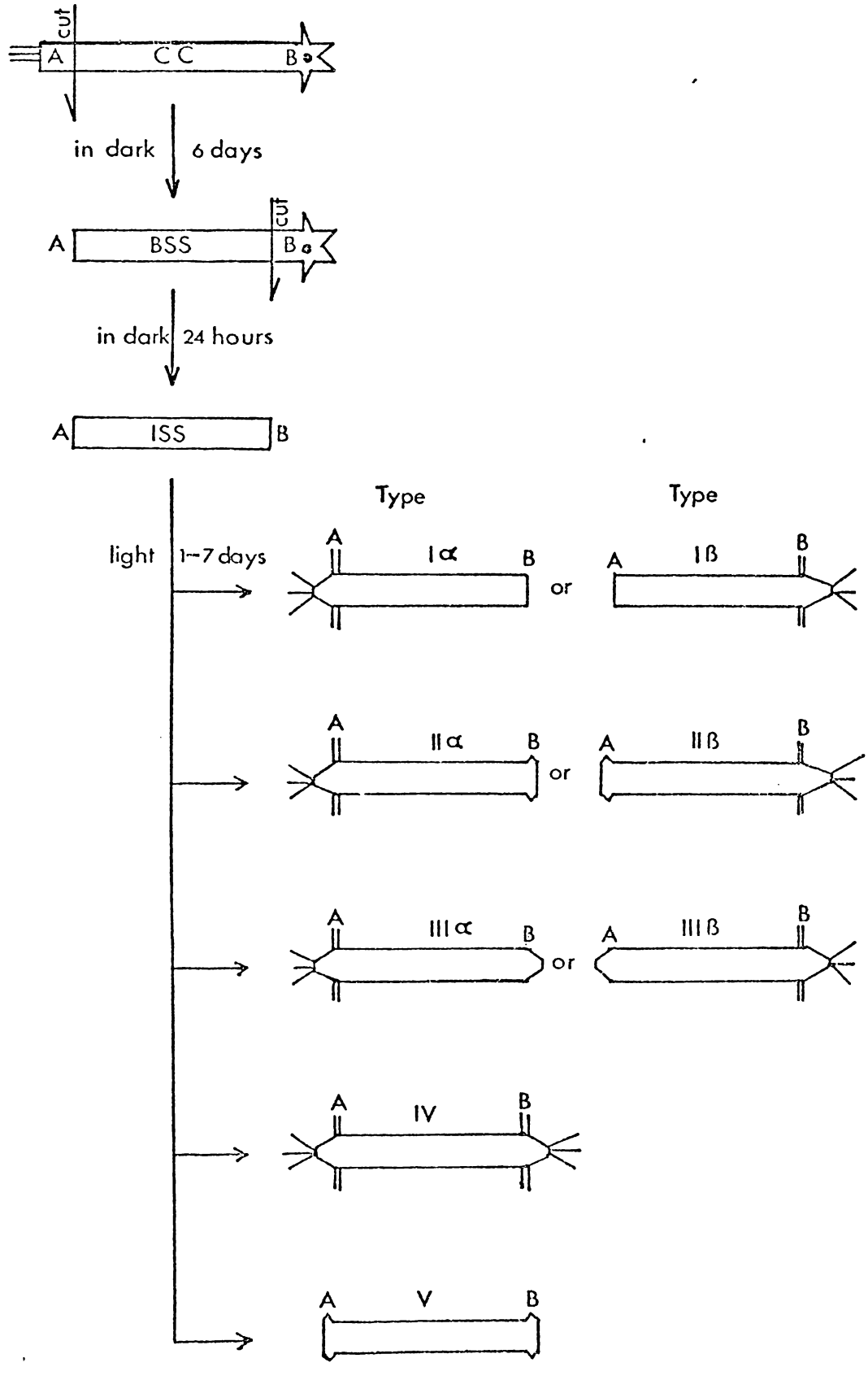

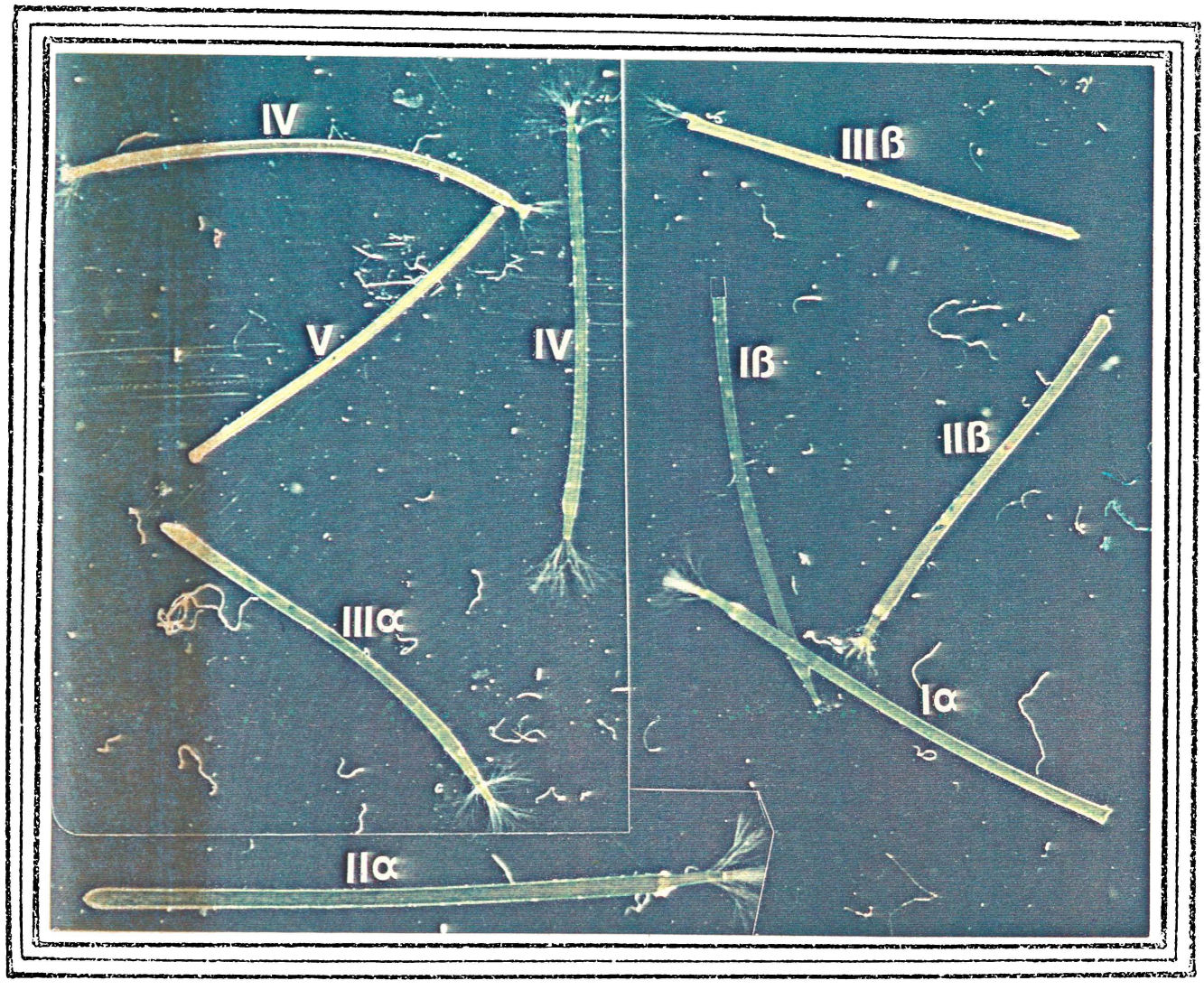

Plate 5.2.2. Five Major Types of Re-development of ISS's. (cf. Fig. 5.2.2)

Scale: ⊢⊣ 0.75mm for IIα

1.0mm for others.

(Specimen Iβ regenerated at former basal end but the apical end was damaged, i.e. small clear patch was formed, at the time when the photo was taken.)

and result in two hairy whorls or young caps very similar in shape and size (Plate 5.2.2).

Type V Negligible Regeneration at Either End.

The ISS just seals off both ends and remains in this form or exhibits just a slight dome-shaped extension of each end.

In Table 5.2.1 the polar regeneration of the ISS's prepared by the standard cutting procedure (Section 2.4) for the main experiment series (Section 5.5) is categorised according to the scheme described above. The majority ($\simeq$ 66%) of the 356 ISS's exhibited apical-type regeneration at the previous apical ends (types Iα and IIα, Fig. 5.2.2), suggesting that the dark treatment did not induce a complete loss of the previous polarity in all cells. However, a sufficient number did exhibit reversed polarity on regeneration for the purposes of the present work. The typical times taken for regeneration to become visible are summarised in Table 5.2.2.

The ISS's prepared by the reversed standard procedure (i.e. the rhizoids were cut first, the resulting ASS's then being left in the dark for 5 - 7 days before removing the apices) rarely survived. They usually formed long clear patches in the cytoplasm. Those that formed short patches were found capable of some early apical-type regeneration but no young caps were seen. The most common case was that these cells showed no regeneration at all, and regeneration at both ends was extremely rare. Because of these difficulties no ISS's prepared in this way were used in the electrophysiological experiments.

Table 5.2.1: SUMMARY OF THE OBSERVED POLAR REGENERATION ON THE ISS's PREPARED FOR THE MAIN EXPERIMENT SERIES

Expt.	Age of cell/wks.	Regeneration Type [1]			
		Iα,IIα,IIIα	Iβ,IIβ,IIIβ	IV	V
A1	60	9	3	-	-
A2,A3	61-62	4	1	-	-
B1,B2	62-63	3	-	-	-
A4	17	4	-	-	-
A5,A6	19-20	17	7	1	-
A7	21	9	6	-	-
A9	23	11	4	1	3
B3	22	12	7	-	1
B4	24	28	10	3	1
B5	25	20	12	1	7
B6	27	19	4	-	2
B7	27	53	14	1	2
B8	28	46	10	1	21
Total (356)		235	78	8	35
Percentage		66	22	2	10

[1] Regeneration at former apical end (Types Iα, IIα, and IIIα; cf. Fig. 5.2.2), basal end (Types Iβ, IIβ, and IIIβ); both ends (Type IV) and no regeneration (Type V) respectively.

Table 5.2.2: OBSERVED REGENERATION TIMES.

Regeneration Time/days	Number of cells	Percentage (Approx.)
< 1	69	21
1-2	114	36
2-3	73	23
3-4	17	5
4-5	20	6
5-6	16	5
> 6	12	4
Total	321 cells	

Young cells (aged 12-16 weeks) were used for producing ISS's by cutting both ends at nearly (< 1 min. interval) the same time. They showed a higher percentage of survival than those prepared by the reversed standard procedure and a capability of redeveloping into any of the five types of redevelopment mentioned previous (Fig. 5.2.2) provided they were exposed to light within 10 hours after being cut. However, any movement or handling of these specimens or the medium in which they were floating could result in the formation of clear patches in the cytoplasm. Consequently they were not able to be used as specimens in the main series of experiments. It was of interest that when two portions of equal length from both ends of a CC were cut off at the same time, the longer the resulting ISS the more complicated its redevelopment and the shorter the time this redevelopment took.

Keeping either an ISS or an ASS (before the second cut to produce an ISS) in the dark for < 7 days did not destroy their ability to redevelop. For a BSS this period could be much more longer

(< 30 days).

No investigation of the effects of gravitational or illumination intensity gradients along the length of the cell was made in this work. The cell SS was maintained horizontal under uniform illumination in all experiments to eliminate any such effects. Even so, there was some indication that geotropism or phototropism may be important in the re-developmental process from the fact that the redeveloping apical ends were sometimes observed to grow off-axis in the upper part of the stalk segment (e.g. see Plate 5.2.3). In further developments of this work a careful investigation of such effects would probably be worthwhile.

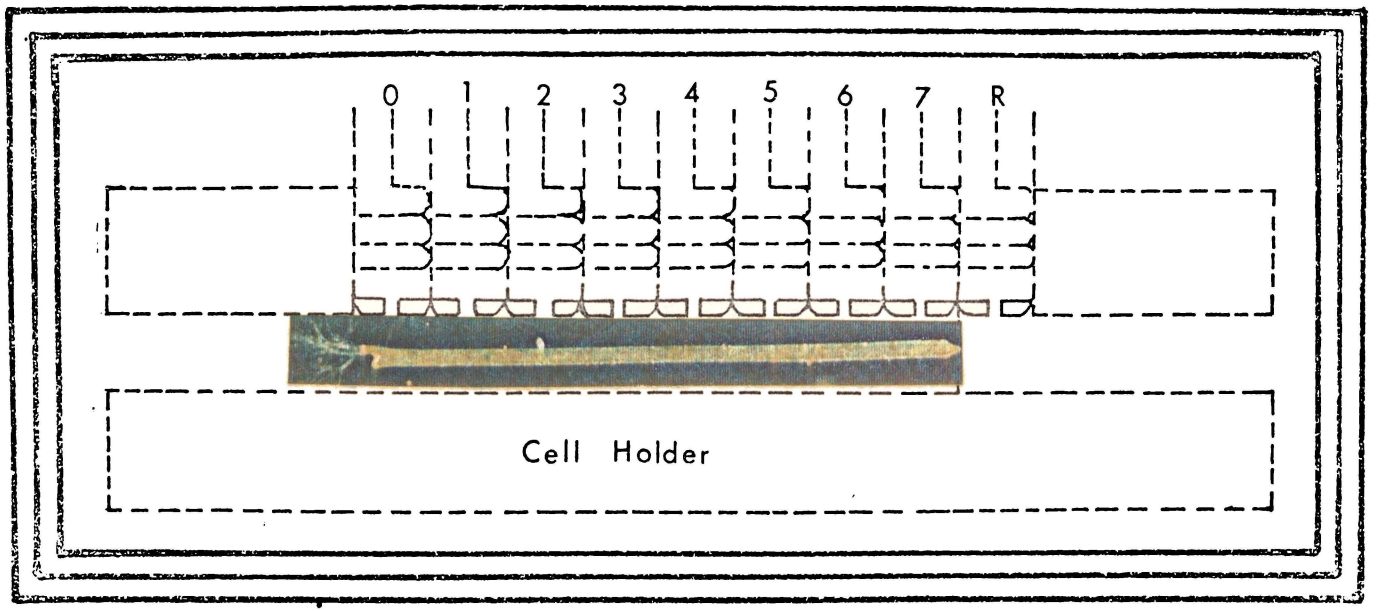

Scale: 2mm

(for specimen only)

Plate 5.2.3. Eccentric Protuberance of Regenerating end.

Specimen was taken from experiment B3 (Section 5.5)
Re-development Type IIIβ.
Schematic Diagram of the set-up is shown in broken lines.

5.3 Results of Preliminary Experiment Series on Complete Cells.

The aim of this series of experiments was to briefly observe the electrical behaviour of complete cells growing in normal culture conditions (Section 2.2) and their response to puncturing with a micropipette, (i.e. to physical damage).

5.3a Behaviour of a Normally Developing Complete Cell.

In Fig. 5.3.1 an X-T chart record of the potential recorded by a single external electrode from a normally developing young cell is shown. Over the 15 hour period covered the cell is seen to exhibit a fairly steady sequence of small amplitude local depolarisations (mean interval ~ 20 mins.) and a smaller number of spontaneous propagating AP's (mean interval $\simeq 80$ mins.). This behaviour is quite typical - see Section 3.3 for a discussion of the similarities and differences between local depolarisations and AP's.

The AP's initiate predominantly at the developing apical end and have waveforms very similar to those shown in Fig. 4.5.4 except that they are generally very 'simple' i.e. no secondary depolarisations or other complications (Appendix 5). They are slow rising and falling curves with a typical duration $\lesssim$ 2 mins.

5.3b Responses to Puncturing.

When a glass micropipette (or metallic needle) is introduced into the cytoplasm, the cell immediately displays a sequence of repetitive AP's. Typically they are sharp rising curves and show initiation at the point of insertion. The initial frequency of these AP's may be as high as $\simeq$ 2 min. per AP. However, it decreases as the cell recovers from the injury. Normal AP's (waveforms) are obtained after $\simeq$ 2 - 8 hours. At this time the tip of a pipette is also found to be 'blocked', presumably due to the formation of new cell membrane round the inserted tip and over its end. For the set-up of this experiment

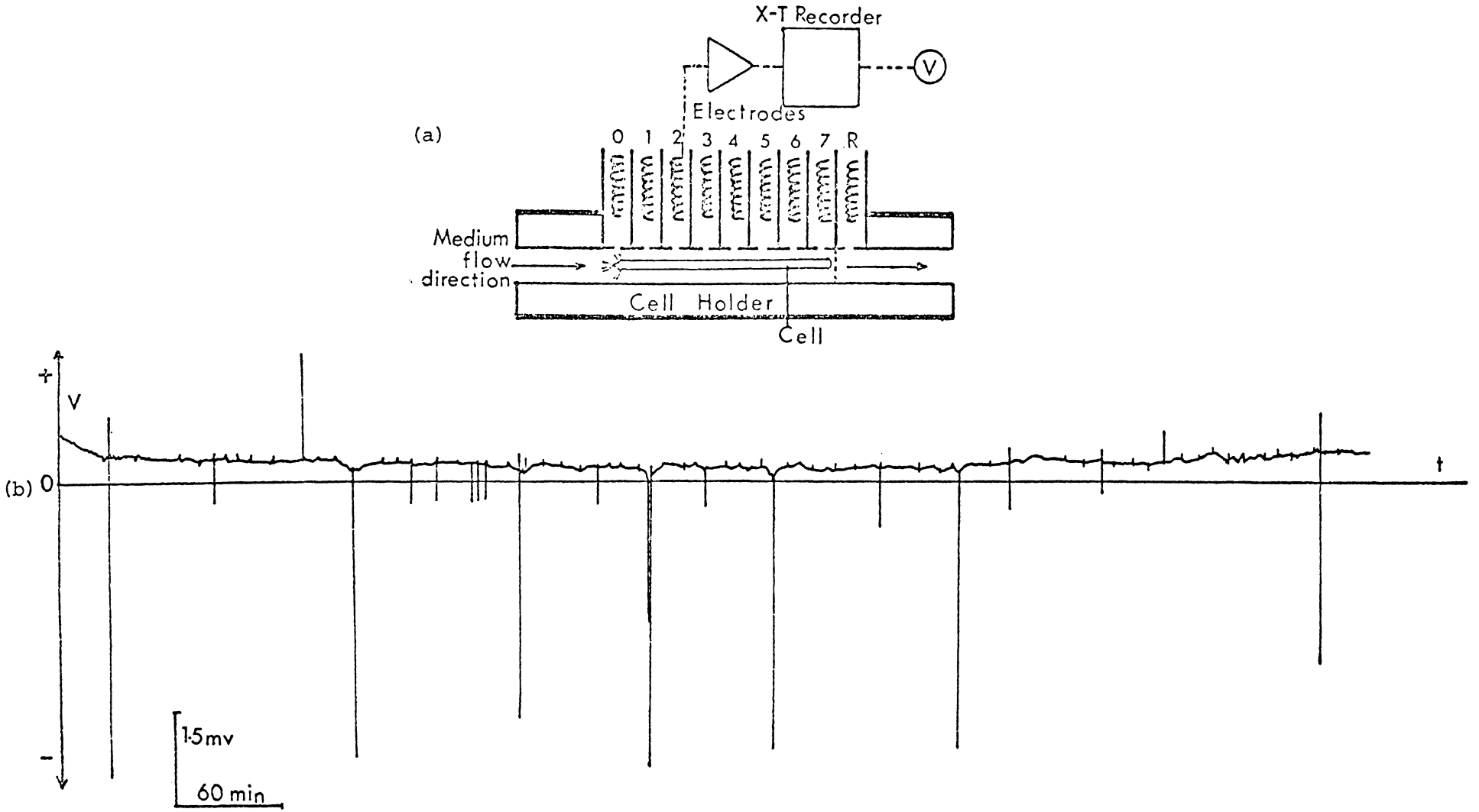

Fig. 5.3.1. Occurence Times of Local Depolarisations (small amplitudes) and AP's (large amplitudes) recorded on an X-T Chart-Recorder (b) from the set-up in diagram in (a).

and the relevant waveforms, see Fig. 5.3.2 a to c respectively.

If a second glass micropipette is introduced into the cell it becomes even more sensitive. The AP's in this situation are more frequent (< 2 min. per AP, see Fig. 5.3.3).

Fig. 5.3.2. Responses of an CC to Puncturing by one micropipette.

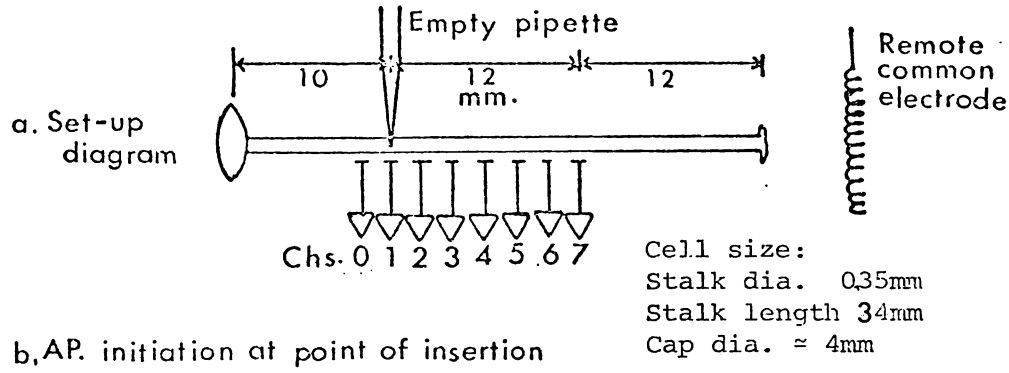

b, AP. initiation at point of insertion

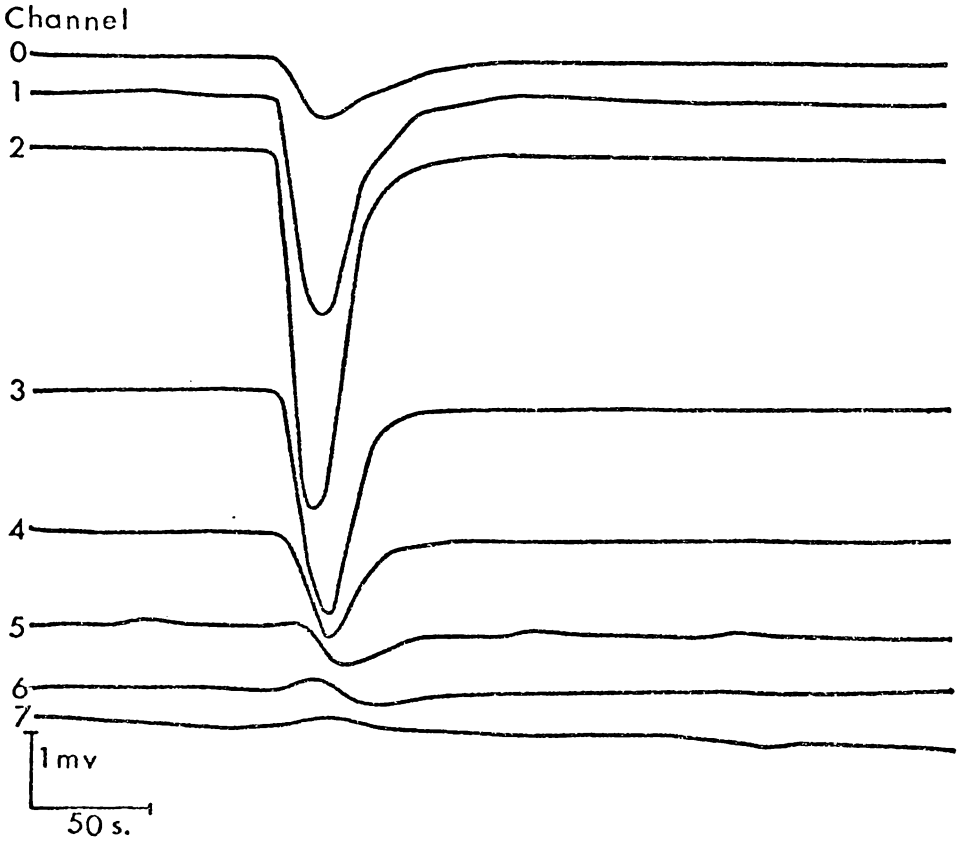

c, Normal AP. initiation elsewhere

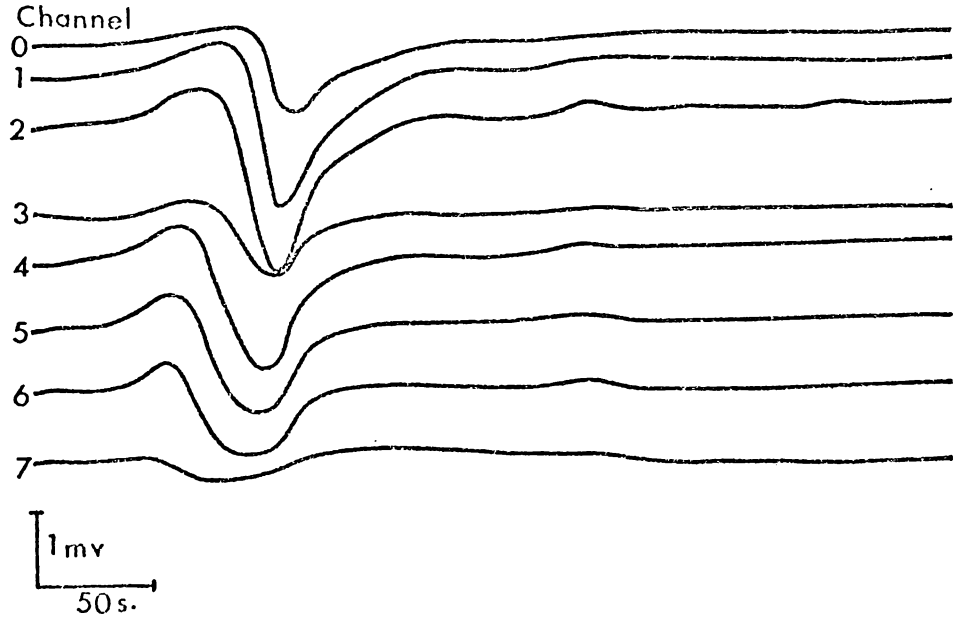

Fig. 5.3.3. Responses of a CC to Puncturing by two microelectrodes.

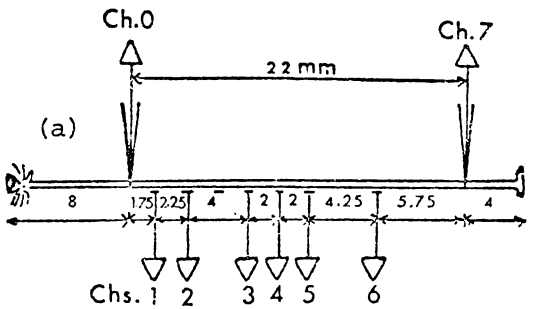

Cell size:
Stalk dia. 0.35 mm.
Stalk length 34 mm.
Young cap dia. ~ 2mm

(a) Diagram of the Set-up

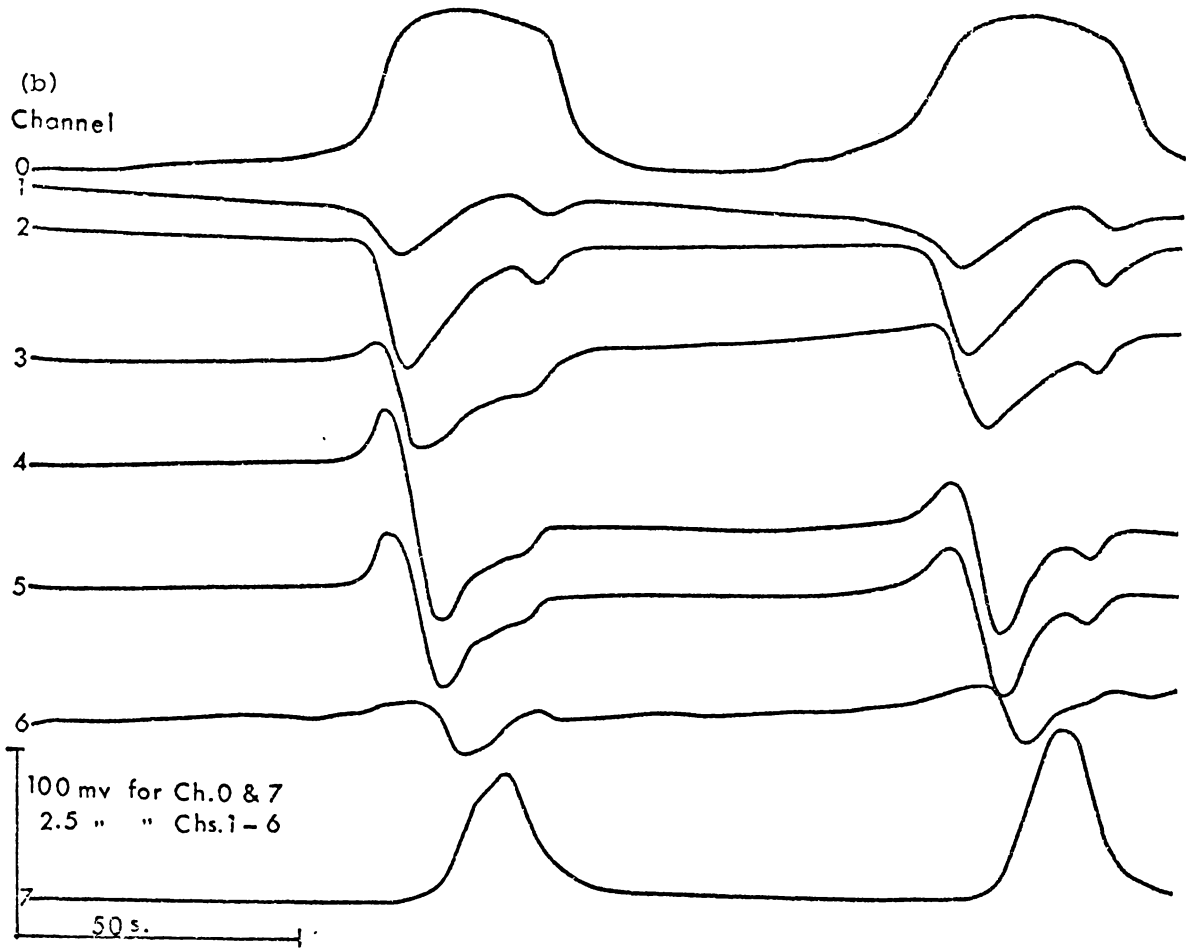

(b) Typical Intra (Ch.0 & Ch. 7) and Extra cellular (Chs. 1 → 6) Potentials Simultaneously Recorded.

5.4 Results of Intermediate Experiment Series.

In this series of experiments, the AP's relating to known (re)developments were studied. They were 'normal' AP's with waveforms similar to those exhibited by complete cells (e.g. Fig. 4.5.4). Conditions under which 'abnormal' AP's recurred were also investigated and criteria for the distinction of these abnormal AP's are proposed.

5.4a Abnormal AP's.

Owing to the fact that the cut cells including the injured CC's and ISS's are extremely sensitive to the surroundings, under the unfavourable experimental conditions they response abnormally. This is indicated both by an anomalously high repetition rate of the depolarisations (mostly AP's, Fig. 5.4.1) and anomalous AP waveforms. Typical waveforms obtained from various defects in experimental conditions (summarised in Table 5.4.1) are shown in Fig. 5.4.2.

5.4b Relation between the Region of AP Initiation and Redevelopment of a Single Cut Cell.

Since single cut cells (ASS's or BSS's) have an established and unambiguous morphogenetic gradient, it is of considerable interest to attempt to correlate the AP initiation characteristics with the known form of regeneration. The result of five such experiments are summarised in Table 5.4.2 (along with one experiment on a CC and two on ISS's) and these will be discussed in some detail later in this section. Firstly however some general conditions and criteria are noted.

(i) In general, a specimen that has a length of 7½ paired electrode spacings (see Sections 2.4 and 4.2a) is imagined divided into three regions corresponding to the spaces between electrode numbers 0 to 2, 2 to 6, and 6 to R respectively (Fig. 5.4.3). The end regions are labelled A and B according to whether they are the (former) apical or basal parts of the cell, and the AP's are categorised as A, B, or M

Fig. 5.4.1. Typical Responses from a Cut Cell being starved (seen in both Intermediate and Main Experiment Series; Sections 5.4 and 5.5). For the Set-up, see Fig. 5.3.1a.

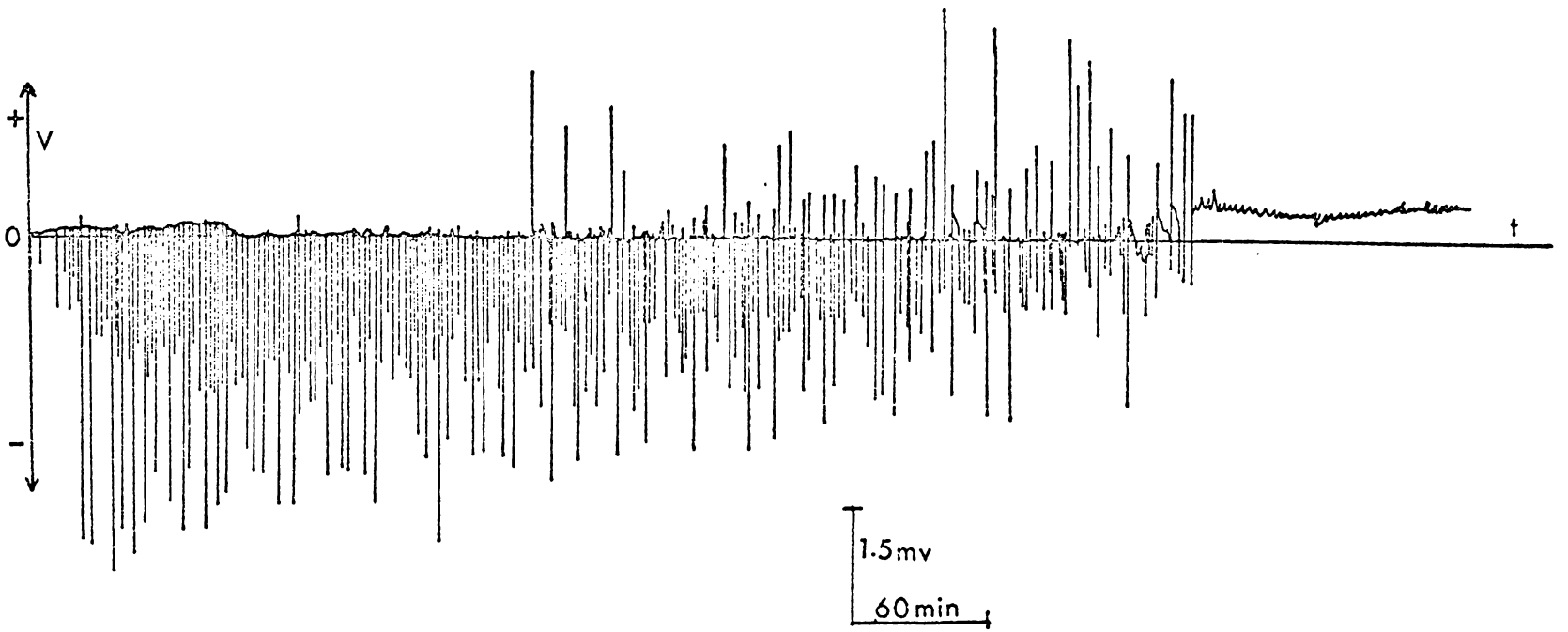

Table 5.4.1 TYPICAL AP's OBTAINED DURING RELEVANT NORMAL AND ABNORMAL TREATMENTS

Case	Cause	Sample AP's	Characteristics of Waveforms	Specifications of Experiments	Similar AP's		AP Initiation at
					Number	in a period of	
(a)	Clear patch	TA 2017	Sharp turning, relatively long lasting	Clear patch developed at near basal end (Ch.7)	46	230 min (5 min/AP)	Ch.6 and Ch.7
		TB 1124 (Fig.5.4.2a)	" " " "	" " " " " (Ch.0)	~100	400 min (4 min/AP)	Ch.0
		TA 6016	Sharp turning, double peaks, long lasting	Clear patch developed near apical end (Ch.0)	48	240 min (5 min/AP)	Ch.0 and Ch.1
		TQ 1018	Highest negative voltage magnitude only at Ch.3	Clear patch developed at near rhizoid, between Ch.0 and Ch.3	10	110 min (11 min/AP)	Ch.3
(b)	A particle irritates cell	TB 4004 (Fig.5.4.2b)	Confusing initiation positions	A large particle collided at the basal end (proximal) and an air bubble developed	7	10 min (1.5 min/AP)	?
(c)	Air Bubbles	TA 7015	Normal waveforms (cf. Fig. 4.5.4)	Air bubble developed at middle region outside of cell	~248	510 min (2 min/AP)	Ch.2 to Ch.4
		TA 8087 (Fig.5.4.2c)	Confusing initiation positions	Air bubble developed at region between electrodes 3 and 7			Ch.6,Ch.7
		TT 8815	Normal waveforms (cf. Fig. 4.5.4)	" " " " "			Ch.3-Ch.7
(d)	Starvation	TA 7069 (Fig.5.4.2d)	> 2 spikes in one transient	Cell near dead, insufficient medium supply	250	500 min (2 min/AP)	Ch.3-Ch.4
		TT 7072	Confusing initiation positions	Cell being starved, insufficient medium supply, cell was not yet killed.	77	850 min (11 min/AP)	Ch.0→ Ch.7
(e)	Contamination	TA 1010 (Fig.5.4.2e)	Long lasting, slow propagating	Cell being surrounded by oblong motile contamination	112	700 min (6 min/AP)	Ch.0-Ch.7
(f)	Direct Sunlight	TA 3015 (Fig.5.4.2f)	Double spikes, long lasting	Direct sunlight shone on cell	49	170 min (3.5min/AP)	Ch.3

Fig. 5.4.2. Typical Abnormal AP's. Relevant to Various Unfavourable Experimental Treatments (cf. Table 5.4.1).

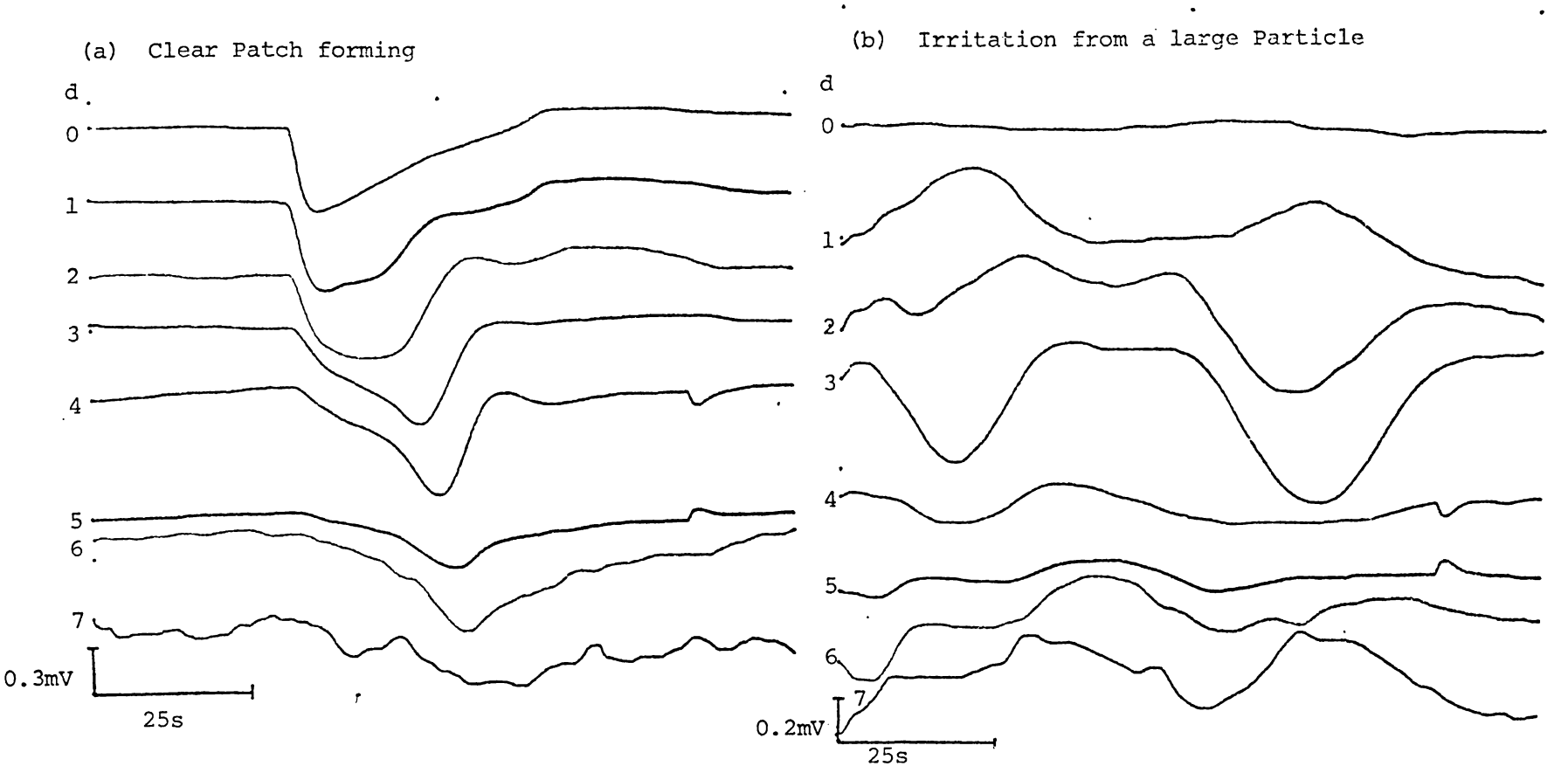

TB1124.ZX.

CHAN	MINVAL	MINPOS	MAXVAL	MAXPOS	SPAN
0-1	-0069	78	+0078	173	+0147
1-2	-0142	81	-0034	179	+0108
2-3	-0074	100	-0001	173	+0073
3-4	-0001	118	+0077	194	+0078
4-5	-0235	124	-0158	62	+0077
5-6	-0114	129	-0002	219	+0112
6-7	+0183	135	+0210	52	+0027
7-R	-0083	187	-0076	61	+0007

TB4004. ZX.

CHAN	MINVAL	MINPOS	MAXVAL	MAXPOS	SPAN
0-1	-0003	195	+0004	8	+0007
1-2	-0006	251	+0039	47	+0045
2-3	-0010	158	+0044	65	+0054
3-4	-0047	172	+0016	79	+0063
4-5	-0034	219	+0040	76	+0074
5-6	+0005	11	+0092	219	+0087
6-7	-0040	6	+0016	91	+0056
7-R	-0011	3	+0014	70	+0025

Fig.5.4.2 (Cont.1)

(c) Irritation from Air Bubbles.

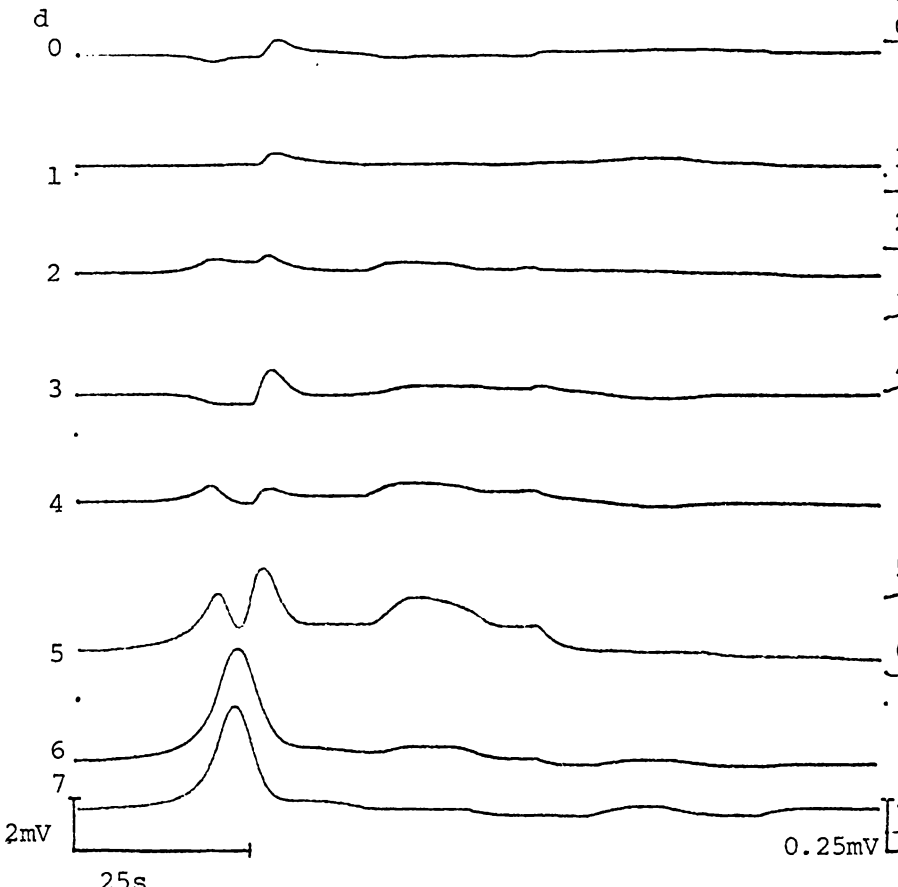

TA8087. ZX.

CHAN	MINVAL	MINPOS	MAXVAL	MAXPOS	SPAN
0-1	-0070	45	+0237	65	+0307
1-2	-0030	223	+0152	63	+0182
2-3	-0117	148	+0117	62	+0234
3-4	-0029	45	+0380	61	+0409
4-5	-0012	179	+0205	60	+0217
5-6	+0045	255	+1317	59	+1272
6-7	+0078	205	+1641	51	+1563
7-R	-0156	149	+0268	50	+0424

(d) Starvation due to Insufficient Medium supply

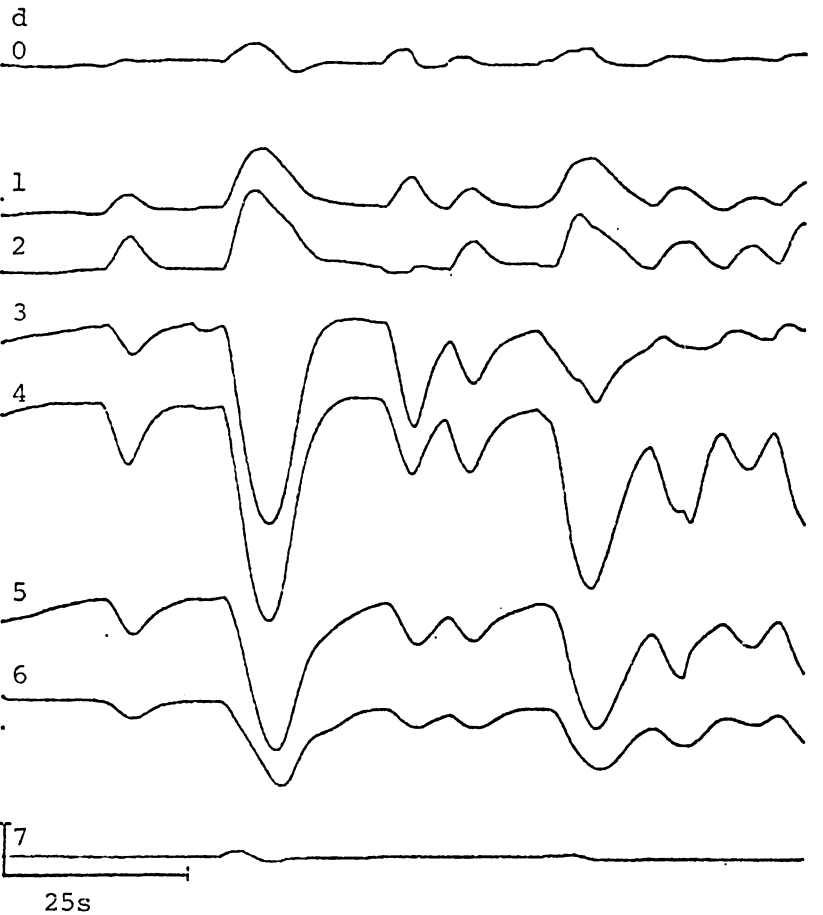

?TA7069. ZX.

CHAN	MINVAL	MINPOS	MAXVAL	MAXPOS	SPAN
0-1	-0032	133	+0006	124	+0038
1-2	-0015	3	+0017	80	+0032
2-3	-0042	124	+0030	79	+0072
3-4	-0045	84	+0058	247	+0103
4-5	-0115	219	-0017	110	+0098
5-6	-0036	85	+0065	219	+0101
6-7	-0048	88	-0009	0	+0039
7-R	+0051	84	+0059	72	+0008

(Fig. 5.4.2. Cont.2)

(e) Contamination in Cell Holder

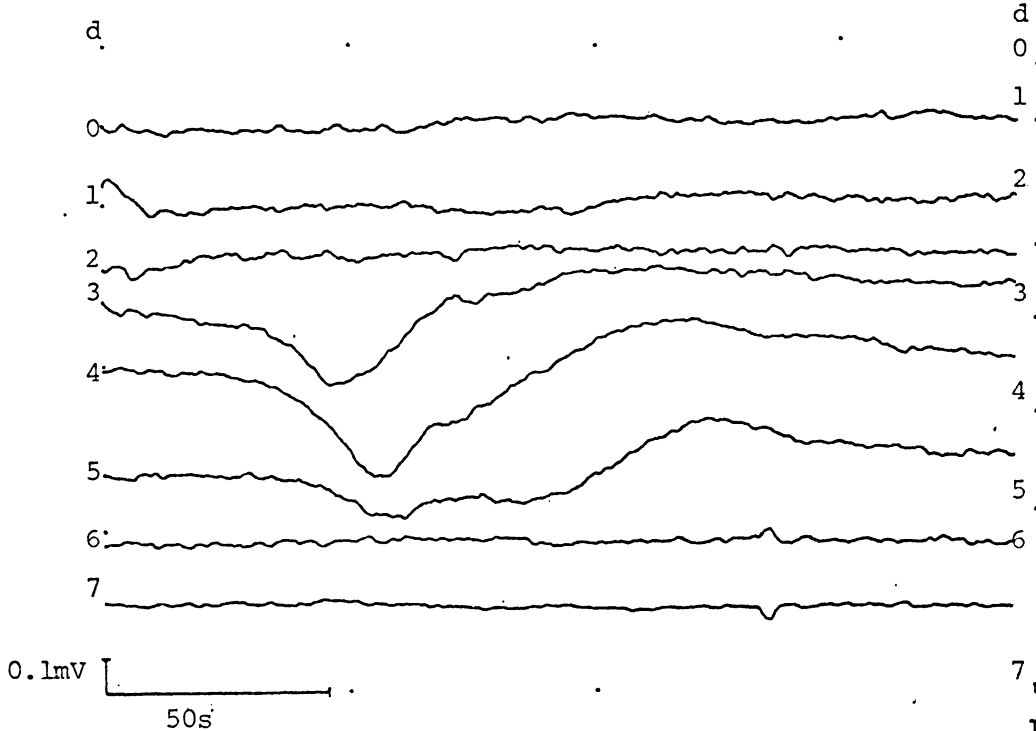

(f) Direct Sunlight shining on Cell

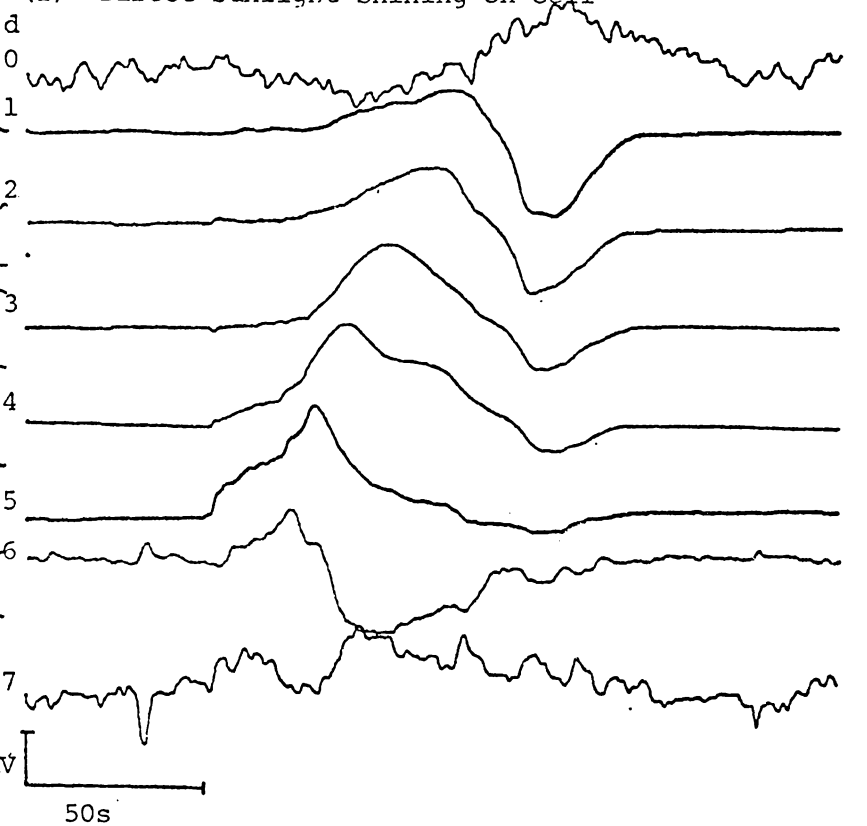

TA1011.ZX.

CHAN	MINVAL	MINPOS	MAXVAL	MAXPOS	SPAN
0-1	+0012	10	+0018	362	+0006
1-2	+0302	50	+0315	3	+0013
2-3	-0274	28	-0265	418	+0009
3-4	-0012	230	+0016	503	+0028
4-5	-0067	270	-0029	608	+0038
5-6	-0133	275	-0109	616	+0024
6-7	-0237	54	-0232	670	+0005
7-R	+0275	670	+0281	134	+0006

TA3015

?ZX.

CHAN	MINVAL	MINPOS	MAXVAL	MAXPOS	SPAN
0-1	-0108	405	-0099	662	+0009
1-2	-0079	659	+0021	528	+0100
2-3	+0041	629	+0152	510	+0111
3-4	-0164	642	-0056	446	+0108
4-5	-0171	660	-0081	394	+0090
5-6	+0315	637	+0382	359	+0067
6-7	-0133	417	-0107	327	+0026
7-R	-0121	146	-0114	401	+0007

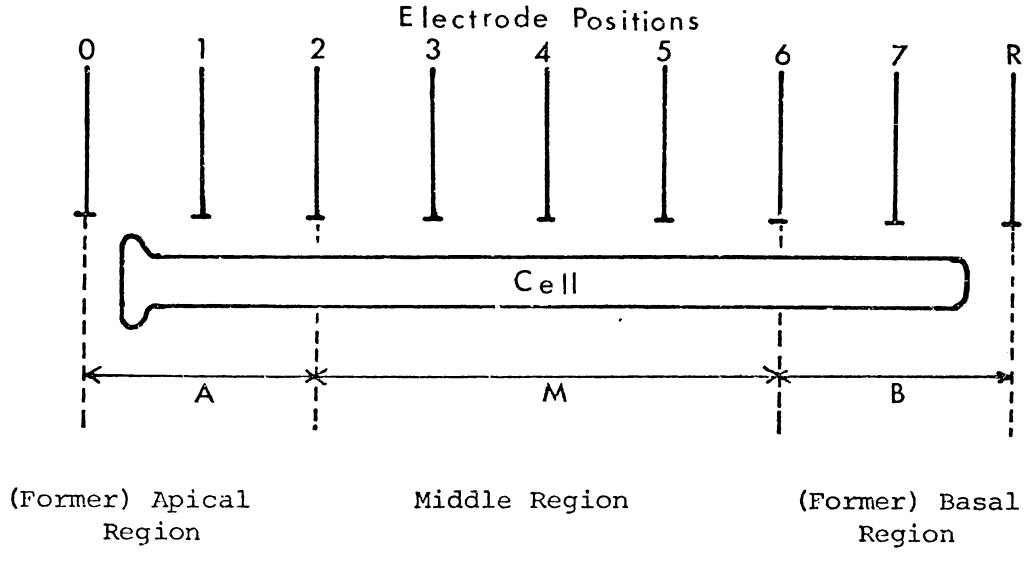

Fig. 5.4.3. Definition of Cell Regions for Comparing AP Initiation.

(middle) - according to where they initiate. (In the case when a specimen is shorter, the related percentages corresponding to those three regions are then applied. For a special case all particulars are mentioned in the discussion of that experiment).

(ii) Only normal AP's (as discussed above in Section 5.4a) exhibited while the cell is clearly seen to be redeveloping (under the 20 × microscope) are accepted to be analysed for the initiation region (as described in Section 4.5b, Figs. 4.5.4 to 4.5.6).

The experiments summarised in Table 5.4.2 are now discussed in detail.

Experiment N1 (Normal young complete cell).

This young cell clearly showed the differentiation at the apex, by developing from the original hairy whorl into a young cap of ~ 1 mm. in diameter within 36 hours. There were 27 AP's (and > 30 local depolarizations) recorded in the 45 hour experiment. Three AP's were rejected as abnormal owing to medium feed system and handling problems. The rest were analysed for the initiation positions, and then plotted as a function of actual experimental time (Fig. 5.4.4).

The diagrams of the experimental arrangement and the observed development are also shown in Fig. 5.4.4.

The result shows predominancy of the AP initiation (18 normal AP's, i.e. 75%) at the developing apex.

Experiment P2 (Basal Stalk Segment)

In this experiment the hairy whorl of a young cell was cut off and the remaining stalk was kept in the dark for ~ 21 hours. It was exposed to the light during the 88 hour experiment. The regeneration (a pointy end) was seen at ~ 31 hours after exposure to light. The new apex developed to be a hairy whorl by the end of the experiment. The regenerated portion (excluding the hairy whorl) was ~ 2.5 mm. long.

Table 5.4.2: SUMMARY OF RESULTS OF INTERMEDIATE EXPERIMENT SERIES

Expt.	Expt. Period /hrs.	Specimen Specifications									No. of AP's / Regenerating periods/hrs.	% ages of AP Initiation at		
		Type	Aged /wks.	Orig. Apex	Stalk dia. / mm.	Stalk length		Regenerating		Redev.[2] Type		A	M	B
						Orig. /mm	cut	end	time[1] /hrs.					
N1	42	CC	25	hairy	0.30	25	-	-	-	-	23/(42)	75	12.5	12.5
P2	88	BSS	23	"	0.25	18	13	A	32	-	28/(56)	91	9	0
X1	90	ASS	18	"	0.25	20	13	B	43	ABX	83/(47)	8	2	90
X2	45	ASS	26	"	0.30	20	14	N	-	ABC	19/(45)	67	22	11
X3	47	ASS	26	"	0.30	20	14	N	-	ABC	15/(47)	60	0	40
Y1	150	ASS	15	"	0.25	22	16	B	25	ABX	63/(83)	35	14	51
T7	61	ISS	21	"	0.30	22	13	A	24	IIα	60/(61)	50	30	20
T8	90	ISS	22	"	0.35	26	13	A	24	IIα	62/(90)	65	21	14

[1] Changes observable under 20 × microscope after being exposed to light.

[2] cf. Figs. 5.2.1 and 5.2.2. A,B = former apical, basal end. N = no regeneration.

Figs. 5.4.4. to 5.4.11 are Plots of Position of AP Initiation as a function of time after illumination of cell segments.

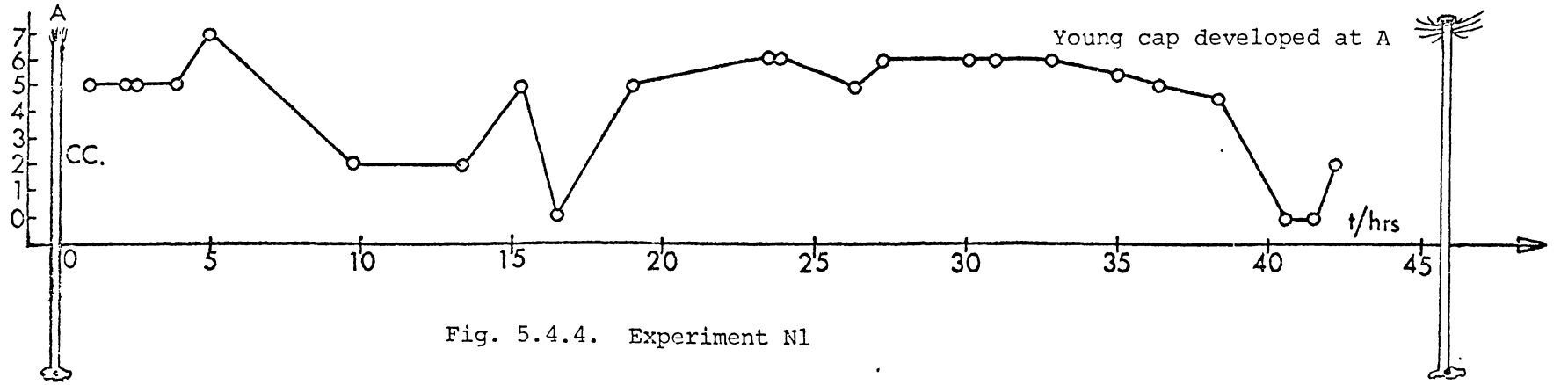

Fig. 5.4.4. Experiment N1

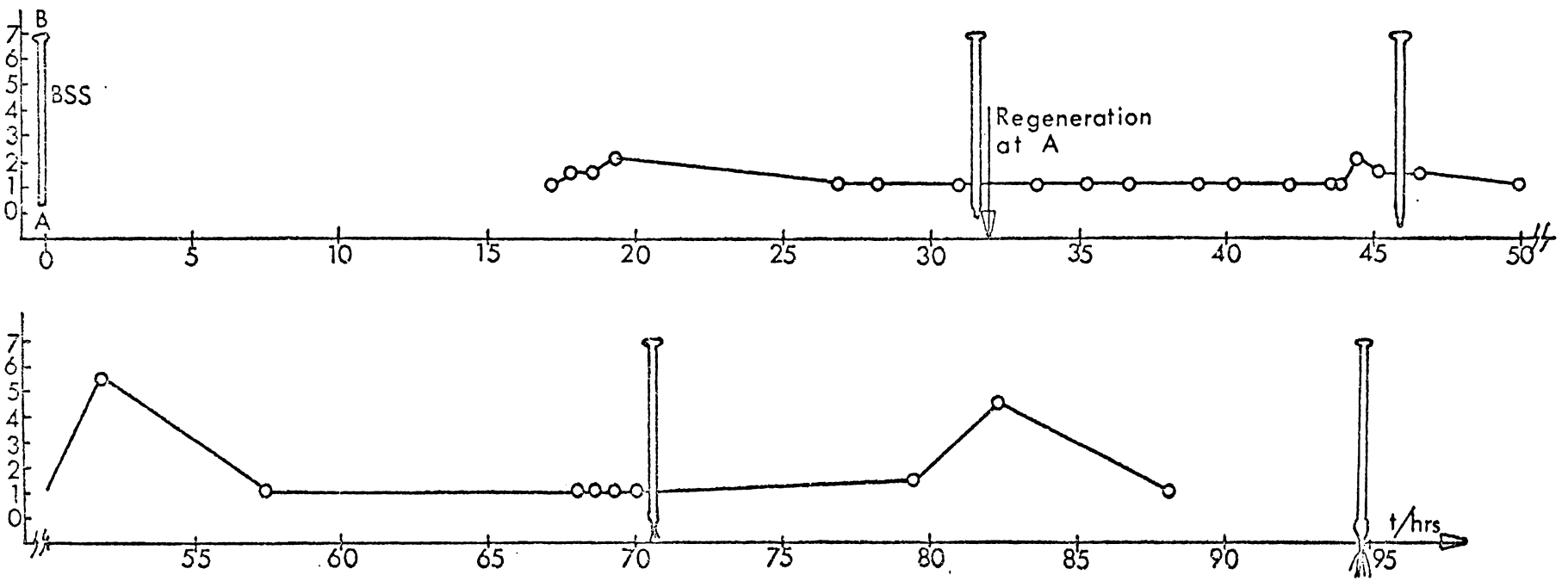

Fig. 5.4.5. Experiment P2

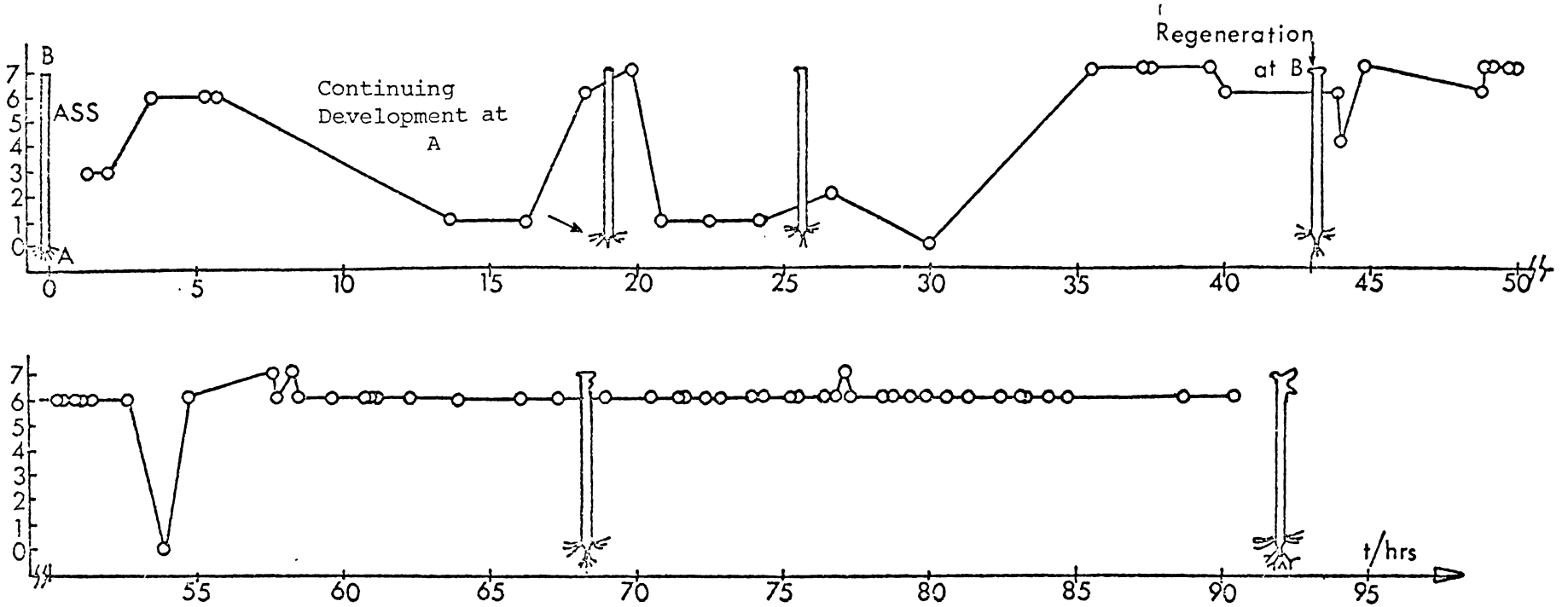

Fig. 5.4.6. Experiment X1

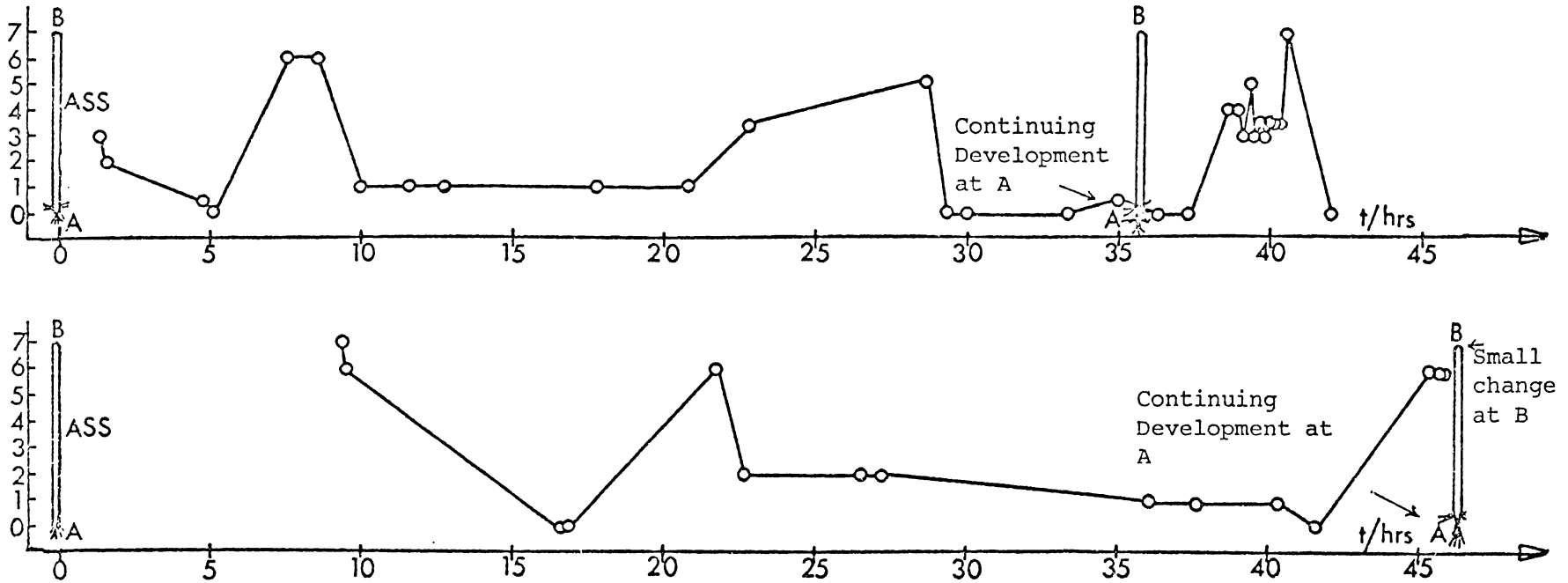

Fig. 5.4.7. Experiment X2 (Upper trace)

Fig. 5.4.8. Experiment X3 (Lower trace)

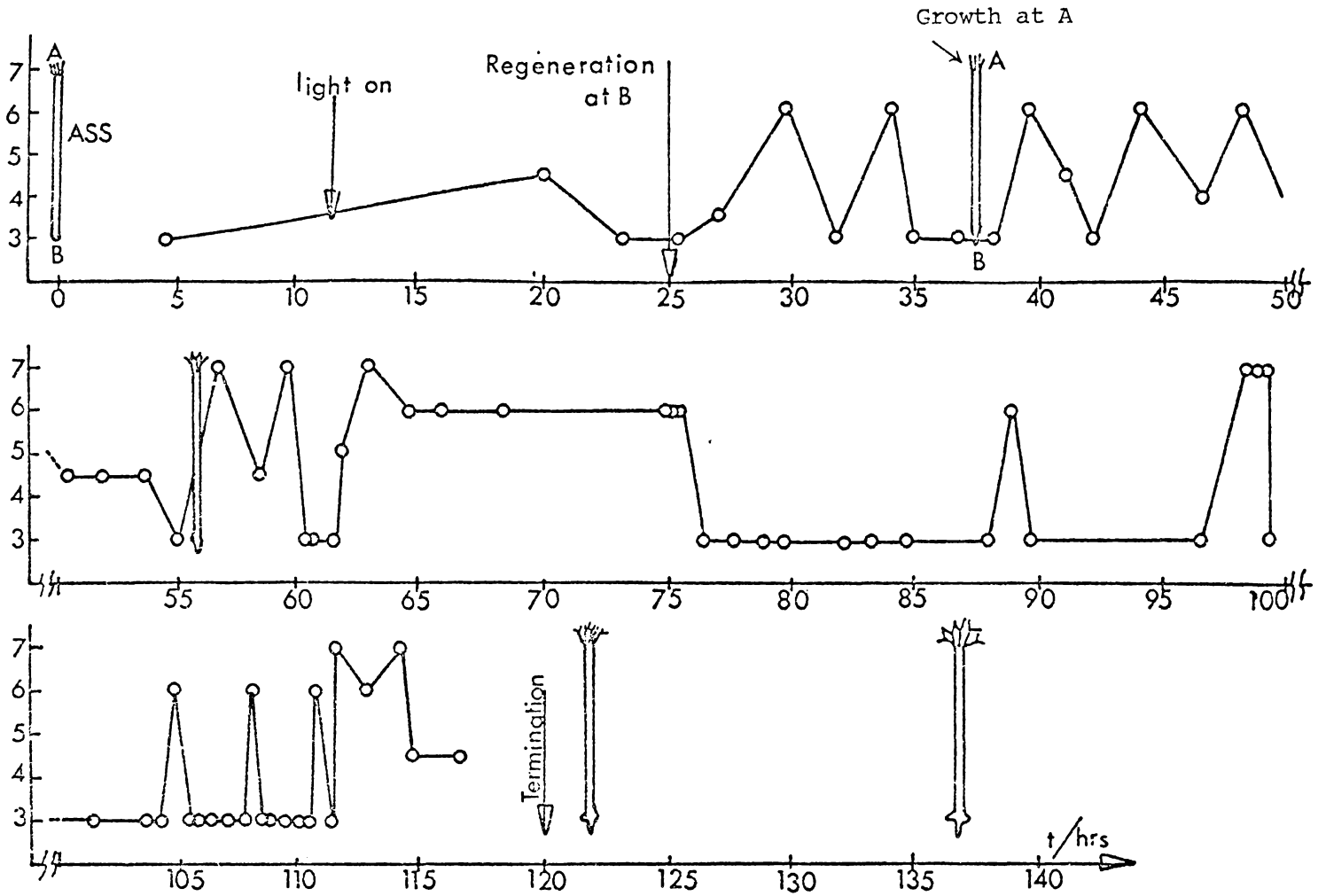

Fig. 5.4.9. Experiment Y1

Note: The Electrode spacing ≃ 3.2mm.

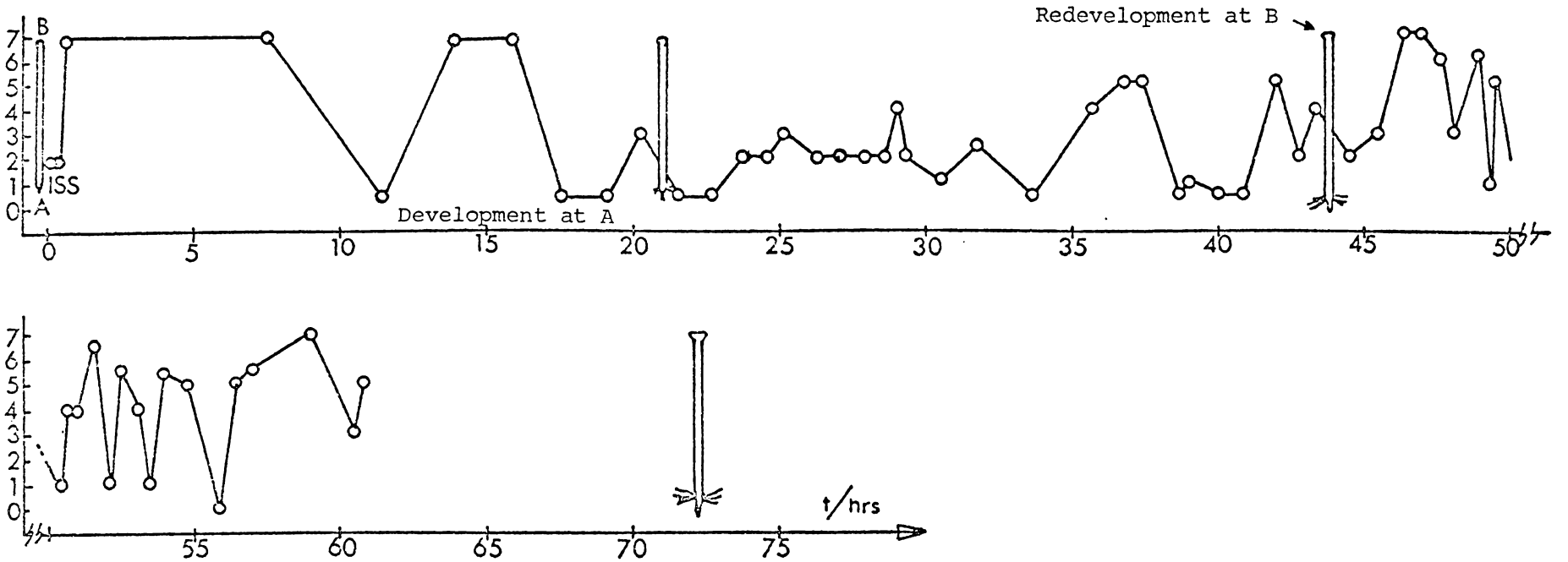

Fig. 5.4.10. Experiment T7

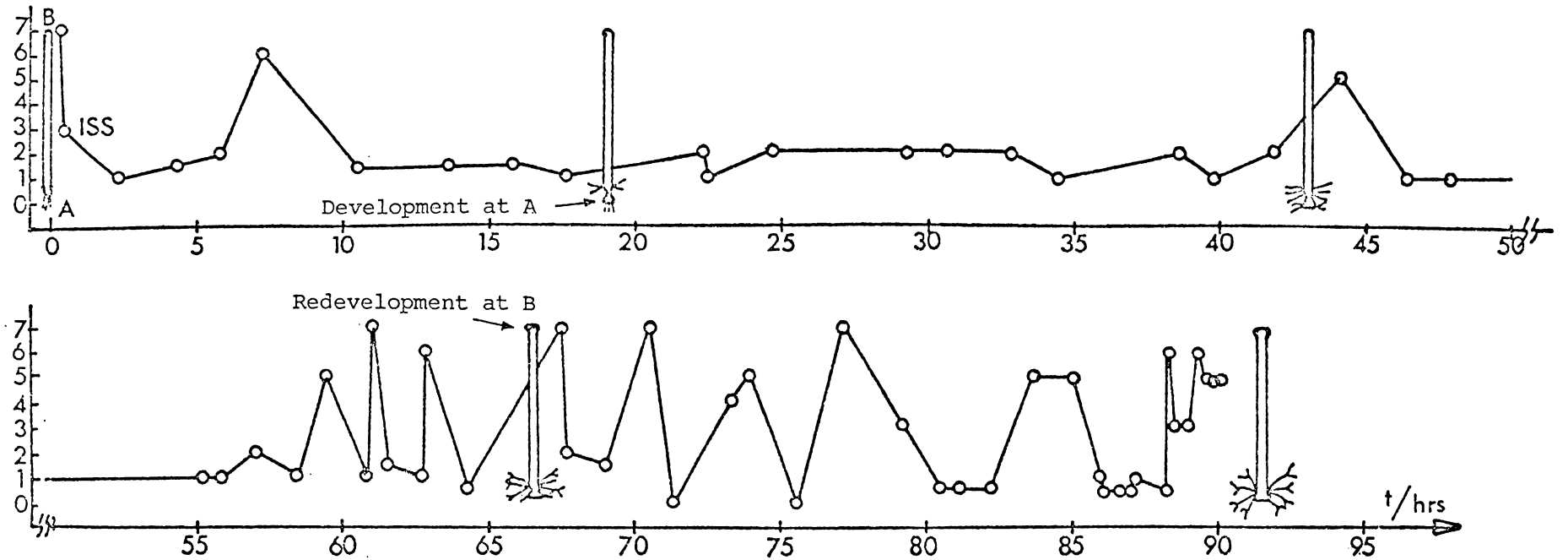

Fig. 5.4.11. Experiment T8

There were 31 AP's recorded, the first was at the ~ 17th hour, and none were anomalous. Twenty nine AP's (~ 91%) initiated in the developing apical region (Fig. 5.4.5).

Experiments X1, X2, X3 and Y1 (Apical Stalk Segments)

An ASS can go on developing the existing apex to a more advanced differentiated cap as well as regenerate a new rhizoid-like end (Section 5.2, Fig. 5.2.1).

In experiments X1, X2 and X3 the rhizoids were cut off and the specimens then kept in the dark for ~ 2, ~ 17 and ~ 65 hours respectively before commencing the experiments.

In experiment X1, the specimen regenerated at the cut basal end at ~ 46 hours after starting the experiment (exposure to light). The apex started further development before the basal regeneration was seen, i.e. during the first period of the experiment ($\lesssim$ 46 hours). After this period, the apex showed differentiation into a whorl as well as the regeneration at the basal end becoming a more complicated, rhizoid-like formation. Although ~ 120 AP's were recorded during ~ 90 hours experiment, only 85 were accepted as normal: 7 AP's (8%) initiated at the apical end mostly before the regeneration was seen, as well as 3 AP's (4%) initiated at the middle region of the cell; and 75 AP's (88%) initiated at the regenerating basal end (Fig. 5.4.6).

The ASS's in experiments X2 and X3 definitely developed at the apices only. No sign of regeneration at the cut basal end was seen during the experimental periods (37 and 47 hours for Expts. X2 and X3 respectively). Only 19 AP's were recorded for Expt. X2, i.e. initiating at growing apex (A), M, and B are respectively 13(67%): 4(22%): 2(11%) (Fig. 5.4.7). In Expt. X3, 15 AP's were recorded, 9(60%) and 6(40%) were initiated at A (growing apex) and B respectively (Fig. 5.4.8).

The results from these three experiments suggests the coincidence

of the AP initiation with growth (at either end) and its predominancy corresponds to the region of most growth.

In experiment Y1 the ASS was placed in the cell holder in the reverse direction to all the other experiments i.e. with the apex at the distal end of the medium feed system. The ASS was kept in the dark for 24½ hours before starting the experiment by exposure to light. The existing apex developed from a hairy into a branched whorl and the cut basal end also regenerated, starting at the 37th hour, into a three branched rhizoid-like end. The regeneration was relatively dominant in this cell (Fig. 5.4.9).

Out of 88 recorded AP's 72 were accepted as normal during the 120 hour period. The predominant region of AP initiation was found to alternate between the two ends. The alternation was seen frequently (1-3 hour intervals) during the first ≈ 42 hour period, and less frequently after that. However, on average there was a predominant initiation at the basal end (A:B:M = 35%: 51%: 14%).

From regular observation of the cell throughout the experiment the above AP initiation behaviour strongly appears to be correlated to growth at the ends, i.e. continuing development at the apex and redevelopment (regeneration) at the former basal end. During the period before the rhizoid-like regeneration was seen, the changes at both ends were negligible, i.e. the AP initiation was possible in any region of the cell with frequent alternation between two ends. After that period the AP initiation was seen predominantly at the terminal regions, with more frequent repetition and less frequent alternation between ends. Also the repetitiveness at the regenerating basal end during any particular interval was relatively greater than that at the apex. This corresponds with the observed dominant redevelopment of the former basal end during the period of regeneration. It therefore suggests that the AP

initiation relates to the growth at either end rather than the overall polarity of the cell.

Experiments T7 and T8 (Isolated Stalk Segments)

These two experiments were done on regenerating ISS's which clearly showed single regenerations (type Iα) at the previous apices at < 24 hours after exposure to light. The previous basal ends were seen as uniform cylindrical shapes. Before commencing these experiments, the specimens for experiments T7 and T8 respectively had been exposed to light for 3 and 7 days after enucleation, i.e. the new apex of the specimen for experiment T8 had differentiated more than the other.

During the experiment periods (61 hours for T7, 90 hours for T8), both new apices developed to a more advanced form. At about 26 hours for T7, and about 58 hours for T8, after commencing the experiments both basal ends started to show some degree of redevelopment. At these times the predominancy of the initiation of the AP at the apical end diminished. Before the basal redevelopments, the AP initiation at A was ~ 70% for T7, and ~ 92% for T8. The overall AP initiation at A was ~ 50% for T7, and ~ 65% for T8. For the AP initiation at other regions, see Figs. 5.4.10 and 5.4.11.

Again, this is another illustration of the AP initiation correlating with the growth region.

5.5 Results of Main Experiment Series.

In this series of experiments dark-treated ISS's were studied exclusively. In the 'A' experiments (Table 5.5.1) the previous apical ends were placed against the medium flow (i.e. at the low electrode number end of the cell holder), and in the reverse direction in the 'B' experiments.

Since ISS's are the most sensitive of the various cut cells to their surroundings, 'abnormal' AP's (as defined in Section 5.4) were produced more frequently and some experiments had to be abandoned. These cell segments also exhibited more complex 'normal' AP waveforms e.g. a local depolarisation accompanied by a propagating AP (Figs. 5.5.1a and b). Also, although rare with more complete cells, simultaneous or near simultaneous AP initiation in two regions of the cell (Figs. 5.5.2a and b) was seen in several of the experiments in this series. (A5, A9, B1, B3 and B6). These more complex 'normal' AP's have been incorporated in the analysis as far as possible.

The AP transient data were analysed for the region of AP initiation in the same way as in Section 5.4, and the results of the eleven complete experiments are summarised in Table 5.5.1. Diagrams of the experimental arrangement, observed redevelopment and a detailed record of the transient initiation position as a function of time are given for each experiment in Figs. 5.5.3 - 5.5.13.

All results, including those from Section 5.4, clearly suggest that the AP initiation coincides not only with the regeneration but any forms of (physiological) developmental changes (e.g. growth) at any region (end) of a cut cell. Although it can't be indicated in the data presented, due to the absence of any photographic or similar quantitative record of the cell redevelopments, from observations throughout the experiments a very clear impression of strong correlation between the

region of current growth and the region of AP initiation was obtained.

Table 5.5.1: SUMMARY OF RESULTS OF MAIN EXPERIMENT SERIES ON ISS's

Expt.	Expt. Period /hrs.	Specimen Specifications								No. of AP's / (regenerating period/ hrs.)	% ages of AP Initiation at		
		Aged /wks.	Cap. dia. /mm.	Stalk dia. /mm.	Stalk length		Regenerating		Redev. Type[2]		A	M	B
					orig. /mm	cut. /mm	end	Time /hr.[1]					
A3[3]	90	60	5	0.30	32	26	A	48	IIα	26/(32)	44	3	53
A4	92	17	hairy	0.25	20	14	B	34	Iβ	24/(58)	64	-	36
A5	113	19	"	0.30	22	14	[4]B,A	63,72	IIIα	63/(50)	41	18	41
A7	59	21	"	0.30	24	13	A	24	Iα	29/(35)	43	11	46
A8	75	22	"	0.30	24	14	B	30	Iβ	36/(45)	8.6	1.4	80
A9	75	23	"	0.35	26	13	A	30	IIα	26/(45)	73	-	27
B3	85	22	"	0.25	22	12	B,A	24,33	IIIβ	61/(61)	30	27	43
B4	105	24	"	0.30	18	12.5	A	36	Iα	36/(69)	47	20	33
B5	72	25	"	0.30	20	14	B	50	IIβ	42/(22)	15	50	35
B6	75	27	"	0.35	22	14	B,A	47,49	IIIα	53/(28)	59	24	17
B7	77	27	"	0.35	24	14.5	N	-	V	63/(77)	60	24	16

[1] Changes observable under 20 × microscope after specimen being exposed to light.

[2] cf. Fig. 5.2.2. A, B = former apical, basal end. [4] B, A = regeneration at B and then A

M = middle region of SS. N = no regeneration.

[3] The specimen in Expt. A3 was kept in the dark for monitoring the depolarisation for 10 hours.

Fig. 5.5.1. AP's accompanied by Local Depolarisation(s) Obtained from ISS's
(d(t) Waveforms and the Relevant Printouts are shown on upper and lower part respectively)

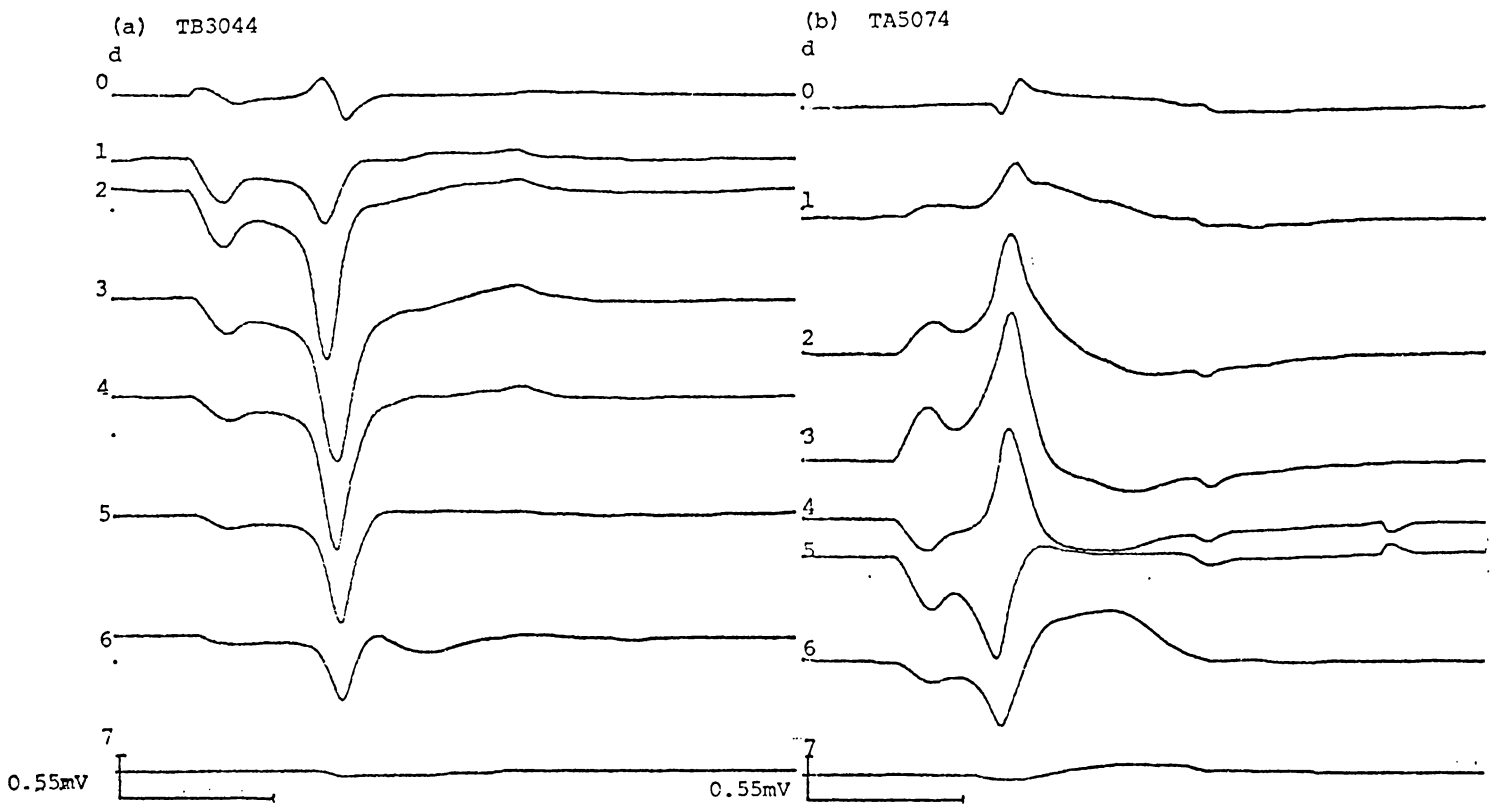

TB3044. ZX.

CHAN	MINVAL	MINPOS	MAXVAL	MAXPOS	SPAN
0-1	-0056	88	+0039	33	+0095
1-2	-0070	80	+0013	119	+0083
2-3	-0181	81	+0018	151	+0199
3-4	-0120	83	+0060	150	+0180
4-5	-0232	84	-0056	152	+0176
5-6	-0180	86	-0053	101	+0127
6-7	-0007	86	+0071	96	+0078
7-R	-0028	84	-0016	168	+0012

TA5074. ZX.

CHAN	MINVAL	MINPOS	MAXVAL	MAXPOS	SPAN
0-1	-0035	76	+0031	82	+0066
1-2	-0013	151	+0057	80	+0070
2-3	+0054	151	+0224	77	+0170
3-4	-0090	152	+0106	78	+0196
4-5	-0086	219	+0116	77	+0202
5-6	-0099	74	+0068	219	+0167
6-7	-0097	75	+0023	115	+0120
7-R	+0149	73	+0167	119	+0018

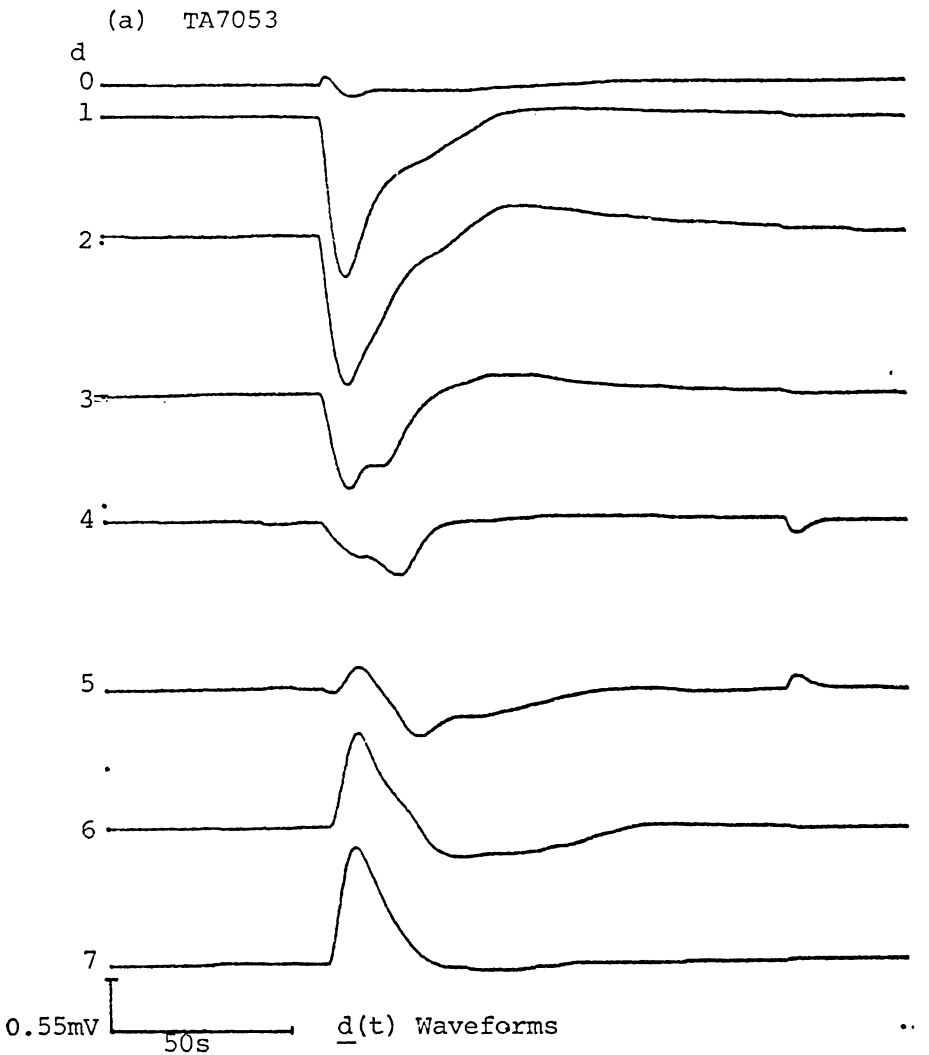

Fig. 5.5.2. Simultaneous initiation of AP's at the two poles of an ISS

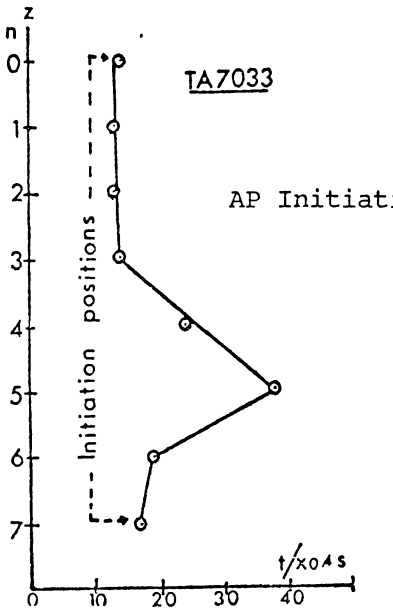

AP Initiation/Propagation Plot

?TA7033. ZX.

CHAN	MINVAL	MINPOS	MAXVAL	MAXPOS	SPAN
0-1	-0061	74	+0119	73	+0180
1-2	-0171	73	-0004	133	+0167
2-3	-0182	73	+0007	127	+0189
3-4	-0071	74	+0034	122	+0105
4-5	-0072	219	-0005	140	+0067
5-6	-0001	98	+0102	219	+0103
6-7	-0056	111	+0053	79	+0109
7-R	+0001	116	+0110	77	+0109

Printout of the Extremal Differential Voltage Values and Positions.

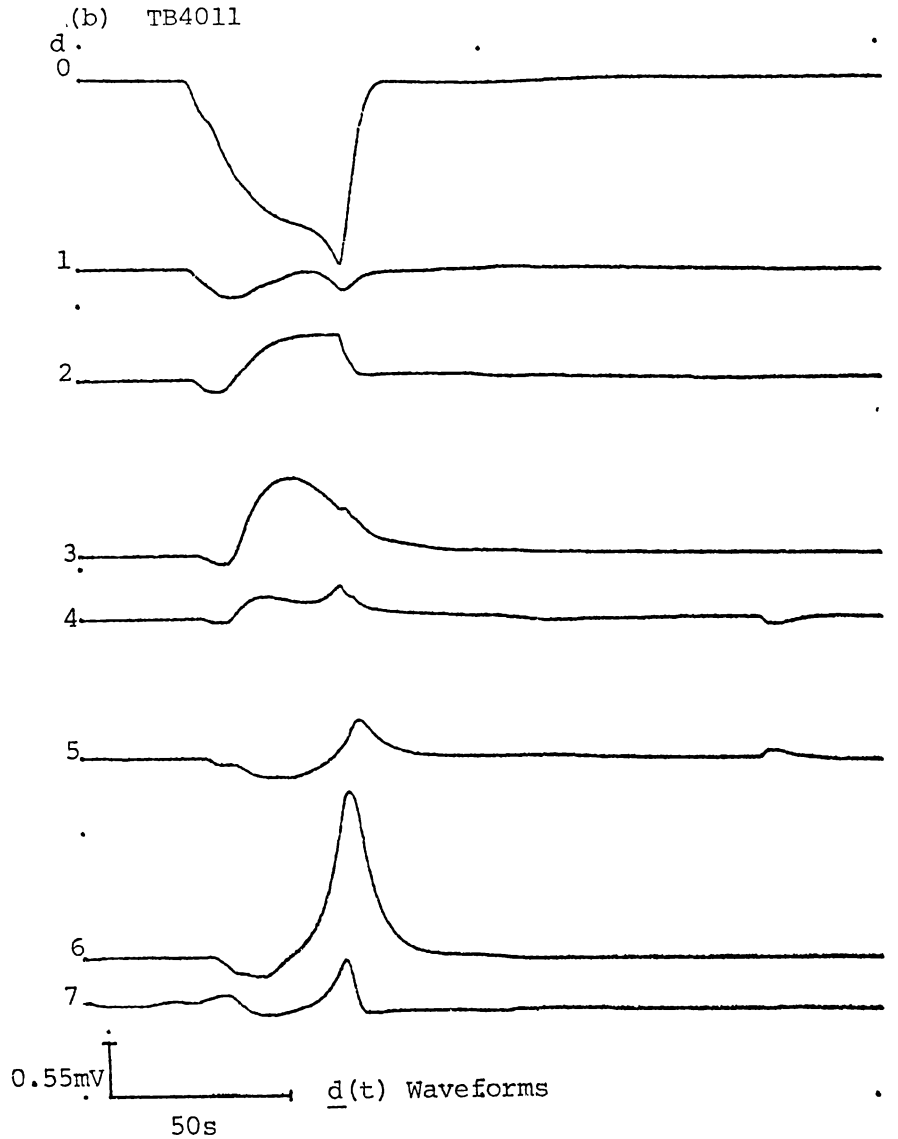

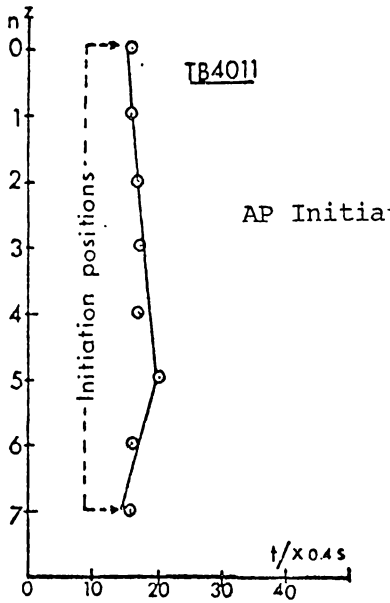

AP Initiation/Propagation Plot

?TB4011. ZX.

CHAN	MINVAL	MINPOS	MAXVAL	MAXPOS	SPAN
0-1	-0330	86	+0066	91	+0396
1-2	-0068	86	-0002	133	+0066
2-3	-0105	87	+0099	83	+0204
3-4	-0046	47	+0132	87	+0178
4-5	-0033	87	+0133	86	+0166
5-6	-0011	58	+0121	90	+0132
6-7	-0128	51	+0275	86	+0403
7-R	-0034	88	+0052	86	+0086

(Fig. 5.5.2. Cont.)

Figs. 5.5.3 to 5.5.13 are Plots of Position of AP Initiation as a function of time after illumination of cell segments.

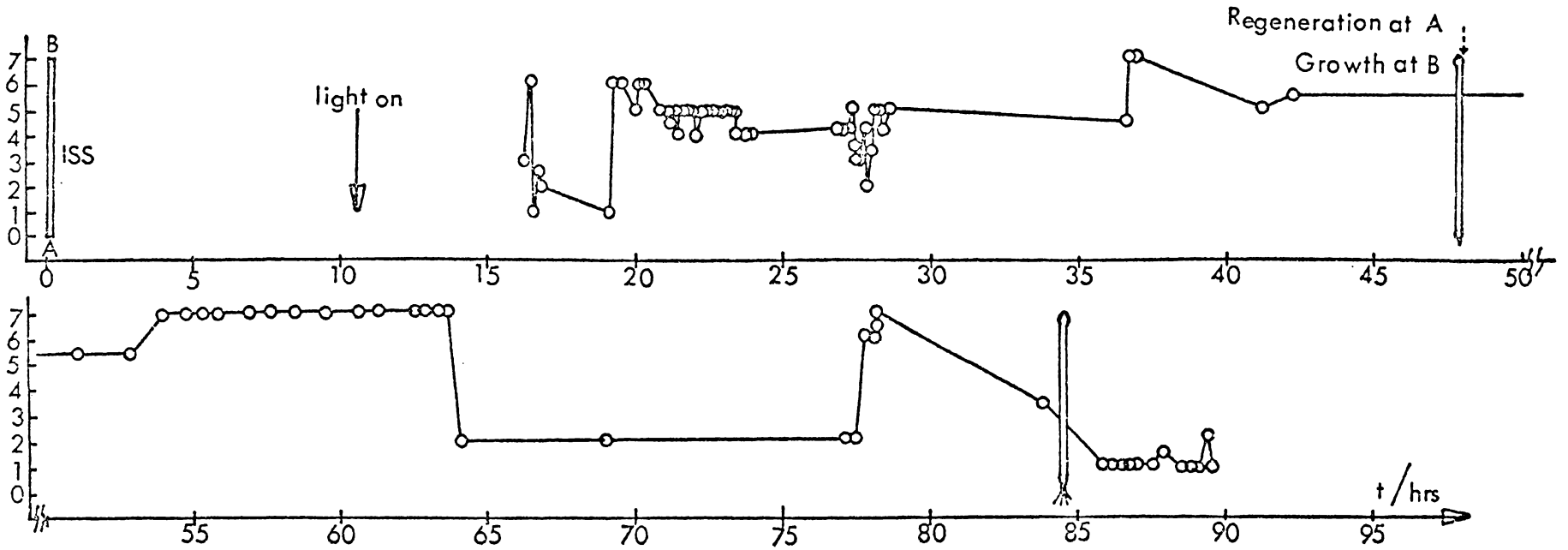

Fig. 5.5.3. Experiment A3

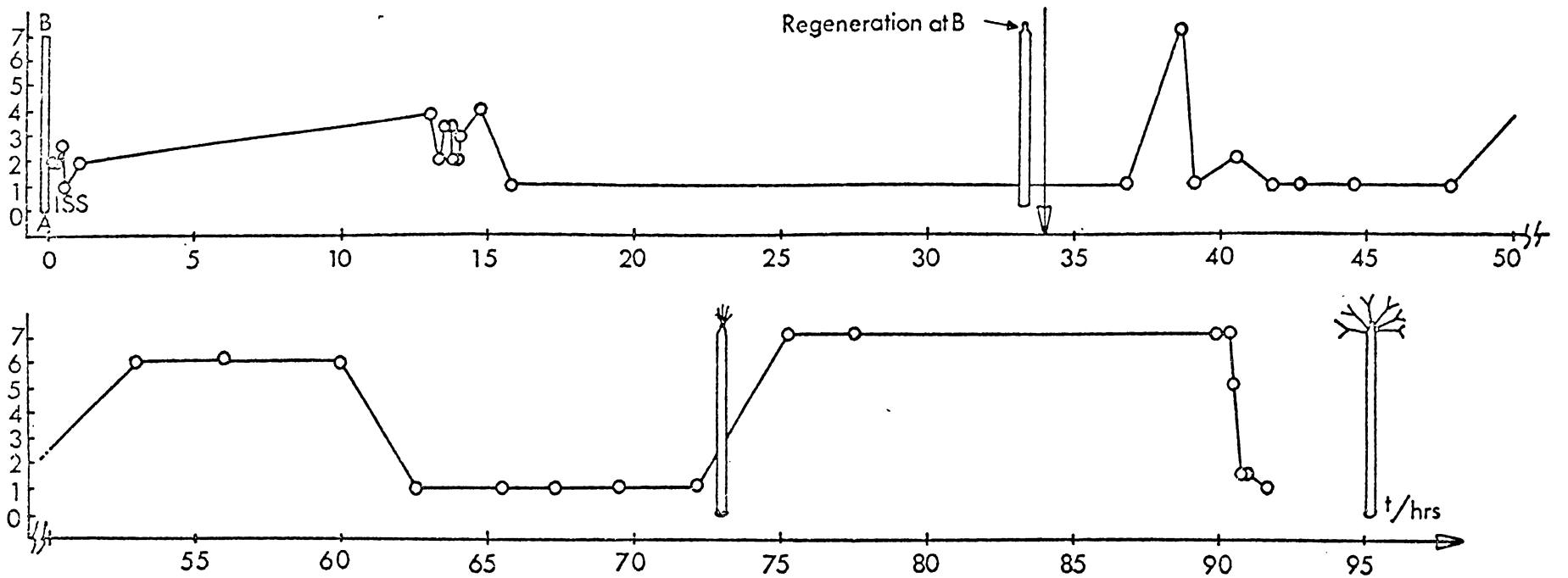

Fig. 5.5.4. Experiment A4

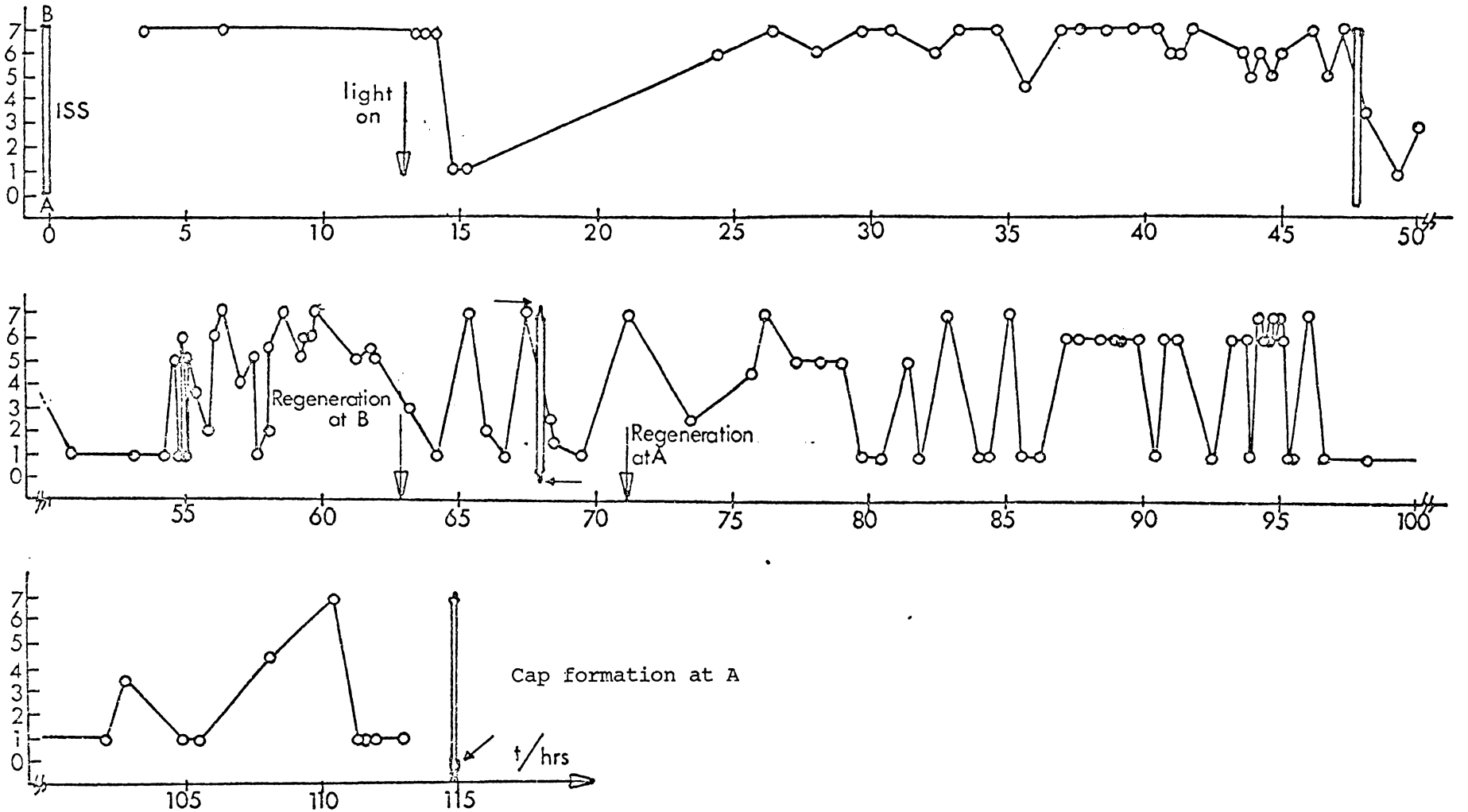

Fig. 5.5.5. Experiment A5

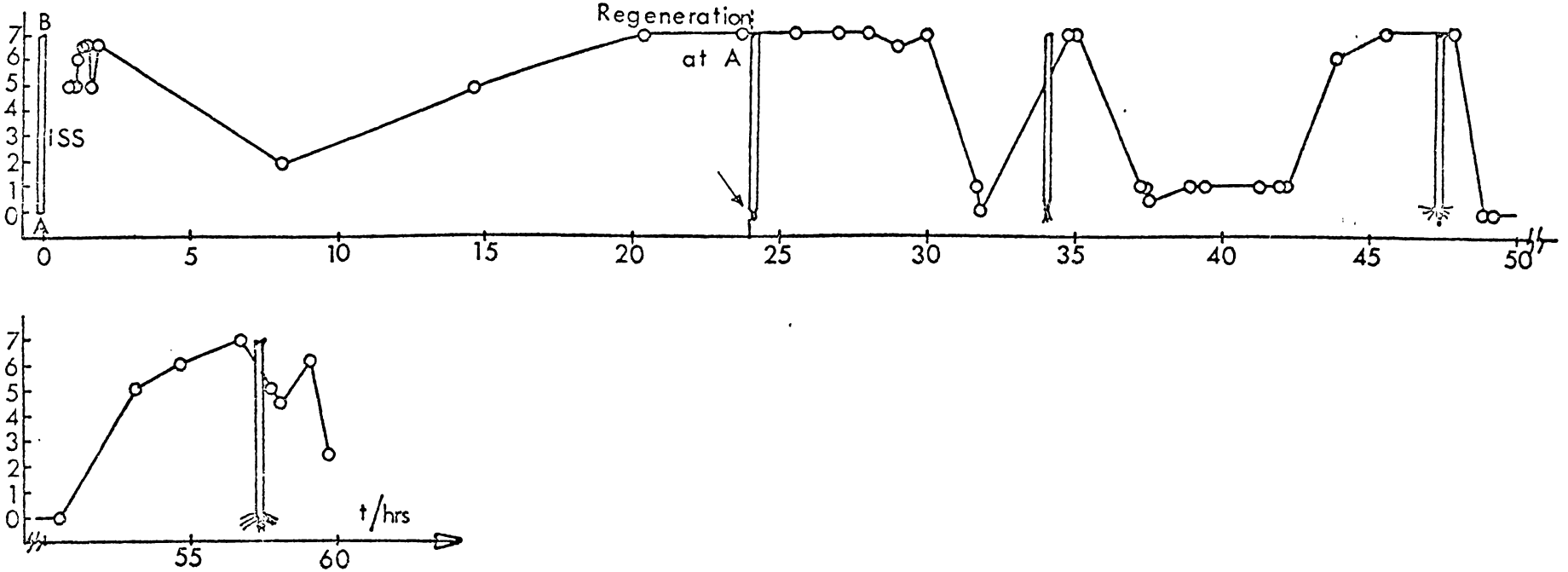

Fig. 5.5.6. Experiment A7

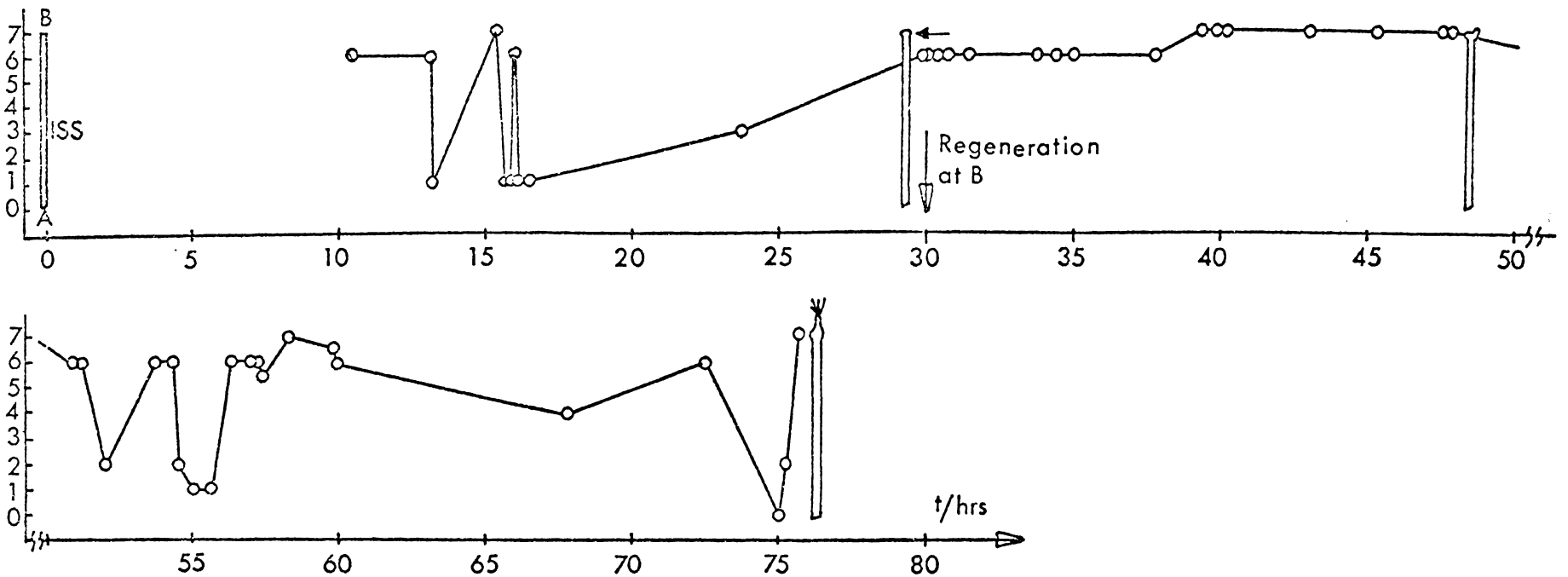

Fig. 5.5.7. Experiment A8

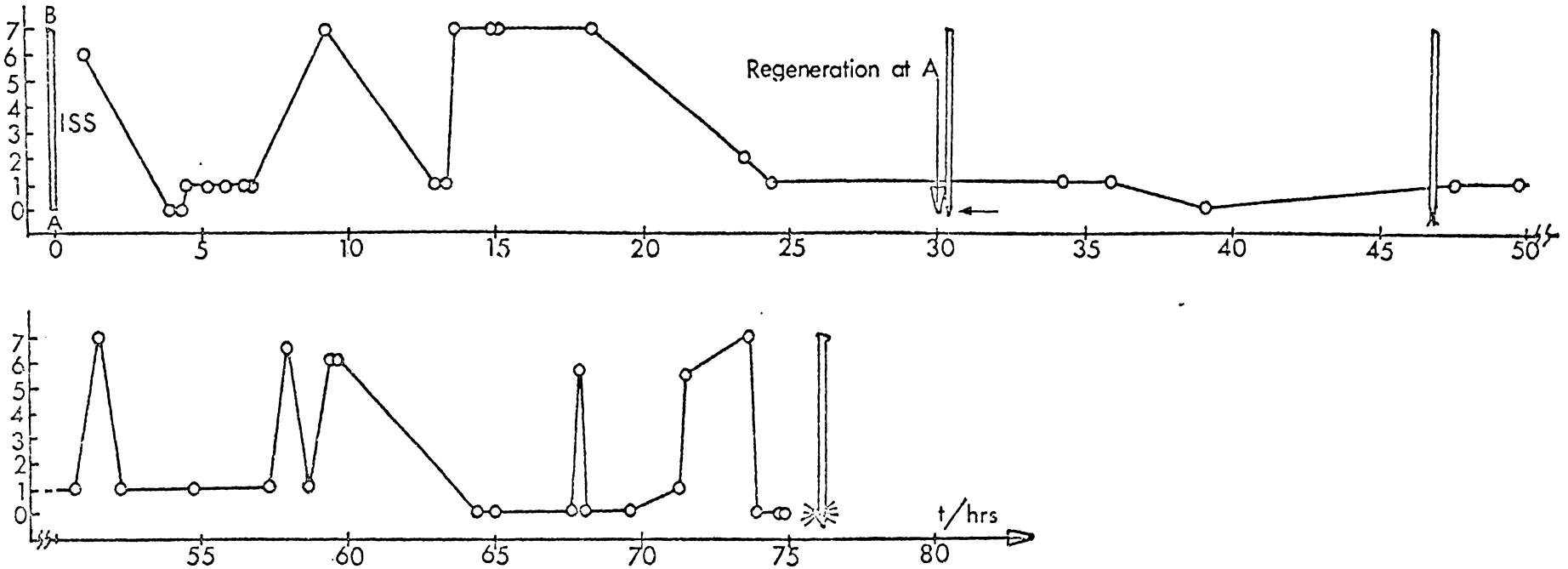

Fig. 5.5.8. Experiment A9

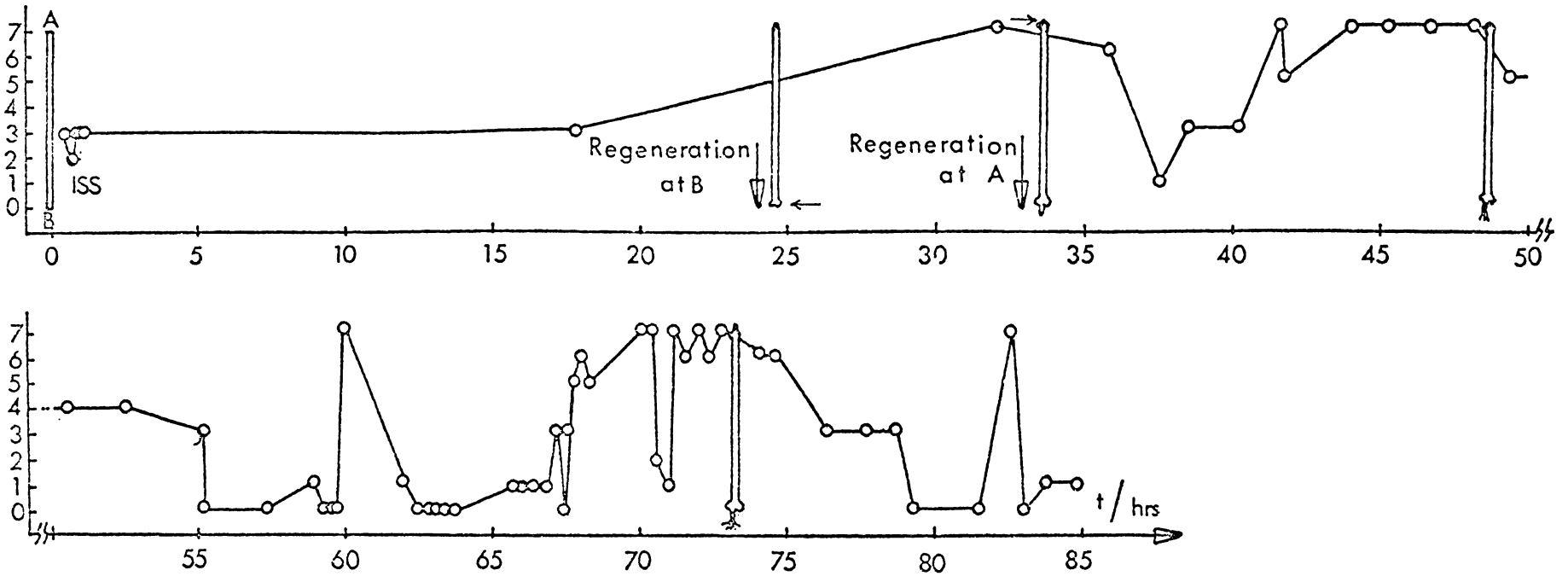

Fig. 5.5.9. Experiment B3

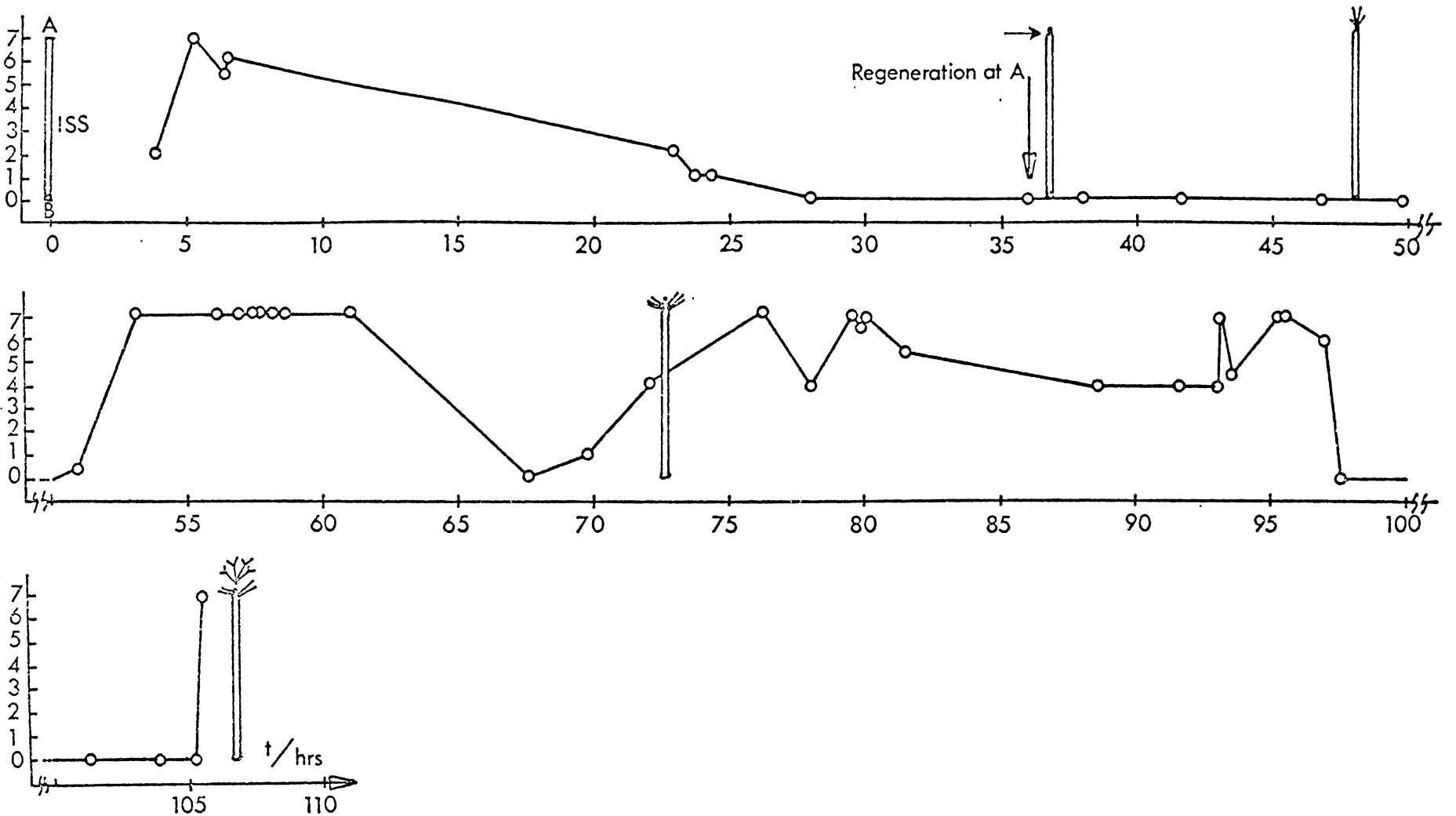

Fig. 5.5.10. Experiment B4

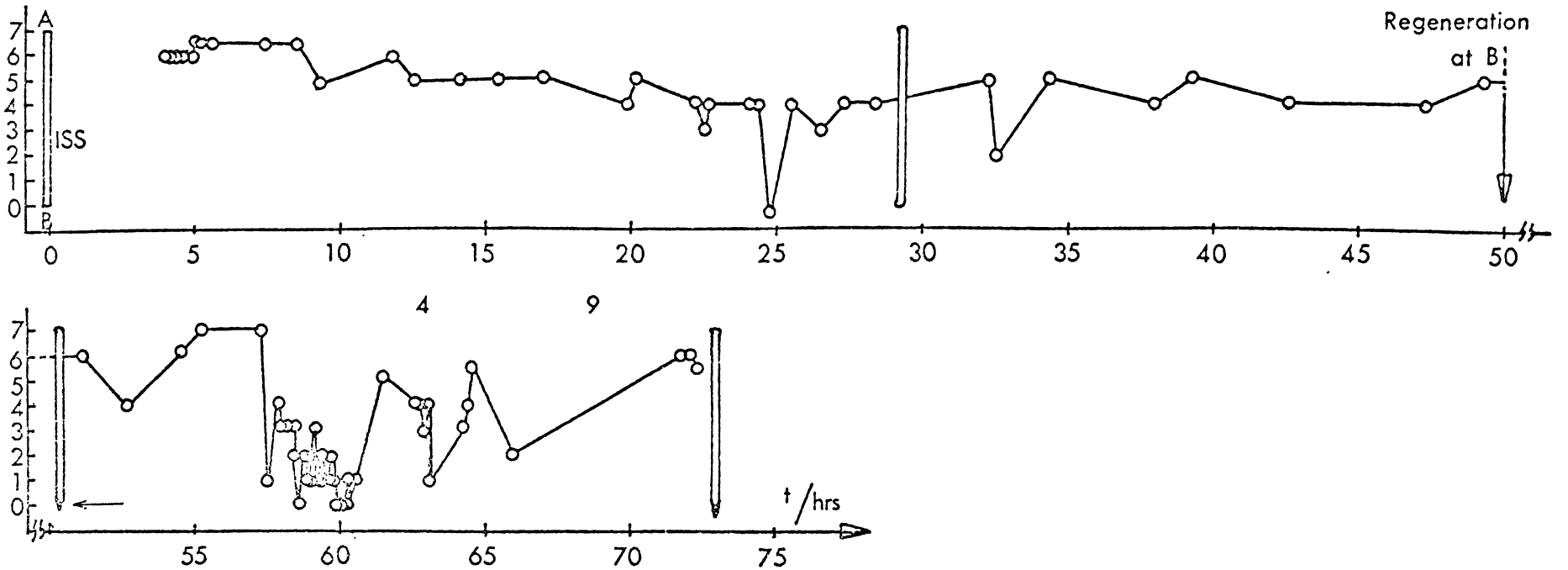

Fig. 5.5.11. Experiment B5

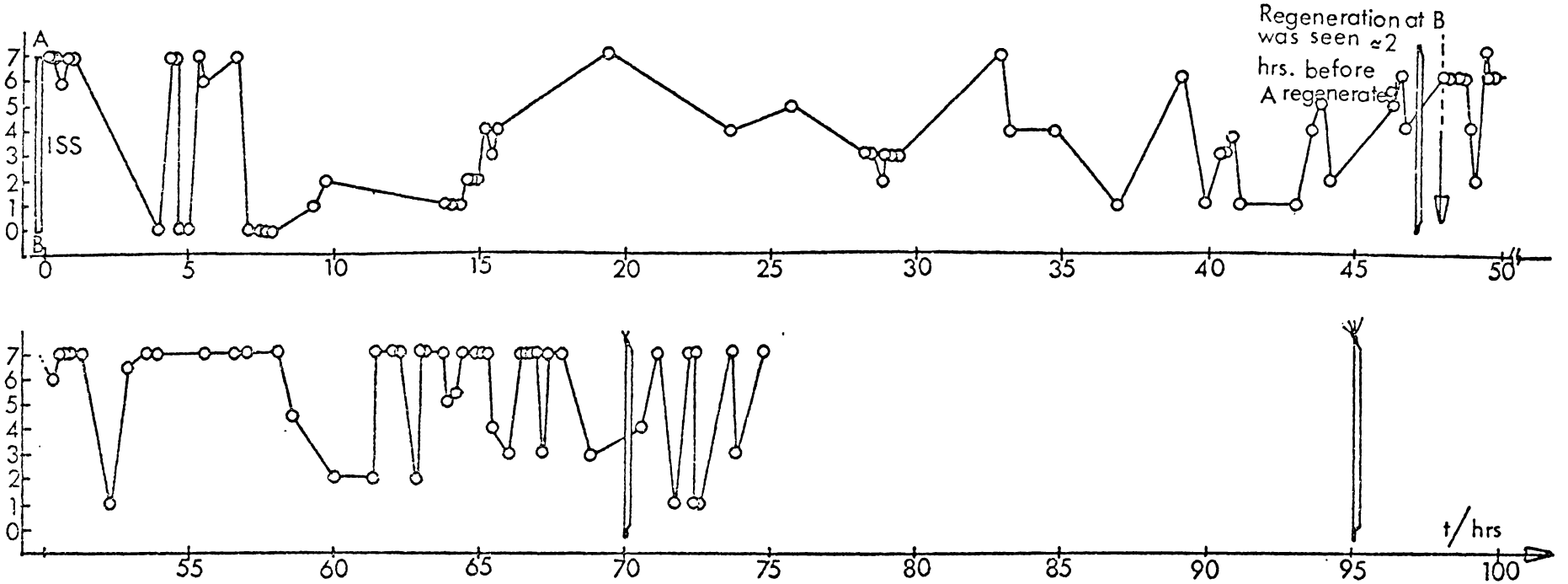

Fig. 5.5.12. Experiment B6

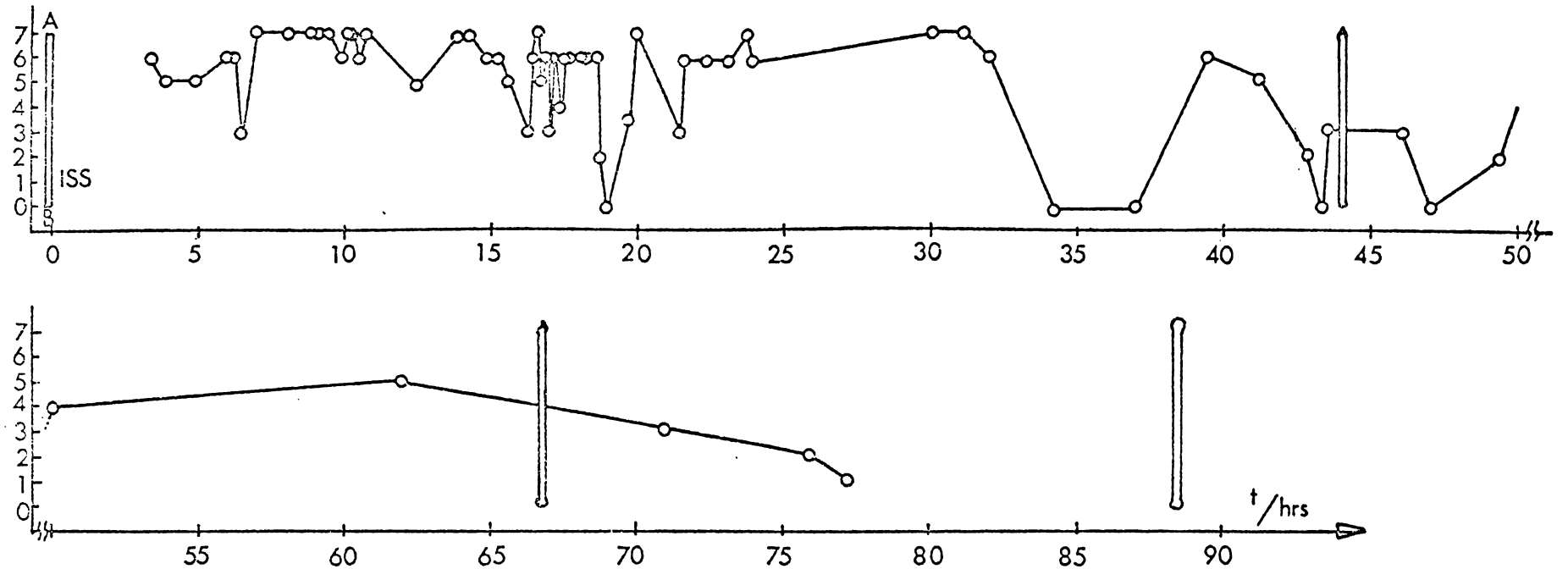

Fig. 5.5.13. Experiment B7
No visible morphogenetic structural forms were seen at both ends, i.e. all AP's recorded during whole experiment period were regarded relevant to the growth of this ISS.

CHAPTER 6

DISCUSSION

6.1 Summary of Experimental Results

In general the overall features of the redevelopment of the cut cells (BSS's, ASS's and ISS's) observed in this work are in good agreement with the classical results reported previously (Sections 1.2 and 5.2). The young cells are generally more capable of redevelopment, i.e. more suitable for preparation of cell segments for electrophysiological studies. The higher percentage of apical-type regeneration at the former apical ends of ISS's (Table 5.2.1) indicates the dark treatment (24 hrs) does not induce the former cell polarity (i.e. morphogenetic map) to disappear completely. There is also indication that the phototropism and/or geotropism may affect the regeneration of an ISS (plate 5.2.3). However the occurrence of a significant fraction of ISS redevelopments in the reverse direction was satisfactory for this work.

The results suggest that a normally growing CC under favourable experimental conditions exhibits normal AP's (Fig. 4.5.4) at a low rate (typically $\simeq$ 80 min/AP). When the membrane of such a cell is damaged, for example by an insertion of a micropipette into the cytoplasm, it becomes very sensitive. Frequent AP's (with sharp turning voltage waveforms) recur at the point of injury (Fig. 5.3.2b). The cell shows capability of healing, i.e. the pipette tip is eventually ($\simeq$ 2-8 hrs) blocked up, and the cell's electrophysiological activity becomes normal.

A cut cell segment is, not surprisingly, even more sensitive to the unfavourable experimental conditions than a damaged CC. Several examples of the experimental conditions that cause abnormal responses are given in Table 5.4.1. In most cases, the differences between the normal and abnormal AP's are indicated by their individual voltage waveforms and the repetitiveness of the occurrence (Figs. 4.5.4, 4.5.7, 5.3.1, 5.4.1 and 5.4.2).

This distinction is important from the point of view that the abnormal AP's may not reflect the genuine electrical activity relevant to the (re)developmental processes but rather the immediate conditions that perturb the cell membrane. Abnormal AP's were therefore not considered in obtaining the relationship between the AP initiation and propagation and the (re)development in cut cells.

The results of the intermediate experiment series clearly show that the AP initiation and propagation is strongly correlated with the well defined (observable) growth (Table 5.4.2). For a young developing CC, the predominant AP initiation is seen at the growing apex (Fig. 5.4.4). This is even clearer in the case of a regenerating BSS (Fig. 5.4.5). However since ASS's and ISS's can (re)develop into several types (Figs. 5.2.1 and 5.2.2), the region of initiation is only rarely seen to remain at one end at all times. Usually the growth is dominant at one end during one period of time and the AP initiation occurs predominantly at that end during that particular period (Figs. 5.4.6 to 5.4.11). An ASS or ISS (re)developing at both ends typically exhibits alternating predominance of AP initiation corresponding to alternating period of growth at the ends (e.g. Fig. 5.4.9). In addition some AP's obtained from such cells are found to initiate simultaneously (or almost simultaneously) at both ends (Fig. 5.5.2).

The same essential behaviour was observed in redeveloping ISS's in the main experiment series. These cell segments showed all redevelopment types except type IV (Fig. 5.2.2. and Table 5.5.1). The AP's were found to initiate at any region of the cell stalk, but predominantly at the redeveloping ends. In three experiments (A3, A4 and A7) however, the overall predominance of AP initiation was not obtained at the end with more growth. For instance, in experiment A3 more frequent AP initiation (53%) was observed at the end with less growth (B) with respect to the apical type regeneration at the other end (A, 44%). In comparison with the others (e.g. experiments A5, B3, B6 and B7), these three experiments may suggest not only the correlation of predominant AP initiation at the redeveloping end(s) but that the number of AP initiation does not necessarily relate simply to the amount of growth.

It may be concluded that the experimental results suggest a strong correlation between the region of AP initiation and the current growth and no obvious correlation with the establishment of the morphogenetic gradients or map.

6.2 Comparisons with Other Work

In spite of the highly unnatural conditions (Section 1.4), the experimental techniques for the external membrane potential measurement employed by Novak and Bentrup (1972a) have dominated most of the subsequent electrophysiological studies of complete cells and cell fragments of *Acetabularia* (see e.g. Christ-Adler and Bentrup, 1976; Goodwin and Pateromichelakis, 1979). Hence it is important to identify the points of agreement and disagreement between these results and the present work.

Before an ISS begins to regenerate, i.e. < 10 hrs after exposure to light, it exhibits very few AP depolarisations. This result is common to this and other work and is believed to be the period in which the morphogenetic map or gradients are being re-established. After this period more frequent AP's occur. According to Novak and Bentrup (1972a) these occur at the regenerating end where the cap forming MS's are concentrated as an apico-basal gradient. This is the stage of the expression of these substances by which the new cell wall at that end is formed. Therefore the recurrence of the AP's at that end does not only coincide with the apico-basal gradient of MS's (as suggested by Novak and Bentrup, 1972a), but also with cell wall synthesis or growth (single regeneration at the apical end in this case). This result is comparable with the (rare) singly redeveloped ISS's in this work (type I, Fig. 5.2.2., see also experiments A8 and A9).

In the relatively more common redevelopment types found in this work (types II, III, Fig. 5.2.2, see also Section 5.2) where the ISS can grow at both ends the electrical activity is quite different, consisting typically of alternation of the region of AP initiation between the two ends (Sections 5.4 and 5.5). It is interesting that these types of redevelopment have apparently not been observed in the more restrictive experiments.

The very recent work of Goodwin and Pateromichelakis (1979) is in better agreement with this work, although they too used a specimen holder of the Novak and Bentrup (1972a) type. They reported that in a non-growing ISS the spatial potential gradient was not stable, i.e. its sign alternated between the ends and AP's arose at both ends. They also reported that either an apical differentiating (into caps) or apical elongating (without cap forming) BSS showed a stable electrophysiological polarity and the AP initiation at the hyperpolarised growing end. These results agree with the conclusion of the present work that the AP initiation is correlated with the mechanisms of growth rather than the establishment of the morphogenetic gradient (since there were no visible morphogenetic structural forms at the apical end of the growing BSS, i.e. the expression of the MS's is suppressed).

The quite different experiments of Jaffe and his coworkers (e.g. Jaffe, et.al., 1974) on sea plant eggs may be interpreted to support the conclusions of the present work. In these experiments, fertilized fucus eggs are placed in array in a capillary tube (100 μm in diameter). The cells germinate in the same direction and the external electric currents are measured by an extra-cellular vibrating electrode. The results show that AP's initiate at the growing end. They propose that the membrane at that end is relatively more active and leaky to ionic exchange and that this gives rise to spontaneous AP's. They conclude that the electrical activity is related to the growing region and this may imply that the AP's arise at any regions showing current growth but not restricted in particular to the new growing apex as interpreted by Novak and Bentrup (1972a).

6.3 Conclusions

6.3a Thesis Summary.

The overall experimental work described in this thesis can be summarised as follows:

I Development of the Culture Technique

The *Acetabularia* culture technique used for this work has been developed to meet the local availability of medium ingredients and the requirement of specimens for electrophysiological experiments. The culture maintenance (Appendix 2) is relatively simple and has proved completely reliable and satisfactory over several years. The simplified cyst germination procedures (Section 2.3) give a large safety margin and a reasonably contamination-free culture, adequate for the requirements of the electrophysiological studies.

II Development of the Multiple Extracellular Electrode Recording System

This newly developed measurement technique enables measurements electrical activity to be made over a long period with minimum perturbation from the measuring system. The fabrication of durable Ag/AgCl electrodes has been developed and proved to meet the required long term measurements (up to 30 days) with a minimum drift of electrode potential (< 10 μV r.m.s., see also Section 4.2b and Appendix 3b). Analytical techniques for the identification of the AP initiation position (Sections 4.4 and 4.5b) and a computerised data acquisition system (Section 4.3) enable much more precise and detailed AP propagation characteristics from intact cells and cell fragments to be reported for the first time (cf. e.g. Novak and Bentrup, 1972a; Gradmann, 1976).

The medium feed system (Section 4.2c) ensures a relatively normal regeneration of ISS's (with respect to the normal regeneration of these cell floating in the shallow petri-dishes containing medium, i.e. comparable regeneration times, 24-72 hrs., see Tables 5.2.2 and 5.5.1, and types of redevelopment, Fig. 5.2.2. and the above tables).

This technique therefore enables an ISS to redevelop in a relatively natural way while the electrical activity is monitored in some detail.

III Range of Experimental Results

Membrane electrical activity from various specimen cells (i.e. intact and damaged CC's, single cut cells (ASS's and BSS's) and ISS's normally or poorly treated during experimentation) have been investigated for comparisons.

For a well defined developing CC or a redeveloping BSS, AP's initiate and propagate predominantly from the growing end. In an anucleate cell (an ASS or an ISS) for which, typically, both ends are capable of redeveloping, the predominant AP initiation alternates from time to time between ends (AP's simultaneously initiating at both ends are also obtained). Microscope observations of growth suggest a strong relationship between the current growth region and the region of AP initiation as concluded in Sections 5.4, 5.5, 6.1 and 6.2.

6.3b Suggestions for Future Work

As is appropriate for a pilot study, the techniques and results presented in this thesis suggest several possible modifications and extensions. Some of the more obvious developments are:

i) Obtaining a more detailed picture of the behaviour of the AP's.

As indicated in Appendix 5, the measured potential distribution along the cell surface in the conducting medium at various particular times could be analysed (on line) to give a graphical display of the full time and spatial dependence of the membrane current distribution. This would give a much more detailed picture of the AP initiation and propagation characteristics.

ii) Measurement of steady membrane potential gradients.

These cannot be measured by the simple Ag/AgCl external electrodes owing to the problem of long term drifts. This problem may be overcome by the replacement of the Ag/Cl electrodes with vibrating external electrodes of the type described by Jaffe and his coworkers (e.g. Jaffe, et.al., 1974; Weisenseel, et.al., 1975). This would enable information about static or slowly varying current distribution to be reliably recorded in addition to the relatively rapid changes associated with AP's.

iii) Development of a quantitative recording technique of the cell growth.

Quantitative records of the developmental changes of the cells could be made periodically during the electrical activity monitoring. In this way the correlation between the growth region and the site of AP initiation could be demonstrated in a more objective and quantitative way.

iv) Investigation of the physical factors affecting the morphogenesis.

The present apparatus could readily be used for investigations of various physical factors, e.g. gravitational and/or illumination gradients, applied electric fields, which are believed to affect both the morphogenesis in an ISS (i.e. the re-establishment of the morphogenetic gradients) and the electrophysiological behaviour.

APPENDICES

APPENDIX 1

AE 50 MEDIUM PREPARATION

(A) ASP2 Solution.

Recipe for Stock Solutions:

(A1) Major Salts

NaCl	290 g
$MgSO_4$	80 g
KCl	9.6 g
$CaCl_2$	8.76g
Dist. Water	4 l.

Autoclave at 15 psi. 121°C 20 min.

(Add $CaCl_2$ and $MgSO_4$ into large volume of dist. water, then others)

(A2) Metals

$FeCl_3.6H_2O$	0.77 g
$ZnCl_2$	0.0624 g
$MnCl_2.4H_2O$	0.86 g
$CoCl_2.6H_2O$	0.0024 g
$CuCl_2.2H_2O$	0.00064 g
H_3BO_3	6.84 g
Na_2EDTA	6.0 g
Dist. water	4 l.

Autoclave

(A3) Tris

Tris (hydroxy methyl-amino methane)	
$NH_2.C.(CH_2OH)_3$	40 g
Dist. water	1 l.

Autoclave

(A4) Minor Salts

$NaNO_3$	5.0 g
K_2HPO_4	0.5 g
Dist. water	100 ml

Autoclave

(A5) Vitamins

(A5.1) Major Vitamins

Thiamine	10 mg
Nicotinic Acid	2 mg
Calcium pantothenate	2 mg
p-aminobenzoic acid	02 mg
Inositol	100 mg
Thymine	60 mg
Sterile dist. water	96 mg

(A 5.2) Minor Vitamins

Biotin	0.5 mg
Folic Acid	1.0 mg
Vit. B12	1.0 mg
Sterile dist. water	100 ml.

- Add 4 ml. of Minor Vitamin - solution (A5.2) into 96 ml of Major vitamin solution (A5.1) to make 100 ml. of Vitamin stock solution.
- Sterilise by filtration through 0.22 µm filter.
- Store in refrigerator
- Discard any vitamin stock solutions stored over 1 year.

(B) Erd-Schreiber Solution.

*	Natural filterd seawater	2 l.
**	Soil extract	100 ml.
***	$NaNO_3$	0.4 g
	Na_2HPO_4	0.0236 g

Autoclave

---

* Natural seawater is collected from non-polluted off-shore sea by pumping it from about 1 metre below sea surface. It is filtered through 0.22 µm filter, autoclaved and kept in a dark cold place.

** Soil extract is prepared from humus (fertile, dried, free from insecticides and fungicides) and sieved earth. The preparation procedures are:

1. Mix soil with distilled water by ratio 2:1 by volume, i.e. pour 1 l. of distilled water into a large beaker and add soil until the volume reaches 1.5 l.
2. Stir well and autoclave at 15 psi/121°c for 20 min.
3. Decant when it is cooled.
4. Leave solution to stand overnight.

5. Decant and throw away sediment.
6. Centrifuge at 5000 rpm for 30 min.
7. Filter the clear solution gradually from large pore size filter, 3.0 µm, down to 0.22 µm.
8. Separate them into required amounts.
9. Autoclave at 15 psi., 121°C, 20 min.
10. Keep them in a refrigerator.

*** $NaBO_3$ 4g, Na_2HPO_4 0.236 g in 100 ml. seawater. Use 10 ml of this stock solution for every 2 l. of seawater for Erd-Schreiber Solution.

(C) Preparation of AE 50 Medium.

1.	Take filtered distilled water	1500 ml.
2.	Add Major salts	500 ml.
3.	Add Tris	50 ml.
4.	Adjust pH to 7.6-7.8, use filtered 1.0N.HCl	(≃ 12 ± 1 ml)
5.	Add Metals	40 ml.
6.	Add Minor salts	2 ml.
7.	Add Erd-Schreiber Solution	2,110 ml.

8. Separate into required amounts then autoclave at 15 psi. 121°C, 15 min.
9. Add stock solution of all vitamins 10 ml. when medium is cooled.
10. Medium with or without vitamins should be kept in a refrigerator.

NB. 1. For a richer medium, double the amount of soil extract can be used.

2. All stock solutions should be kept in a dry, cold and dark

place, i.e. a refrigerator.

APPENDIX 2

STANDARD PROCEDURES OF CULTURE MAITENANCE

1. Select 50 mature cells; colourless stalks, full-sized caps from several flasks; wash several times with sterile sea water and leave them in 400 ml. AE 50, 12/12 hours. light/dark, 21 ± 1°C for a month to ensure complete maturation of the caps.
2. Transfer them into sterile seawater and leave in dark, 10 ± 1°C for a month.
3. Expose them to light for 12 hours, then renew sterile seawater, and leave in the same conditions for another month with sea water being changed every week. (Steps 2 & 3 are to minimise contaminations).
4. Transfer into AE 50 medium and leave in the dark at room temperature (20 ± 5°C) for three months, exposing them to light 12 hours/month and renew medium monthly. Cysts should be mature after this period.
5. Second selection for mature cysts. Under (20 times) microscope, only caps containing cysts are harvested from several flasks. Separate 50 caps from their stalks and leave them in a sterile dish containing sterile seawater. To free the cysts cut or tear the caps along the rays with a pair of aseptic scissors or an aseptic needle. Wash the cysts (with cap fragments) several times through 50 µm sterile nylon filter with sterile seawater. Cysts (with cap fragments) are retained on the filter and contaminants should be washed away at this state. Transfer the cysts into a flask containing 400 ml. AE 50.
6. Keep them in 12/12 hrs., light/dark, 21 ± 1°C for 5 days.
7. Place in dark at 14 ± 1°C for 2 days.
8. Repeat (6).
9. Repeat (7).

10. Return to 12/12 hrs. light/dark, 21±1°C for 11 days. Gametes should be released; if not, repeat procedures starting from step (7).

11. Renew AE 50 and leave (in the same conditions) for 10 days.

12. Thin out 0.2 mm long cells to $0.5^{ml}/cell$ and leave for 4 days.

13. Renew AE 50, thin out 1mm long cells to $1^{ml}/cell$ and leave for 6 days.

14. Renew AE 50, thin out 2mm long cells to $5^{ml}/cell$ and leave for 6 days.

15. Renew AE 50, thin out 4mm long cells to $8^{ml}/cell$ and leave for one month.

16. Renew AE 50, thin out to $10^{ml}/cell$ and leave for one month.

17. Renew AE 50, thin out to $20^{ml}/cell$ and leave until caps are developed *. AE 50 is renewed monthly.

18. While the mature caps are developing, renew AE 50 every three days for three times. The colourless stalks should be seen; if not, renew AE 50 every week until caps are mature. Mature caps are to be harvested, then repeat step (1).

---

* Cap development among cells in the same flask may not be synchronous, i.e. if they are individually separable, select them for the same cap sizes; if they are attached together into a bunch, use majority of the cap size for this selection.

APPENDIX 3

FABRICATION OF A GLASS MICRO-ELECTRODE

(a) Glass pipettes.

Glass micropipettes are made from borosilicate glass tubes[1] of I.D. 0.5 - 1.0mm and O.D. of 1.0 to 2.0mm. The I.D. : O.D. ratio of 1:2 is preferable. The commercial capillary tubes[2], made by Clark Electromedical Instruments, England, are very convenient for consistent results. The I.D. (0.58mm) and O.D. (1.0 ± 0.1mm) have less than 10% error. The single capillaries with inner filament(s) (Fig.A3.1a) make it easier for the pulled micropipettes to be filled with electrolyte.

Micropipette pulling.

Before they are pulled, glass capillary tubes must be cleaned thoroughly by soaking in 10% chromic acid (or HNO_3 or equivalent) overnight, rinsed well with hot water, then distilled water, and dried in the oven.

The micropipette puller can be either a horizontal or a vertical type. The horizontal type[3] was used here. The micropipette tip profile produced by the machine is controllable by a selection of the combination of the variations from the tube dimensions, the pulling force, the heater temperature and the time delay before the pull. The pulling procedure begins with clamping a clean glass capillary tube firmly in the position within the nichrome heater strip. When the time delay is

---

(1) See Lavallee, et.al., 1969, for types of glasses used for micropipettes.
(2) They were introduced into market in 1977-78.
(3) Microelectrode puller Model 8104, C.F. PALMER, London.

Fig.A3.1

a)

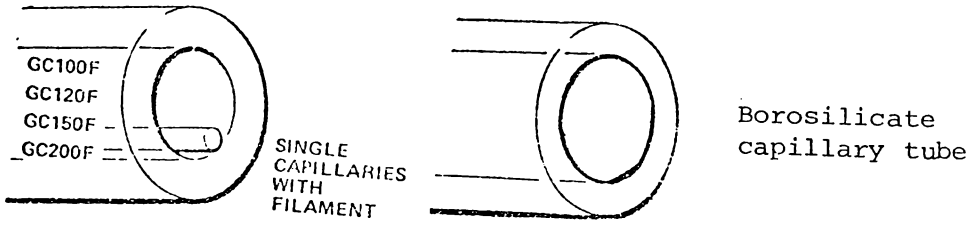

b)

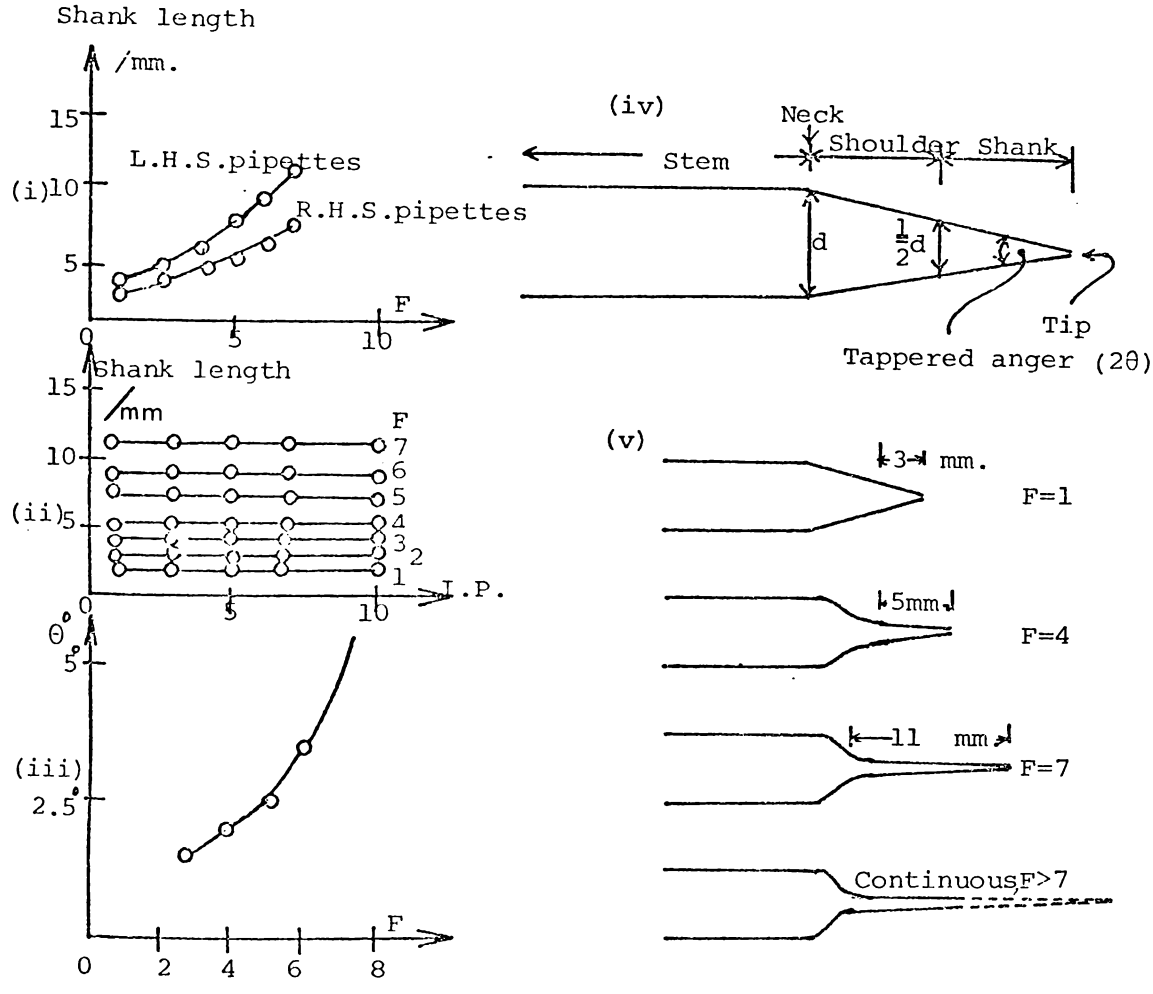

a) Capillary tubes

b) Pulling Conditions

Capillary tubes = Hard Capillary tube
I.D = 1.2mm
O.D. = 1.6mm (±10%)
length = 75mm

(i) shank length vs. Heater Current (Furnace = F)
(ii) shank length vs. Initial Pulling Force (I.P.)
(iii) Estimated tappered angle (θ) vs. F.
(iv) Terminology of a micropipette
(v) Typical shape of micropipette pulled at different F's.

selected and the pulling force and the heater current are set, the start switch is pressed. Heat is then applied to the tube until it reaches a plastic state. When the pre-set time delay is reached, a solinoid is actuated releasing the pulling mechanism and the micropipette is pulled. The tip sizes of the workable micropipettes are estimated in the range of 1.5 ± 1 μm. The shank is 10 ± 2mm long (Fig. A3.1b).

Fillant.

Generally the fillant for glass microelectrodes is saturated or 3M KCl. There are several advantages of this solution mainly the minimum diffusion potential, the obviation of the liquid junction potential, and keeping the electrode resistance as low as possible.

For a larger tip size micropipette (the resistance is relatively lower) the medium (AE 50) can be used to minimise the ionic diffusion between the cytoplasm and the fillant.

The filling method.

The pipettes can be filled with electrolyte directly or indirectly. The classical indirect or alcohol method (Tasaki,et.al.,1954)is well known. It takes 2-3 days to complete the procedure and may introduce a high tip potential (see e.g. Agin & Holtzman, 1966; and Gotow, et.al., 1977). The direct filling method is much easier and offers a smaller tip potential. However the micropipettes must be drawn from the tube (I.D. ≤ 1mm) that contains some (5-10) glass fibres (≃ 20 μm in diameter), or the commercial capillary tube with filaments built in. To fill these pipettes, the pressure in the filling jar may need reducing - see Fig. A 3.2. For quicker filling, it is helpful to warm up the fillant. This may enable the pipettes to be filled within 10 seconds. Otherwise the pipettes may be left to be filled by surface tension effect. The

Fig.A3.2

a Micropipette Holder

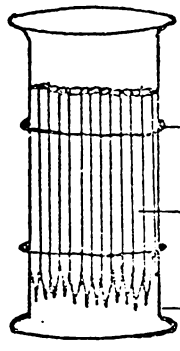

b Filling Jar

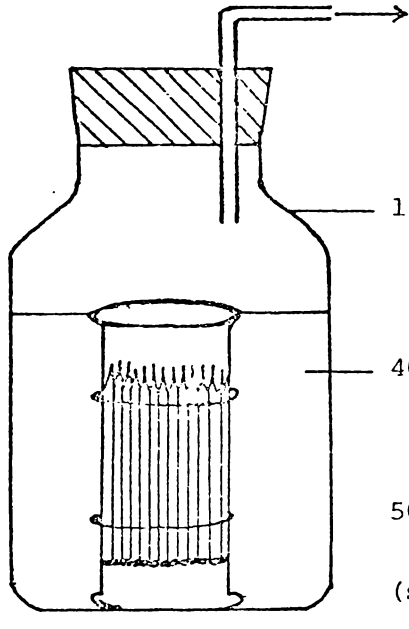

micropipettes produced by tubes with filaments have a smaller tip size but stronger shank and lower tip potential (Tasaki, et.al., 1968).

Storage of Micropipettes.

It is recommended to store the micropipettes by holding with a pipette holder in closed container and avoiding exposure to light and heat. The pipettes should be filled with and soaked in distilled water. This is to minimise the contaminations and their growth that could cause higher tip potential, tip resistance or even blocking the tip of the pipette.

(b) Ag/AgCl Electrodes.

Standard Procedures for Making a Set of 10 Tight Helix Ag/AgCl Electrodes.

1. High purity (99.999%) silver wire of 0.3mm in diameter is cut into ten 200mm long segments.
2. Each wire is soldered at one end to a small flexible wire of ~200mm long. The joint is kept as small as possible (< 1mm in diameter).
3. They are wiped with acetone, rinsed in distilled water and dried in a closed cabinet.
4. The joints and the surface that is not to be chlorided is coated with varnish (see Section 4.2) and allowed to dry.
5. The wires are dipped into 50% (by vol.) HNO_3 for 1 min. (to get rid of surface impurities, as well as to make a larger rough surface for a better chloriding).
6. The wires are wound around a 0.3 - 0.4mm drill (or any similar cylinders) to give a tight helix of 0.7 - 1.0mm. in diameter, ~ 100 turns and ~ 60mm long.
7. The wires are tied together and arranged at equal radial distances

and spacings.

8. They are dipped into acetone for 10 seconds, let dry, then dipped into distilled water several times, and into 50% HNO_3 for another 10 sec. and rinsed with distilled water several times.

9. The chloriding circuit is set as in Fig. 4.2.2 :

Electrolyte	= 800 ml, 0.1N HCl in 1 l. beaker,
Cathode	= Pt. or Ag. wire coiled to fit in the beaker,
Anode	= Ag-wires to be chlorided, hung centrally,
Battery	= 1.5V dry cell,
10 kΩ	= variable 10 kΩ resistor,
A	= Ammeter - ranges 1 - 100 mA.

10. The resistor is adjusted to give a current density of about 5 - 7 mA/cm^2 of Ag-wire surface, and the wires are left chloriding for 1-3 hours in the dark.

11. The circuit is opened to let chlorided electrodes age for ~ 20 min.

12. The circuit is then closed for another 1-3 hours chloriding. The required electrodes are then left for ageing in 0.01N HCl (or equivalent - see Section 4.2), in the dark for at least 2 days.

NB. (i) Amount of chloride coated on Ag-wire is calculated by:

$$m = \frac{it \times m_{AgCl}}{96500} \text{ g.,}$$ where i = applied current/amp,

r = chloriding time/sec.,

m_{AgCl} = gram equivalent wt. of AgCl (143.5 g).

(ii) During chloridizing the current decreases as the Ag-wires are coated more thickly, i.e. higher resistance layer.

(iii) Typical resistance of these electrodes (as measured by an A.C. bridge meter) ≃ 10 ± 5 kΩ in AE 50.

(iv) For ageing and storing these electrodes, see Section 4.2.

Tip Resistance and Tip Potential of Microelectrodes.

A glass microelectrode is made up of a glass micropipette containing electrolyte and an Ag/AgCl electrode. It has two important electrical characteristics; tip resistance and tip potential.

High tip resistance comes from a smaller tip pore size (in the order of 1 μm - determinable only under an electron microscope), and a dilute electrolyte. Pore size of < 0.5 μm, in 3M KCl, may have a resistance over 100 MΩ. This can distort the input signals and a very high input impedance amplifier is required. However, the small tip pipette favours the experiments in terms of prolonging the cell survival time because of the smaller rate of diffusion. A compromise for these is found in a microelectrode that gives tip resistance in the range of 1 - 5 MΩ, the tip pore size is 1 - 2 μm and tip potential is 1 ± 0.5 mV.

Tip potential is measurable experimentally by taking the difference of the potential between two microelectrodes. Another possibility is to measure the difference of the potentials before and after breaking the tip (Lavellée, et.al., 1969).

APPENDIX 4

LABORATORY COMPUTER PROGRAMS

This appendix contains outline descriptions of the suite of programs developed for date acquisition and analysis.

The detailed coding was done by Dr. R.A. Sherlock.

I TRANSIENT RECORDER PROGRAMS - TR3 SERIES OUTLINE STRUCTURE

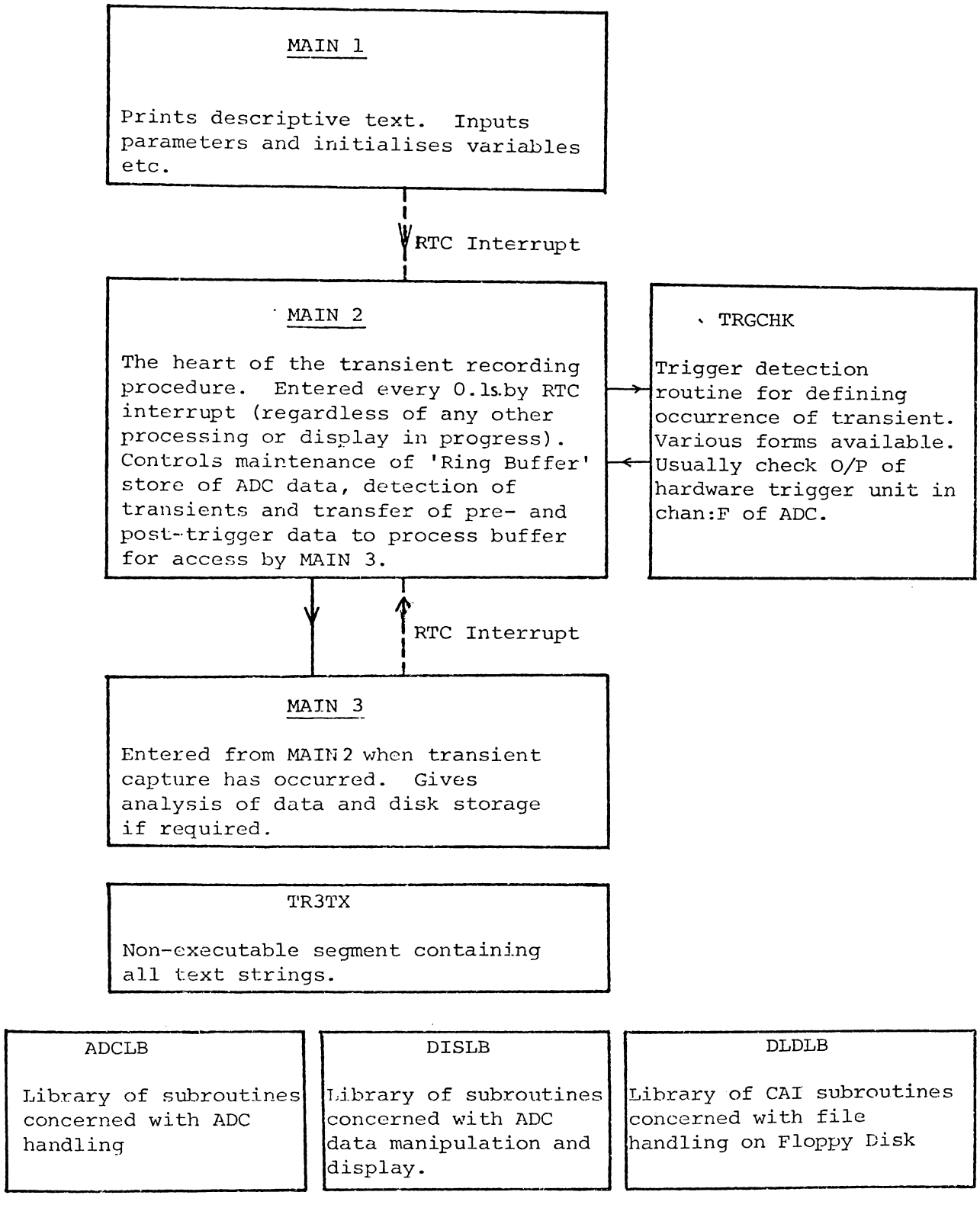

Ia MAJOR PROGRAM VARIABLES - TR3 PROGRAM.

HHCTR — "Half hour counter" counts clock beats to initiate a logging printout every 30 mins.

CIFLG — "Console Interrupt Flag" Data word which is incremented by the CPU console Interrupt switch being depressed or by the "half hour counter". If CIFLG is set (i.e. has value > 0) a logging printout of the current scan is produced.

DBUF — 16 word buffer in which ADC read subroutine RADC 22 stores the ADC data words.

RBUF — "Ring Buffer". 8192 word buffer containing current and preceeding (SCANL X RECLEN - 1) ADC words.

TRCNT — "Transient end Count" - negative if no. of samples remaining before end of transient record is reached. Set at + 1 if transient capture under way. As soon as a trigger occurs TRCNT set to - TPOS then incremented with every succeeding sample. End of transient record when TRCNT = 0

ABUF1, ABUF2 — Auxillary 16 word storage buffers used for holding DBUF contents so these are not destroyed by subsequent calls to RADC2

TYFLG — Flag to indicate that a (slow) teletype printing operation is under way.

PBUF — "Process Buffer" 8192 word buffer. Captured transient immediately transferred from RBUF to PBUF will be destroyed by continual updating of RBUF.

Ib TERMINOLOGY

ADC word 16 bit data word from multiplex ADC in form

12 ms bits	4 ls bits
2's complement ADC O/P	chann. addr.

TTY Print in form C ± XXXX (-2048 to +2047)

Sample Set of data words from successive ADC channels (time separation ≃ 60 μs. is negligible compared with the minimum Sample Interval of 0.1s in these experiments. Hence can consider all words in sample being taken at approximately same point in time).

Scan Length (SCANL) Number of data words in sample, i.e. no. of channels scanned in each sample.

Transient Record or Record Sequence of samples containing the time record immediately before and after a trigger condition was detected.

Record length (RECLEN) Total number of samples in a Transient Record.

Trigger Position (TPOS) defines time point within the Record at which the trigger condition first occurred, e.g. if Record length = 256 and Trigger Position = 176 then Record consists of the 80 samples immediately prior to the trigger and the 176 samples immediately after.

N.B. Underlined upper case names are program variables or symbolic labels.

General and Hardware Abbreviations.

RTC	Real Time Clock
LIFO	Last in - First out
CPU	Central Processing Unit
A - REG	The two general purpose storage registers in the CPU.
X - REG	All data manipulations involve one or both of these.

Ic DETAILED FLOW DIAGRAM - TRANSIENT RECORDER PROGRAM TR3M15

(TR3, MAIN 1, VERSION 5)

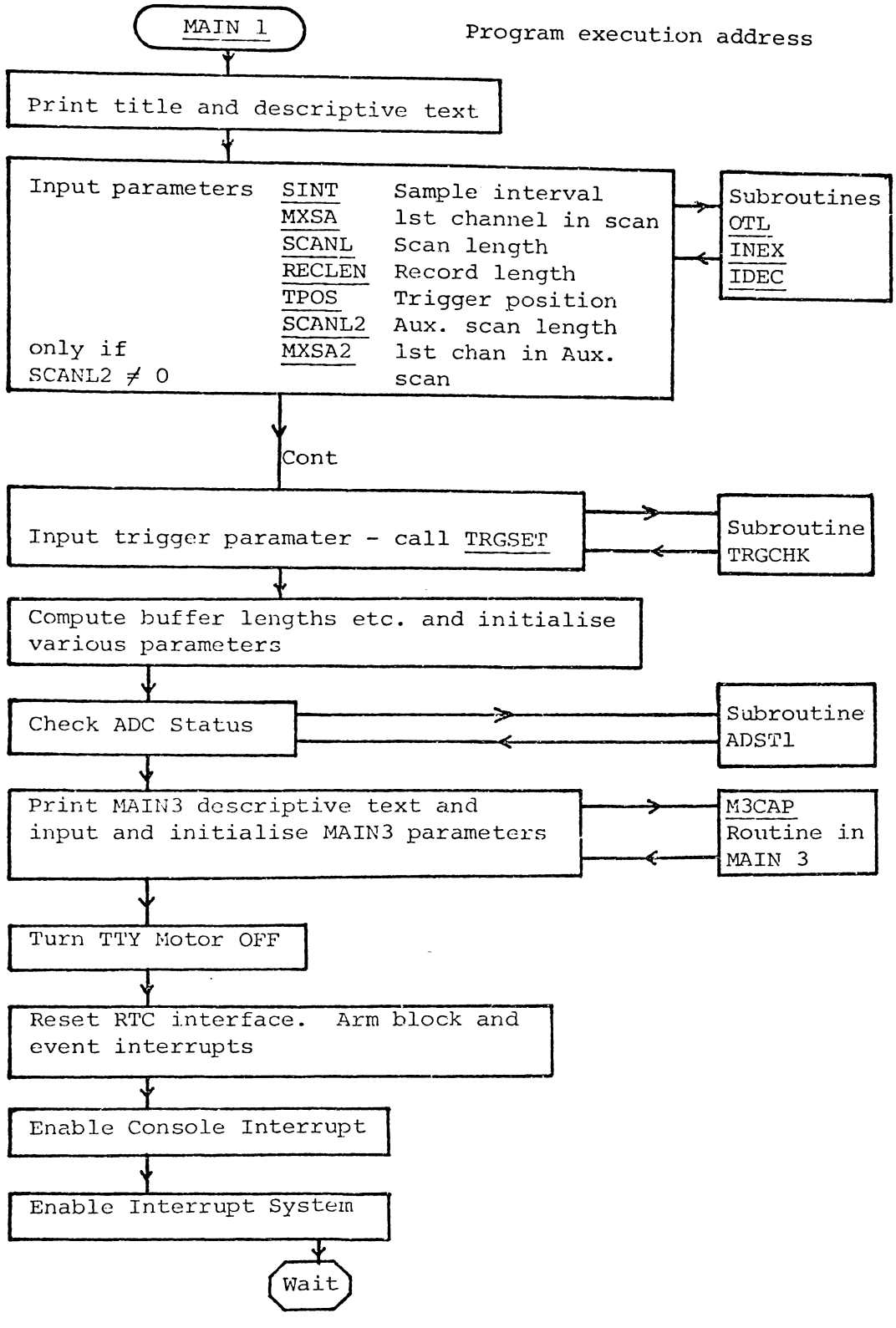

Await RTC Interrupt to transfer to MAIN 2

Id DETAILED FLOW DIAGRAM - TRANSIENT RECORDER PROGRAM TR3M25

(TR3, MAIN 2, VERSION 5)

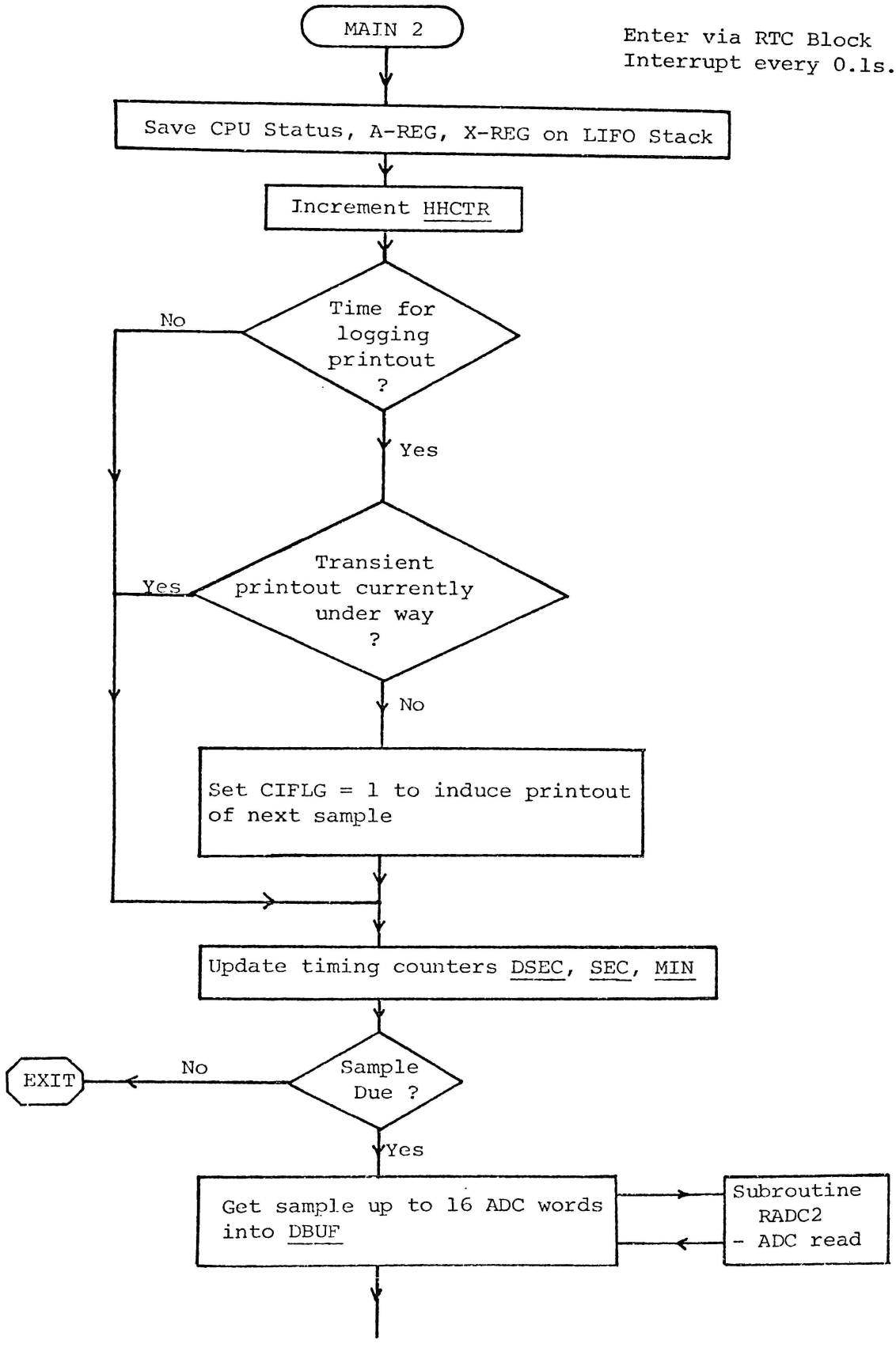

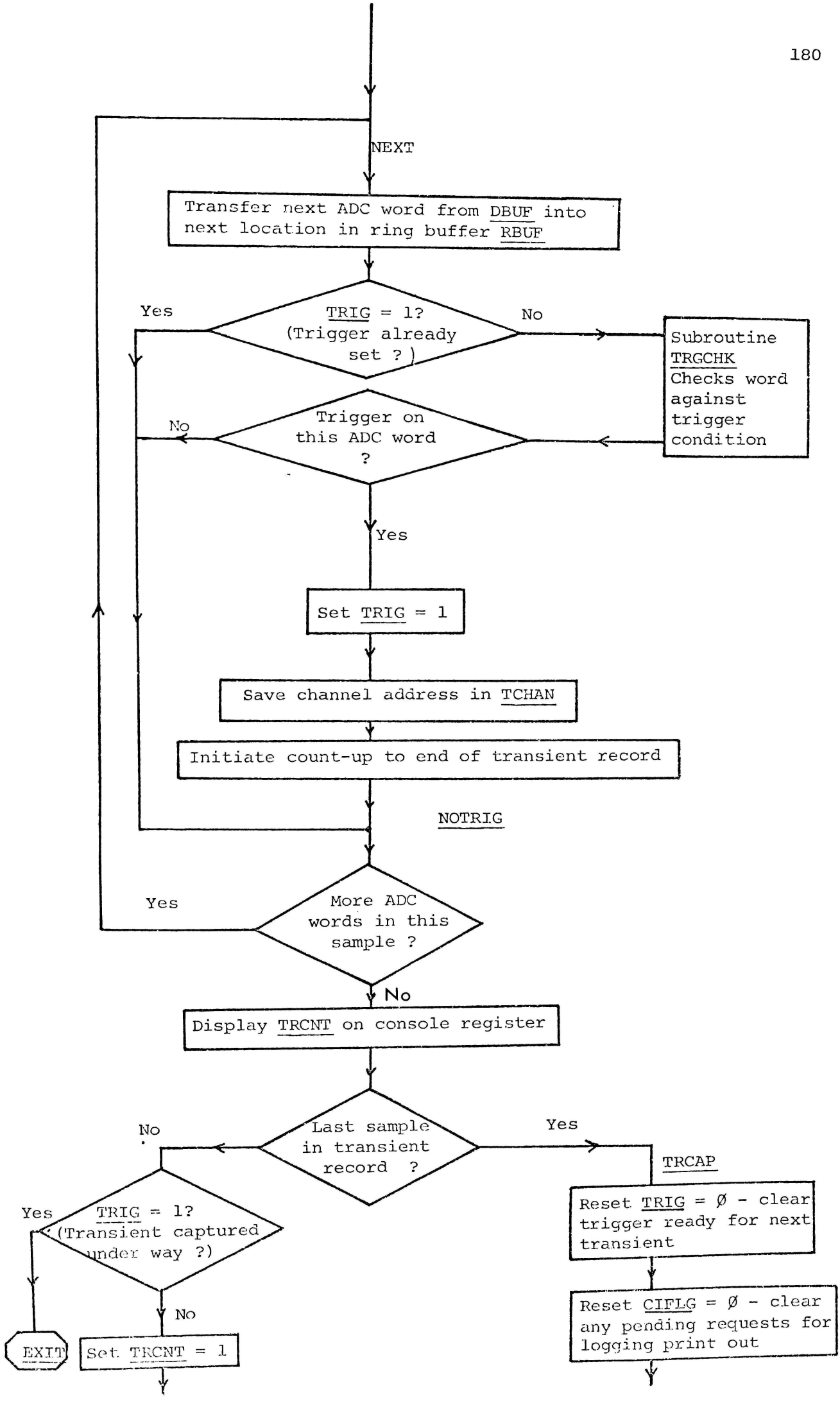
NEXT
Transfer next ADC word from DBUF into next location in ring buffer RBUF
TRIG = 1? (Trigger already set ?)
Yes
No
Subroutine TRGCHK Checks word against trigger condition
Trigger on this ADC word ?
No
Yes
Set TRIG = 1
Save channel address in TCHAN
Initiate count-up to end of transient record
NOTRIG
More ADC words in this sample ?
Yes
No
Display TRCNT on console register
Last sample in transient record ?
No
Yes
TRCAP
TRIG = 1? (Transient captured under way ?)
Yes
No
Reset TRIG = Ø - clear trigger ready for next transient
Reset CIFLG = Ø - clear any pending requests for logging print out
EXIT
Set TRCNT = 1

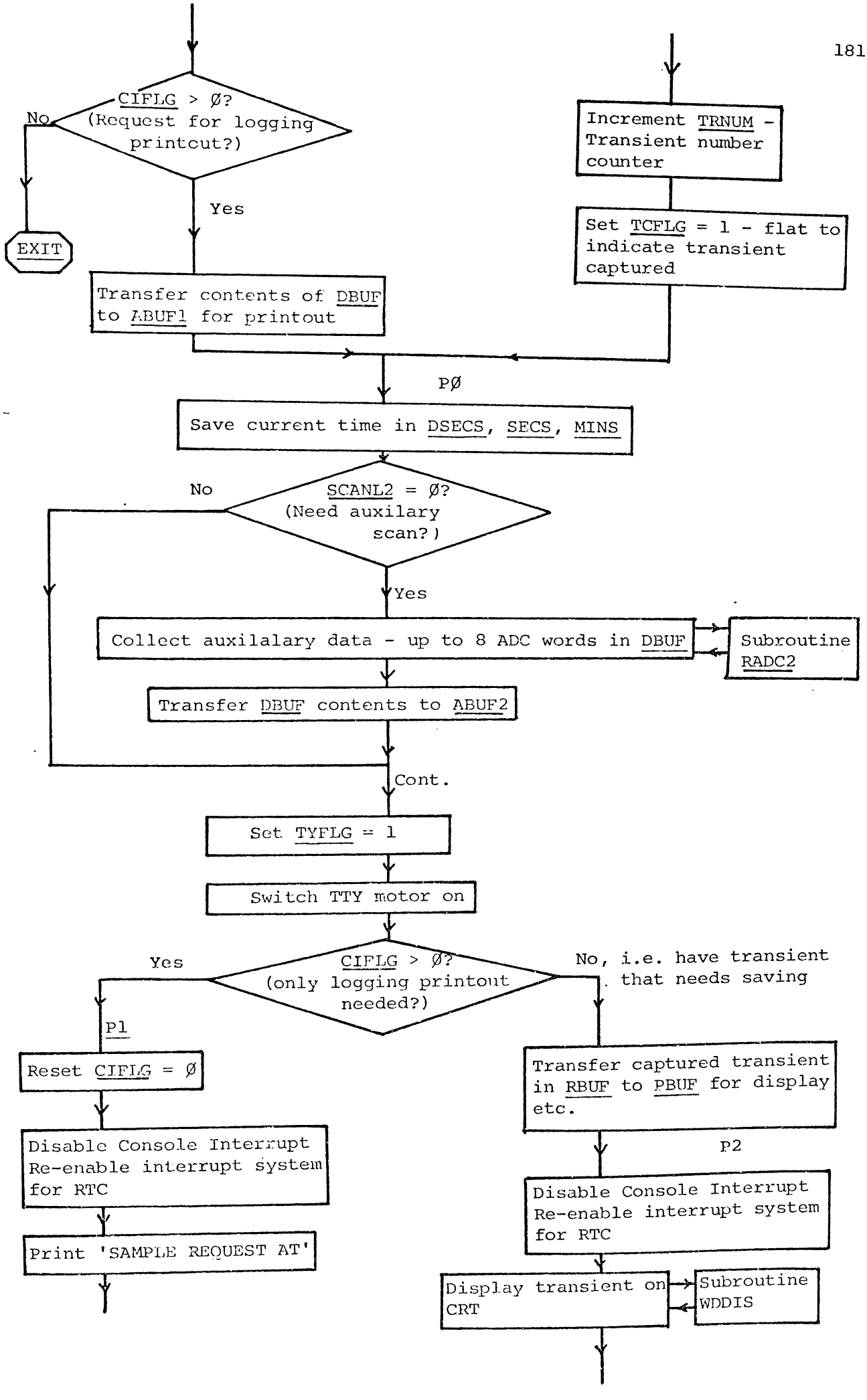
CIFLG > Ø?
(Request for logging printout?)
No
Yes
EXIT
Transfer contents of DBUF to ABUF1 for printout
Increment TRNUM - Transient number counter
Set TCFLG = 1 - flat to indicate transient captured
PØ
Save current time in DSECS, SECS, MINS
SCANL2 = Ø?
(Need auxilary scan?)
No
Yes
Collect auxilalary data - up to 8 ADC words in DBUF
Subroutine RADC2
Transfer DBUF contents to ABUF2
Cont.
Set TYFLG = 1
Switch TTY motor on
CIFLG > Ø?
(only logging printout needed?)
Yes
No, i.e. have transient that needs saving
P1
Reset CIFLG = Ø
Disable Console Interrupt
Re-enable interrupt system for RTC
Print 'SAMPLE REQUEST AT'
Transfer captured transient in RBUF to PBUF for display etc.
P2
Disable Console Interrupt
Re-enable interrupt system for RTC
Display transient on CRT
Subroutine WDDIS

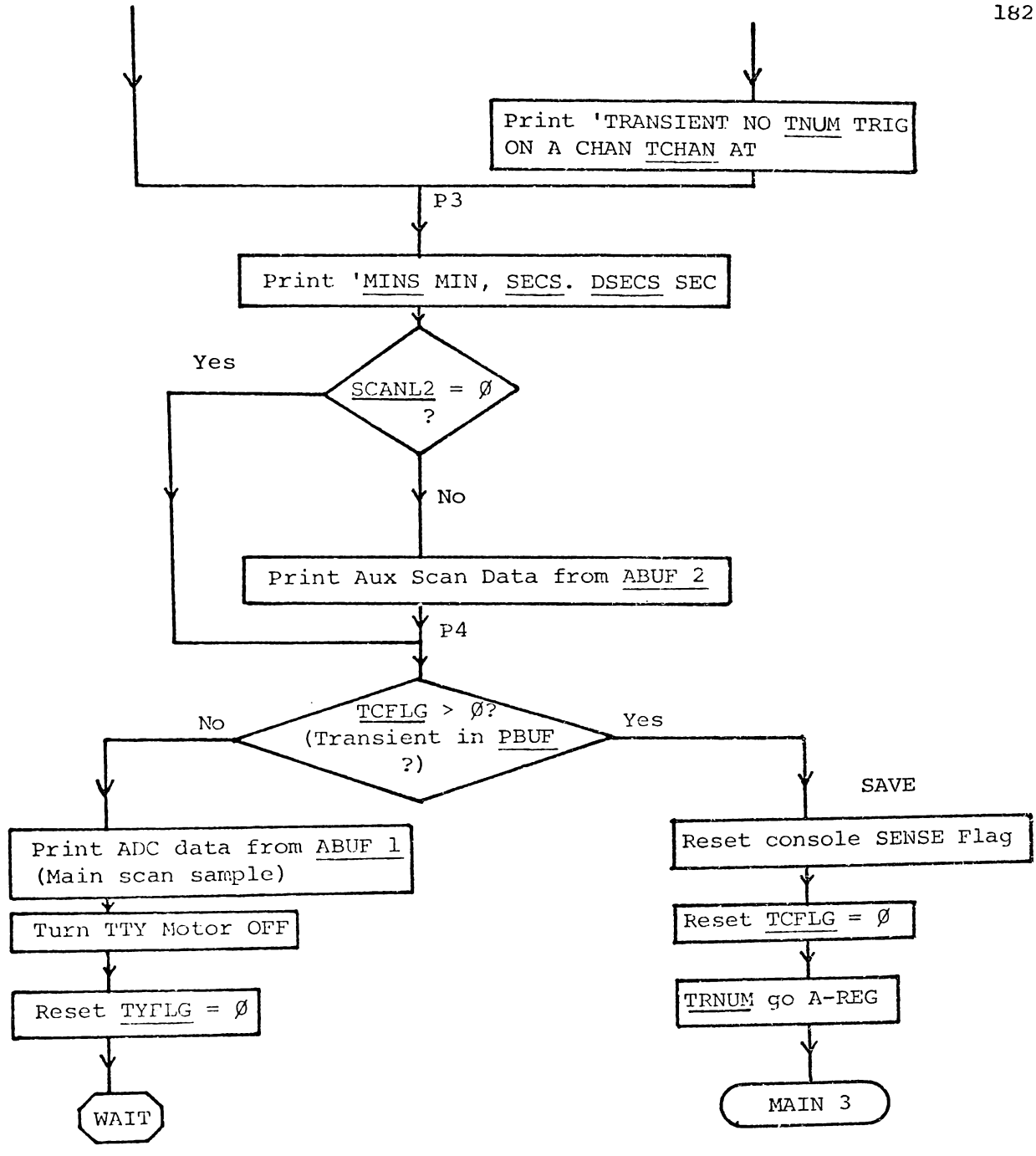

(Await next RTC interrupt which will cause re-entry into MAIN2)

(Further processing and storage of transient handled in next segment of Main Program).

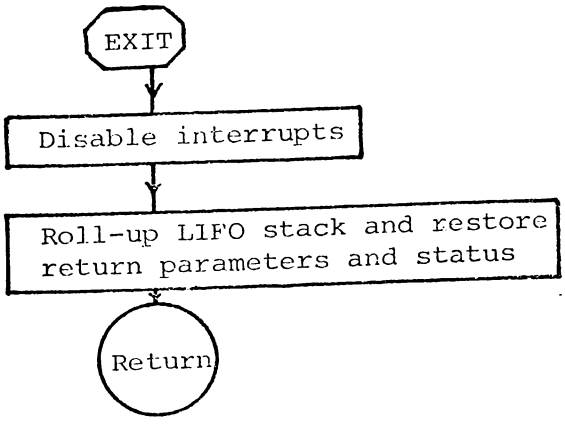

Normal EXIT, returns program to point where RTC interrupt caused branch to MAIN2

Ie DETAILED FLOW DIAGRAM - TRANSIENT RECORDER PROGRAM TR3M35

(TR 3, MAIN 3, VERSION 5)

This segment contains two entry points, M3CAP and MAIN3. The M3CAP section is entered from MAIN 1 and handles descriptive text printout, parameter input and initialisation. Returns to MAIN 2 on completion.

The MAIN3 section is entered from end of MAIN2 when a captured transient has been transferred to PBUF. The data in PBUF is analysed for peak values and positions and baseline values which are printed on the TTY, and unless inhibited by setting console SENSE Flat PBUF contents are saved on Floppy Disk.

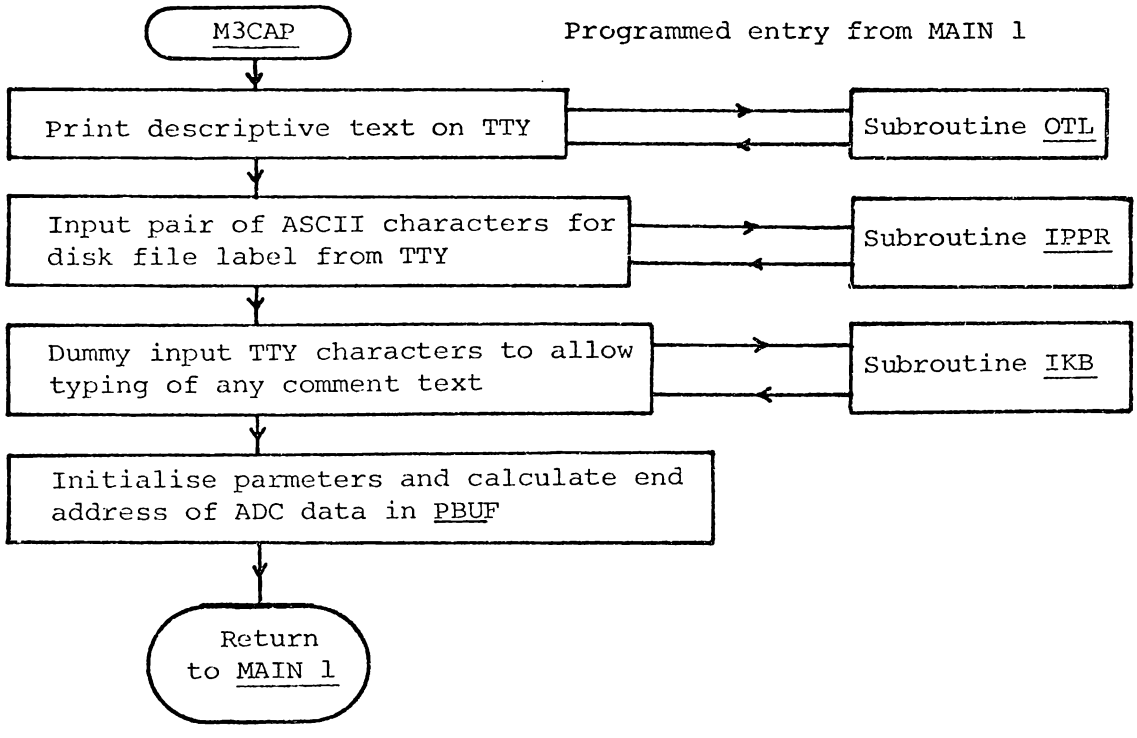

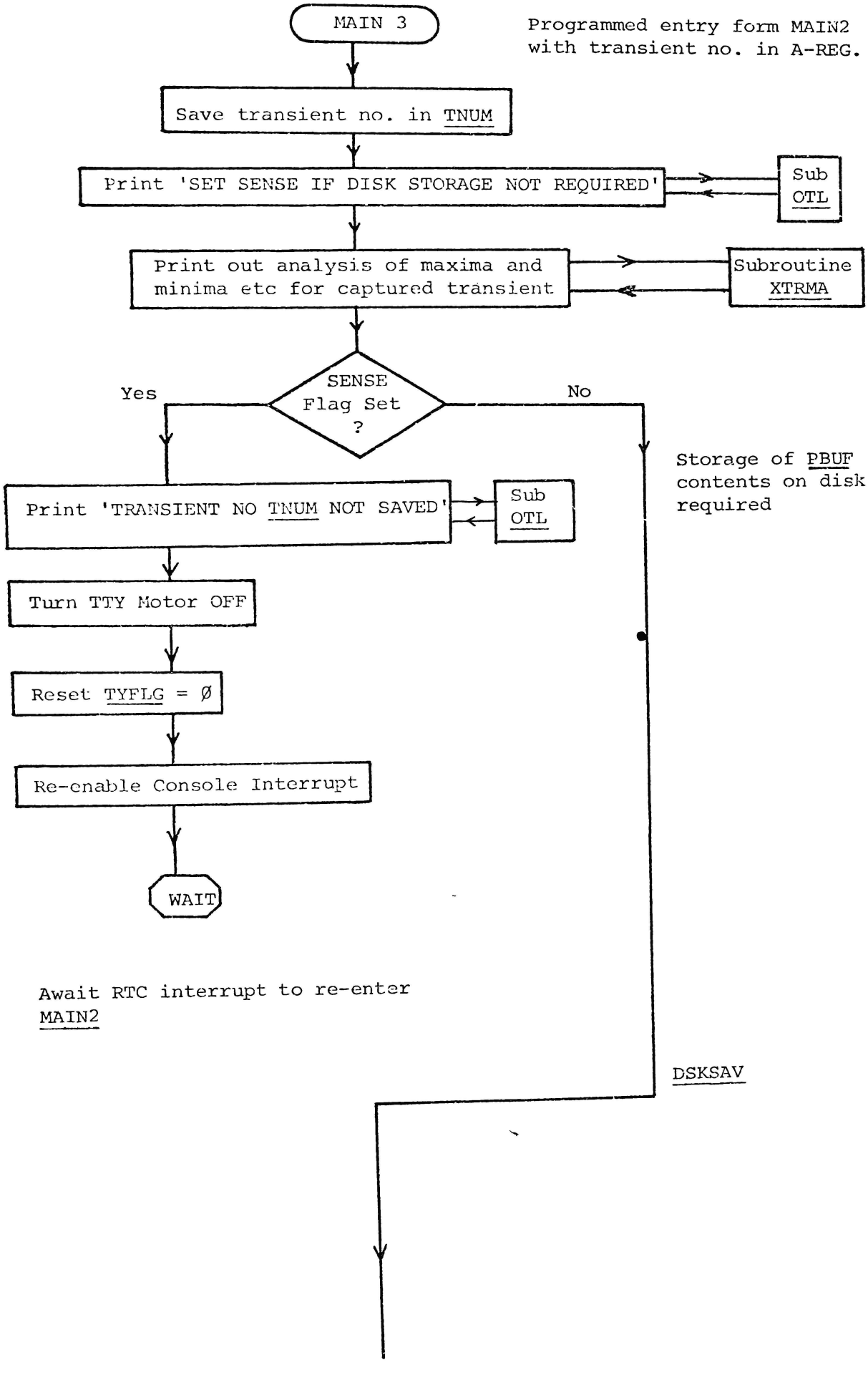
MAIN 3
Programmed entry form MAIN2 with transient no. in A-REG.
Save transient no. in TNUM
Print 'SET SENSE IF DISK STORAGE NOT REQUIRED'
Sub OTL
Print out analysis of maxima and minima etc for captured transient
Subroutine XTRMA
SENSE Flag Set ?
Yes
No
Print 'TRANSIENT NO TNUM NOT SAVED'
Sub OTL
Storage of PBUF contents on disk required
Turn TTY Motor OFF
Reset TYFLG = Ø
Re-enable Console Interrupt
WAIT
Await RTC interrupt to re-enter MAIN2
DSKSAV

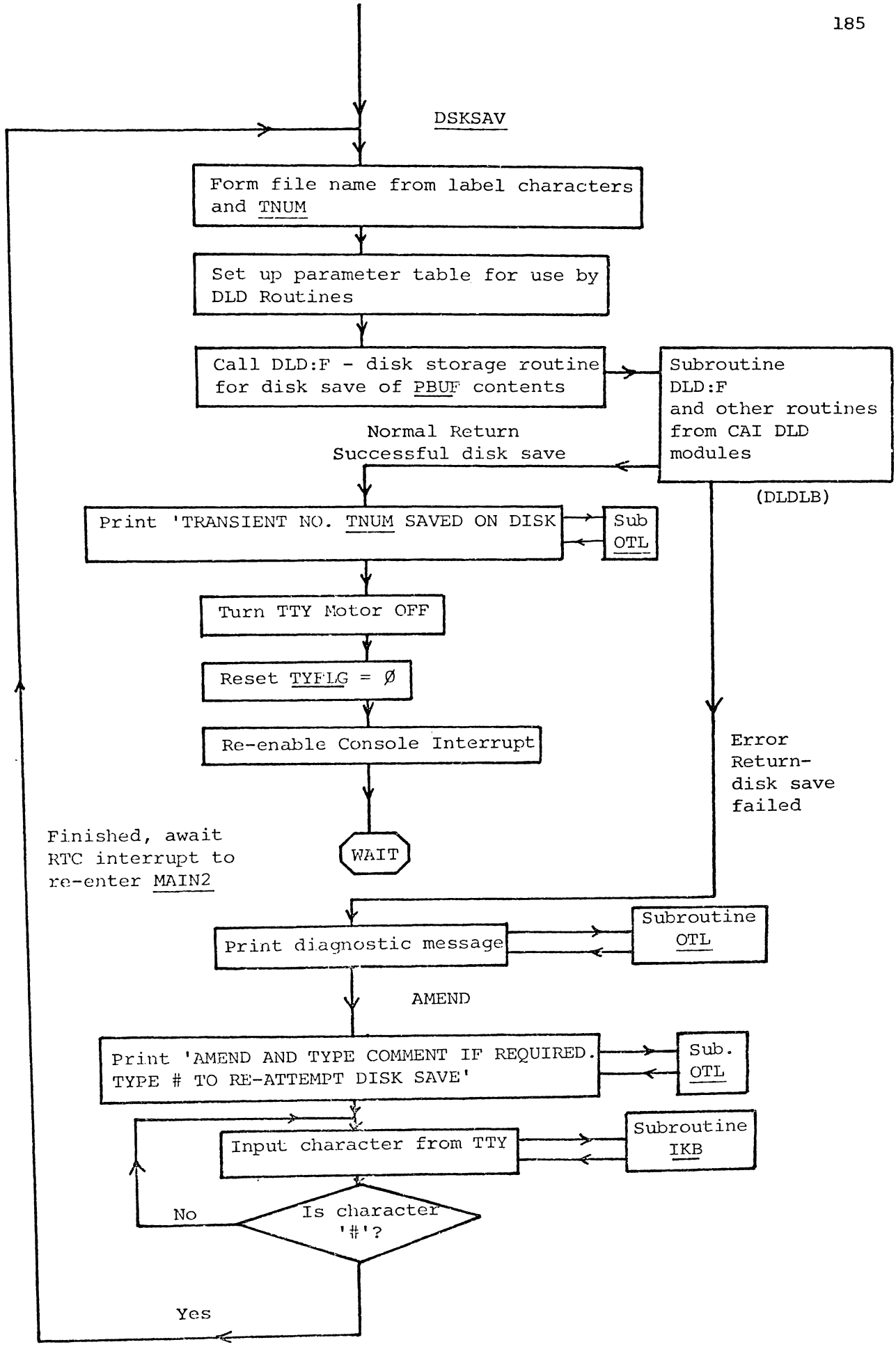
DSKSAV
Form file name from label characters and TNUM
Set up parameter table for use by DLD Routines
Call DLD:F - disk storage routine for disk save of PBUF contents
Subroutine DLD:F and other routines from CAI DLD modules
(DLDLB)
Normal Return
Successful disk save
Print 'TRANSIENT NO. TNUM SAVED ON DISK
Sub OTL
Turn TTY Motor OFF
Reset TYFLG = Ø
Re-enable Console Interrupt
WAIT
Finished, await RTC interrupt to re-enter MAIN2
Error Return- disk save failed
Print diagnostic message
Subroutine OTL
AMEND
Print 'AMEND AND TYPE COMMENT IF REQUIRED. TYPE # TO RE-ATTEMPT DISK SAVE'
Sub. OTL
Input character from TTY
Subroutine IKB
Is character '#'?
No
Yes

II DATA STRUCTURE IN PBUF (in TR3 and TDDP Programs) and OBUF (in TDDP)

PBUF contains standard ADC data format words defining the complete transient record (i.e. voltage as a function of time for several input channels) in the following structure.

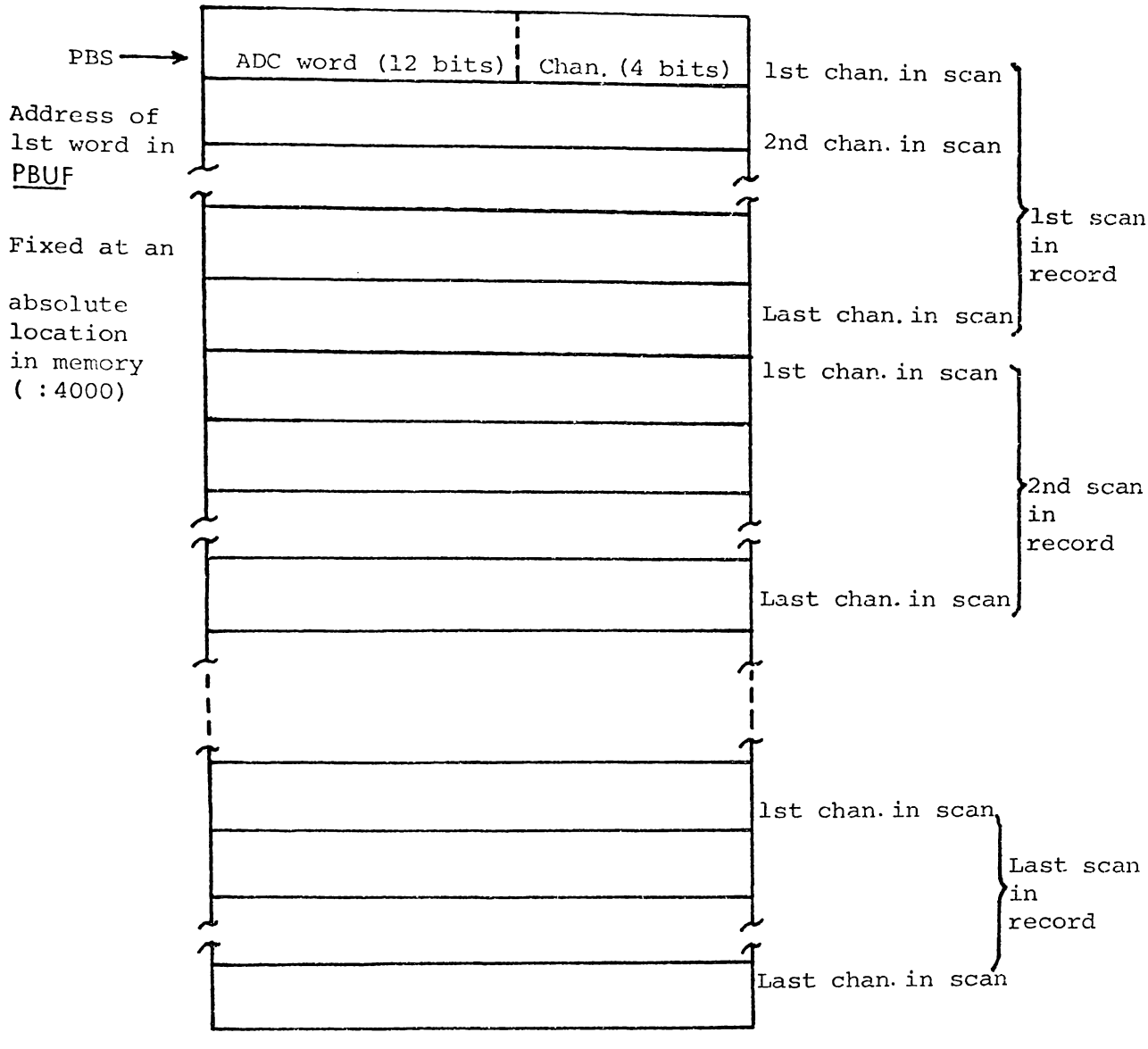

Transient data is written into PBUF in this form by TR3 MAIN2, stored onto Floppy Disk in this form by TR3 MAIN3, and reloaded into PBUF in the same form by TDDP2.

Thus when a disk file is loaded by TDDP2 the complete data set for one transient is loaded into cone in PBUF.

For all processing and graphical display operations the transient record for one channel only is handled at any one time. A second buffer OBUF (Output buffer) is used to set up alternate X(time) and Y (ADC output) values for access by the CRT and XY plotter drive routines. Thus the data structure in OBUF is as follows.

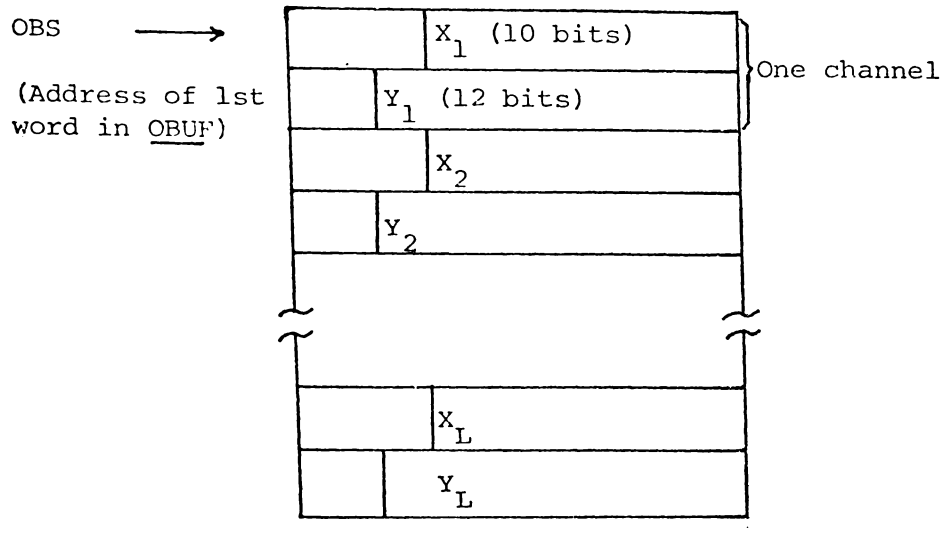

The Y values are successive ADC data words from the same channel (shifted right 4 bits to eliminate the channel index) and the X values normally increment from $X_1 = 0$ to X_L = (RECLEN - 1)

The Digital-to-Analog converters in the CRT/Plotter interface are set up to give the following sensitivites.

X	X = 0, $V_x = 0$;	X = 1023, V_x = + 10.24V
Y	Y = -2048,	V_y = 0.V
	Y = 0,	V_y = 5.12V
	Y = +2047,	V_y = + 10.24V

III TRANSIENT DATA DISPLAY AND PROCESS PROGRAM (TDDP)

Program runs "off line" (i.e. not during actual experiments) and enables data files to be read from Floppy Disk and various display and analysis procedures to be performed.

Operates under control from Teletype in a conversational mode.

Program types '?' when requires a command.

Operator responds with one of the following command strings.

TRANSIENT DATA DISPLAY & PROCESS COMMANDS

Complete data for a transient loaded into PBUF from disk in F1. This can be accessed for TTY printout or transferred to OBUF for manipulation and display, but it is never altered or destroyed except by being replaced with another load (L) command.

1. Load PBUF from floppy disk in F1

   L ffffff. ffffff - 6 character filename

2. Processing with TTY Printout

   T aaaa ∩ bbbb. Type all channel data from sample aaaa to bbbb inclusive aaaa, bbbb +ve decimal in range 0 - 1023, bbbb > aaaa

   X. Type maximum and minimum values and their positions, averages of 1st and last 100 samples and peak to peak span for all channels.

   Vaaaa ∩ bbbb. Type average value of samples aaaa to bbbb inclusive for channel data currently in OBUF.

   ZX. Print extrema of differential signals.

3. Transfer of Data from PBUF to OBUF & Manipulation of OBUF Data

   R. Reset OBUF: All Y-vals set to 0 and X-vals. set in ascending sequence 0-1023

Ah. (Sh.) Adds (Subtracts) data from channel h (hex character) to Y-vals in OBUF.

± ddddc. Adds or subracts decimal integer to all c-vals in OBUF. c = X or Y)

* aaaa/bbbbc. Multiplies all c-vals in OBUF by rational fraction aaaa/bbbb where aaaa, bbbb are +ve decimal integers.

Na. Normalises and shifts Y-vals. so that they are centred about Y=0 and occupy 1/a of FS. (+2000 to -2000). a = +ve integer.

B. Shifts all Y-vals. so extrema are symmetrical about Y=0 baseline.

I. All Y-vals. multiplied by -1 (any -2048 converted to -2047 before inversion).

4. Graphical Output device d = C (CRT) or G (XY Graph Plotter)

Wd. Displays all data in PBUF, automatically scaled and displayed (i.e. all channels).

E. Erase CRT display.

C. CRT display of complete OBUF contents (single channel).

C aaaa ∩ bbbb. CRT display of points in OBUF from aaaa to bbbb inclusive.

D. X-Y graph plotter display of complete OBUF contents.

C aaaa ∩ bbbb. XY trace of points aaaa to bbbb inclusive.

P aaaa ∩ bbbb. As Daaaa ∩ bbbb but individual point plotted instead of single trace. (Takes ~ 1 sec/pt).

Qd. Plots 16 pts. on device d to define full, half and quarter scale values on both X and Y axes (Y max. ±2000, X max. 0,1000)
min. min.

Mxxxx ∩ (-) yyyyd. Plots single point on device d with coordinates xxxx, yyyy.

Zd. Display full set of differential signals auto scaled and display on C or G.

5. Annotation Text and Exit

Any character typed simply printed until next # encountered.

APPENDIX 5

PROPAGATION CHARACTERISTICS OF ACTION POTENTIALS FROM A REDEVELOPING ANUCLEATE ISOLATED STALK SEGMENT

By the methods described in Section 4.4.c, the $\underline{d}(t)$ vs. n plots at various times (as given in Fig. 4.2.2) can be constructed from the recorded v_n waveforms (although recognising that errors may arise from electrode potential and amplifier gain drifts, and other complications e.g. inhomogeneity of the medium in the cell holder). From this the propagation characteristics of an AP initiating at any position can be studied, i.e. how it generates, propagates and decays during the whole course of the event.

To illustrate this procedure five common spontaneous AP's (2 initiating at the far left, 2 at the middle and 1 on the far right of the SS) obtained from the ISS in experiment A8 (Fig. 5.5.7, Section 5.5) are transformed. Their transformed $\underline{d}(t)$ vs. n plots, the corresponding movements of the depolarised regions on the ISS, and the differential voltage waveforms (d_n vs. t) of the whole active period are schematically shown in Figs. A5 a to e respectively. Several other normal and abnormal AP's (Sections 4.5 and 5.4) have been similarly transformed (not shown).

The results suggest that the depolarised region does not propagate uniformly as a whole (contrary to the case of a nerve cell). The boundaries move independently with various speeds, directions and distances. The speeds range from < 0.1 to > 20 mm/s and the propagation patterns are so varied that they are difficult to group.

Although many AP waveforms initiating at the same position on the SS may look alike, they can in fact be different from each other by some of the following factors for example:

Fig.A5

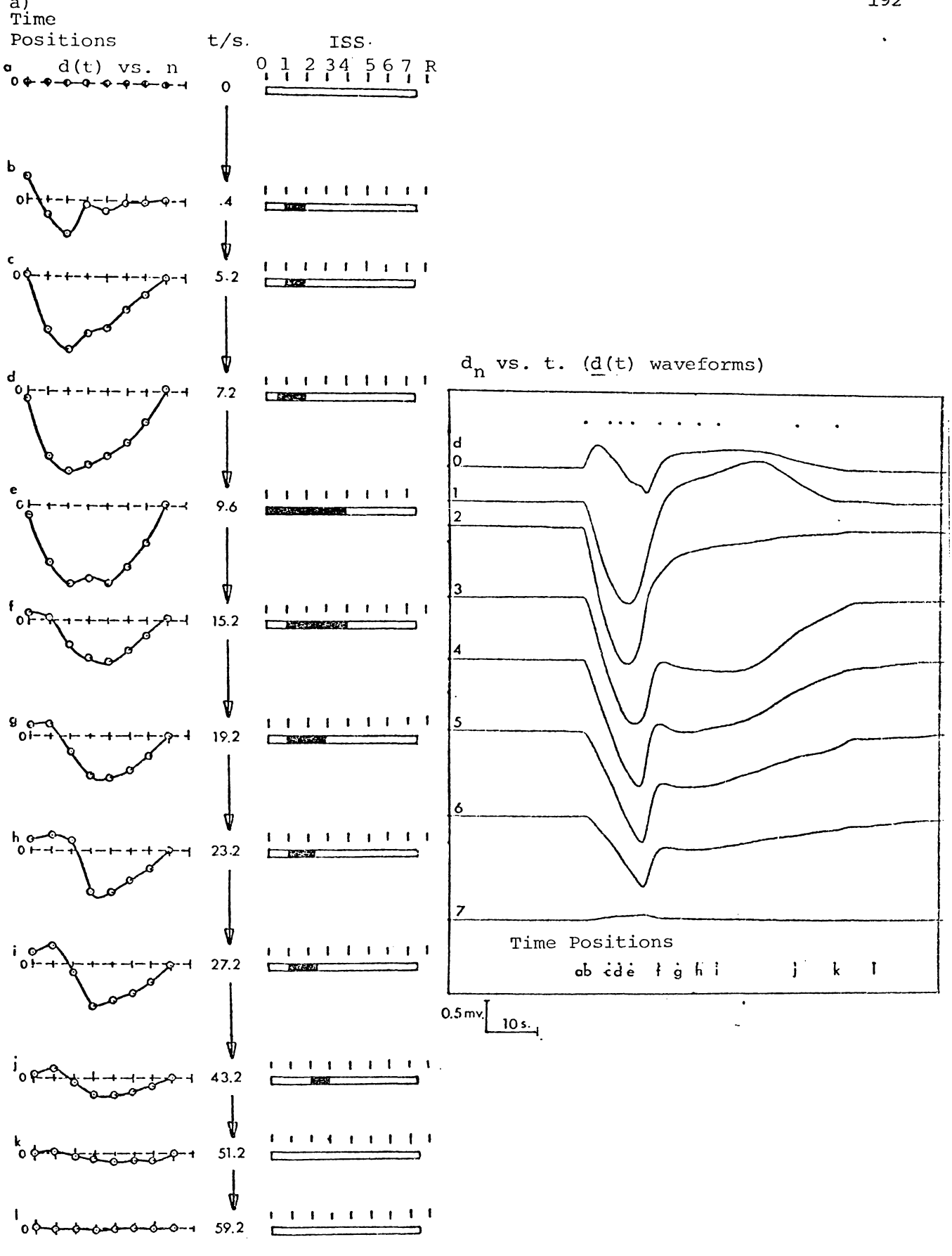
a)
Time
Positions
t/s.
ISS.
0 1 2 3 4 5 6 7 R
a d(t) vs. n
0
.4
5.2
7.2
9.6
15.2
19.2
23.2
27.2
43.2
51.2
59.2
1mv
n
0 1 2 3 4 5 6 7 R
Electrode Positions
Electrode Spacings = 1.9 mm.
d_n vs. t. ($\underline{d}$(t) waveforms)
d
0
1
2
3
4
5
6
7
Time Positions
a b c d e f g h i j k l
0.5 mv.
10 s.

Fig. A5 (Cont. 1)

b)

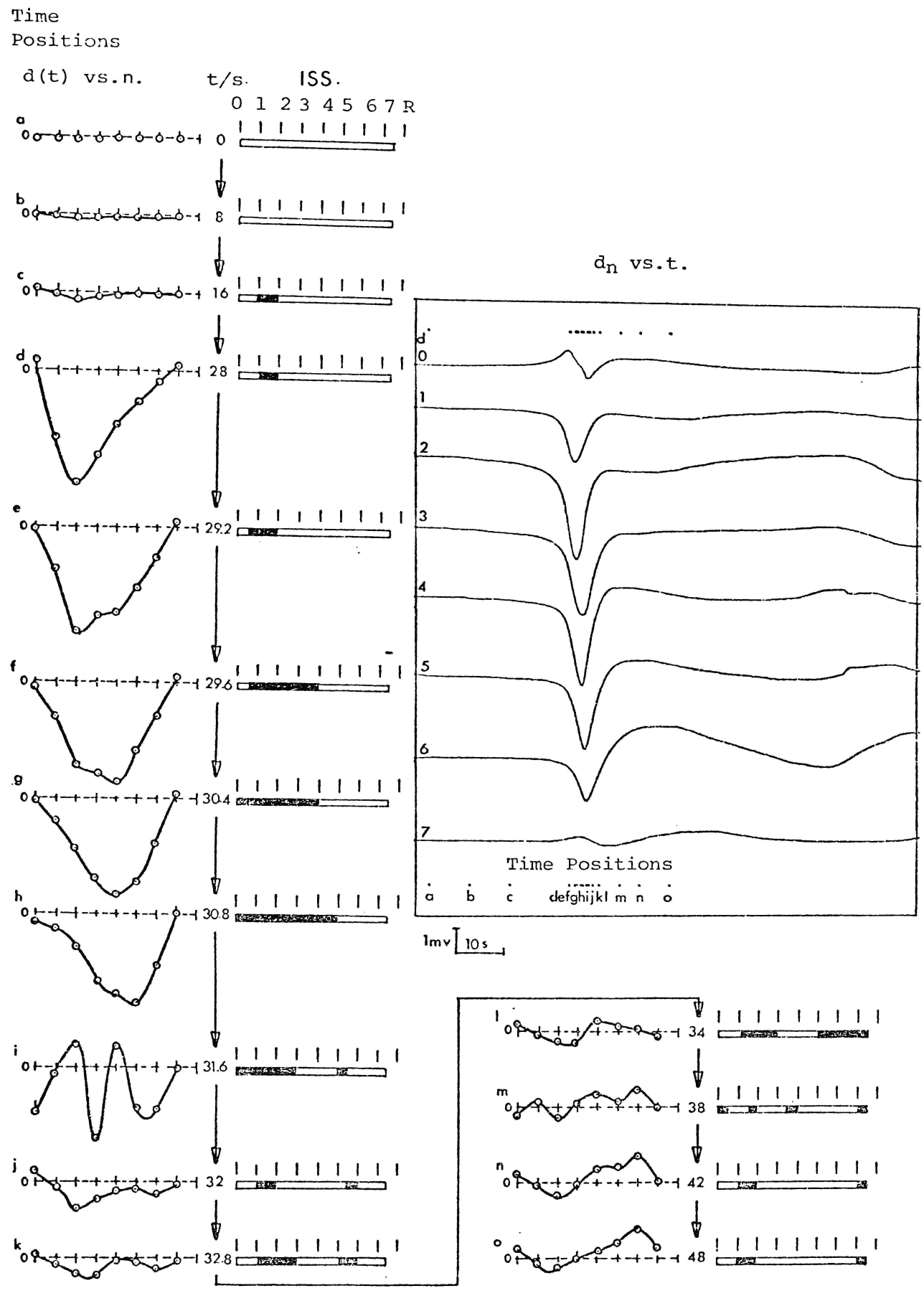

Fig.A5 (Cont.2)
c)

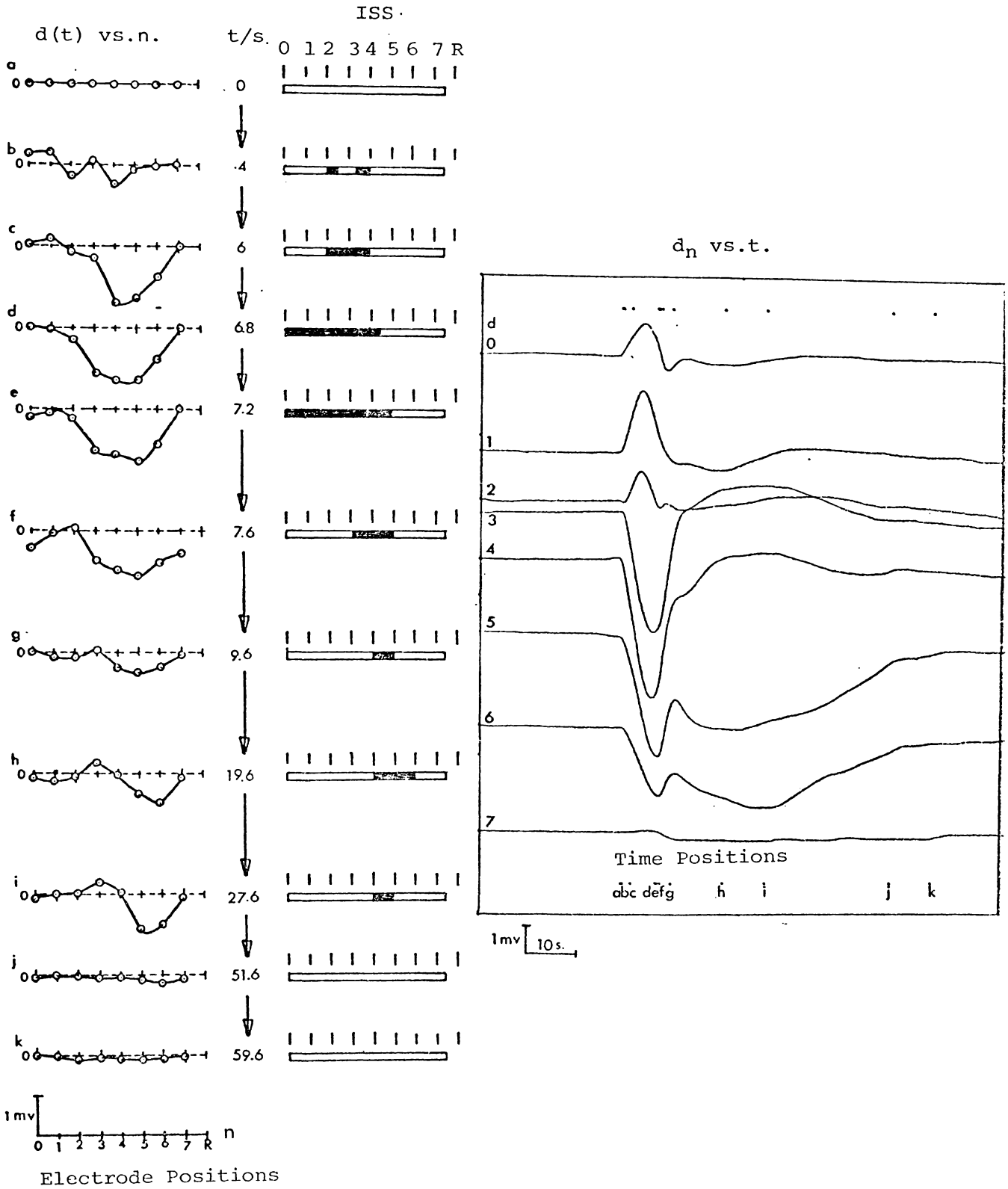

Electrode Positions

Electrode Spacings = 1.9 mm.

Fig. A5 (Cont. 3)

d)

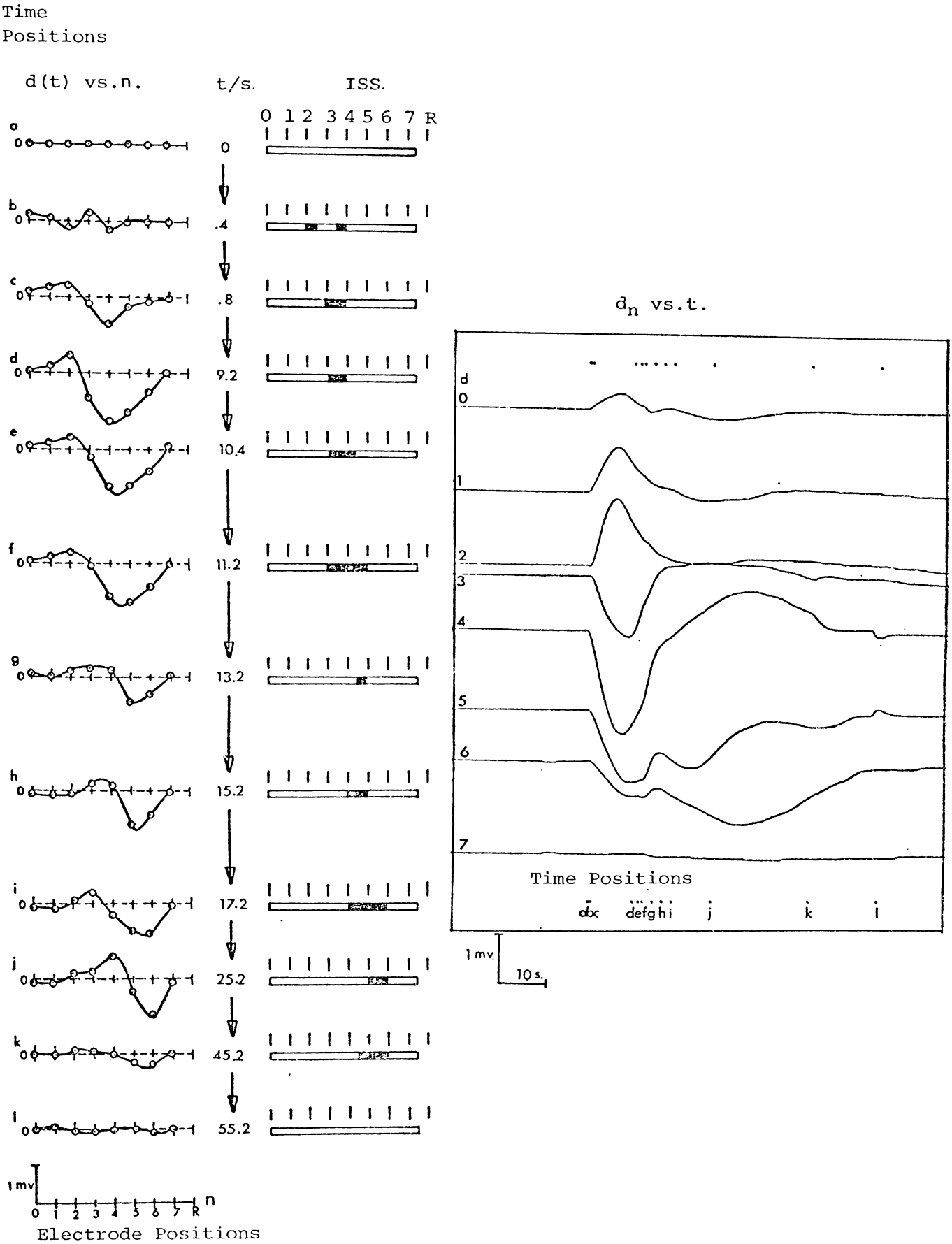

Fig. A5 (Cont. 4)

e)

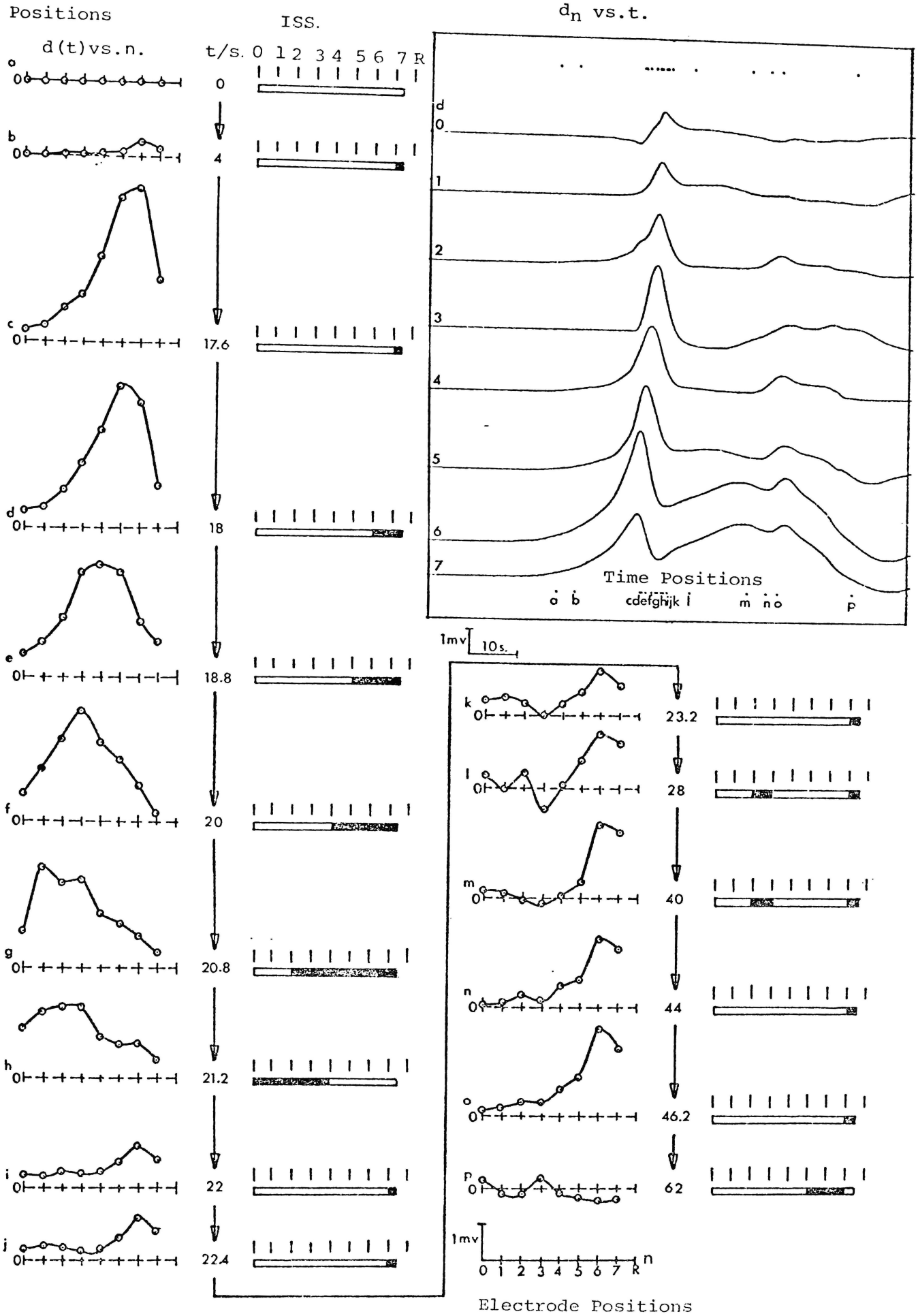

i) The occurrence of some additional depolarisations (usually local depolarisations) during the active period.

ii) The 'build-up' period during the initial stage of the AP generation before it begins to propagate differs in length.

iii) The whole active period may range from 15 to 200 s.

iv) The peak voltage amplitudes (among AP's detected from the cell can range from $\simeq$ 2 to $\simeq$ 7 mV.)

v) Some AP's originate from the summation of more than one local depolarisations (see Fig. 3.3.1, Section 3.3)

This variability of the AP characteristics is undoubtedly due to the sensitivity of the AP propagation to the state of the membrane activity, as suggested by several authors e.g. Jaffe et.al.(1974), Gradmann (1975, 1976, 1978) and Bentrup (1977) (see also Section 3.4). Thus more detailed measurements of AP initiation and propagation may well be a useful probe of membrane process.

REFERENCES

REFERENCES

Adrian, R.H., 1956. The Effect of Internal and External Potassium Concentration on the Membrane Potential of Frog Muscle. *Journal of Physiology (London) 133*, p.631-658.

Agin, D., and D. Holtzman , 1966. Glass Microelectrodes : the Origin and Elimination of Tip Potentials. *Nature (London) 211*, p.1194-5.

Babloyantz, A., & J. Hiernaux, 1974. Models for Positional Information and Positional Differentiation. *Proceedings of the National Academy of Sciences 71(4)*, p.1530-33.

Babloyantz, A., and J. Hiernaux, 1975. Models for Cell Differentiation and Generation of Polarity in Diffusion - Governed Morphogenetic Field. *Bulletin of Mathematical Biology 37*, p.637-657.

Barker, A.T., B.H. Brown, and I.L. Freeston, 1979. Modeling of an Active Nerve Fibre in a Finite Volume Conductor and Its Application to the Calculation of Surface Action Potentials. *IEEE Transactions on Biomedical Engineering BME 26(1)*, p.53-56.

Bentrup, F.W., 1977. Electric Events During Apex Regeneration in *Acetabularia mediterranea*. *In Progress in Acetabularia Research*, p.249-254. Ed. C.L.F. Woodcock. Academic Press, New York.

Bonotto, S., P. Lurguin, and A. Mazza, 1976. Recent Advances in Research on the Marine Algal *Acetabularia*. *Advance Marine Biology 14*, p.123-250.

Bonotto, S., and C. Sironval, 1977. Experimental Studies on the Phototropism of *Acetabularia mediterranea* and *Acetabularia crenulata*. *In Progress in Acetabularia Research*, p.241-247. Ed. C.L.F. Woodcock. Academic Press, New York.

Brachet, J., and S. Bonotto, 1970. *Biology of Acetabularia*, Academic Press, New York.

Brazier, M.A., 1968. *The Electrical Activity of the Nervous System*, London Pitman Medical Publishing Co., London.

Christ-Adler, M., and F.W. Bentrup, 1976. Effects of K^+ and Cl^- Ion Gradients upon Apex Regeneration in *Acetabularia mediterranea*. *Planta (Berlin) 129*, p.91-93.

Clark, J., and R. Plonsey, 1966. A Mathematical Evaluation of the Core Conductor Model. *Biophysical Journal 6*, p.95-112.

Clark, J., and R. Plonsey, 1968. The Extracellular Potential Field of the Single Active Nerve Fibre in a Volume Conductor. *Biophysical Journal 8*, p.842-64.

Finean, J.B., R. Coleman, and R.H. Michell, 1974. *Membranes and Their Cellular Functions*, Blackwell Scientific Publication, Oxford.

Ferris, C.D., 1974. *Introduction to Bioelectrodes*, Plenum Press, New York.

Frank, K., and M.C. Becker, 1964. Microelectrodes for Recording and Stimulation. *In Physical Techniques in Biological Research 5A*, p.23-84. Ed. W.L. Nastuk. Academic Press, New York.

Geddes, L.A., 1972. *Electrodes and the Measurement of Bioelectric Events*, John Wiley, New York.

Gibor, A., 1966. *Acetabularia* : A Useful Giant Cell. *Scientific American 215(5)*, p.118-124.

Gibor, A., 1977. Cell Elongation in *Acetabularia*. *In Progress in Acetabularia Research*, p.231-239. Ed. C.L.F. Woodcock. Academic Press, New York.

Gibor, A., and M. Izawa, 1963. The DNA Content of the chloroplasts of *Acetabularia*. *Proceedings of the National Academy of Sciences 50(6)*, p.1164-9.

Goldman, D.E., 1943. Potential, Impedance and Rectification in Membranes. *Journal of Physiology(London) 27*, p.37.

Goodwin, B.C., 1975, A Membrane Model for Polar Ordering and Gradient Formation. *Advances in Chemical Physics 29*, p.269-280.

Goodwin, B.C., 1976. *Analytical Physiology of Cells and Developing Organisms*, Academic Press, London.

Goodwin, B.C., 1980. Pattern Formation and Its Regeneration in the Protozoa. *In The Eukaryotic Microbial Cell. Society for General Microbiology Symposium 30*, p.377-404. Eds. G.W. Gooday, D. Lloyd, and A.P.J. Trinci. Cambridge University Press, London.

Goodwin, B.C., and S. Pateromichelakis, 1979. The Role of Electrical Fields, Ions, and the Cortex in the Morphogenesis of *Acetabularia*. *Planta (Berlin) 145*, p.427-435.

Gotow, T., M. Ohba, and T. Tomita, 1977. Tip Potential and Resistance of Micro-Electrodes Filled with KCl Solution by Boiling and Nonboiling Methods. *IEEE Transactions on Biomedical Engineering*, BME 24(4), p.366-371.

Gradmann, D., 1975. Analog Circuit of the *Acetabularia* Membrane. *Journal of Membrane Biology 25*, p.183-208.

Gradmann, D., 1976. "Metabolic" Action Potential in *Acetabularia*. *Journal of Membrane Biology 29*, p.23-45.

Gradmann, D., 1978. Green Light (550 nm) Inhibits Electrogenic Cl^- Pump in the *Acetabularia* Membrane by Permeability Increase for the Carrier Ion. *Journal of Membrane Biology 44(1)*, p.1-24.

Gradmann, D., and W. Klemke, 1974. Current-Voltage Relationship of the Electrogenic Pump in *Acetabularia mediterranea*. *In Membrane Transport in Plants*, p.131-138. Eds. U. Zimmermann and J. Dainty. Springer-Verlag Berlin Heidelberg, New York.

Gradmann, D., G. Wagner, and R.M. Gläsel, 1973. Chloride Efflux During Light - Triggered Action Potentials in *Acetabularia mediterranea*. *Biochimica et Biophysica Acta 323*, p.151-155.

Haken, H., 1978. *Synergetics - An Introduction Nonequilibrium Phase Transitions and Self-Organisation in Physics, Chemistry and Biology*, 2nd Edition. Springer-Verlag Berlin Heidelberg, New York.

Hammerling, J., 1931. Entwicklung und Formbildungsvermögen von *Acetabularia mediterranea*, I. Die normale Entwicklung. *Biologisches Zentralblastt 51*, p.633-647.

Hammerling, J., 1963. Nucleo-Cytoplasmic Interactions in *Acetabularia* and other Cells. *Annual Review of Plant Physiology 14*, p.65-92.

Hodgkin, A.L., and A.F. Huxley, 1939. Action Potentials Recorded from Inside a Nerve Fibre. *Nature (London) 144*, p.403.

Hodgkin, A.L., and A.F. Huxley, 1952. A Quantitative Description of Membrane Current and Its Application to Conduction and Excitation in Nerve. *Journal of Physiology (London) 117*, p.500-44.

Hodgkin, A.L., and B. Katz, 1949. The Effect of Sodium Ions on the Electrical Activity of the Giant Axon of Squid. *Journal of Physiology (London) 108*, p.37.

Hodgkin, A.L., and R.D. Keynes, 1955. The Potassium Permeability of a Giant Nerve Fibre. *Journal of Physiology (London) 128*, p.61-68.

Hope, A.B., and N.A. Walker, 1975. *The Physiology of Giant Algal Cells*, Cambridge University Press, London.

Hoursiangou-Neubran, D., J.P. Dubacq, and S. Puiseux-Dao, 1977. Heterogeneity of the Plastid Population and Chloroplast Differentiation in *Acetabularia mediterranea*. *In Progress in Acetabularia Research*, p.175-194. Ed. C.L.F. Woodcock. Academic Press, New York.

Jack, J.J.B., D. Noble, and R.W. Tsien, 1975. *Electric Current Flow in Excitable Cells*, Clarendon Press, Oxford.

Jaffe, L.F., K.R. Robinson, and R. Nuccitelli, 1974. Local Cation Entry and Self Electrophoresis as in Intracellular Localization Mechanism. *Annals New York Academy of Sciences 328*, p.372-89.

Katz, B., 1966. *Nerve, Muscle, and Synapse*, McGraw-Hill, New York.

Keck, K., 1964. Culturing and Experimental Manipulation of *Acetabularia*. *In Method in Cell Physiology 1*, p.189-212. Ed. D.M. Prescott. Academic Press, New York.

Khodorov, B.I., 1974. *The Problem of Excitability, Electrical Excitability and Ionic Permeability of the Nerve Membrane*, Plenum Press, New York.

Koop, H.-U., 1975. Multi nuclear Stages of the Life Cycle of *Acetabularia mediterranea*. *Protoplasma 86*, p.351-362.

Lateur, L., and S. Bonotto, 1973. Culture of *Acetabularia mediterranea* in the Laboratory. *Bulletin de la Societé royale de Botanique de Belgique 106(1)*, p.17-38.

Lavallée, M., O. Schanne, and N.C. Hébert, 1969. *Glass Microelectrodes*, John Wiley, New York.

Lehninger, A.L., 1975. *Biochemistry*, 2nd Edition, Worth Publishers Inc., New York.

Mazza, A., S. Bonotto, and B. Felluga, 1977. Ultrastructure of DNA of Basal, Middle and Apical Chloroplasts of Individual *Acetabularia mediterranea* cells. *In Progress in Acetabularia Research*, p.123-136. Ed. C.L.F. Woodcock. Academic Press, New York.

Mullins, L.J., 1962. Efflux of Chloride Ions During Action Potential of *Nitella*. *Nature (London) 196*, p.986.

Mummert, H., and D. Gradmann, 1976. Voltage Dependent Potassium Fluxes and the Significance of Action Potentials in *Acetabularia*. *Biochimica et Biophysica Acta 443*, p.443-50.

Nicolis, G., and I. Prigogine, 1977. *Self-Organisation in Nonequilibrium Systems*, John Wiley, New York.

Novak, B., 1975a. Sustained Current Pulses and Transcellular Current During the Regeneration of *Acetabularia mediterranea*. *Protoplasm 83*, p.178.

Novak, B., 1975b. Periodical Signals in the Spatial Differentiation of Plant Cells. *In Advances in Chemical Physics 29*, p.281-299. Eds. G. Nicolis and R. Lefever. John Wiley, New York.

Novak, B., and F.W. Bentrup, 1972a. An Electrophysiological Study of Regeneration in *Acetabularia mediterranea*. *Planta (Berlin) 108*, p.227-244.

Novak, B., and F.W. Bentrup, 1972b. Transcytoplasmic Electric Currents through Regenerating Stalk Segments of *Acetabularia mediterranea*. *Protoplasma 75*, p.483.

Novak, B., and C. Sironval, 1975. Inhibition of Regeneration of *Acetabularia mediterranea* Enucleated Posterior Stalk Segments by Electrical Isolation. *Plant Science Letters 5*, p.183-188.

Novak, B., and C. Sironval, 1976. Circadian Rhythm of the Transcellular Current in Regenerating Enucleated Posterior Stalk Segments of *Acetabularia mediterranea*. *Plant Science Letters 6*, p.273-283.

Nuccutelli, R., and L.F. Jaffe, 1974. Spontaneous Current Pulses through Developing Fucoid Eggs. *Proceedings of the National Academy of Sciences 71*, p.4855.

Ohki, S., 1979. Membrane Potential, Surface Potential and Ionic Permeability. *Physics Letters 75A(1,2)*, p.149-152.

Okada, Y., and A. Inouye, 1976. Studies on the Origin of the Tip Potential of Glass Microelectrode. *Biophysics of Structure and Mechanism 2*, p.31-42.

Puiseux-Dao, S., 1970. *Acetabularia and Cell Biology*, Logos Press Ltd., London.

Saddler, H.D.W., 1970a. The Ionic Relations of *Acetabularia mediterranea*. *Journal of Experimental Botany 21*, p.345-359.

Saddler, H.D.W., 1970b. The Membrane Potential of *Acetabularia mediterranea*. *Journal of General Physiology 55*, p.802-821.

Saddler, H.D.W., 1970c. Fluxes of Sodium and Potassium in *Acetabularia mediterranea*. *Journal of Experimental Botany 21*, p.605-616.

Saddler, H.D.W., 1971. Spontaneous and Induced Changes in the Membrane Potential and Resistance of *Acetabularia mediterranea*. *Journal of Membrane Biology 5*, p.250-260.

Schweiger, H.G., H. Bannwarth, S. Berger, and K. Kloppstech, 1975. *Acetabularia*, a Cellular Model for the Study of Nucleocytoplasmic Interactions. *In Molecular Biology of Nucleocytoplasmic Relationships*, p.203-215. Ed. S. Puiseux-Dao. Elsevier, Amsterdam and New York.

Schweiger, H.G., P. Dehm, and S. Berger, 1977. Culture Conditions for *Acetabularia*. *In Progress in Acetabularia Research*, p.319-330. Ed. C.L.F. Woodcock. Academic Press, New York.

Shephard, D.C., 1970. Axenic Culture of *Acetabularia* in a Synthetic Medium. *In Methods in Cell Physiology 4*, p.49-69. Ed. D.M. Prescott. Academic Press, New York and London.

Sironval, C., S. Bonotto, M. Paques, and E. Dujardin, 1977. Temporary Periodic Localization of the Chloroplasts in the Form of Transverse Bands, in the Stalk of *Acetabularia mediterranea*. *In Progress in Acetabularia Research*, p.207-212. Ed. C.L.F. Woodcock. Academic Press Inc., New York.

Tasaki, I., E.H. Polley, and F. Orrego, 1954. Action Potentials from Individual Elements in Cat Geneculate and Striate Cortex. *Journal of Neurophysiology 17*, p.454-474.

Tasaki, K., Y. Tsukahara, M.J. Wayner, and W.Y. Wu, 1968. A Simple Direct and Rapid Method for Filling Microelectrodes. *Physiology and Behaviour 3*, p.1009-1010.

Turing, A.M., 1952. The Chemical Basis of Morphogenesis. *Philosophical Transactions of the Royal Society Series B237*, p.37-72.

Weisenseel, M.H., R. Nuccitelli, and L.F. Jaffe, 1975. Large Electrical Currents Traverse Growing Pollen Tubes. *Journal of Cell Biology 66*, p.556-567.

Werz, G., 1974. Fine Structural Aspects of Morphogenesis in *Acetabularia*. *In International Review of Cytology38*, p.319-367. Eds. G.H. Bourne, J.F. Danielli, and K.W. Jeon. Academic Press, New York.

White, A., P. Handler, E.L. Smith, R.L. Hill, and I.R. Lehman, 1978. *Principles of Biochemistry*. 6th Edition. McGraw-Hill, New York.

Wolpert, L., 1969. Positional Information and the Spatial Pattern of Cellular Differentiation. *Journal of Theoretical Biology 25*, p.1-47.

Wolpert, L., 1975. The Development of Pattern : Mechanisms Based on Positional Information. *In Advances in Chemical Physics 29*, p.253-267. Eds. G. Nicolis and R. Lefever. John Wiley, New York.

Zubarev, T.N., and N.P. Rogatykh, 1975. On the Nature of the Signal Inducing the Synthesis of "Morphogenetic Substances" in the *Acetabularia* nucleus in Cap Regeneration. *In Molecular Biology of Nucleocytoplasmic Relationships*, p.259-262. Ed. S. Puiseux-Dao. Elsevier, Amsterdam and New York.